The role of floodplains on the propagation of land management signals in the Vale of York

HILL, CATHERINE,JANE

The role of floodplains on the propagation of land management signals in the Vale of York

Catherine Jane Hill

MSc by Research

Department of Geography

Durham University

October 2010

Declaration of Copyright

I confirm that no part of the material presented in this thesis has previously been submitted by me or any other person for a degree in this or any other university. In all cases, where it is relevant, material from the work of others has been acknowledged.

Catherine Jane Hill

Department of Geography

Durham University

October 2010

Abstract

The floodplains of many UK rivers are heavily managed to reduce the risk of flooding. The presence of levées is thought to increase peak flows, decreasing the ability of the floodplains to attenuate flood waters. Understanding the role of floodplains for reducing flood risk is vital in order to create flood management strategies that utilise the natural attenuation properties of floodplains to reduce future flood risk. The impact of flood levées on the propagation of upstream land management signals has been assessed in this thesis. The study utilised the 1-D model HEC-RAS to determine the impact of levées on the transmission of possible land management signals (from moorland grips) in the Ouse catchment, and establish the resulting flood risk for the City of York. A link between rural land management in the upper catchments and flood routing was demonstrated. The flow was scaled in relation to the hypothesised effect of blocking grips to examine the scale of possible downstream consequences. At upstream cross-sections the reduction in peak discharge was higher, suggesting that the positive impact of removing the levées, in terms of decreasing the flood peak, is dissipated as the flood wave propagates downstream. Further downstream the attenuation reduced suggesting that land use signals are dissipated with distance downstream. Solely removing the levées reduced peak flows by only 1.3%. Crucially, by combining the positive effects of levée removal and grip blocking, peak discharge downstream at York could be reduced by 4.2% for the York 2000 flood event. This approach also reduced the peak flow for the York 2000 flood event below the threshold for peak flows associated with a 25 year return period. Peak discharge was more sensitive to flow scaling with the levées, suggesting that levées do make the grip effect more noticeable, although the influence of the levées is not large. The findings suggest that levées do transmit the flood signal further downstream to York due to a reduction in floodplain attenuation. The removal of levée sections combined with grip blocking in the upland catchments could prove an effective and sustainable approach for future flood risk management in the Ouse catchment.

Acknowledgements

I would like to express my thanks to Professor Stuart Lane and Dr Richard Hardy for their constant support, guidance and enthusiasm which have been greatly appreciated. I am very grateful for their direction and inspiration throughout this project. Many thanks to Jeff Pacey for initiating this project and providing data, and to all others at the Environment Agency who have made datasets available and given their time for this investigation. Thank you to Ian for his modelling expertise and guidance during the early stages of the project and to Calum, Carly, Charlie, Ed, Emma, George, I-Hsien and many others in the department who offered their advice, time and company during tea breaks. A special thank you goes to Luke for his continuous support and encouragement throughout this year. Finally, I thank my family for supporting me throughout my University studies and for moving my vast collections of 'stuff' to and from Yorkshire.

Contents

Chapter One: Introduction **1**

1.1 Introduction **2**

1.2 Aim and Research Questions **2**

1.3 Explanation of Research Questions **2**

1.4 Justification of research focus **3**

1.5 Case study – flooding in the City of York **5**

1.6 Study location **5**

1.6.1 Catchment characteristics 5

1.6.2 Model extent 8

1.7 Thesis structure **9**

Chapter Two: Literature Review **10**

2.1 Introduction **11**

2.2 In what way can the floodplain be used to reduce flood risk downstream? **11**

2.2.1 Floodplains for flood alleviation 11

2.2.2 Hydrograph timing 12

2.2.3 Design and location of storage areas 13

2.2.4 Flood wave propagation 15

2.2.5 Woodland planting on the floodplain 16

2.2.6 Manning's *n* 18

2.3 To what extent are land management signals impacted upon by flow attenuation? **20**

2.3.1 Upland drainage 21

2.3.2 Grip blocking practice 22

2.3.3 Flow attenuation 23

2.4 Do flood levées aid the transmission of the upstream hydrograph? **23**

2.5 Case Study – flooding at York **25**

2.5.1 The York floods of 2000 25

2.5.2 Land use and flooding at York 26

2.5.3 Subcatchment landuse projects 27

2.6 Summary **28**

Chapter Three: Methodology **29**

3.1 Introduction **30**

3.2 Modelling overview **30**

3.2.1 Modelling approach 30

3.2.2 Model choice and set-up 33

3.2.3 Basic 1-D flow equations 34

3.3 Description of HEC-RAS **35**

3.3.1 Hydrological boundary conditions 35

3.3.2 Geometric Data 36

3.4 Data Sources **41**

3.4.1 ISIS 1-D hydrodynamic model 41

3.4.2 Hydrology data 42

3.5 Model building – unsteady flow model structure **43**

3.5.1 Hydrological boundary conditions 43

3.5.2 Lateral inflows 44

3.5.3 Geometry: river channel 48

3.5.4 Geometry: floodplains 49

3.5.5 Structures 51

3.5.6 Roughness coefficient 52

3.6 Modelling practice **53**

3.7 Summary **54**

Chapter Four: Model sensitivity and calibration **55**

4.1 Introduction **56**

4.2 Methodology **56**

4.2.1 Purpose of sensitivity analyses 56

4.2.2 Experimental design 57

4.2.3 Variation of each input parameter 58

4.2.4 Input matrix – one-at-a-time approach 58

4.2.5 Evaluation – objective functions 61

4.3 Results – model predictions **64**

4.3.1 Discharge response to Manning's *n* 64

4.3.2 Discharge response to weir coefficient 77
4.3.3 Discharge response to changing both inflow and Manning's *n* 80
4.4 Results – model performance 86
4.4.1 Discharge response to Manning's *n* 88
4.4.2 Discharge response to changing both inflow and Manning's *n* 96
4.5 Discussion 97
4.5.1 Discharge response to Manning's *n* 97
4.5.2. Discharge response to weir coefficient 99
4.6 Calibration 99
4.6.1 Calibration process 99
4.6.2 Calibration results 102
4.7 Conclusion 106

Chapter Five: Simulation – Results 108
5.1 Introduction 109
5.2 Methodology 109
5.2.1 RQ 1 – In what way can the floodplain be used to reduce flood risk downstream? 109
5.2.2 RQ2 – To what extent are land management signals impacted upon by flow attenuation? 110
5.2.3 RQ 3 – Do flood levées aid the transmission of the upstream hydrograph? 113
5.3 Results: Research Question 1 – In what way can the floodplain be used to reduce flood risk downstream? 116
5.3.1 Initial hydrographs 116
5.3.2 Varying Manning's *n* for all reaches 120
5.3.3 Varying Manning's *n* for the River Ouse 126
5.3.4 Varying Manning's *n* for the River Swale 132
5.3.5 Varying Manning's *n* for the River Nidd 136
5.3.6 Four levée scenarios 141
5.4 Results: Research Question 2 – To what extent are land management signals impacted upon by flow attenuation? 147

5.4.1 Grip blocking scenarios 147
5.4.2 Effect on output hydrographs – with levées 151
5.5 Results: Research Question 3 – Do flood levées aid the transmission of the upstream hydrograph? 157
5.5.1 Effect on output hydrographs – without levées 157
5.5.2 Effect on output hydrographs – half levées and added height levées 165
5.5.3 Effect on hydrograph with changes to roughness – with levées 168
5.5.4 Effect on hydrograph with changes to roughness – without levées 171
5.5.5 Effect on hydrograph with changes to roughness – half levées 174
5.5.6 Effect on hydrograph with changes to roughness – added height levées 176
5.5.7 Influence of the changes on peak discharge 178
5.5.8 Comparison of the four levée scenarios 185
5.6 Conclusion 186

Chapter Six: Simulation – Discussion 188
6.1 Introduction 189
6.2 Research Question 1 – In what way can the floodplain be used to reduce flood risk downstream? 189
6.2.1 Varying Manning's *n* for the levée scenarios 193
6.2.2 Varying Manning's *n* for the Rivers Ouse, Swale and Nidd 196
6.3 Research Question 2 – To what extent are land management signals impacted upon by flow attenuation? 197
6.4 Research Question 3 – Do flood levées aid the transmission of the upstream hydrograph? 198
6.4.1 Scaling the flow and varying levée heights 198
6.4.2 Scaling and shifting the flow and varying levée heights 199
6.4.3 Varying channel Manning's *n*, flow and levée heights 200
6.4.4 Varying floodplain Manning's *n*, flow and levée heights 201
6.4.5 Reducing peak discharge below a threshold 202
6.5 Conclusion 203

Chapter Seven: Conclusions **204**

7.1 Introduction **205**

7.2 Impact of levées on propagation of the upland grip signal in the Ouse catchment **205**

7.3 Summary of Research Questions **206**

7.3.1 Research Question 1 – In what way can the floodplain be used to reduce flood risk downstream? 207

7.3.2 Research Question 2 – To what extent are land management signals impacted upon by flow attenuation? 207

7.3.3 Research Question 3 – Do flood levées aid the transmission of the upstream hydrograph? 208

7.4 Recommendations for future work **209**

7.5 Wider lessons learnt **210**

7.6 Assessment of the study **210**

7.7 Summary **211**

References **213**

Appendix One: Number, grid reference, roughness and distance downstream for Left Over Bank (LOB), channel and Right Over Bank (ROB) for each cross-section in the HEC-RAS model **229**

Appendix Two: Changes to the output hydrographs after varying Manning's *n* of the channel and floodplain **233**

Appendix Three: Hydrographs produced after scaling and shifting the flow for each of the levée scenarios **243**

Appendix Four: Comparing the hydrographs for each variation in roughness and flow **247**

List of Figures

Figure Number	Figure Title	Page Number
	Chapter One	
1.1	Location of the Ouse catchment in a national context	**6**
1.2	Extent of the model and location of flow gauging stations in the Ouse catchment	**8**
	Chapter Two	
2.1	Attenuation and translation of the flood hydrograph as a result of floodplain storage (source: Morris *et al.*, 2004)	**12**
2.2	Effect of washland storage on flood hydrographs (source: English Nature *et al.*, 2002)	**14**
2.3	Effect of floodplain woodland on flood hydrographs (source: Thomas and Nisbet, 2007)	**17**
	Chapter Three	
3.1	Location of the lateral inflows entering the modelled reach	**46**
3.2	Model schematic illustrating the location of rivers, reaches, point and lateral inflows and gauging stations	**47**
3.3	Calculating LOB and ROB to complete the cross sectional geometry data	**48**
3.4	Calculating the volume of each storage area	**49**
3.5	Removal and alteration of the levées within the model	**51**
	Chapter Four	
4.1	Discharge response to changes in global Manning's *n* for all reaches	**65**
4.2	Peak discharge response to varying global Manning's *n*	**66**
4.3	Discharge response to changes in channel Manning's *n* for all reaches	**68**
4.4	Peak discharge response to varying channel Manning's *n*	**68**
4.5	Discharge response to changes in floodplain Manning's *n* for all reaches	**69**
4.6	Peak discharge response to varying floodplain Manning's *n*	**69**
4.7	Discharge response to left bank floodplain changes in Manning's *n* for all	**70**

reaches
4.8 Discharge response to right bank floodplain changes in Manning's *n* for all reaches **70**
4.9 Peak discharge response to varying floodplain Manning's *n* for the left (a) and right (b) banks **71**
4.10 (a) Discharge response to changes in global Manning's *n* for the River Ouse; (b) for the River Swale; (c) for the River Nidd **72**
4.11 Peak discharge response to varying global Manning's *n* in each of the three tributaries **74**
4.12 (a) Discharge response to changes in channel Manning's *n* for the River Ouse; (b) for the River Swale; (c) for the River Nidd **75**
4.13 (a) Discharge response to changes in floodplain Manning's *n* for the River Ouse; (b) for the River Swale; (c) for the River Nidd **76**
4.14 Effect of the weirs on the simulated hydrograph **78**
4.15 Effect of Linton weir coefficient on discharge **79**
4.16 (a) Discharge response to a 20% increase in inflow and changes in global Manning's *n*; (b) Discharge response to a 20% increase in inflow and changes in channel Manning's *n*; (c) Discharge response to a 20% increase in inflow and changes in floodplain Manning's *n* **81**
4.17 (a) Discharge response to a 20% decrease in inflow and changes in global Manning's *n*; (b) Discharge response to a 20% decrease in inflow and changes in channel Manning's *n*; (c) Discharge response to a 20% decrease in inflow and changes in floodplain Manning's *n* **82**
4.18 Peak discharge response to a 20% increase in inflow and changes in Manning's *n* **84**
4.19 Peak discharge response to a 20% decrease in inflow and changes in Manning's *n* **85**
4.20 Observed hydrograph and the simulated hydrograph returned after initial model building / RMSE calculated for five sections of the original modelled and observed flow data **87**
4.21 Nash-Sutcliffe values for varying global Manning's n **88**
4.22 Nash-Sutcliffe values for each Manning's *n* value modelled **89**
4.23 Percentage error in the peak of the simulated hydrograph compared to the **89**

observed hydrograph with changes in global Manning's *n*

4.24 Percentage error in the peak for each of the Manning's *n* values modelled **90**

4.25 Root Mean Square Error for each of the Manning's *n* values modelled **91**

4.26 Mean absolute error values after varying global Manning's n **92**

4.27 Mean absolute error values for each Manning's *n* value modelled **92**

4.28 Stages involved in the calibration process of model building (source: Janssen and Heuberger, 1995) **101**

4.29 Varying Manning's *n* for calibration **103**

4.30 Manning's *n* decreased globally by 20% and the weir geometries changed differently in each run **105**

4.31 Manning's *n* of the River Ouse decreased globally by 25% and 20% for both the River Swale and River Nidd and the weir geometries changed differently in each run **105**

Chapter Five

5.1 A schematic diagram of the whole system showing the possible outcomes for flood risk through model assessment **115**

5.2 Locations of the cross-sections within the modelled reach that were used for flow analysis **117**

5.3 Output hydrograph at the downstream boundary for the original flow using the 'with levées' and 'without levées' scenarios **117**

5.4 Output hydrographs at selected cross-sections in the model for the original flow using the 'with levées' and 'without levées' scenarios **118**

5.5 Difference in peak discharge between the scenarios for different cross-sections in the model **119**

5.6 Difference in peak timing delay between the scenarios for different cross-sections in the model **119**

5.7 Change in peak discharge with relation to Manning's *n* values of the channel for the 'with levées' and 'without levées' scenarios **121**

5.8 Change in peak discharge with relation to Manning's *n* values of the floodplain for the 'with levées' and 'without levées' scenarios **121**

5.9 Change in peak discharge with relation to Manning's *n* values varied for both the channel and floodplain for the 'with levées' and 'without levées' **122**

scenarios

5.10 Change in peak timing delay with relation to Manning's *n* values of the channel for the 'with levées' and 'without levées' scenarios **123**

5.11 Change in peak timing delay with relation to Manning's *n* values of the floodplain for the 'with levées' and 'without levées' scenarios **123**

5.12 Change in peak discharge with relation to Manning's *n* values of the Ouse channel for the 'with levées' and 'without levées' scenarios **127**

5.13 Change in peak discharge with relation to Manning's *n* values of the Ouse floodplain for the 'with levées' and 'without levées' scenarios **127**

5.14 Change in peak discharge with relation to Manning's *n* values varied for both the channel and floodplain for the 'with levées' and 'without levées' scenarios **128**

5.15 Change in peak timing delay with relation to Manning's *n* values of the Ouse channel for the 'with levées' and 'without levées' scenarios **129**

5.16 Change in peak timing delay with relation to Manning's *n* values of the Ouse floodplain for the 'with levées' and 'without levées' scenarios **129**

5.17 Change in peak discharge with relation to Manning's *n* values of the Swale channel for the 'with levées' and 'without levées' scenarios **132**

5.18 Change in peak discharge with relation to Manning's *n* values of the Swale floodplain for the 'with levées' and 'without levées' scenarios **133**

5.19 Change in peak timing delay with relation to Manning's *n* values of the Swale channel for the 'with levées' and 'without levées' scenarios **133**

5.20 Change in peak timing delay with relation to Manning's *n* values of the Swale floodplain for the 'with levées' and 'without levées' scenarios **134**

5.21 Change in peak discharge with relation to Manning's *n* values of the Nidd channel for the 'with levées' and 'without levées' scenarios **136**

5.22 Change in peak discharge with relation to Manning's *n* values of the Nidd floodplain for the 'with levées' and 'without levées' scenarios **137**

5.23 Change in peak timing delay with relation to Manning's *n* values of the Nidd channel for the 'with levées' and 'without levées' scenarios **137**

5.24 Change in peak timing delay with relation to Manning's *n* values of the Nidd floodplain for the 'with levées' and 'without levées' scenarios **138**

5.25 (a) Output hydrographs for each of the four levée scenarios using the original input hydrographs; (b) Peak discharges at the downstream boundary of the model for each of the four levée scenarios **142**

5.26 Change in peak discharge with relation to Manning's *n* values of the channel for all four levée scenarios **143**

5.27 Change in peak discharge with relation to Manning's *n* values of the floodplain for all four levée scenarios **144**

5.28 Change in peak timing delay from the original timing with relation to Manning's *n* values of the channel for all four levée scenarios **145**

5.29 Change in peak timing delay with relation to Manning's *n* values of the floodplain for all four levée scenarios **146**

5.30 Ouse input hydrograph scaled by 1.01, 1.05, 1.10, 1.20, 1.25 and 1.50 and subsequently shifted by 1 hour **150**

5.31 Effect of the scaled flow on peak discharge for the 'with levées' scenario **151**

5.32 Peak timing delay in relation to each scaled flow under the 'with levées' scenario **151**

5.33 Peak discharge at selected cross section locations using the 'with levées' scenario for each of the scaled flows **152**

5.34 Change in peak discharge after scaling and shifting the flow using the 'with levées' scenario **153**

5.35 Change in peak timing delay after scaling and shifting the flow using the 'with levées' scenario **154**

5.36 Peak discharge at selected cross section locations using the 'with levées' scenario for each of the scaled and shifted flows **156**

5.37 Effect of the scaled flow on peak discharge for the 'with levées' and 'without levées' scenarios **157**

5.38 Peak timing delay in relation to each scaled flow under the 'with levées' and 'without levées' scenarios **158**

5.39 Peak discharge at selected cross section locations using the 'without levées' scenario for each of the scaled flows **159**

5.40 Change in peak discharge after scaling and shifting the flow using the 'without levées' scenario **160**

5.41 Change in peak timing after scaling and shifting the flow using the 'without levées' scenario **160**

5.42 Peak discharge at selected cross section locations using the 'without levées' scenario for each of the scaled and shifted flows **163**

5.43 Difference in peak discharge between the 'with levées' and 'without levées' scenarios at selected cross section locations for each of the scaled and shifted flows **164**

5.44 Difference in peak timing delay between the 'with levées' and 'without levées' scenarios at selected cross section locations for each of the scaled and shifted flows **164**

5.45 Effect of the scaled flow on peak discharge for all levée scenarios **165**

5.46 Change in peak discharge with each shift to the flow using the 'half height levées' and 'added height levées' scenarios **166**

5.47 Change in peak discharge from the original peak discharge after shifting the flow using the 'half height levées' and 'added height levées' scenarios **167**

5.48 Change in peak timing delay after shifting the flow for each of the four levée scenarios **167**

5.49 Change in peak discharge after scaling and shifting the flow using the 'half height levées' and 'added height levées' scenarios **168**

5.50 Change in peak discharge with channel Manning's *n* for each of the scaled and shifted flows using the 'with levées' scenario **169**

5.51 Change in peak discharge with floodplain Manning's *n* for each of the scaled and shifted flows using the 'with levées' scenario **169**

5.52 Change in peak timing delay with Manning's *n* for each of the scaled and shifted flows using the 'with levées' scenario **170**

5.53 Change in peak discharge with channel Manning's *n* for each of the scaled and shifted flows using the 'without levées' scenario **171**

5.54 Change in peak discharge with floodplain Manning's *n* for each of the scaled and shifted flows using the 'without levées' scenario **172**

5.55 Change in peak timing delay with Manning's *n* for each of the scaled and shifted flows using the 'without levées' scenario **173**

5.56 Comparing the change in peak discharge for the 'with levées' and 'without levées' scenarios after varying both Manning's *n* for the channel and **173**

floodplain and scaling and shifting the flow with original Manning's *n* values

5.57 Change in peak discharge with channel Manning's *n* for each of the scaled and shifted flows using the 'half height levées' scenario **175**

5.58 Change in peak discharge with floodplain Manning's *n* for each of the scaled and shifted flows using the 'half height levées' scenario **175**

5.59 Change in peak discharge with channel Manning's *n* for each of the scaled and shifted flows using the 'added height levées' scenario **177**

5.60 Change in peak discharge with floodplain Manning's *n* for each of the scaled and shifted flows using the 'added height levées' scenario **177**

5.61 -5.63 Comparing the peak discharge for each variation using the 'with levées' and 'without levées' scenarios **180**

5.64 Comparisons of varying (1) Manning's *n*; (2) scaled flow; (3) shifted flow; and (4) scaled and shifted flow for each of the levée scenarios **185**

5.65 Comparisons of varying Manning's *n* and the scaling of the scaled and shifted flows for each of the levée scenarios **186**

Chapter Six

6.1 Effect of raising and reducing levée heights in the system on the flood hydrograph **193**

Chapter Seven

-

List of Tables

Table Number	Table Title	Page Number
	Chapter One	
	-	
	Chapter Two	
2.1	Possible interventions to modify the frequency and duration of washland flooding and the downstream hydrograph	**18**
2.2	Manning's *n* values for channel and floodplain used in the literature	**20**
	Chapter Three	
3.1	Descriptors used in the allocation of Manning's *n* values for each cross-section (source: Chow, 1959; HEC-RAS user manual, 2008)	**39**
3.2	Name and location of each of the reaches within the river system	**44**
3.3	Residual inflows to the model	**45**
	Chapter Four	
4.1	Stages in performing a sensitivity analysis (Based on Fisher (1935) and Saltelli *et al.* (2000))	**57**
4.2	Summary of parameters assessed in the sensitivity analysis	**61**
4.3	Difference in mean peak timing delay between the simulated and observed hydrographs after varying Manning's *n* globally, for the channel and for the floodplain	**66**
4.4	Sensitivity of discharge to variations in roughness, inflow and weir coefficients	**67**
4.5	Peak timing delay between the simulated and observed hydrographs after varying the weir coefficient by 20%	**79**
4.6	Peak timing delay between the simulated and observed hydrographs after increasing and decreasing inflow by 20% and varying Manning's *n* globally	**86**
4.7	(a) RMSE of the simulated hydrograph compared to the observed hydrograph with changes in global Manning's *n*; (b) RMSE was also calculated for	**90**

separate sections of the simulated and observed hydrographs

4.8 Nash-Sutcliffe indicies, percentage error in the peak, Root Mean Square Error and Mean Absolute Error values comparing the simulated hydrograph with the observed for varying channel Manning's *n* **93**

4.9 Nash-Sutcliffe indicies, percentage error in the peak, Root Mean Square Error and Mean Absolute Error values comparing the simulated hydrograph with the observed for varying floodplain Manning's *n* **94**

4.10 Nash-Sutcliffe values for varying Manning's *n* for the floodplain on the left and right sides of the river system **94**

4.11 Nash-Sutcliffe values for Manning's *n* variations in global, channel and floodplain *n* along the three tributaries **96**

4.12 Nash-Sutcliffe calculated for each of the Manning's *n* values modelled with inflow increased and decreased by 20% **97**

4.13 Summary of the calibration runs **102**

4.14 Objective functions for calibration runs **104**

Chapter Five

5.1 Statistics for peak discharge and peak timing delay for the 'with levées' and 'without levées' scenarios for different cross-sections in the model **120**

5.2 Peak discharge and peak timing results for simulations using the 'with levées' scenario **125**

5.3 Peak discharge and peak timing results for simulations using the 'with levées' scenario for the River Ouse **131**

5.4 Peak discharge and peak timing results for simulations using the 'with levées' scenario for the River Swale **135**

5.5 Peak discharge and peak timing results for simulations using the 'with levées' scenario for the River Nidd **139**

5.6 Comparison of the results for the three tributaries using the 'with levées' scenario **140**

5.7 Statistics for each of the four levée scenarios showing change in peak discharge after varying both Manning's *n* for the channel and floodplain **144**

5.8 Statistics for each simulation varying both Manning's *n* for the channel and floodplain using the 'half height levées' scenario **145**

5.9 Statistics for each simulation varying both Manning's *n* for the channel and floodplain using the 'added height levées' scenario **145**

5.10 Statistics for each of the four levée scenarios showing change in peak timing delay after varying both Manning's *n* for the channel and floodplain **147**

5.11 Statistics for each variation to the input hydrograph: (1) scaled; (2) shifted; (3) scaled and shifted; using the 'with levées' scenario **155**

5.12 Statistics for each variation to the input hydrograph: (1) scaled; (2) shifted; (3) scaled and shifted under each levée scenario **162**

5.13 Statistics for each simulation varying both Manning's *n* for the channel and floodplain and flow (scaled and shifted) using the 'with levées' scenario **170**

5.14 Statistics for each simulation varying both Manning's *n* for the channel and floodplain and flow (scaled and shifted) using the 'without levées' scenario **172**

5.15 Statistics for each simulation varying both Manning's *n* for the channel and floodplain and flow (scaled and shifted) using the 'with levées' and 'without levées' scenarios **174**

5.16 Statistics for each simulation varying both Manning's *n* for the channel and floodplain and grip flow (scaled and shifted) using the 'half height levées' scenario **176**

5.17 Statistics for each simulation varying both Manning's *n* for the channel and floodplain and flow (scaled and shifted) using the 'added height levées' Scenario **178**

Chapter Six

6.1 Peak reductions after varying Manning's *n*, levée height and flow in relation to each of the research questions **191**

6.2 Peak timing delay after varying Manning's *n*, levée height and flow in relation to each of the research questions **191**

Chapter Seven

-

Chapter One

Introduction

1.1 Introduction

The link between rural land use management and flood risk is becoming increasingly pertinent to both government agencies and stakeholders, but also to the general public (Parrott *et al.*, 2009). There are a number of linkages being explored; one area of particular focus is the relationship between moorland grips (shallow (< 0.80 m) and narrow (typically 0.5 m) surface drains in upland environments) and local flood risk in the UK (Environment Agency, 2000; Lane *et al.*, 2003a; Beven *et al.*, 2004; Robinson, 2006; Lane *et al.*, 2007). The extent to which the impacts of upland land management scale up to impact downstream flood risk remains inconclusive and is surrounded by debate (Lane, 2003a, 2008). The critical issue is whether or not observed upstream responses propagate downstream. This propagation will be related to attenuation processes, including the role of floodplains. Floodplain flows have typically different hydraulic properties to channel flows (lower depth, greater width) and commonly contribute to attenuation. But floodplain flows are, themselves, also managed. Thus, there may be a linkage between possible land management signals (the impact of grip blocking specifically) and floodplain management activities in determining downstream flood hazard.

1.2 Aim and Research Questions

The overall aim of the study is to determine the extent to which floodplains impact upon the propagation of upstream land management flood signals. In order to meet this aim, the following research questions will be addressed:

1. In what way can the floodplain be used to reduce flood risk downstream?
2. To what extent are land management signals impacted upon by flow attenuation?
3. Do flood levées aid the transmission of the upstream hydrograph?

1.3 Explanation of Research Questions

RQ1 In what way can the floodplain be used to reduce flood risk downstream?

By storing and gradually releasing water that would normally contribute to flood volumes, floodplains are believed to aid flood risk reduction (Whiting and Pomeranets, 1997). Throughout this study, flood risk is defined as:

Risk = probability x exposure x consequence

Lowering peak discharge is the aim of this study because this will reduce the probability of the hazard occurring and reduce exposure to it. Storage on a floodplain has been shown to attenuate flood flows, reducing the peak flow downstream (Larson and Plasencia, 2001). The precursor to the wider project is determining whether this is the case as the reduction in peak flow may depend on river-floodplain configuration. The introduction of levées into a river system may decrease the attenuation provided by the floodplains if the channel-floodplain connection is removed.

RQ2 To what extent are land management signals impacted upon by flow attenuation?

The impact of land management on flooding is surrounded by uncertainty due to the effects of attenuation. The balance between the effects of attenuation (naturally causing peak flow to fall with distance downstream) and flow augmentation (as tributaries deliver more water to a system) is key to determining the size of flow. Addressing this research question will determine whether or not the impact of grip blocking is translated downstream and remains noticeable. There may be evidence that grip blocking impacts upon downstream flood risk but the question that arises here is how far downstream this impact extends given the intervening attenuation effects.

RQ3 Do flood levées aid the transmission of the upstream hydrograph?

With the presence of levées in a river system (a section of raised river bank constructed to restrain floodwater (Morris *et al.*, 2007)), peak flows are decoupled from the floodplains as the channel-floodplain connection is removed. As the flow is constricted within the channel, conveyance increases and attenuation decreases as the water is no longer free to flow on the floodplains. Consequently, discharge increases. The key question here is to determine whether the presence of levées means that land management signals are more or less strongly propagated downstream.

1.4 Justification of research focus

The government publication of *Making Space for Water* in July 2004 came during a move in flood management towards a holistic 'whole catchment' approach following significant flood events around the year 2000 (DEFRA, 2005). This integrated strategy aimed to involve stakeholders at all levels, with focus on making greater use of rural land solutions

for flood risk. It recognised that hard engineering solutions are not always justified and the benefits must be measured holistically, with environmental, social and economic considerations (DEFRA, 2005). As a result, the Environment Agency (EA) is increasingly using storage areas to mitigate floods, particularly with wetland creation for which they have minimum targets (DEFRA, 2005). However, those in favour of flood control, such as through levées, have a strong voice in flood management as they are likely to be those who will be harmed by flooding or owners of land who benefit from defences (Cuny, 1991). If land is to be flooded, it is necessary to use poor quality land, or provide compensation to farmers (Morris *et al.*, 2003; Coultish, 2008).

It has been recognised that using natural floodplains for flood control may provide more societal benefits than using hard engineering: levées increase water levels because width is restricted, and so floodplain storage is eliminated (Leopold, 1994). Driving this change in ideology is the perceived increased frequency of flooding in Europe in recent years and the associated economic costs (Olsen *et al.*, 2000; Blackwell and Maltby, 2005). Past agriculture and industrial development has altered the function of floodplains such that "as little as 2 percent of European rivers and associated floodplains can be considered as 'natural'" (Blackwell and Maltby, 2005: 9). Encroachment of floodplains allows flood waves to be routed more rapidly downstream (Larson and Plasencia, 2001). 85% of lowland rivers in England and Wales have been modified with channels becoming disconnected from the floodplain (DEFRA, 2002). Acreman *et al.* (2003) crucially showed that the presence of levées increased peak flow downstream by between 50-150% for the River Cherwell. Recent studies have shown that storage areas can effectively reduce peak discharges: McCartney and Naden (1995) modelled a reduction of 24% whilst Woltenmade and Potter (1994) found that peak discharge can be reduced by as much as 49%. Increasing floodplain roughness is also effective, reducing peak discharge by 27% in a study by Diehl (1990). The variance in peak flow reduction shown between studies is not unexpected because it does depend on storage zone configuration.

Recent literature has also shown that gripping of upland peatlands alters the hydrological response of a catchment. For example, yield was increased by 15% in a gripped catchment in upper Teesdale between 1950s and 2000s (Holden *et al.*, 2006), giving evidence that gripping has a direct influence on flow. Grip blocking (restricting the movement of water within upland drains) in the last 15 years has been found to reduce

travel times, thus reducing flood risk (Lane *et al.*, 2003b). There have been few catchment-scale investigations of the effects of gripping on downstream flow, nor exploration of linkages between propagation of grip signals and modification of floodplains.

1.5 Case study – flooding in the City of York

This research aims to use the City of York as a case study to determine the link between rural land management in the upper catchments and flood routing. York is a particularly pertinent case as it has experienced a dramatic rise in flood frequency and magnitude since the 1940s, which has been related to land use changes in the Yorkshire Dales (Lane, 2003a, 2008). Furthermore, it is expected that the extensive levée system upstream of York has a control on the conveyance of this land management signal, particularly resulting from grips, as they cut off natural storage areas. Upstream impacts should be lost with distance downstream due to attenuation, but as levées decrease attenuation, it is possible that they propagate upstream changes downstream. Hence, the main question addressed within this study is whether or not the presence of levées upstream of York makes it easier to transmit change in the upstream hydrograph downstream. If this relationship is demonstrated, and the associated results accepted by relevant agricultural communities, this research could suggest that the flood management strategy for York be radically modified to use floodplains to reduce flood risk. The Environment Agency have used 1-D hydraulic models of the River Ouse in previous studies to identify areas benefiting from defence and potential areas for further storage of floodwater. This investigation was commissioned following the Environment Agency's requirement for a study to investigate the effect of the levées within the Ouse catchment on the flood wave travelling towards York.

1.6 Study location

1.6.1 Catchment characteristics

Hydrology

The Ouse catchment, situated within the Yorkshire and Humber region, is the focus of this study. Figure 1.1 shows the catchment's location in the UK. Upstream of York, the Ouse catchment is a large, predominantly rural catchment (3315 km^2) that drains the Yorkshire Dales and Vale of York. The hydrology of the Ouse catchment is largely influenced by

three key subcatchments upstream: the Ure, Swale and Nidd (Lane, 2003a). The River Ure rises in the Yorkshire Dales within a catchment area of 915 km^2. The upper catchment receives an average annual rainfall of >2000 mm (Environment Agency, 2010a). The River Swale has a flashy response to rainfall, draining an area of 1363 km^2 of the northern Yorkshire Dales (Environment Agency, 2010a). The River Nidd runs from moorland headwaters through a rural catchment with an area of 484 km^2 (Environment Agency, 2010a).

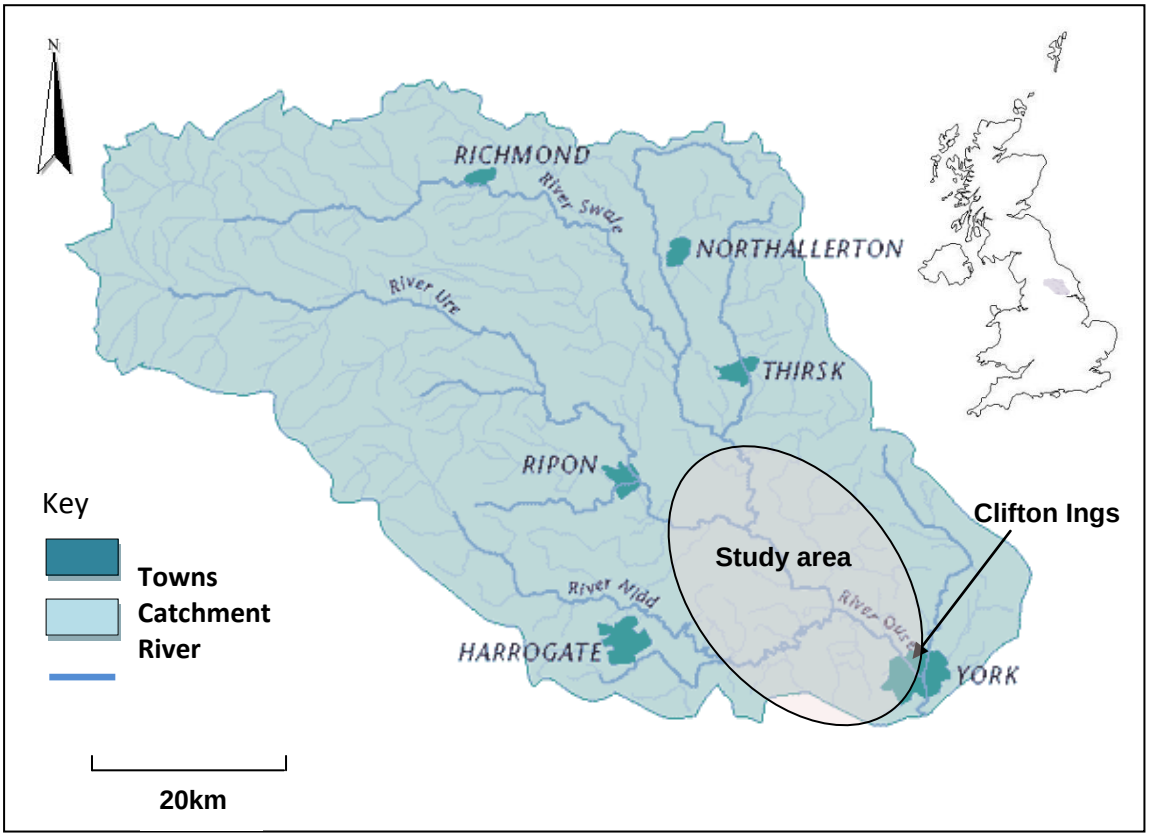

Figure 1.1 Location of the Ouse catchment in a national context. The study area is also highlighted.

The Ouse catchment has a long history of flooding. A detailed flood record exists for York, recording numerous historical floods within the catchment. More recently, the most notable floods are those of 1947 and 1982 which, due to the severe damage caused, prompted the building of the most recent current flood defences (Environment Agency, 2010b). The highest recorded flood occurred in 2000 when over 550 properties flooded downstream of York between Linton-on-Ouse and Selby (Environment Agency, 2010b). Flooding from the River Ouse is the result of prolonged rain in the upper Ouse catchment and takes a long time to develop. The tributaries of the Ouse have a flashier regime,

responding to rainfall more quickly. The washlands upstream of York, such as the Clifton Ings, are important in reducing risk (Environment Agency, 2010b).

Geomorphology and geology

The headwaters of the main river systems are characterised by steep river gradients which flow through rural areas and some small settlements. Both the River Nidd and the River Ouse begin to meander as the gradient reduces at the lower part of the catchment and the river becomes less confined by valley topography. The area downstream of Ripon on the River Ouse is generally low lying with space for the floodplains to widen. Large areas of the Ouse catchment are underlain by Carboniferous limestone, but there are exposures of Millstone Grit in the west, Permian Magnesian limestone in the centre and Triassic sandstone in the east (Environment Agency, 2010a). The Carboniferous limestone geology creates the steep valleys in the headwaters of the catchment, whilst further downstream the Millstone Grit forms gentle hills and in the downstream reaches the Magnesian limestone forms a plain (Environment Agency, 2010a).

Land use and history

The land use of the Ouse catchment is primarily arable, with large areas of moorland within the Yorkshire Dales. There are a number of towns within the catchment, such as Ripon and Boroughbridge along the River Ure, Richmond on the River Swale and the large settlement of York on the River Ouse. Since the 1940s, the land use of the upper catchments has changed significantly with the addition of grips, shallow (< 0.80 m) and narrow (typically 0.5 m) surface drains. Coinciding with this change was an increase in stocking densities, notably of sheep, within upland agricultural communities. In addition to the changes in the upper catchments, the floodplains of the River Ouse have been modified. Agricultural land was protected by the introduction of levées along both banks of the river and was also enhanced via widespread underdrainage. It is estimated that approximately 78 km of levées line the River Ouse, often located on both banks of the river (Environment Agency, 2004).

1.6.2 Model extent

The study reach (Figure 1.2) comprises the River Ure and River Ouse from Westwick Weir down to Skelton Railway Bridge (a distance of 32.7 km) and the following main tributaries:

- River Swale from Crakehill to its confluence with the Ure, approximately 4km downstream of Boroughbridge (12.2 km)
- River Nidd from the Old Corn Mill at Hunsingore to the confluence with the River Ouse, approximately 15 km downstream of the confluence with the River Swale (25.7 km)

These reaches were chosen as they were included in the 1-D model provided by the Environment Agency for this study. The River Ure is renamed the River Ouse approximately 2 km downstream of Aldwark Toll Bridge. The total length of the model is approximately 71 km.

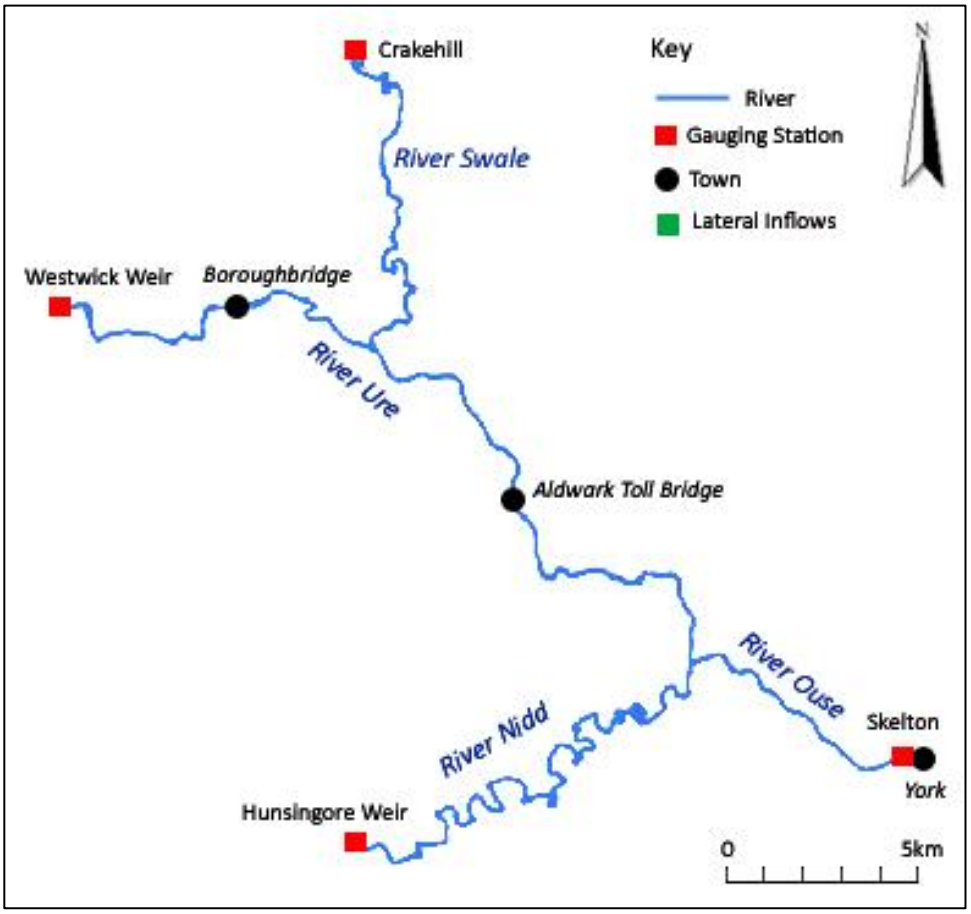

Figure 1.2 Extent of the model and location of flow gauging stations in the Ouse catchment.

Gauging stations

Discharge of the Rivers Ure, Swale, Nidd and Ouse is estimated for four locations using EA gauging stations (Figure 1.2):

- River Ure: Westwick Weir - records dating from 1955 to present
- River Swale: Crakehill - records dating from 1980 to present
- River Nidd: Hunsingore Weir - records dating from 1934 to present
- River Ouse: Skelton - records dating from 1886 to present

1.7 Thesis structure

This thesis is structured around the investigation of floodplains and the propagation of land management signals in the catchment. Chapter Two introduces the literature relevant to each of the research questions covering temporary storage of flood waters, the impact of grip blocking and levées. Chapter Three reviews different types of hydraulic model available for flood propagation studies and provides a justification for the chosen modelling approach. Chapter Three also explores the model building procedure and how the chosen model represents a river system. Chapter Four presents the sensitivity analysis and calibration of the model. Chapter Five presents the results of the model simulations within the framework of the research questions. The results are discussed in Chapter Six with reference to the findings of previous relevant studies and the implications for flood management are reviewed. Core findings, recommendations and areas for future research are presented in Chapter Seven.

Chapter Two

Literature Review

2.1 Introduction

This chapter aims to assess the role of floodplains in flood management through the review of published literature. Previous work and findings will be discussed and structured around each of the research questions outlined in Chapter One. Section 2.2 focuses on the use of floodplains for reducing flood risk in terms of storage. Section 2.3 addresses the link between land management and flow attenuation, whilst Section 2.4 assesses the impact of levées on the transmission on the upstream hydrograph. Section 2.5 will focus specifically on the literature addressing the case study of York. Section 2.6 outlines the findings of the chapter and the direction the project will take as a result of the findings of this chapter.

2.2 Research Question 1 – In what way can the floodplain be used to reduce flood risk downstream?

2.2.1 Floodplains for flood alleviation

Current flood reduction schemes aim to use natural floodplains (typically used as agricultural land) as an effective method to decrease the impact and magnitude of flooding (McCartney and Naden, 1995; Svensson *et al.*, 2006; Lane, 2008). The Environment Agency has seen promise in using strategic floodplain storage to reduce flood risk (Morris *et al.*, 2004). This idea is based upon the hypothesis that floodplains, by storing and gradually releasing water that would normally contribute to flood volumes, help to reduce flood risk (Whiting and Pomeranets, 1997). The adoption of temporary storage areas should increase the incidence of flooding in the storage areas whilst alleviating high levels of flood risk downstream (Morris *et al.*, 2003), provided they are designed properly. Restoring the connection between channel and floodplain allows the reach to temporarily store water thus dissipating the passing flood wave (Sholtes, 2009).

Storage in a floodplain has been shown to attenuate flood flows between large tributaries (Larson and Plasencia, 2001). Attenuation is a natural process associated with the interaction between a river and its floodplain, formally defined as loss of the magnitude of flux (Lane and Thorne, 2007). Flows on a floodplain are shallower, and when combined with turbulence-related momentum at the channel-floodplain interface, this should result in enhanced attenuation as compared with a channel-confined flow. For instance, Archer (1989) showed that above bankfull, floodplain flows reduce the rate of downstream flow.

However, he also showed that as flow peak and volume continue to increase, attenuation effects diminish (Archer, 1989).

2.2.2 Hydrograph timing

The temporary storage of water on the floodplain changes the flood hydrograph by firstly, forming a 'shoulder' on the rising limb as water enters the store, and secondly by reducing the flood peak and increasing the duration of the flood event due to the attenuation of the flood wave (Figure 2.1) (Leopold, 1994; McCartney and Naden, 1995; Whiting and Pomeranets, 1997; Hornberger *et al.*, 1998; Pepper *et al.*, 1998; Morris *et al.*, 2004; Blackwell and Maltby, 2005). Reducing peak discharge decreases the likelihood of a flood occurring (Blackwell and Maltby, 2005). These effects are particularly evident in locations with a large capacity for water storage (Svensson *et al.*, 2006; Acreman *et al.*, 2007) such as washlands. Flood control reservoirs serve the same role in alleviating floods (Chuntian *et al.*, 2001). Montaldo *et al.* (2004) showed that reservoirs can be used to mitigate major floods in the Toce River basin, Italy, through flood peak attenuation. The study showed a reduction in the beneficial effects of the reservoirs as the drainage basin area increased. However, if initial storage conditions are managed at lower levels than modelled, significant flood attenuation could be achieved (Montaldo *et al.*, 2004).

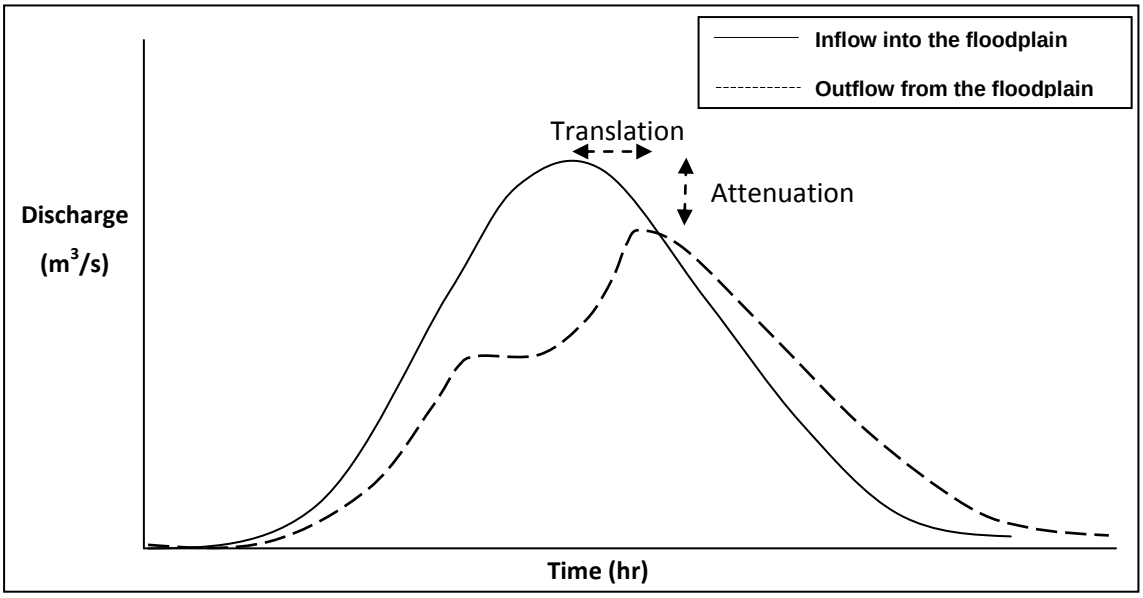

Figure 2.1 Flood hydrograph is attenuated and translated in time to reduce downstream flood peaks as a result of flood water storage on the floodplain (Morris *et al.*, 2004). The degree of attenuation is determined by the difference between the rate of inflow and outflow.

2.2.3 Design and location of storage areas

The design and location of storage areas within the catchment is crucial to ensure that all sites work hydraulically, contributing to flood management (English Nature *et al.*, 2002; Morris *et al.*, 2003; Morris *et al.*, 2005). The storage areas must be designed to 'engineer' the shape and timing of the flood hydrograph (English Nature *et al.*, 2002). They need to be able to capture the flood peak at the right time with little management; too early and the storage areas reach capacity too soon and have little influence on peak discharge, but too late and the peak is allowed to pass and initiate flooding (Morris *et al.*, 2005; Hall, 2008) (Figure 2.2). Furthermore, if the storage area drains too slowly after a flood, the area might not be available for a subsequent event (English Nature *et al.*, 2002). Wollf and Burges (1994) also found that the reduction in peak flow depended on the effective storage of the reach. Flood events can require different amounts of storage volume depending on the shape of the hydrograph (Yue *et al.*, 2002). For example, a hydrograph with a negative skew (later peak) requires a larger volume than a positively skewed hydrograph (earlier peak) to provide the same degree of protection of both floods.

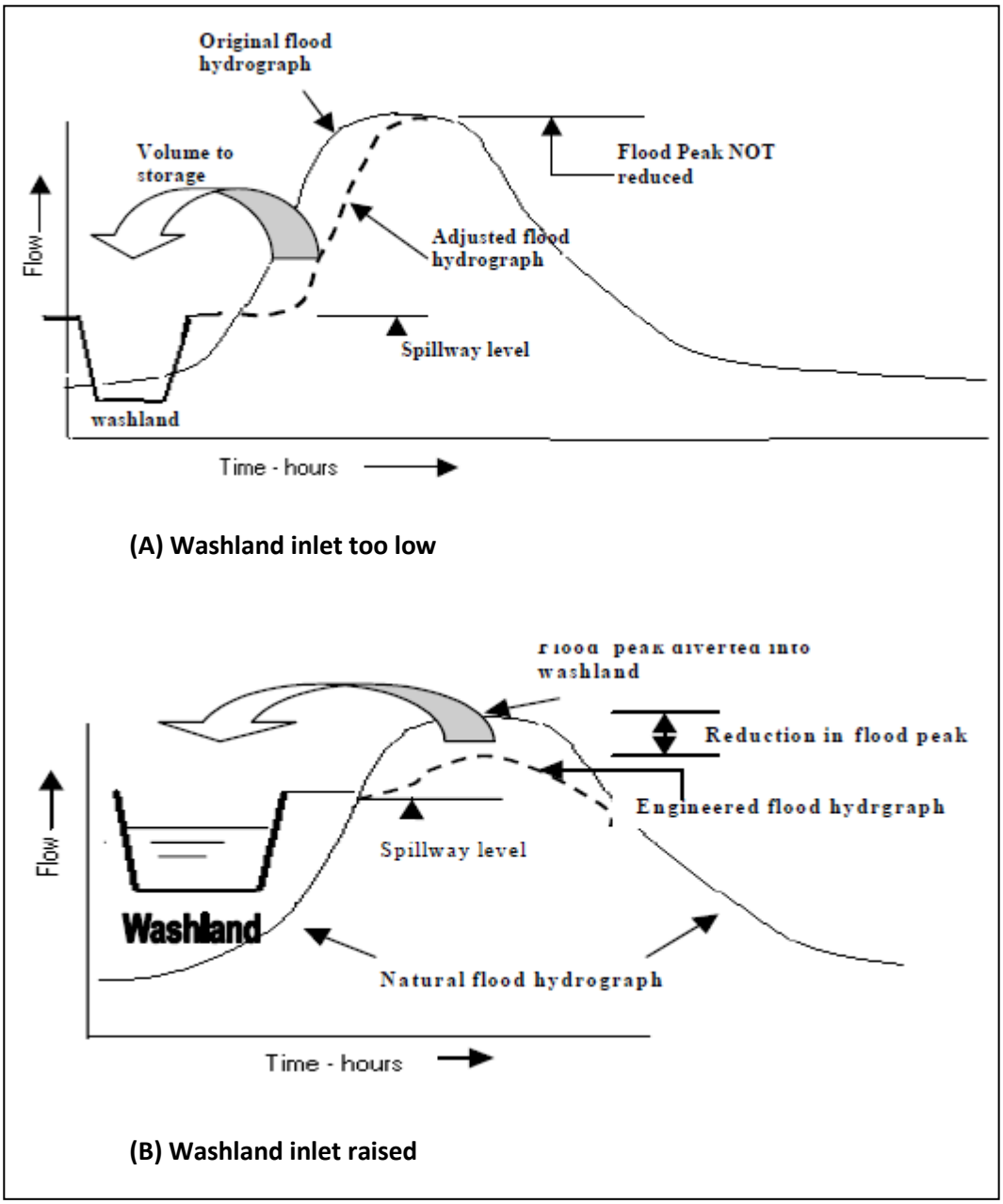

Figure 2.2 Effect of washland storage on flood hydrographs. (A) flood peak not reduced; (B) flood peak effectively reduced (Source: English Nature *et al.*, 2002).

Conveyance, or the capacity to convey water downstream, is an important process which must be addressed when discussing the issue of runoff generation and flood risk. For attenuation to be increased via the floodplain, conveyance must decrease. By changing the morphology and roughness of the channel and floodplain, conveyance can be managed (Lane and Thorne, 2007). The reduction of river channel conveyance leads to a greater transfer to the floodplain (Lane *et al.*, 2007). As conveyance is slower on the floodplain, this leads to attenuation of the flood peak.

2.2.4 Flood wave propagation

The hydraulic and geometric properties of both the channel and floodplain have a bearing on flood frequency and hydrograph shape as a flood wave propagates downstream. Wollf and Burges (1994) used a 1-D flood routing model, DAMBRK, to simulate the flood from a dam failure. This model used the 1-D Saint Venant equations, a mathematical representation of coupled channel-floodplain flow, to take into account differences in parameters between the channel and floodplain. Larger inundation levels were found for a channel with lower capacity as more water flows out of banks across the rougher surface (Wollf and Burges, 1994). Also, a wider floodplain caused higher attenuation of the flood peak due to the larger storage area available. The lateral inflow from hillslopes influences the storage of water. Thus, it also has a bearing on flood wave attenuation (Burt *et al.*, 2002). Floodplain storage provides a buffer zone preventing hillslope water flowing rapidly into the river system (Burt *et al.*, 2002).

Hydraulic models can be used to estimate the impact of washlands on the shape of the downstream hydrograph (Morris *et al.*, 2004) and to predict the propagation of a flood wave through the river system (Mujumdar, 2001). Woltenmade and Potter (1994) recognised that the storage of water can effectively reduce peak discharge but not in all catchments due to geomorphic factors that affect the storage and conveyance of flood water. They found that peak discharges varied by as much as 49% from the original peak discharge.

McCartney and Naden (1995) used a simple routing model to investigate the effect of floodplain storage on floodplain flows. The study demonstrated that the availability of natural floodplain can significantly reduce the magnitude of major floods: the mean annual flood of the River Severn at Montford was reduced by 24%. The importance of wetland storage can also be demonstrated for much smaller river systems. Following a beaver dam failure in 1994 in Alberta the estimated peak of the flood wave was 15 m^3/s, over 3.5 times the maximum discharge recorded in the creek for 23 years (Hillman, 1997). The flood wave peak was significantly reduced to 6% of the estimated upstream peak due to its passage over 90 hectares of wetland (Hillman, 1997).

Anderson *et al.* (2006) used a 1-D model to explore the impact of vegetation on the flood hydrograph. They found that channel roughness is a significant determinant of flood

hydrograph skew and the speed of propagation of flood waves. Smaller floods were found to be more sensitive to channel roughness than larger floods (Anderson *et al.*, 2006). Wave celerity was reduced with higher roughness values, which would increase catchment response times and thus decrease peak discharges.

2.2.5 Woodland planting on the floodplain

Attenuation caused by the floodplain can be exacerbated by planting floodplain woodland (English Nature *et al.*, 2002; Nisbet and Broadmeadow, 2003; Nisbet, 2004; Thomas and Nisbet, 2007; Nisbet and Thomas, 2008). Floodplain planting increases hydraulic roughness which in turn reduces velocity. In its simplest sense, discharge can be described as a function of area and velocity:

$$Q = UA$$

where: Q is discharge (m^3/s) *Equation 2.1*
U is the average velocity in that section (m/s)
A is the cross-sectional area (m^2)

Equation 2.1 is based on the principle of mass conservation (Beven, 2004). As velocity is reduced, area must increase in order for discharge to remain constant (Albertson *et al.*, 1966). It must be recognised that the attenuation effects created by roughness and by storage areas are generated in different ways; a flood wave must travel along a long reach of roughened river in order to reduce the flood peak as much as a moderate storage area can achieve in a short distance (Hornberger *et al.*, 1998).

Within the last 15 years research and interest in floodplain woodlands has expanded with focus on their function in floodplain control (Nisbet, 2004). Nisbet and Broadmeadow (2003) outlined the main ways that woodland can help reduce flooding: (1) delaying floodplain flows; (2) delaying channel flows; (3) delaying soil runoff; (4) increasing water use. A scoping report was required by the Forest Research to assess the effects of restoring floodplain woodland, focusing on flooding in the River Parrett, southwest England (Nisbet, 2004). A 2.2 km reach with the potential to be completely forested was modelled using HEC-RAS and River2D. Initial findings showed that floodplain woodland provides considerable scope for reducing downstream flooding, particularly with use of an area of woodland greater than 133 ha. The scale of woodland is important for producing an effective strategy, but land ownership reduces the availability of land thus

the greatest potential for using woodland is at the middle and upper reaches (Nisbet *et al.*, 2008). Combined with other defences, this strategy could prove valuable for downstream protection (Nisbet, 2004).

Thomas and Nisbet (2007) used hydraulic models to simulate the role of floodplain woodland in flood reduction (Figure 2.3). They demonstrated the potential for flood storage to increase by 15-71% and for the flood peak to be delayed by 30 to 140 minutes compared to without the inclusion of floodplain woodland (Thomas and Nisbet, 2007). This strategy has the potential to mitigate against flood risk resulting from climate change (Thomas and Nisbet, 2007). Hewlett and Helvey (1970) analysed storm hydrographs following felling of mature forest in the Appalachians. Storm flow volume was significantly increased by 11% and the peak discharge was increased. Timing of the peak was not affected by felling in the case study. Similarly, Helmio (2002) used a 1-D model to explore the effects of vegetated floodplains on flood wave conveyance. When vegetation density was decreased, the total conveyance (from the channel and floodplains) increased. Further decreases in vegetation density increased the contributing width of the floodplain, thus the main channel conveyance decreased causing a decrease in total conveyance. Water levels during individual simulations ranged from millimetres to centimetres as a result of vegetation loss.

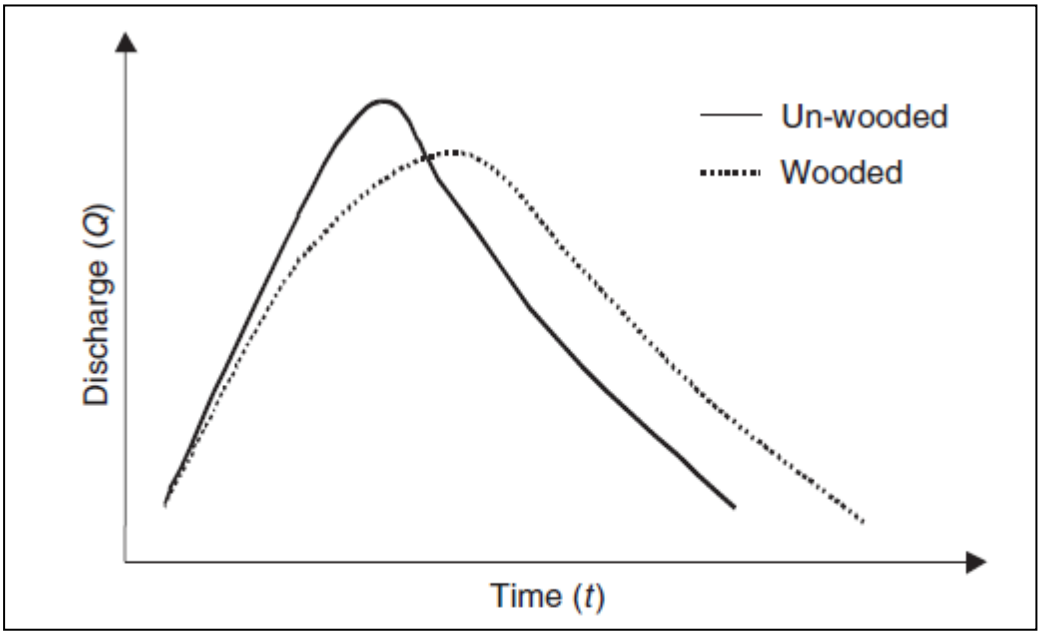

Figure 2.3 Hydrograph showing the expected effect of floodplain woodland on flood flows (Thomas and Nisbet, 2007). Discharge is reduced with planting on the floodplain, and the flood peak translated in time.

It must be recognised that this delay in the flood peak could be beneficial or disastrous at the catchment scale according to whether or not it synchronises (disastrous) or desynchronises (beneficial) tributary flood peaks. Delivery of flow to the network is also important here. By reducing the speed at which overland flow is conveyed to the river channel using rural land management strategies, flood risk can be reduced (Lane *et al.*, 2007). Table 2.1 outlines a selection of interventions available to enhance floodplain flows in order to modify the propagation of the flood wave downstream.

Action	**Hydraulic impact**	**Washland impact**	**In-channel impact**
Set back levées	Increased on-line storage	Increased area	Reduced peak stage/discharge
Removal of levées	Increased on-line storage	Increased area	Reduced peak stage/discharge
Woodland planting	Reduced rate of inflow and outflow	Change in duration of flooding	Increased floodplain roughness
Increased siphoning into washland	Variable	Increased frequency and duration of inundation	Reduced in-channel discharge (up to capacity of washland)
Decreased channel maintenance leading to increased river and bank vegetation	Change in stage-discharge relationship	Increased frequency of inundation	Increased stage at all discharges, depending on the extent of vegetation

Table 2.1 Possible interventions to modify the frequency and duration of washland flooding and the downstream hydrograph (Adapted from: Morris *et al.*, 2005). On-line storage refers to storage provided by out-of-bank flow where the floodplain is not separated from the channel.

2.2.6 Manning's *n*

As it is clear that there is a strong relationship between conveyance and catchment storage (Lane *et al.*, 2007), it is hoped that by increasing hydraulic roughness to reduce conveyance, an increase in flood inundation will be seen on the floodplains. Manning's *n* is a roughness coefficient and the standard approach to assigning a hydraulic resistance value to a river channel (Lane and Thorne, 2007). It is included in the energy loss term in all 1-D models as Manning's equation solves the relation between water level, velocity and river bed characteristics (Whatmore and Landstrom, 2009). Typically, it is determined

through visual assessments of the character of a channel or floodplain (Whatmore and Landstrom, 2009). It must be recognised that the value of Manning's *n* depends on multiple factors, particularly vegetation, surface roughness, channel irregularity and obstruction (Chow, 1959). In a model experiment, a higher value of *n* increases the water depth in the channel and focuses more water onto the floodplain, allowing floodplain roughness to exert a greater influence on peak discharge and travel times (Hunter *et al.*, 2006) (Figure 2.3).

Woltenmade and Potter (1994) varied hydraulic roughness to see the effect on peak discharge. Minor changes to floodplain roughness had a large effect on discharge, particularly on high magnitude floods. Reducing floodplain roughness from between 0.039 and 0.046 to between 0.03 and 0.036 increased the flood peak by 1-18% whilst a very rough floodplain (0.057-0.064) decreased the flood peak by 1-21% (Woltenmade and Potter, 1994). Diehl (1990) also showed that increasing floodplain roughness from 0.053 to 0.10 can decrease the peak discharge of moderate floods by up to 27%. Sholtes (2009) used unit hydrographs to assess how attenuation varied with increasing flood magnitudes. Similar to Woltenmade and Potter (1994) he demonstrated that higher magnitude floods were primarily influenced by channel and floodplain roughness. The hydraulics of the flood response of the Charlotte area of North Carolina were explored by Turner-Gillespie *et al.* (2003) using a coupled model. Peak discharge increased by 1% with a decrease in floodplain roughness from 0.055 to 0.047 whilst the decrease in peak discharge was approximately 3% for an increase in floodplain roughness from 0.053 to 0.070. Table 2.2 presents values of Manning's *n* used in previous studies that were used to inform the values used for the sensitivity analysis in Chapter Four.

Source	Channel *n*	Floodplain *n*
Akanbi and Singh (1997)	0.02	0.03-0.1, 1.0
Anderson *et al.* (2006)	-	0.043-0.15
Carson (2006)	0.02-0.2	-
Fathi-Magham and Kouwen (1997)	-	0.089
Ghavasieh *et al.* (2006)	0.033, 0.067	0.067, 0.2
Hunter *et al.* (2006)	0.01-0.05	0.01-0.1
Kalyanapu *et al*. (2009)	-	0.012-0.4
Nisbet (2004)	-	0.035-0.15
Nisbet and Thomas (2008)	0.03-0.1	0.05-0.3
Pasche and Rouve (1985)	0.01	0.01
Sholtes (2009)	0.035-0.045	0.05-0.15
Swiatek (2007)	0.05-0.09	0.1
Thomas and Nisbet (2007)	0.04	0.035-0.15
Turner-Gillespie *et al.* (2003)	0.03	0.047, 0.055, 0.070
Wollf and Burges (1994)	0.02, 0.06	0.035, 0.12
Woltenmade and Potter (1994)	0.023-0.049	0.03-0.015

Table 2.2 Manning's *n* values for channel and floodplain used in the literature.

2.3 Research Question 2 – To what extent are land management signals impacted upon by flow attenuation?

Previous research provides evidence that grips have a local impact upon flood risk as a result of their ability to connect runoff more readily to the drainage network (Holden, *et al.,* 2006; Lane *et al.*, 2007). An extensive grip network was introduced to the Yorkshire Dales in the 1940s as a result of a major land management change for the region (Robinson, 1989). It is believed that 15% of the Yorkshire Dales is gripped (Robinson, 2006), increasing to as much as 60% in areas of steep hill slopes (Robinson, 2006). In addition, the region was greatly affected by the grants implemented in the 1970s to encourage land improvement and drainage, combined with increased stocking densities (Posthumus and Morris, 2010). The extent to which these impacts scale up to impact downstream flood risk (e.g. for the City of York) remains inconclusive (Lane, 2003a, 2008; O'Donnell *et al.*, 2008). Research to date does not concur that local-scale changes in runoff can generate larger-scale catchment impacts downstream (DEFRA, 2005; O'Connell *et al.*, 2007; Ball, 2008). There have been few catchment-scale investigations of the effect of gripping on downstream flood risk (Lane, 2003a). However, small-scale land management changes offer the potential for attenuation and improving warning times

even though the overall flood risk benefits at the catchment-scale are difficult to determine (Parrott *et al.*, 2009). It is difficult to study the effects of land management on flood risk as the intervening processes have a major influence on the system, increasing its complexity (Beven *et al.*, 2004; Lane *et al.*, 2007). New multidisciplinary and multiscale approaches are needed in order to understand the link between land use changes and the consequences for downstream flood risk (DeFries and Eshleman, 2004; O'Connell *et al.*, 2007; O'Donnell *et al.*, 2008). Whilst the relationship between the rural land management practice of gripping and downstream flood risk within the Ouse catchment is closely related to my research and thus needs to be highlighted, it is being addressed in a separate project at Durham University. Therefore, this study focuses more on the ways in which possible land management signals are propagated in the downstream direction by the presence of levées.

2.3.1 Upland drainage

Early research by Conway and Miller (1960) showed that areas of extensive gully networks and artificial drainage created rapid runoff rates. The sensitivity of the peatland to heavy rainfall increased with larger peak flows which occurred earlier. In contrast, catchments that were not eroded had longer lag times as they could retain more water. These findings suggest that drainage increases flooding downstream. Robinson (1986) also found that upland drainage alters the volume and timing of flow. In storms the drains channelled the flow to the river network, creating higher peaks and shorter response times. In contrast, Holden *et al.* (2006) compared data from the 1950s to 2002/2004 for the same sites as Conway and Miller (1960) in upper Teesdale, finding a 15% annual increase in yield and lower peak flows, giving evidence that gripping has a direct influence on peak flows. The location of the drainage in the catchment is a key issue, particularly large drainage schemes in headwater regions, because if the peak is delayed so that it becomes synchronised with the main channel it can cause an overall increase in the flood peak (Holden *et al.*, 2004).

A different method for reducing the impact of land management on flooding was investigated by Jackson *et al.* (2008). The Pont Bren catchment has a history of intensive sheep farming with recent notable increases in runoff. They showed that strip planting of trees on the hillslopes could reduce the flood peak by 40% at field scale by reducing overland flow volumes.

Upland drainage has also been linked with decreases in flood peaks (Holden *et al.*, 2004). A study by Bullock and Acreman (2003) found no indication that upland peatlands aid the reduction of floods. This was because upland peatlands retain large quantities of water thus having little space for storing fresh rainfall. Therefore most water runs across the surface and rapidly enters the river network. It is important to understand the conditions under which increases and decreases in flood peaks occur as local impacts can have a large influence on the conveyance of water (Holden *et al.*, 2004). Furthermore, a study at Glenamoy, Ireland in the 1960s (Burke, 1975; Dooge and Keane, 1975) found that areas of drainage reduced the water table, increasing storage capacity to attenuate storm flows (Robinson, 2006). However, this study is now seen as anomalous because of how very closely spaced the drains were. Recent drainage studies have indicated that grips can both increase and decrease peak flows downstream in a catchment, thus the evidence remains unclear (Robinson, 2006).

2.3.2 Grip blocking practice

Recent research suggests that by blocking the grips, there is the potential to delay and attenuate floods through the creation of surface storage and water retention on the moorland (Environment Agency, 2000). A project in Upper Wharfedale blocked grips using straw bales and peat dams, finding that the East Camm grip showed a reduction in runoff volume of 24% after blocking (Environment Agency, 2000). This effect reduces with distance downstream as the proportion of storage created by the blocked grip to the total runoff in the catchment reduces. Lane *et al.* (2003a) used a quasi-distributed numerical model to assess the impact of flooding arising from grip blocking. The results showed that the effect of grips on overland flow generation depended on local topography, connection of saturated areas to the network by grips and rainfall characteristics. Lane *et al.* (2003b) used SCIMAP, a hydrological model which represents connectivity across a range of spatial scales, to assess the effects of grip blocking. The findings suggested that blocking grips reduces travel times to the catchment outlet, thus reducing flood risk as rainfall is delivered more slowly (Lane *et al.*, 2003b). Both Lane *et al.* (2003a) and Lane *et al.* (2003b) recognised that the focus for grip blocking should be on individual grips with the largest impact on flood generation and travel times. The practice of grip blocking has evolved within the last 15 years (Armstrong *et al.,* 2009) and continues within upland

environments with continual assessment of the benefits for flood reduction (e.g. EA project in Upper Wharfedale (Environment Agency, 2000)).

2.3.3 Flow attenuation

The uncertainty surrounding the impact of land management on flooding is also due to the effects of attenuation. During a flood event this process can become significant as water moves more slowly on the floodplain than in the main channel. Attenuation should naturally cause the peak flow of a river to fall with distance downstream. However, the effect of tributaries increases the flow downstream as more water is delivered to the river. Consequently the size of a flow at any one point will be a balance between the effects of attenuation and the effects of flow augmentation (Lane and Thorne, 2007). The volume of water in each tributary influences the flow characteristics of the river to which they join, thus any tributary which contributes more water as a result of land use practices in upstream catchments could have a negative effect on attenuation downstream. Similarly, a tributary with large areas of floodplain storage could contribute greatly to the reduction of downstream flood flow. Pattison *et al.* (2008) demonstrated that land use practice in one sub-catchment of the Eden catchment can cause a shift in the timing of the flow peak. The magnitude of downstream flood peaks was primarily controlled by the flow magnitude in the sub-catchments and the peak timing of the contributing catchments was also crucial. Thus, in order to understand the impacts of land management practices upon downstream flood risk, this study must consider:

1. the land management itself – does it increase the rate of runoff generation?;
2. how runoff from tributaries combines in time; and, crucially,
3. the effects of attenuation.

2.4 Research Question 3 – Do flood levées aid the transmission of the upstream hydrograph?

Once the effects of flood storage and upstream tributaries on downstream flood flows have been explored, this knowledge can be used to address research question 3. It is necessary to relate decisions over grip blocking to decisions over how to manage the flood banks as one may be related to the other. Grip blocking results in the attenuation of flows within hillslopes, reducing flows such that removing downstream levées and

reducing maintenance is feasible (Environment Agency, 2000). The sustainability of removing the flood banks may be more easily realised if by blocking grips there are fewer small floods. This project aims to understand this crucial link and if demonstrated, it may be possible to progress in the use of floodplains for flood risk management.

In relation to this problem, it is necessary to determine whether or not levées should be integrated into flood management schemes. Typically, flood banks have been raised to contain high flows (Pepper *et al.*, 1998) in order to protect developments. More recently it has been suggested that the removal of defences may more effectively mitigate floods. By reducing the levels of flood protection for agricultural land on the floodplain, this land provides additional floodplain storage to aid the reduction of the downstream flood peak (Morris and Wheater, 2007). The removal of minor levées is thought to increase the frequency and duration of flooding over the floodplain (Buijse *et al.*, 2002). The impact of the removal of levées along floodplains was investigated by Acreman *et al.* (2003) through the use of both hydraulic and hydrological modelling which simulated changes to flood hydrographs for the River Cherwell. Extreme scenarios of levées height (up to +1.5 m) were used to show the maximum range of possible outcomes. It showed evidence that levées increased peak flow downstream by between 50-150%, a significant increase. Peak water levels on the floodplain increased between 0.5 m to 1.6 m (Acreman *et al.*, 2003). Another project, funded by EU LIFE Nature, used hydrological modelling to determine the hydrological impacts of floodplain restoration for the River Cherwell (English Nature *et al.*, 2002; Wise Use of Floodplains, 2002). As for Acreman *et al.* (2003), the model showed that embanking the channel led to much higher peak flows and stages, thus showing the effectiveness of reconnecting the river with its floodplain. Even a small decrease in flood level could be effective for reducing flooding as a small decrease in peak stage could prevent large losses (Leopold, 1994).

A report by Akanbi and Singh (1997) outlined future work to evaluate the benefits of converting levées along the River Illinois, USA, into flood storage using a 1-D flow model. They simulated the effect of levée flood storage on flood peaks by modelling (1) no overtopping of levées; (2) overtopping of some levées; (3) no levées; and (4) levées converted to storage. The model was run for different flows in order to determine the reductions in peak discharge that can be produced by converting levées to temporary storage. Further to removing levées completely, Ervine and MacLeod (1999) presented

the idea of setting back flood banks from the river channel allowing a significant part of the floodplain to remain for attenuation purposes. Results from the 1-D modelling tool HEC-RAS showed that using set-back flood banks will help the reduction of flooding downstream. There is much scope for using floodplain areas previously defended for agriculture to 'set-back' or remove levées in order to create storage areas for floodwater retention (English Nature *et al.*, 2002; Morris *et al.*, 2003; Morris and Wheater, 2007).

Removal of levées currently protecting agricultural land may be a method for reducing downstream flood risk as it leads to increased inundation of the floodplain, and thus increased attenuation (Acreman *et al.*, 2003). There is scope to set back current defences in the UK to create storage areas for flood water (Ervine and MacLeod, 1999; Morris and Wheater, 2007). This effect is well established but the intriguing question is whether or not the presence of levées makes it easier to transmit upstream hydrograph changes downstream. If the floodplains are not managed effectively and the effects of attenuation are lost, flood magnitudes could be higher than they would otherwise be at York (Lane, 2008).

2.5 Case study - flooding at York

2.5.1 The York floods of 2000

The City of York is extremely prone to flooding as it was originally built at the confluence of the River Ouse and River Foss. Increased pressure for development has caused the city to encroach onto the floodplains, land previously thought unsuitable for development. In October and November 2000 York experienced the worst flooding in nearly 400 years with high flood waters lasting 14 days (The Guardian Online, 2000). The water level peaked at 5.3 m above normal levels on 4th November 2000 at 0300. The cost of the damage was estimated at more than £1.3 million (Yorkshire Post, 2006) . Over 550 homes were flooded, whilst 3000 people were made homeless as water levels rose (Environment Agency, 2010b). This event provided the catalyst for new flood alleviation schemes and strategies to deal with the increasing frequency and magnitude of floods events at York. The 2000 flood event will be used for this study as this large magnitude event provides the scope to demonstrate that large reductions can be made in terms of peak discharge and thus losses can be reduced. The results of this study could prove crucial information to reduce future flood risk at York.

2.5.2 Land use and flooding at York

A valuable flood record exists for York from 1878 and illustrates a dramatic rise in the flood magnitude and frequency, particularly in the 1940s and between the 1980s and 1990s. It has been suggested that the increase in both magnitude and frequency of flooding is a result of changes in land use in the upland catchments, as the hydrology of the Ouse catchment is largely influenced by three key sub-catchments upstream – the Ure, Swale and Nidd.

There is evidence to suggest that grips do increase the rate of runoff generation in the case of the Yorkshire Dales (Lane, 2006). Tributary timing is also shown to impact upon the magnitude of downstream flood risk (Lane, 2003a). However, there is no evidence that these impacts, as affected by tributary delivery and attenuation, scale up to explain the increased occurrence of flooding in York that has been observed since the 1940s, albeit coincident with the onset of gripping (Longfield and Macklin, 1999; Lane, 2003a; Lane *et al.*, 2003b; Lane, 2006, 2008). It is difficult to correlate the flood signal at York with gripping impacts partly due to the large area and distances involved (Lane, 2006). This relationship is also difficult to unravel as other variables correlate with the York flood record, for example, the changing frequency of flood-producing weather types. It is widely believed that gripping has increased downstream flooding frequency and magnitude even though urbanisation and climate change could generate a larger impact (Lane, 2006).

In addition to changes in stocking densities and gripping that have been introduced in the upper catchments in the Yorkshire Dales (Posthumus and Morris, 2010), the floodplains of the River Ouse upstream of York have been modified (Lane, 2008). Agricultural land was protected using levées set back from the river channel (Longfield and Macklin, 1999). The water level needed to induce flooding is much higher now than prior to the building of the defences. If the introduction of the levée system has reduced flood wave attenuation associated with the floodplains, with reduced transfer to the floodplain, the flood magnitude at York could have increased (Lane, 2008). The question is whether the levée system is exacerbating the translation of the grip signature further downstream. One place where flooding of a large area appears to have a positive effect on flood levels is at Clifton Ings, a large natural floodplain upstream of York, which reduces peak food levels in the River Ouse. Storage capacity was increased in 1982 by the construction of new levées

(Environment Agency, 2004). It must be recognised that urbanisation restricts floodplain storage as available land for flooding is reduced (Svensson *et al.*, 2006). As a result the flood management schemes aiming to flood large areas of land will increasingly come against resistance due to increasing pressures for land.

2.5.3 Sub-catchment land use projects

Recent projects have been initiated in upstream catchments in an attempt to reduce the amount of runoff resulting from land use changes. The Ripon Multi-Objective Project (MOP) set up in 2004 aimed to integrate flood risk management and catchment-scale objectives (such as the implications of land use changes over a long period of time), whilst involving stakeholders and local farmers (DEFRA, 2007). As a branch of this project, English Nature commissioned consultants to model moorland runoff affecting the River Laver and River Skell at Ripon (DEFRA, 2007). The Laver and the Skell flow into the River Ure which in turn influence the River Ouse downstream. A hydrological model was used to examine the effect of grip blocking. The large rainfall event during October and November 2000 was modelled, finding that water flow was positively affected by grip blocking; a reduction in the rate of initial runoff and peak flow was seen, decreasing the duration of the flood hydrograph (DEFRA, 2007). As at York, the potential for temporary storage of runoff water to reduce flood flow downstream was seen at Ripon. Although changing practices may not provide significant benefits for extreme floods, there is potential to increase travel times, thus improving warning times (Parrott *et al.*, 2009). Posthumus *et al.* (2008) and Posthumus and Morris (2010) discovered that local farmers had a good knowledge of factors influencing flooding, including moorland drainage, field drainage and hard surfaces. Farmers acknowledged that they could help to retain runoff using their land but needed an incentive to participate in the project as they felt they were bearing the costs whilst downstream communities benefitted (Posthumus *et al.*, 2008).

In conjunction with the Ripon MOP, the effectiveness of woodland planting for flood alleviation was demonstrated along the River Laver using the 1-D hydraulic model ISIS (Nisbet and Thomas, 2008). The results were significant, showing that the combined effects of the three planted locations could create an overall lag of one hour in the flood peak at Ripon. This could desynchronise the flood flows of the River Skell and River Laver thus lowering the peak discharge by an estimated 1-2% at Ripon (Nisbet and Thomas,

2008). With increased woodland planting in the study area, a much greater reduction could be realised (Nisbet *et al.*, 2008). The critical question that arises here is whether, if desynchronised, the other tributaries of the River Ouse can reduce the flood peak through the effects of upstream storage. Demonstration sites need to be used to encourage landowners to participate in this technique which could prove highly significant for flood warning downstream (Nisbet and Thomas, 2008).

2.6 Summary

Chapter Two has reviewed the relevant published literature to this project. Recent flood management policy has recognised that the removal of flood defences may effectively mitigate floods. Many previous studies have demonstrated the beneficial effects of using the natural floodplains to alleviate flooding downstream (McCartney and Naden, 1995; Svensson *et al.*, 2006; Lane, 2008). The flood waves passing over the floodplain are attenuated and travel times increased as a result of the increased roughness of the surface (McCartney and Naden, 1995; Whiting and Pomeranets, 1997; Morris *et al.*, 2004; Blackwell and Maltby, 2005). This attenuation effect can be increased using floodplain planting (Thomas and Nisbet, 2007; Nisbet and Thomas, 2008). In addition to the heavily modified floodplains, increased upland drainage and stocking densities are expected to increase peak flows and are thus linked with increased frequency and magnitude of flooding at York. The extensive stretch of levées lining the River Ouse at York is now believed to have increased water levels. The effect of removing levées or setting current defences back has been well established (Ervine and MacLeod, 1999; Acreman *et al.*, 2003), but the intriguing question is whether or not the presence of levées is exacerbating the translation of the grip signature further downstream. This study focuses on the ways in which possible grip signals are propagated in the downstream direction to determine whether the levée system has reduced flood wave attenuation associated with the floodplains. Different roughness, flow and levée scenarios will be simulated, directed by the literature in this chapter.

Chapter Three

Methodology

3.1 Introduction

This chapter details the study location, the modelling approach and the process of model building. Section 3.2 reviews the different types of hydraulic model available for flood inundation and propagation studies and presents the justification for the chosen model and approach. Section 3.3 describes how HEC-RAS represents the river system, structures and storage areas. Section 3.4 presents the data sources for the model. Section 3.5 illustrates the methods used to build the model, from the input of hydrological conditions to the geometry and structures. Section 3.6 discusses general modelling practice. Section 3.7 summarises the methodology.

3.2 Modelling overview

3.2.1 Modelling approach

Currently there are a number of different hydraulic models available for modelling both river channels and floodplains. These range from a simple 1-D approach used by models such as HEC-RAS (U.S. Army Corps), ISIS (Halcrow and HR Wallingford) and MIKE 11 (Danish Hydraulic Institute), through 2-D approaches including TELEMAC-2D (Horritt and Bates, 2001), MIKE 21 (DHI) and JFLOW (JBA) to the more complex 3-D approaches including FLUENT (Fluent Inc., 1993). There is debate in the literature as to which approach is preferable when modelling open channel hydraulics (Environment Agency/DEFRA, 2009).

A 1-D approach has, until recently, been the most popular approach to modelling open channel hydraulics at the reach scale (Bates and De Roo, 2000). This approach is very suited to simulating flood risk at both a catchment and sub-catchment scale as it can be used to model 10-100s of km depending on catchment size (Pender and Neelz, 2007). Originally 1-D models could only model single branches of river but now have the capacity to simulate dendritic networks as part of more complex systems (Environment Agency/DEFRA, 2004). Unsteady 1-D models allow the variation of flow conditions in time to be simulated. They can then be easily modified to include flood defence techniques that influence flooding processes at both a local scale (walls) and catchment scale (flood attenuation) (Environment Agency, 2004; Wright and Baker, 2004). Floodplains can be modelled by use of storage reservoirs or cells, by extended cross-sections, or by parallel virtual rivers (Lin *et al.*, 2006; Tayefi *et al.*, 2007). However, the accuracy of floodplain

geometry (cross-sections) used by the model greatly influences the predictions made (Pender and Neelz, 2007).

Horritt and Bates (2002) compared the performances of both 1-D (HEC-RAS) and 2-D (TELEMAC-2D and LISFLOOD-FP) approaches to model flood hydraulics on the River Severn. Quite different predictive performances were observed, with the 1-D model HEC-RAS surprisingly outperforming the 2-D models in predictions of inundated area. The difference in predictive outcome is thought to have been a result of different responses to friction parameterisation (Horritt and Bates, 2002). Tayefi *et al.* (2007) showed that storage units can affect prediction in an unrealistic way. They found that, in their model, water moved instantaneously between adjacent storage cells, skipping the channel and solely being rapidly conveyed across the floodplain. Storage cells must be carefully designed and checks performed to ensure that they are functioning in a realistic and expected manner.

1-D approaches have been readily used for some time to describe flood inundation over >1 km reaches (Tayefi *et al.*, 2007). Complex networks can be built from separate units using 1-D models, and current computer power allows a whole catchment to be contained within a single model (Wright and Baker, 2004). Advances in software and hardware and the availability of accurate terrain data have prompted a commercial move towards 2-D modelling of floodplains (Wright and Baker, 2004; Evans *et al.*, 2007; McMillan and Brasington, 2007). However, work by the Environment Agency indicates that the use of 2-D models is not yet standard practice (Wright and Baker, 2004) and focus remains on 1-D models, although work is currently being carried out to determine which 2-D models best suit the Environment Agency's current needs (Environment Agency/DEFRA, 2009).

1-D models are also particularly well suited to simulating flood wave propagation and attenuation within a system over larger reaches. The influence of channel and floodplain hydraulic and geometric properties on peak flow can then be investigated as the flood wave propagates downstream. Wollf and Burges (1994) used a 1-D flood routing model, DAMBRK, in this way to investigate the potential for reducing peak flow using effective storage within the river system. 1-D models are less suitable for providing local predictions of flood inundation, whereas 2-D models can incorporate more detailed processes, notably the 2-D effects of floodplain topography on flow.

Tayefi *et al.* (2007) argued that although it is acknowledged that in-channel flows can be satisfactorily modelled using a 1-D approach (e.g. Hamer and Mocke, 2002; Wallingford, 2006), out-of-bank flows may be less readily represented as they incorporate significant 2-D and 3-D effects where topography impacts upon the flow (Bates and De Roo, 2000; Environment Agency/DEFRA, 2004; Wright and Baker, 2004). Tayefi *et al.* (2007) compared three different treatments of floodplain inundation in HEC-RAS using (1) extended cross sections; (2) a series of storage cells connecting to the channel or other storage cells and (3) a 2-D diffusion wave with explicit representation of floodplain topography, connected to 1-D channel treatment. They concluded that the optimal approach to modelling complex floodplains involves combining a 1-D channel model and 2-D floodplain model. Approach (1) displayed the expected results, with increases in channel friction reducing peak discharge, whereas in approach (2) water moved unrealistically rapidly between the storage cells (Tayefi *et al.*, 2007). Farahi *et al.* (2009) also compared the use of storage cells and extended cross sections in HEC-RAS for calculating flood extent. The inundation extent recorded was highest for the storage cell mode, with the advantage that any water conveyed to the floodplain can be moved between cross-sections (Farahi *et al.*, 2009). Similarly, Hamer and Mocke (2002) presented the floodplain as a series of connected reservoir units using an ISIS model. They found that the results were consistent and repeatable, giving greater confidence in the 1-D model for simulating flood propagation.

Kohane and Westrich (1994) reviewed the use of 1-D models within river flood management. They concluded that a 1-D strip model, which divides the channel into subsections of different flow depths and roughness along the reach, would be useful for an engineering application as it can account for the significant difference in flow velocities between the main channel and floodplains during a flood. During laboratory tests, changing the alignment of levées created great variability in flow rate and water level between channel and floodplain. More accurate results were presented when using this approach, compared to modelling flow depth and roughness along the whole reach, as flow depth and discharge could be calculated for each strip individually. Helmio (2005) used a simple 1-D model to measure the effect of vegetation on the floodplains of the Rhine. Despite the simplicity of modelling one-dimensional flow in a compound channel, the simulated hydrographs matched well with the observed.

Although 2-D and 3-D models may address problems with the more simplistic 1-D approach, many authors still find 1-D models adequate for some modelling problems. For example, Downs and Thorne (2000) found that HEC-RAS was able to represent different channel scenarios at reach and basin scales, concluding that the model is readily accepted by flood defence specialists. Wright and Baker (2004) stated that if studying an entire length of river, it is not necessary to have the large amount of detail that can be provided by 3-D equations, and that such models can be reduced to 1-D equations in order to make the model parsimonious with available data. Often 2-D solutions are only required in parts of a river model. Thus, for most of the system a 1-D approach is adequate (Wright and Baker, 2004). It must be remembered that "model complexity does not always guarantee success!" (Michaelides and Wainwright, 2004: 123). Recent advances in the predictive ability of 3-D models have led to increased usage, mainly used in simulations of flow patterns (Michaelides and Wainwright, 2004). However, as 3-D models rely on the specification of complex topography and are difficult to parameterise, they are primarily used over small spatial and temporal scales (Krishnappan and Lau, 1986; Michaelides and Wainwright, 2004).

Following the evaluation of 1-D, 2-D and 3-D modelling approaches to flow modelling, the application of a 1-D model was deemed suitable for the study of flow within the Ouse catchment. As three main tributaries are to be assessed over a large distance of 71 km, and detailed measurements of velocities were not required, the computational time and expense of 2-D and 3-D approaches were deemed unsuitable. In addition, although 1-D models tend to just give discharge and water level results, this is sufficient for this study thus a more complex model is not necessary (Knight, 2005). Kirkby (1996) argues that few models are too simple and thus models should be in the simplest form necessary for the required predictions. A 1-D approach is widely used commercially for flood risk assessments (Environment Agency/DEFRA, 2004; Wright and Baker, 2004; Lin *et al.*, 2006). As a 1-D approach can be used to successfully model hydraulic structures and treat floodplains with extended cross sections and storage units, it was deemed suitable for this investigation.

3.2.2 Model choice and set-up

A 1-D approach was adopted for this modelling problem (Section 3.2.1). The flood inundation model HEC-RAS 4.0 (U. S. Army Corps of Engineers, 2008) was chosen for a

number of reasons. First, it is commercially used and freely available to download and use from http://www.hec.usace.army.mil/software/hec-ras/hecras-download.html. Second, it was necessary to produce results that would fit with previous work and existing understanding of the Ouse system by the Environment Agency, whose work is primarily done using 1-D models. Third, the scale of the modelling required for this study (71 km river) indicated that a 1-D approach was most suitable. Fourth, it uses the generally accepted equations for both 1-D flow routing and flood prediction described by Lane and Ferguson (2005) and in Section 3.2.3. Fifth, the simple data requirements allowed the model to be built quickly, as the data needed (geometric and hydrologic) were already available from the Environment Agency. Sixth, HEC-RAS allows the assignment of distributed values of *n* within cross-sections (channel, left and right bank) (Kitson *et al.*, 2006) and they are easily altered. Finally, HEC-RAS provides a user-friendly interface to aid the speed of model development.

HEC-RAS allows the user to perform one-dimensional steady and unsteady flow calculations as well as undertake sediment transport and water quality modelling. It can be used to model both natural and constructed channels, and HEC-RAS is in widespread use in consultancy firms as it is effective for floodplain modelling (Environment Agency, 2004) . As it can model floodplain flows in different ways, for example using extended cross sections and hydraulic structures (Lin *et al.*, 2006), it can effectively simulate situations that could not be realised in reality (Lane, 2003b).

3.2.3 Basic 1-D flow equations

The model is based on the major flow equations that govern all 1-D approaches to hydrodynamic modelling. The standard continuity equation forms the foundation of all numerical schemes for 1-D treatments of flow. The principle of mass conservation implies that the mass of water can neither be created or destroyed: the (Beven, 2004). In 1-D the continuity or mass conservation equation states that:

$$\frac{\partial Q}{\partial x} + \frac{\partial A}{\partial t} = 0$$

Equation 3.1

where Q is the flow discharge (m^3/s) given by $Q = UA$ where U is the cross-sectional averaged velocity and A is the cross-section surface area (m^2).

The rate of change of momentum through time at a point is governed by the spatial change of the momentum plus the driving forces via the conservation of momentum equation:

$$\frac{\partial(Av)}{\partial t} = -\frac{\partial(Av^2)}{\partial x} + \ driving\ forces$$

Equation 3.2

These driving forces are (1) pressure gradients; (2) potential energy; (3) friction that causes energy expenditure:

$$\frac{\partial(Av)}{\partial t} + \frac{\partial(Av^2)}{\partial x} = \ -Ag\frac{\partial h}{\partial x} + \ gA(S_o - S_f)$$

Equation 3.3

where h is mean flow depth (m), S_o is the bed slope of the channel (defining the potential energy term), and S_f is the friction slope (i.e. the friction term).

One equation often used in flow modelling to describe friction is Manning's roughness equation.

$$\left(\frac{vn}{R^{2/3}}\right)^2 = S_f$$

Equation 3.4

where v is velocity (m/s), R is hydraulic radius (m), S_f is the friction slope and n is Manning's resistance coefficient (dimensionless).

The HEC-RAS model is based on these equations which provide the method by which flow routing and channel characteristics, such as velocities and depths, can be calculated.

3.3 Description of HEC-RAS

HEC-RAS can be used to determine water surface elevations and discharges at any location within the model for either a set of flow data (steady flow simulation) or by routing hydrographs through the model (unsteady flow simulation). In order to perform a steady state simulation, as required for this study, unsteady flow data and geometric data are required.

3.3.1 Hydrological boundary conditions

Boundary conditions must be entered for all of the reaches in the system. For an unsteady flow model, the boundary conditions are a combination of flow and stage time

series which can either model an observed event or generate a hypothetical event such as a dam break. The accuracy of the boundary conditions used will affect the accuracy of the reproduction of the observed event.

The upstream boundary condition defines the input which will be routed through the model. Those available in HEC-RAS are flow hydrograph, stage hydrograph and flow and stage hydrograph combined. A flow hydrograph is the typically used boundary condition, where discharge is routed downstream and the corresponding stages are computed by the model. The downstream end of the system can be modelled using these boundary conditions: rating curve; normal depth (Manning's *n*); flow hydrograph; stage hydrograph; flow and stage hydrograph. The classic downstream boundary condition is the stage hydrograph where the corresponding discharge is computed by the model. Boundary conditions are also required for lateral inflows internally within the model. The boundary conditions available are lateral inflow hydrograph, uniform lateral inflow hydrograph, groundwater and internal stage and flow hydrograph, which are linked to specific cross-sections. Lateral inflows can either be located at a point or uniformly distributed along a reach. Initial conditions must also be entered for all of the reaches in the system before simulations can be run. The most common method is to enter flow data for each reach, specifying the initial flow as bankfull. HEC-RAS then runs a steady flow backwater run to establish the corresponding stages at each cross-section. An initial water surface elevation must also be defined for each of the storage areas present in the model.

3.3.2 Geometric Data

The basic geometric data consist of cross-section data, reach lengths, energy loss coefficients (friction losses and contraction and expansion losses), stream junction information and hydraulic structure data. Similarly, data collection is required downstream of the modelled system to prevent any user-defined boundary condition from affecting the results.

Cross-sections

Coupled with the hydrological data, the geometric data determine the conveyance of water downstream, both within the channel and across the floodplain. The boundary geometry for the analysis of flow is specified in terms of ground surface profiles (cross-sections) and the distance between them (reach lengths). The cross-sections are located at intervals along the river in order to characterise and accurately represent the flow

carrying capacity and geometry of the channel and its floodplain. Cross-sections are required where changes to roughness, discharge, shape and slope occur, as well as before and after weir and bridge structures. In HEC-RAS the cross-sections extend across the entire floodplain, perpendicular to anticipated flow.

Each cross-section is labelled with a river, a reach and a river station label. The cross-section is described by entering the station and elevation (x-y) data from left to right. All cross-section data are defined looking in the downstream direction. The specific points at which 'overbank flow' is defined along the channel cross-section are called 'left and right overbank stations'. The reach lengths between cross-sections must be specified for the left bank, right bank and channel. Channel lengths are typically measured along the thalweg and overbank distances along the expected centre of mass of the overbank flow. These values differ more greatly as river bends.

Levées can be designated within the geometry data by identifying a left or right bank levée station and elevation on a cross-section. Once established, water can only pass the levée station if the water level exceeds the elevation of the levée. The levées are usually established at an existing point on the cross-section.

The spacing of cross-sections depends on slope, stream size and uniformity, but also the purpose of the study in question. For example, studies analysing the effect of local geomorphology on flow depths will require more closely spaced cross-sections than a study investigating the deposition of sediment in reservoirs. Interpolation is often required where the velocity head is too large to accurately determine the change in energy gradient. Inadequate cross-sectional spacing can result in significant computational errors as a result of inaccurate integration within the profile computations. This error can be effectively removed by adding interpolated cross-sections. Increasing the density of the cross-sections will improve the accuracy of the profile computations (the solution of the equations). It is necessary to have frequent cross sections in order to describe the hydraulic behaviour of the channel with acceptable precision, but this must be balanced with time pressures of this procedure (Samuels, 1990). Interpolating over a very small distance between cross sections creates too much data and unnecessary expense, whilst very large spacing can result in calculation instabilities (Samuels, 1990).

Roughness

The Manning's *n* selected for each cross-section is a major influence on the friction slope and hence energy losses. Thus it influences the conveyance of water and therefore the speed at which water can flow through a channel. The amount of friction combined with the channel geometry determines the depth of flow within a channel at a certain location. The application of Manning's *n* values contains an element of subjectivity but there are standard values recommended for different channel and floodplain types. The criteria for selecting *n* values are well documented in U.S. Army Corps of Engineers (2008) and Chow (1959), the main source for obtaining *n* values (Table 3.1). Values for Manning's *n* for left overbank, right overbank and channel are required for each cross-section.

Expansion and contraction coefficients

Energy losses can occur between two cross-sections as a result of contraction or expansion of flow. The loss is computed using the contraction and expansion coefficients specified in the cross-section data editor. The energy loss is calculated by multiplying the coefficients by the absolute difference in velocity heads between one cross-section and the next one downstream. If the change in cross-section is small or gradual, the contraction and expansion coefficients are typically 0.1 and 0.3 respectively. These values are recommended by the HEC-RAS manual to account for gradual changes in river cross-sectional area (U. S. Army Corps of Engineers, 2008). Where the change in effective cross-section area is abrupt (e.g. at bridges) contraction and expansion values of 0.3 and 0.5 are typically used.

Type of Channel and Description	Minimum	Normal	Maximum
Natural Streams			
1. Main Channels			
a. Clean, straight, no rifts or pools	0.025	0.030	0.033
b. Same as above, but more stones and weeds	0.030	0.035	0.040
c. Clean, winding, some pools and shoals	0.033	0.040	0.045
d. Same as above, but some weeds and stones.	0.035	0.045	0.050
e. Same as above, lower stages, more ineffective slopes and sections	0.040	0.048	0.055
f. Same as 'd' but more stones	0.045	0.050	0.060
g. Sluggish reaches, weedy, deep pools.	0.050	0.070	0.080
h. Very weedy reaches, deep pools, or floodways with heavy stands of timber and brush.	0.070	0.1	0.150
2. Floodplains			
a. Pasture no brush			
i). Short grass	0.025	0.030	0.035
ii). High grass	0.030	0.035	0.050
b. Cultivated areas			
i). No crop	0.020	0.030	0.040
ii). Mature row crops	0.025	0.035	0.045
iii). Mature field crops	0.030	0.040	0.050
c. Brush			
i). Scattered brush, heavy weed	0.035	0.050	0.070
ii). Light brush and trees in winter	0.035	0.050	0.060
iii). Light brush and trees in summer	0.040	0.060	0.080
iv). Medium to dense brush, in winter	0.045	0.070	0.110
v). Medium to dense brush, in summer	0.070	0.100	0.160
d. Trees			
i). Cleared land with tree stumps, no sprouts	0.030	0.040	0.050
ii). Same as above, but heavy sprouts	0.050	0.060	0.080
iii). Heavy stands of timber, few down trees, little undergrowth, flow below branches	0.080	0.100	0.120
iv). Same as above but with flow into branches	0.100	0.120	0.160
v). Dense willows, summer, straight.	0.110	0.150	0.200

Table 3.1 Descriptors used in the allocation of Manning's *n* values for each cross-section (Source: Chow, 1959; U. S. Army Corps of Engineers, 2008).

Structures: bridges

In order to model bridge structures, HEC-RAS requires four user-defined cross-sections in order to compute energy losses around the structure. Cross-section one is located far enough downstream so that the flow is not affected by the structure. Field investigations during high flow should determine this distance. A second cross section should be located just downstream of the bridge to represent the topography of the channel and floodplain. A third cross-section should be placed just upstream of the bridge to represent the channel and floodplain upstream. A fourth cross-section should be located upstream of the bridge where flow lines are approximately parallel. This method allows for the changes in water surface profile and energy losses apparent in the vicinity of bridges to be calculated. For a 1-D approach, as for HEC-RAS, expansion and contraction coefficients are used to quantify energy losses as a result of contraction and expansion through a bridge based on the abruptness of the change. Typical bridge sections are given contraction and expansion coefficients of 0.3 and 0.5 respectively which must be specified by the user. The coefficients must be adjusted back to an appropriate value downstream of the structure.

Structures: weirs

HEC-RAS has the ability to model broad-crested, ogee shape and sharp-crested weirs as inline structures across the main river. Like bridges, weirs have an effect on flow as water backs up behind them causing a localised increase in width and depth. The presence of a weir also has an effect on river-floodplain interaction and both the bank and bed can be subject to erosion. In HEC-RAS the flow over a weir is computed using the standard weir equation:

$$Q = CLH^{3/2} \qquad \textit{Equation 3.4}$$

where *Q* is discharge, *C* is the weir flow coefficient (typical values range from 2.6 to 4.0 depending upon the shape of the spillway crest), *L* is the length of spillway crest and *H* is the upstream energy head above the spillway crest.

During very high discharges, a weir can become 'submerged' and, if a flow gauging station is present (such as Westwick and Hunsingore), it will be unable to provide accurate measurements (Rickard *et al.*, 2003). HEC-RAS automatically accounts for submergence if the tailwater is high enough to slow the flow. As submergence increases, the weir flow coefficient is automatically reduced. The shape of the weir selected determines how HEC-

RAS calculates submerged weir flow. In order to model inline structures it requires the same cross-section framework as for bridges. The geometry of the weir is entered using elevation and station data across the river. The same contraction and expansion coefficients apply for weirs as for bridges.

Storage areas

Floodplains and storage areas in a river system are represented in one of two ways in HEC-RAS: either by using a series of extended cross-sections which includes the properties of the floodplain (topography and roughness) within the specification of each cross-section, or by representing the floodplain as a series of discrete flood cells, hydraulically connected to neighbour cells and/or the main channel, through which water is routed (Maidment, 2002; Tayefi *et al.*, 2007). In order to add a storage area to the model, two different methods can be used. Firstly, the area times depth method requires the area of the storage and minimum elevation to be entered. Secondly, the elevation versus volume method requires volume measurements for each elevation of the storage area. This is the recommended method where possible as it is more detailed. HEC-RAS uses lateral structures to link two storage areas together and to link the storage areas to cross-sections. As in Tayefi *et al.* (2007) and Hornberger *et al.* (1998), flow exchanges between the storage areas are calculated using the standard weir equation for a broad-crested weir (Equation 3.4). For a lateral structure connecting a cross-section to a storage area there must be a cross-section upstream and downstream of the lateral structure. For each lateral structure station data, elevation data, weir width and a weir coefficient are required.

3.4 Data sources

3.4.1 ISIS 1-D hydrodynamic model

As part of the Environment Agency's Strategic Flood Risk Management Framework, a hydraulic study of the River Ure and its tributaries was commissioned. An ISIS 1-D hydrodynamic model was developed at the Environment Agency using the ISIS v3.3 modelling software. The main objective of the study was to produce flood outlines and areas benefitting from defences and identify potential areas for further storage of floodwater. In addition to this previous work, the Environment Agency wanted to quantify the extent to which the levées present in the system aid in transmitting changes

in the upstream hydrograph downstream. Thus the ISIS model was provided for this study. A full description of the ISIS model was provided in the *River Ure and Tributaries Modelling Study: Interim Modelling Report* and *Ure Model Handover Annex*. A major challenge to this project became apparent on receiving the ISIS model: the model was created using a more recent version of ISIS software than was available at Durham University and therefore would not run completely. Furthermore, the complexity of the model created many errors which stopped the trial simulations. These errors were due to the large number of structures in the model, which caused problems with water levels at the bridges, particularly on the River Tutt and River Nidd. Reducing the timestep and increasing the depth of the Preissmann Slot (a conceptual narrow slot providing a conceptual free surface condition for the flow) did not solve the problems. Additionally, with little knowledge of how the model was built and how it represented the Ouse catchment, it was very difficult to gain a detailed understanding of the model that would be needed in order to use it to produce useful results. As the ISIS model contained all of the topography data required, and the flow data were available, it was decided that the model could be represented and re-built in the HEC-RAS 1-D software. This simplified the ISIS model down to the key hydrological inputs, structures and geometry without the complexity that caused the ISIS model to not run. Additionally, with greater understanding of the model it could be manipulated more easily in order to meet the objectives of the investigation.

3.4.2 Hydrology data

Flow and stage data were required in order to build the HEC-RAS model. Flow data were retrieved from three upstream locations which form the upstream extent of the model and also the downstream extent at Skelton. These locations were chosen as they coincide with flow gauging stations:

- Westwick Weir gauging station on the River Ure
- Crakehill gauging station on the River Swale
- Hunsingore weir gauging station on the River Nidd

The location of these gauging stations can be seen in Figure 1.2. Flow data from the flood event of 2000 at York were chosen as the basis for this study for a number of reasons. First, the 2000 event caused the highest recorded water level during a flood at York, thus

if by modelling the event the impacts can be shown to be reduced using such a large event, the results could prove crucial information to reduce future flood risk. Second, this event provided the catalyst for new flood alleviation schemes and strategies to deal with the increasing frequency and magnitude of floods events at York. Third, flow data for the gauging stations within the catchment were readily available from the Environment Agency. Data are available for 15-minute flow intervals as well as daily and annual mean flows. For this model, 1-hour flow intervals were seen as sufficient as the studied flow event (2000 flood event) was both a high magnitude and long duration event. A balance was needed between gaining enough detail and time limitations, as using smaller intervals made the model run time too long.

The upstream inflows account for approximately 80% of the discharge within the study catchment area. Discharge hydrographs from each of these locations were generated from the data received from the Environment Agency, from each of the gauging stations mentioned. The Environment Agency also provided the stage data from the Skelton gauging station required for the downstream boundary at Skelton.

In order to include additional flow discharged into the main watercourses by smaller tributaries, residual inflows were included. Inflows for the residual 20% from the ungauged portion of the catchment were taken from the ISIS model. The *Ure Model Handover Annex* cautioned that problems were experienced during calibration of the ISIS model due to the boundaries for the residual inflows overestimating runoff during long duration events. Therefore the inflows were scaled on the advice of a senior hydrologist at the Environment Agency and reported in the *Ure Model Handover Annex*. This scaling was followed for the HEC-RAS model, scaling the residual inflows by a factor of 0.25 for the 2000 event.

3.5 Model building – unsteady flow model structure

3.5.1 Hydrological boundary conditions

The input and output boundaries require hydrological data to specify the amount of water running through the model in a specified time. The upstream boundary conditions were specified by discharge hydrographs. Gauged data from the three tributaries (Ouse, Swale and Nidd) were used to generate the discharge hydrographs. The downstream

boundary condition was specified as a stage hydrograph at Skelton using the gauged data from the station located here.

In addition to the boundary conditions, the initial conditions of the system at the beginning of an unsteady flow simulation must be established. These consist of flow and stage data at each of the cross-sections as well as elevations for any storage areas defined in the model. The initial conditions were set to channel bankfull for each of the rivers. The initial elevation of the storage areas was set to the minimum floodplain elevation.

3.5.2 Lateral inflows

The river system used in this study is a dendritic system, thus the main stem is joined by a number of tributaries. In order to model these tributaries, the main stem of the River Ouse was divided into several sub-reaches. These reaches are listed in Table 3.2 along with the associated river and cross-section reference number. The lateral inflows represent water running into the watercourse between the main inflow and downstream extent of the model. Point inflows represent flow entering the river from specific watercourses and their effect will be observed at the next downstream cross-section. A list of the residual inflows can be seen in Table 3.3 and their location in Figure 3.1. Figure 3.2 shows the locations of the inflows, gauging stations and cross section numbers schematically. Boundary conditions used for the lateral inflows were uniform lateral inflow hydrographs and lateral inflow hydrographs. The River Tutt was not included in the model due to the instabilities experienced in the ISIS model. This was thought to be as a result of the large number of structures present in this short reach. The River Tutt is also relatively unimportant to the Ouse system as it produces a very small discharge and is not influenced by upland grips.

Reach number	River	Reach	Cross-section number
1	Ure-Ouse	Upper	1000-955
2	Ouse	Swale-Nidd	954-922
3	Ouse	Lower	920-902
4	Swale	Lower	100-68
5	Nidd	Lower	100-28

Table 3.2 Name and location of each of the reaches within the river system.

Model cross-section label	Description	Location and schematisation	Reach
97	Birdforth Beck point inflow	Connected to River Swale channel	River Swale
90	Thornton point inflow	Connected to River Swale channel	River Swale
926	River Kyle point inflow	Connected to River Ouse channel	River Ouse
916	River Foss point inflow	Connected to River Ouse channel	River Ouse
100-68	Lateral inflow – River Swale, Crakehill to confluence with River Ure	Connected to channel cross-sections	River Swale
1000 – 955	Lateral inflow – River Ure, Westwick to River Swale confluence	Connected to channel cross-sections	River Ure
954-926	Lateral inflow – River Ure / Ouse, River Swale confluence to River Kyle	Connected to channel cross-sections	River Ure / River Ouse
926-902	Lateral inflow – River Ouse, River Kyle to Skelton	Connected to channel cross-sections	River Ouse
100 – 28	Lateral inflow – River Nidd, Hunsingore to River Ouse confluence	Connected to channel cross-sections	River Nidd

Table 3.3 Residual inflows to the model.

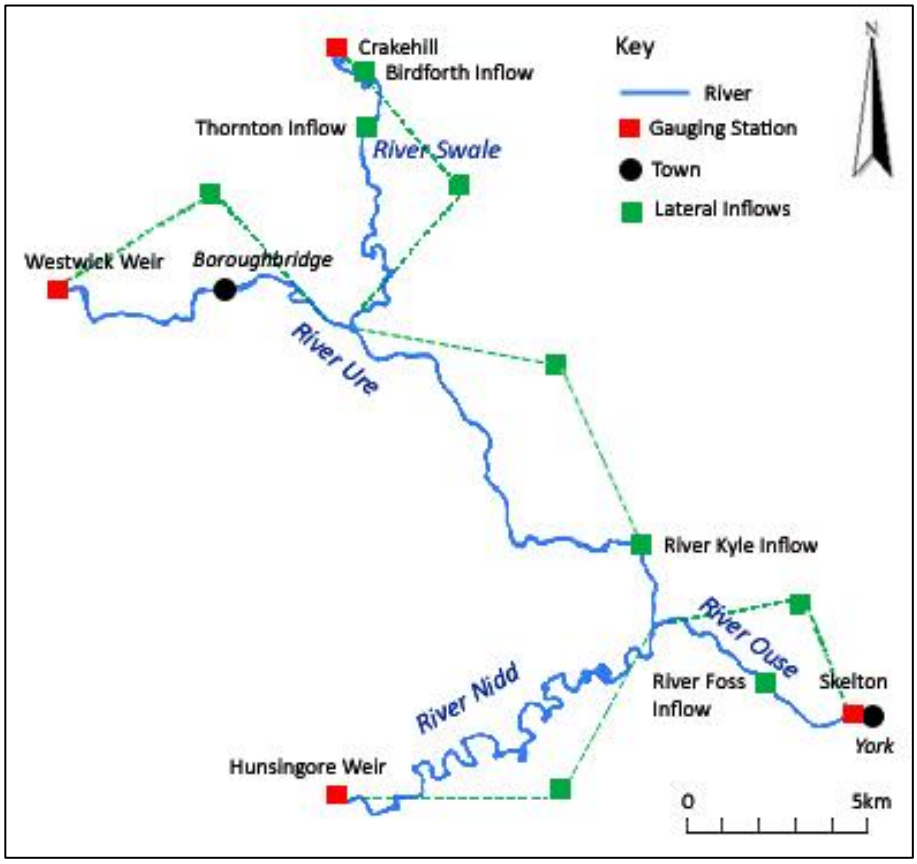

Figure 3.1 Location of the lateral inflows entering the modelled reach. The dashed green lines indicate the points between which the discharge from the lateral inflows was added to the system.

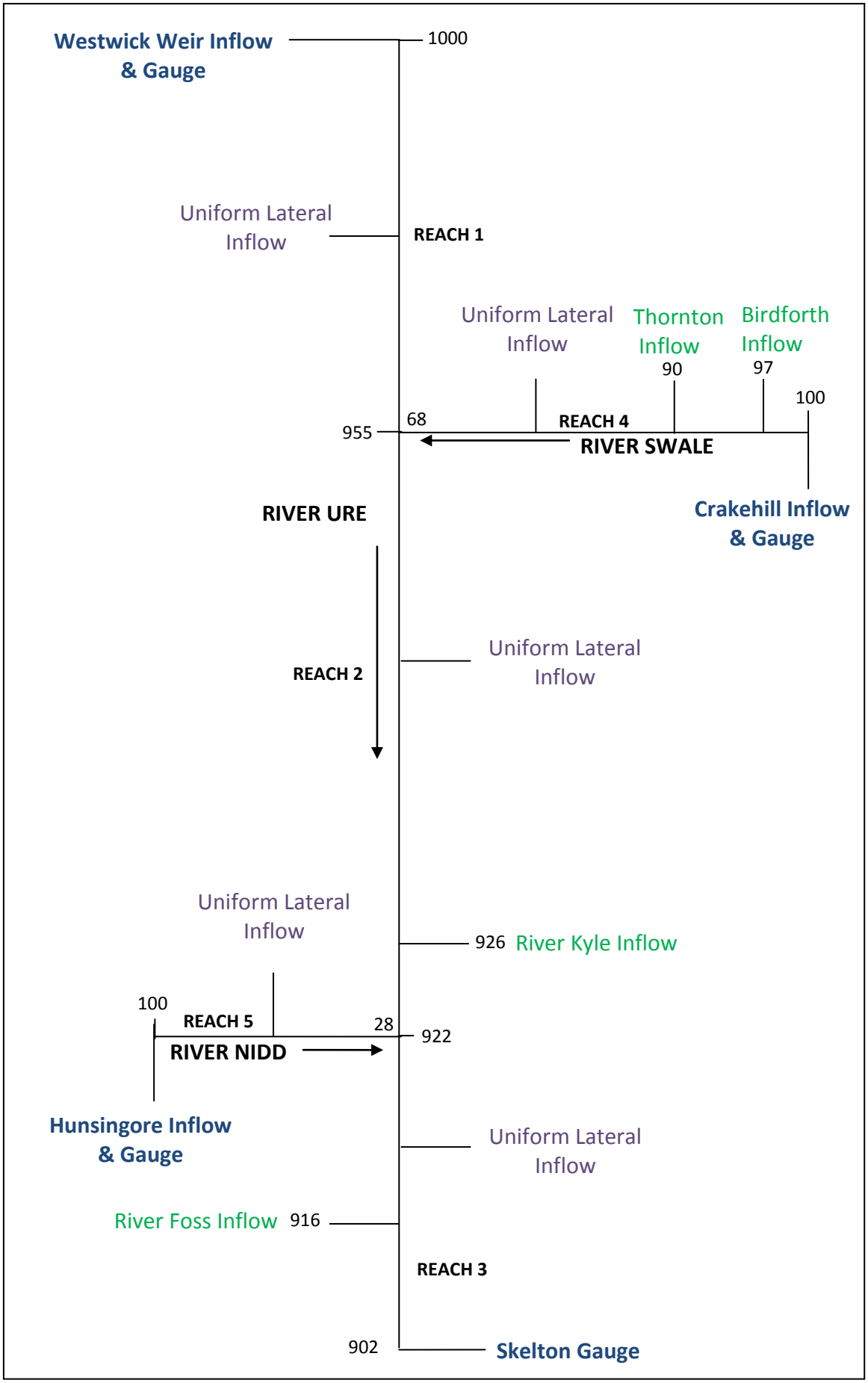

Figure 3.2 Model schematic illustrating the location of rivers, reaches, point and lateral inflows and gauging stations.

3.5.3 Geometry: river channel

Cross-sections

The original ISIS model contains 201 cross sections within the study catchment: 97 along the Ure, 32 along the Swale and 72 along the Nidd. The data were transferred from the ISIS model in order to create the same system in HEC-RAS. Using the HEC-RAS Geometric data tool. Elevation and station information were entered for each cross section, including the elevation of the left and right overbank stations. The contraction and expansion coefficients were kept at the default settings of 0.1 and 0.3 respectively, values used in HEC-RAS to describe small changes between cross-sections. The distance between cross-sections was entered for the channel directly from the ISIS model. However, measurements for LOB and ROB (left overbank and right overbank) were not present in the ISIS model but are required by HEC-RAS, thus the values needed to be calculated following the method in Figure 3.3.

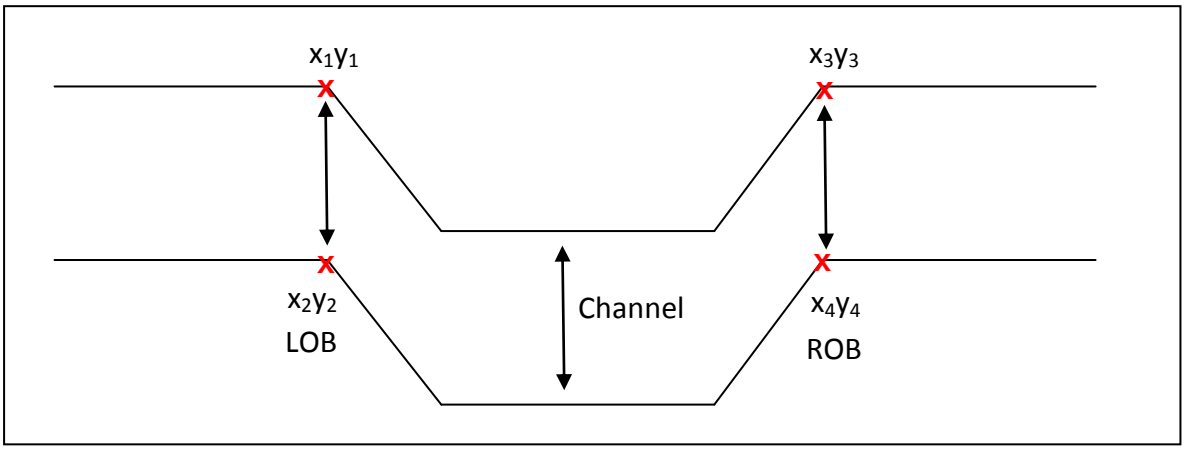

Figure 3.3 Calculating LOB and ROB to complete the cross sectional geometry data. LOB and ROB are the points at which water flows out of the channel at either end of the cross-section. For LOB, equation 3.5 was used: $\left((x_2 - x_1)^2 + (y_2 - y_1)^2\right)^{0.5}$**. For ROB, equation 3.6 was used:** $\left((x_4 - x_3)^2 + (y_4 - y_3)^2\right)^{0.5}$.

Values for Manning's *n* (for channel, left bank and right bank) were also required at this stage. The values entered will be discussed in Section 3.5.6. Appendix One lists the name, location and relative position of each cross-section.

Interpolation

The cross sectional data were interpolated after finding some instabilities following initial runs of the model. This helps to better represent the change in water levels around structures and to aid model stability in deeper parts of the modelled reach. Time was taken over the choice of spacing of the interpolated cross sections as this is "fundamental to the success of modelling applications" (Samuels, 1990: 1). A spacing of 100 m was chosen for the whole model, excluding the River Nidd which showed larger instabilities. A spacing of 50 m was used for the River Nidd.

3.5.4 Geometry: floodplains

Extended cross sections

The floodplains were modelled with the use of extended cross sections. The floodplain spills were combined with the cross-sectional data in order to represent the topography of the floodplain. This is a method often used in hydraulic modelling (e.g. Acreman *et al.*, 2003).

Storage areas

Storage areas were added to the model in order to represent the managed 'reservoirs' of water that are stored within the Ouse catchment during flood events. Firstly, storage areas were drawn and labelled using the *Storage Area Tool* to create a polygon. 31 storage areas were added along the Ure/Ouse, 18 along the Swale and 31 along the Nidd. The data for each storage area were added using the *Storage Areas Editor.* The data for the storage areas were transferred from the reservoir units in the ISIS model. The geometry of the reservoir units is stored as elevation (m) and plan area (m^2) in ISIS, whereas HEC-RAS uses elevation and volume (m^3). In order to calculate the volume of each storage area, they were split into segments (Figure 3.4).

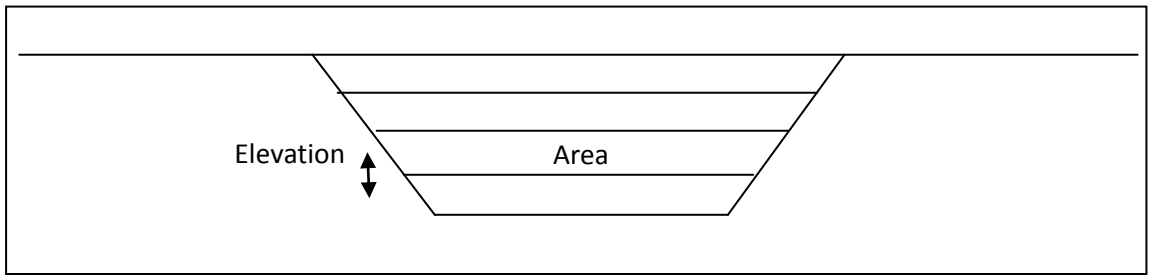

Figure 3.4 Calculating the volume of each storage area. The mean plan-view area between two segments was calculated and multiplied by the difference in elevation of the same two segments. This gave a volume for the storage area at each elevation.

The elevation versus volume curve method was used to represent the storage areas as it is the most detailed method available, representing the storage areas with the most accuracy. Once the data for the storage areas were entered, the storage areas were connected with the river reach using a lateral structure connection. 67 lateral structures were entered in total. In the *Lateral Structure Editor* the reach, the position of the storage area (left or right overbank) and the structure type (weir/gates/culverts/diversion rating curves) were selected. The station, elevation, weir width and weir coefficient data were retrieved from the 'floodplain spills' in the ISIS model and were used to connect the storage areas with the cross sections. The data from the 'embankment spills' in the ISIS model were used to connect the storage areas together, via the *Connection Data Editor.* The station, elevation, weir width and weir coefficient data were all taken from the ISIS model.

Levées

Levées were included in the HEC-RAS model within the cross-sectional topography. The elevation data for the levées were taken from the embankment spills in the ISIS model. The highest elevations of the levées were marked in the model using the *Levée Editor*. When levées are established in this way, no water can go to the left of the left levée station or to the right of the right levée station until either of the levée elevations is exceeded. Figure 3.5 shows how the levées were removed and altered for the different scenarios tested.

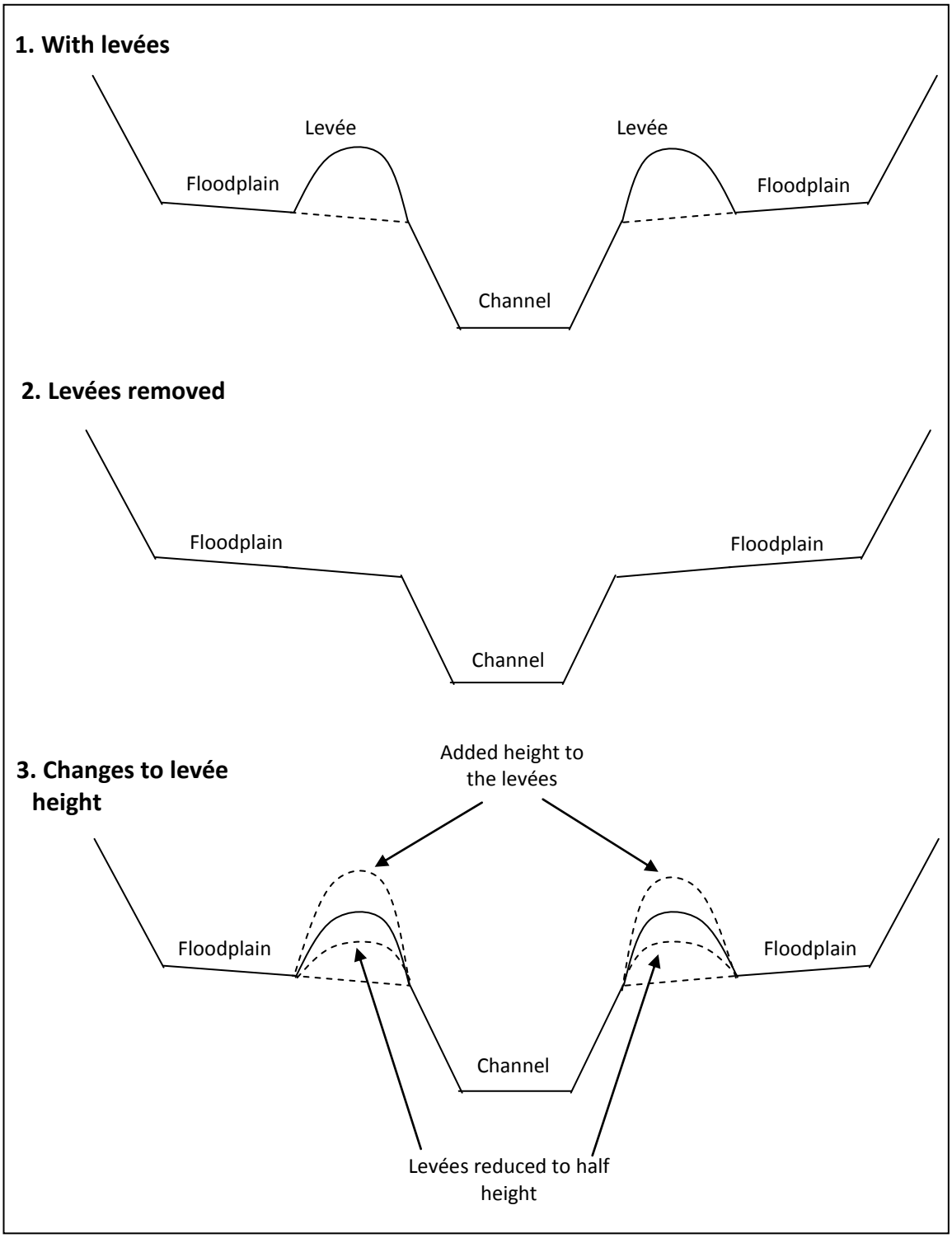

Figure 3.5 Removal and alteration of the levées within the model.

3.5.5 Structures

In order to satisfactorily represent the Ouse catchment using a 1-D model, the structures within the catchment need to be recognised and input into the model. The main structures within the watercourse are bridges and weirs.

Bridges

Bridges were added to the model in the locations defined by the ISIS model: four bridges along the River Ouse and four along the River Nidd. The upstream and downstream bounding cross-sections were taken from the ISIS model, plus the distance between them. The bridge culvert editor was used to enter the required data for the deck and piers, transferred from the ISIS model. The contraction and expansion coefficients were increased to 0.3 and 0.5 respectively at the bounding cross-sections to reflect the flow interactions around the bridge structures. The bridges within the catchment have an effect on flow as water is constricted through the bridge opening, creating a higher water surface profile behind the bridge. During a flood this effect has an even larger influence, as the water running across the floodplain width is constricted and must contract to pass through the bridge (Hamill, 1999). During floods it is large woody debris that often constricts flow even further at bridges, causing exaggerated surcharging. Further research could investigate the impact of surging at bridges, caused by large woody debris, on the modelled output.

Weirs

In addition to bridges, weirs must be modelled in order to satisfactorily represent the Ouse catchment. Weirs were added to the model in the locations defined by the ISIS model. The weirs represented by spill units in the ISIS model at the Old Corn Mill at Hunsingore and Westwick Weir were reproduced with the cross-section data in the HEC-RAS model. Linton weir and Cundall weirs, which were represented by standard weir units in the ISIS model, were reproduced using the *Inline Structure Editor* in HEC-RAS. Weir coefficient values of 1.2 and 0.9 were used for Linton weir and Cundall weir, respectively.

3.5.6 Roughness coefficient

A list of the roughness values used for each cross-section is shown in Appendix One. The Environment Agency used site photographs, observations and aerial photographs in conjunction with photographs from Chow (1959) and professional judgement to select Manning's *n* values for the ISIS model. The values selected were based on channel shape, substrate size and form, and floodplain and vegetation characteristics, and therefore different values were assigned for different parts of the modelled reach.

The values used for channel roughness vary from 0.035 for the River Ouse downstream of Aldwark Toll Bridge to 0.050 upstream of the Swale confluence on the River Ure. Higher values were used for the bank tops, between 0.05 and 0.07, to represent the increased vegetation here. The floodplains were also assigned values for *n*. A site visit found that roughness was fairly high, with fences and hedges causing restrictions to flow on the floodplain. Roughness values were therefore set to 0.05 on the River Nidd and River Swale and 0.06 on the River Ure/Ouse.

Because much of this process is subjective, it was crucial to understand the sensitivity of the model to roughness values and so sensitivity analyses that involved changing the roughness coefficient (*n*) were conducted and the results shown in Chapter Four.

3.6 Modelling practice

Before the HEC-RAS model was used for this particular modelling problem, general modelling practice was considered. It must be recognised that models make a number of assumptions about reality in order for reality to be represented (Mulligan and Wainwright, 2004). Therefore any predictions are only as good as assumptions made in the model (Anderson and Burt, 1985). The main challenge in modelling is determining whether observed behaviour is due to the assumptions made, or actually represents real world processes (Lane, 1998; Lane and Bates, 2000). Successful modelling involves knowing which assumptions are wrong and ensuring that they do not influence the results (Mulligan and Wainwright, 2004). Any major assumptions have to be evaluated and discussed with other modellers to ensure that the modelling process reflects reality as closely as possible. The use of models relies on sufficient knowledge of the whole system by the modeller. The determination of boundary conditions, parameter values and hydraulic structures to be included is controlled by the modeller and therefore model performance may depend on the experience of the modeller (Beven, 1989; Olsen, 2008; JBA, 2009). Error is an inherent problem in the modelling process but it must be remembered that “no measurement can be made without error” (Mulligan and Wainwright, 2004: 59). Some key modelling assumptions for the work undertaken in this study are discussed in Section 7.5.

3.7 Summary

The study reach for this project comprises the River Ure, and the Swale and Nidd tributaries, from Westwick Weir down to Skelton at York in the Ouse catchment. Flow gauging stations along the modelled reach provide the flow and stage data. A large range of hydraulic models are available for modelling floods, from 1-D to 3-D. A 1-D approach was chosen for this study as it aims to simulate flood wave propagation and attenuation within a large system. HEC-RAS was deemed appropriate particularly so that results produced would fit with previous work by the Environment Agency using 1-D models. The way in which HEC-RAS represents features, such as cross-sections and structures, has been discussed and the model building process presented. Chapters Four and Five will present the results of the sensitivity analysis and the main simulations.

Chapter Four

Model sensitivity and calibration

4.1 Introduction

Chapter Four starts with a brief discussion of the purpose of carrying out a sensitivity analysis. Section 4.2 introduces the methodology used for the sensitivity analysis and the objective functions used for evaluating the results. Sections 4.3 and 4.4 present the results of the sensitivity analysis in two parts: the sensitivity analysis of model predictions and the sensitivity analysis of model performance. These results and their implications are discussed in Section 4.5. Section 4.6 presents the results of the calibration process. The results of the sensitivity analysis and calibration process are concluded in Section 4.7.

4.2 Methodology

4.2.1 Purpose of sensitivity analyses

It is necessary to conduct a sensitivity analysis before any modelling occurs in order to focus the investigation and understand the responsiveness of the model to changes in parameters (Aber, 1997; Baker, 2001). It is crucial to present the effects of parameters on the predictions and performance of a model in order to have confidence in the results. Thus, it is normally a requisite part of model building (Aber, 1997; Ratto *et al.*, 2001; Saltelli, 2002). Sensitivity analyses define the sensitivity of model output to variation in input parameters, thus identifying those variables to which the model is most sensitive and which require most attention (Anderson and Burt, 1985; Crosetto *et al.*, 2000; Saltelli *et al.*, 2000; Mulligan and Wainwright, 2004). They aim to quantify and to rank the importance of each input parameter in determining output variability (Homma and Saltelli, 1996). If these parameters are identified, the greatest source of variation can be reduced (Saltelli, 2002).

Lane *et al.* (1994) recognised that the assessment of a model should not solely involve comparing model predictions to observed (external) data as these data may have associated problems such as the reliability of the gauging instruments. Thus assessment of model behaviour should also include internal validation where the model is assessed in terms of imposed conditions in order to gain confidence in the model predictions. Lane *et al.* (1994) and Howes and Anderson (1988) stated that this ensures that:

(1) the model behaviour is realistic in terms of its response to input parameters and boundary conditions;
(2) the model is sufficiently sensitive to represent the variation in the system; and

(3) the input parameters to which the model is most sensitive are identified.

If a model is relatively insensitive to a particular parameter, the uncertainty of that parameter is more acceptable. The sensitivity analysis will be undertaken as part of the model calibration process which aids the refinement of the model (Crosetto and Tarantola, 2001). Model calibration will be discussed in Section 4.6.

4.2.2 Experimental design

The design of the sensitivity analysis was based on that of Saltelli *et al.* (2000) and consisted of five stages (Table 4.1). Each of these stages will be illustrated in turn in this report. Stages 1 to 3 will be discussed in the methodology section (4.2) and stages 4 to 5 in the results and discussion sections (4.3 to 4.5).

The first step of the sensitivity analysis was to determine the input factors to be analysed. It was necessary to test the sensitivity of parameters which typically have the most influence on model results. These are recognised as roughness coefficients, inflows, topography and structures in the system. Similarly, it was important to cover the parameters studied in the EA *River Ure and Tributaries Modelling study* for the ISIS model. This determined the factors that would be studied here: channel and floodplain roughness, hydrograph inflows and the weir coefficient.

1. Design the experiment and determine which input factors should be analysed. Which factors will best reveal the way in which the response is affected by the input parameters?
2. Assign a range of variation to each input factor
3. Generate input matrix through appropriate design
4. Evaluate the model, so creating output distribution for the response of interest
5. Assess the influences/importance of each input on the output variables

Table 4.1 Stages in performing a sensitivity analysis. Based on Fisher (1935) and Saltelli *et al.* (2000).

4.2.3 Variation of each input parameter

Each of the parameters were varied in a systematic way, using an increase and decrease of 20% for all parameters. This follows the method used by the EA in their modelling report. Varying the parameters by a fixed percentage is a method recognised by Hamby (1994) as a reliable way to quantify the change in model output. Manning's *n* values were varied in accord with Chow (1959). The Manning's *n* values determined by the EA for the Ure model range from 0.015 to 0.097 for the channel and 0.02 to 0.16 for the floodplains. The values selected for *n* for the sensitivity analysis lie between 0.02 and 0.2 in order to capture the possible range of responses. Lower values of Manning's *n* were tested but the model became unstable when values of 0.015 were used. A large range of *n* values allows the modeller to view the exact influence of the parameter on the model output.

4.2.4 Input matrix – one-at-a-time approach

For models with a high number of input parameters, screening methods are often used to identify the parameters that control most of the output variability as it reduces the number of model evaluations (Saltelli *et al.*, 2000). The simplest approach is to vary each parameter one-at-a-time. The sensitivity of the parameters can be ranked quickly using this method. Each parameter is increased by a given percentage whilst the others remain constant (Hamby, 1994). The effect of each of the parameters on model output can be quantified, highlighting which has the most influence on model performance (Daniel, 1973). Here, the standard one-at-a-time method was primarily used, varying one factor in each run from the standard condition. A summary of the parameters tested is found in Table 4.2.

Manning's *n* was the main parameter assessed in the analysis as it is noted by many authors to have a significant influence on model output (Werner *et al.*, 2005; Anderson *et al.*, 2006; McGahey *et al.*, 2009). Yu and Lane (2006a) noted that 1-D models often display a high sensitivity to channel roughness. The roughness of the model was varied globally (variation 1 – Table 4.2), then just for the channel (variation 2) and just for the floodplain (variation 3). The roughness of the floodplain (the over-bank zone) was varied for both left over-bank and right over-bank together (variation 3) and then independently (variations 4 and 5). This process was repeated to analyse the sensitivity to roughness

long each of the tributaries in turn; global, channel and floodplain roughness were tested along the River Ouse, River Swale and the River Nidd.

Secondly, the sensitivity of the model outputs to the inflow hydrographs was assessed by increasing and decreasing the flow by 20% (variation 6). These new input values were subsequently used to look at the sensitivity of the model to both changed inflow and roughness values (variations 7-12). Thus the modified inflow hydrographs of +20% and -20% were run together with roughness changes as before. This method deviates from the one-at-a-time technique as a combination of factors is used, often referred to as *factoral design* (Saltelli *et al.*, 2000).

Thirdly, the sensitivity of the model outputs to the weir coefficients was assessed (variation 13). All of the weirs were removed from the model and then individually to see their impact on the output discharge. The values of the weir coefficients were increased and decreased by 20%, as with the inflow hydrographs.

In order to quantify the sensitivity of the model to change in Manning's *n* and the weir coefficient, the following equation was used:

$$Sensitivity = \frac{dQ_{max}}{dn} \cdot \frac{n}{\overline{Q_{max}}}$$

Equation 4.1

This is the sensitivity coefficient which expresses the ratio of change in the output (max. discharge) to the change in input (Manning's *n*) whilst all other parameters remain constant (Hamby, 1994).

Parameter	Variation	Description
1. Global roughness	20%	Manning's *n* increased by 20%
	-20%	Manning's *n* decreased by 20%
	n = 0.02-0.2	Manning's *n* values of 0.02-0.2
2. Channel roughness	20%	Manning's *n* increased by 20%
	-20%	Manning's *n* decreased by 20%
	n = 0.02-0.2	Manning's *n* values of 0.02-0.2
3. Floodplain roughness	20%	Manning's *n* increased by 20%
	-20%	Manning's *n* decreased by 20%
	n = 0.02-0.2	Manning's *n* values of 0.02-0.2
4. Left bank of floodplain	20%	Manning's *n* increased by 20%
	-20%	Manning's *n* decreased by 20%
	n = 0.03-0.2	Manning's *n* values of 0.03-0.2
5. Right bank of floodplain	20%	Manning's *n* increased by 20%
	-20%	Manning's *n* decreased by 20%
	n = 0.03-0.2	Manning's *n* values of 0.03-0.2
6. Inflow	20%	Inflows increased by 20%
	-20%	Inflows decreased by 20%
7. Inflow and global roughness	20%	Inflows increased by 20% and Manning's *n* increased by 20%
	-20%	Inflows increased by 20% and Manning's *n* decreased by 20%
	n = 0.03-0.2	Inflows increased by 20% and Manning's *n* values of 0.03-0.2
8. Inflow and channel roughness	20%	Inflows increased by 20% and Manning's *n* increased by 20%
	-20%	Inflows increased by 20% and Manning's *n* decreased by 20%
	0.03-0.2 *n*	Inflows increased by 20% and Manning's *n* values of 0.03-0.2
9. Inflow and floodplain roughness	20%	Inflows increased by 20% and Manning's *n* increased by 20%
	-20%	Inflows increased by 20% and Manning's *n* decreased by 20%
	n = 0.03-0.2	Inflows increased by 20% and Manning's *n* values of 0.03-0.2
10. Inflow and global roughness	20%	Inflows decreased by 20% and Manning's *n* increased by 20%
	-20%	Inflows decreased by 20% and Manning's *n* decreased by 20%
	0.03-0.2 *n*	Inflows decreased by 20% and Manning's *n* values of 0.03-0.2
11. Inflow and channel roughness	20%	Inflows decreased by 20% and Manning's *n* increased by 20%
	-20%	Inflows decreased by 20% and Manning's *n* decreased by 20%
	n = 0.03-0.2	Inflows decreased by 20% and Manning's *n* values of 0.03-0.2
12. Inflow and floodplain roughness	20%	Inflows decreased by 20% and Manning's *n* increased by 20%
	-20%	Inflows decreased by 20% and Manning's *n* decreased by 20%
	n = 0.03-0.2	Inflows decreased by 20% and Manning's *n*

		values of 0.03-0.2
13. Weir coefficient	20%	Weir coefficient increased by 20%
	-20%	Weir coefficient decreased by 20%

Table 4.2 Summary of parameters assessed in the sensitivity analysis. Manning's n values were assigned to every cross-section in the model, following this matrix. For example, in number 2, the same value for channel Manning's *n* was used throughout the model and the floodplain *n* values remain with the original values (set out in the ISIS model). The parameters above were also assessed for each of the reaches independently, for example, varying only channel *n* for the Ouse whilst all other parameters remained unchanged. Manning's *n* values of between 0.02 and 0.2 (0.02, 0.03, 0.05, 0.07, 0.09, 0.1, 0.15, 0.2) were used for the first three parameter simulations. Parameter simulations 4-13 do not include a simulation at a Manning's *n* value of 0.02. Some of the simulations became unstable at higher values of Manning's *n*.

4.2.5 Evaluation – objective functions

Both qualitative and quantitative methods should be used to compare modelled and observed data: qualitative techniques allow a visual analysis of the results whilst quantitative techniques numerically show the agreement. The examination of the sensitivity analysis results follows that of Green and Stephenson (1986) and Janssen and Heuberger (1995). A number of objective functions have been used to assess the goodness-of-fit of the simulated hydrographs with the observed hydrograph. A range of criteria were chosen as this allows different elements of model prediction to be considered (Green and Stephenson, 1986). Scatter plots were used to represent the output data from the sensitivity analysis as they are one of the most intuitive methods for presenting the results (Saltelli *et al.*, 2000).

Nash-Sutcliffe coefficient

The Nash-Sutcliffe coefficient was derived to evaluate the efficiency of a model (Nash and Sutcliffe, 1970; Green and Stephenson, 1986). It is now used as a standard assessment of model efficiency and is preferred to other objective functions. Thus it was used here to determine the efficiency of the HEC-RAS model.

$$R^2 = \frac{F_o^2 - F^2}{F_o^2}$$

$F_o^2 = \sum_{i=1}^{n}\left[q_o^{(t)} - \bar{q}\right]^2$ where $\bar{q}$ = mean observed discharge (averaged over the 300 hour time period of the modelled event)

$F^2 = \sum_{i=1}^{n}\left[q_o^{(t)} - q_s^{(t)}\right]^2$ where $q_o^{(t)}$ = observed discharge at time t
$q_s^{(t)}$ = simulated discharge at time t

Equation 4.2

F^2 is the *index of disagreement*, defining the difference between the observed and simulated data and F_o^2 is the *initial variance* (Nash and Sutcliffe, 1970). The efficiency of the model can then be defined as R^2.

After calculating R^2, the values received were very low, which did not represent the similarity observed from a visual comparison between the observed and simulated hydrographs. It was evident that $\bar{q}$ was affecting R^2. Instead of using a fixed mean for calculating Nash-Sutcliffe, a moving average presented a better method for comparing the observed and simulated results. This is because the discharge values in the hydrograph were highly varied from the mean, thus a fixed mean created a lower R^2 value than expected for the simulated and observed hydrographs. A 29-point moving average was chosen as this represented 10% of the data returned by the sensitivity analysis (peak discharge was recorded each hour for 300 hours). This relates the simulated and observed data to a benchmark, the mean of the observed. Much higher values of R^2 were returned with this correction.

Percentage error in peak (PEP)

$$PEP = \frac{q_{ps} - q_{po}}{q_{po}} x\ 100$$

where q_{ps} = simulated peak discharge
q_{po} = observed peak discharge

Equation 4.3

PEP compares the observed and simulated data using an average over the time series (Green and Stephenson, 1986; Janssen and Heuberger, 1995). The averaging used in this method smooths out key features of the dataset and is affected by outliers (Janssen and Heuberger, 1995).

Root Mean Square Error (RMSE)

$$RMSE = \left[\frac{1}{n}\sum_{i=1}^{n} \left(q_o^{(t)} - q_s^{(t)}\right)^2\right]^{1/2}$$

Equation 4.4

RMSE is a measure of the average magnitude of the error (Green and Stephenson, 1986; Janssen and Heuberger, 1995). It compares a point in the observed data with the same point in the simulated data, expressing the spread in the data. Since the errors are squared before being averaged, the RMSE gives relatively high weight to large errors, which is a problem if the observed and simulated hydrographs do not match well in places. If model errors are significant, RMSE is not the best method to assess agreement between the model and data objectively (Janssen and Heuberger, 1995). RMSE was calculated for global, channel and floodplain roughness variations. It was also calculated for distinct sections on the observed- simulated graph, to quantify the location of the best fit between the observed and simulated hydrographs. This shows that the falling limbs of the hydrographs skew the data to a higher RMSE whilst in most regions there is a good fit between the hydrographs. For this reason, the Nash-Sutcliffe index is more desirable.

Mean Absolute Error (MAE)

$$MAE = \frac{1}{n}\sum_{i=1}^{n}\left(q_o^{(t)} - q_s^{(t)}\right)$$

Equation 4.5

MAE is another measure of the average magnitude of the errors for a set of continuous variables (Janssen and Heuberger, 1995). It gives the average over the sample of the absolute values of the differences between forecast and observation. MAE is less sensitive to outliers than RMSE.

Peak Timing Error (PTE)

This can be useful to calculate the timing error between the simulated and observed hydrographs. For example, the peaks could be at the same discharge but desynchronised. Green and Stephenson (1986) recognised the need to account for this time-shift error.

$$PTE = \sqrt{\left(Tp_o^{(t)} - Tp_s^{(t)}\right)^2}$$

Equation 4.6

Tp_o = peak timing of observed data

Tp_s = peak timing of simulated data

The peak timing error was calculated for each of the peaks on the hydrograph and the mean error recorded. This gives a good indication of the influence of parameters on model output as attenuation and translation can be identified.

4.3 Results: model predictions

4.3.1 Discharge response to Manning's *n*

Global *n*

Figure 4.1 shows that varying Manning's *n* globally across the whole model has a large influence on the modelled output at Skelton. The baseline used for these comparisons is the output hydrograph at Skelton returned after initial model building. The results are presented to one decimal place because the input hydrographs were recorded to this degree of precision. Low values of *n* (0.02 and 0.03) caused the discharge hydrograph to increase dramatically, particularly at the peaks. A clear trend was shown for higher values of *n* (0.05 to 0.09): the peak was reduced and the timing of the hydrograph shifted. It shows that increasing *n* values by 20% reduces the discharge hydrograph slightly, with a small delay in peak timing. In contrast, decreasing *n* by 20% increases the output discharge and advances the peak slightly. A Manning's *n* of 0.02 increases the peak discharge dramatically, with an increase of over 100 m^3/s for the first peak. The peak discharge is also increased with a Manning's *n* of 0.03. However, Manning's *n* of 0.05 reduces the peak discharge and the peaks occur slightly later. Manning's *n* of 0.07 and 0.09 reduce the peak discharge dramatically and the overall shape of the hydrograph is changed. A large lag is caused in the peak timing as a result of high values of Manning's *n*. Figure 4.2 illustrates the influence of varying global Manning's *n* on peak discharge. With a roughness value of 0.02 the peak discharge is 588.7 m^3/s and at 0.09 the peak discharge has reduced considerably to 395.3 m^3/s, although the reduction in peak discharge is quite gradual as Manning's *n* increases. Table 4.3 shows the change in peak timing delay as global Manning's *n* increased. The mean peak timing error is only 2 hours for the original

simulated run, which increases gradually to 24 hours at a Manning's *n* of 0.09. Using Equation 4.1, the sensitivity of the model to changing Manning's *n* globally was calculated as -0.3, a relatively high degree of sensitivity (Table 4.4).

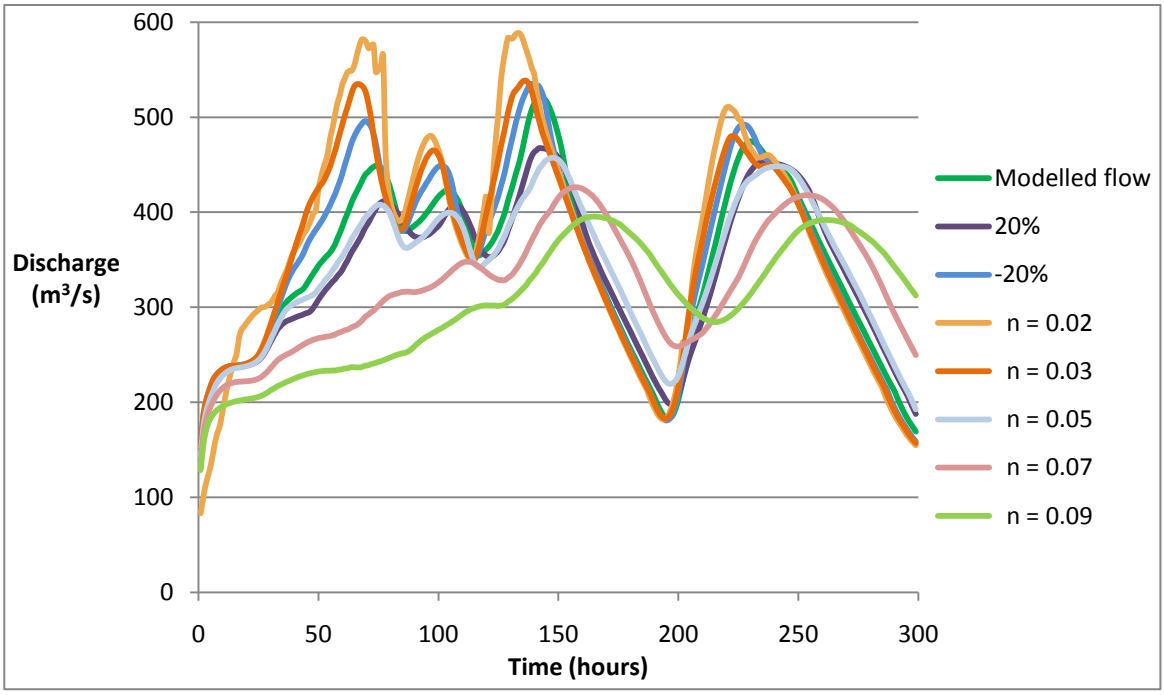

Figure 4.1 Discharge response to changes in global Manning's *n* for all reaches in the model. 'Modelled flow' refers to the output hydrograph at Skelton returned after initial model building. This is the baseline used for these comparisons. The lines labelled '20%' and '-20%' describe scenarios where Manning's *n* was increased or decreased, respectively, for the whole model.

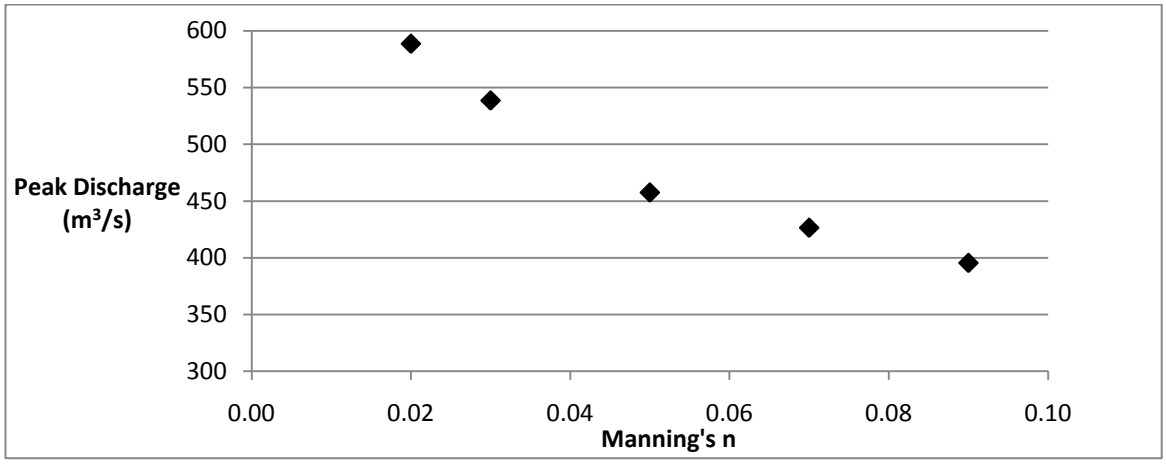

Figure 4.2 Peak discharge response to varying global Manning's *n*.

	Mean Peak Timing Delay (hr)		
Variation	**Global *n***	**Channel *n***	**Floodplain *n***
Modelled	2	-	-
20%	4.5	4	2
-20%	1.75	1.5	1.75
***n* = 0.02**	6.25	6.5	1.5
***n* = 0.03**	5.25	5.25	1.5
***n* = 0.05**	6	6.25	1.75
***n* = 0.07**	16.5	15.5	2
***n* = 0.09**	24	20.3	2.5
***n* = 0.1**	-	25	2.5
***n* = 15**	-	31	2.75
***n* = 0.2**	-	42	3

Table 4.3 Difference in mean peak timing delay between the simulated and observed hydrographs after varying Manning's *n* globally, for the channel and for the floodplain. Timing delay was calculated for each of the four peaks in the hydrographs and the mean peak timing delay is displayed in the table. The lags in mean timing delay in relation to the modelled run (the baseline) are both positive and negative. No results were recorded at high global *n* values due to instabilities in the model.

Parameter	Sensitivity
Global *n*	-0.3
Channel *n*	-0.2
Floodplain *n*	0.0
Left bank *n*	0.0
Right bank *n*	0.0
Ouse global *n*	-0.4
Swale global *n*	0.0
Nidd global *n*	0.0
Inflow+20%, global *n*	-0.3
Inflow+20%, channel *n*	-0.1
Inflow+20%, fplain *n*	0.0
Inflow-20%, global *n*	-0.4
Inflow-20%, channel *n*	-0.2
Inflow-20%, fplain *n*	0.0
Linton weir coefficient	0.2
Cundall weir coefficient	0.0

Table 4.4 Sensitivity of discharge to variations in roughness, inflow and weir coefficients.

Channel *n*

The following sections explore whether the global effects discussed above can be attributed to either the *river channel* or the *floodplain*. Figure 4.3 shows that variations in channel Manning's *n* also greatly influence discharge. In these simulations, floodplain *n* was not varied and the values for Manning's *n* remain the same as in the original 'modelled flow' (the values used in the ISIS model). The hydrographs show that the same patterns are produced after varying channel *n* as with global *n*, however the discharges are slightly lower after varying channel *n*. This can be seen by comparing the discharge hydrograph using *n* = 0.09 in Figure 4.3 with the same hydrograph in Figure 4.1. Figure 4.4 shows that peak discharge is greatly reduced with increasing *n* values for the channel. With *n* = 0.02 the peak discharge is 579.8 m^3/s and at *n* = 0.2 the peak discharge is 393.5 m^3/s. At *n* values greater than 0.1, the influence on peak discharge is negligible. Table 4.3 shows the change in peak timing error as channel Manning's *n* increased. The mean peak timing error is approximately 0.25 to 0.5 hours less than for global changes to *n*, therefore showing that channel Manning's *n* has a smaller influence on peak timing than global *n*. At *n* = 0.09, peak timing error is 3.6 hours less for channel *n* than global *n*. Using Equation 4.1, the sensitivity of the model to changing Manning's *n* for the channel was calculated as -0.2, which is slightly less than for global *n* (Table 4.4).

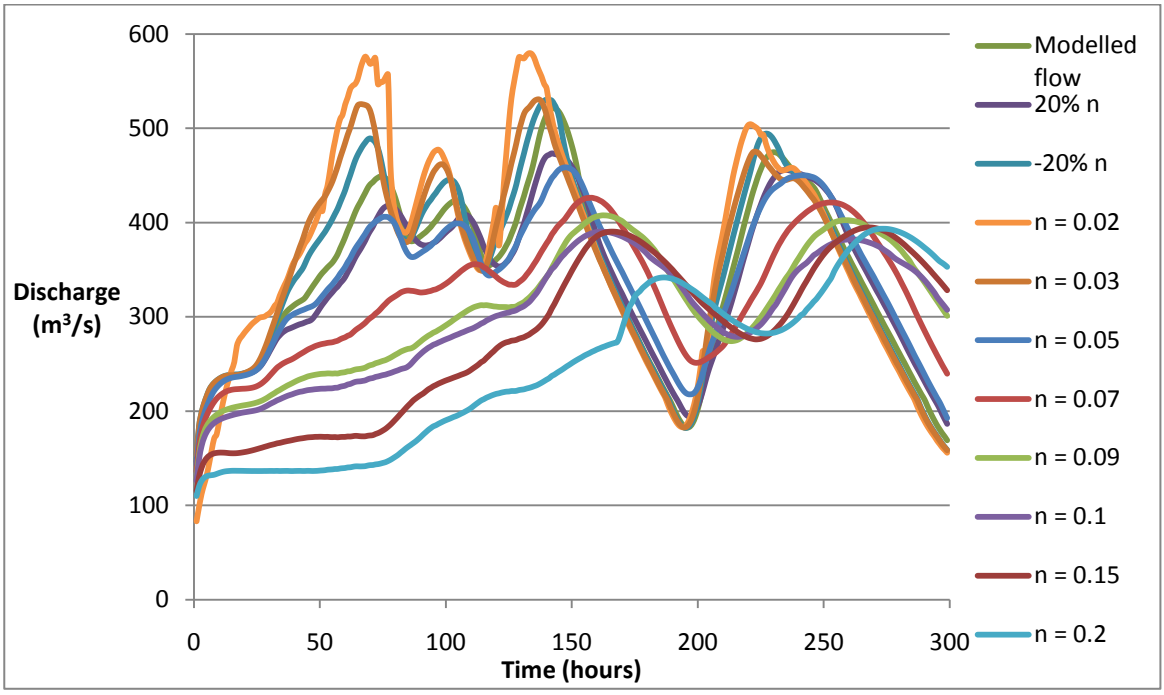

Figure 4.3 Discharge response to changes in channel Manning's *n* for all reaches in the model.

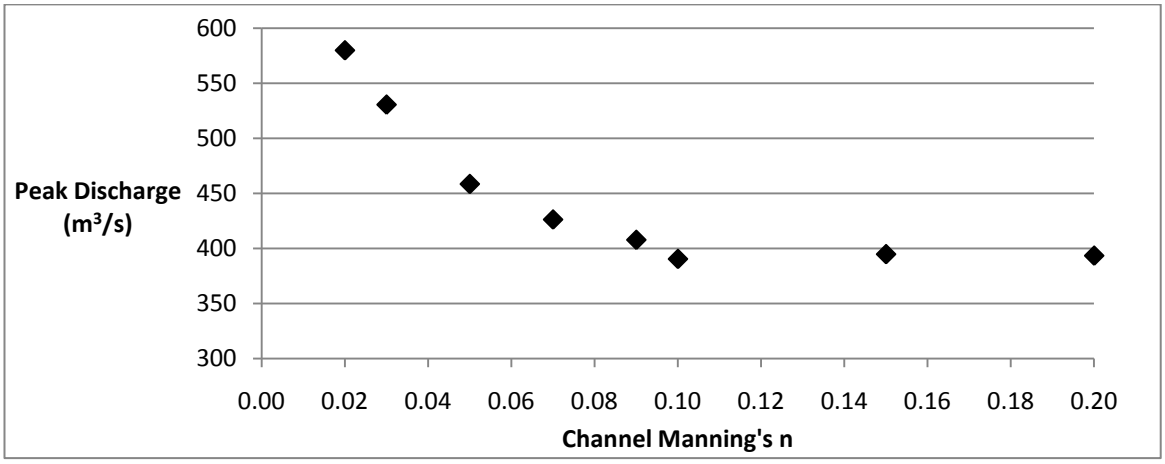

Figure 4.4 Peak discharge response to varying channel Manning's *n*.

Floodplain *n*

Figure 4.5 shows that in contrast to global and channel changes in *n,* varying floodplain Manning's *n* does not have a large effect on discharge. This is a pattern recognised in the literature by Yu and Lane (2006a, 2006b). The discharge hydrographs are slightly reduced for increasing values of floodplain *n* and the peaks are slightly shifted. Figure 4.6 shows the gradual reduction in peak discharge with increasing floodplain *n* values from 531.5 m^3/s at *n* = 0.02 to 498.8 m^3/s at *n* = 0.2. Table 4.3 shows that the mean peak timing error is much smaller than for global and channel *n* changes. A gradual increase in the timing error occurs from 1.5 hours at *n* = 0.02 to 3 hours at *n* = 0.2. The sensitivity of the model to changes in floodplain *n* was calculated as 0.00 (Table 4.4).

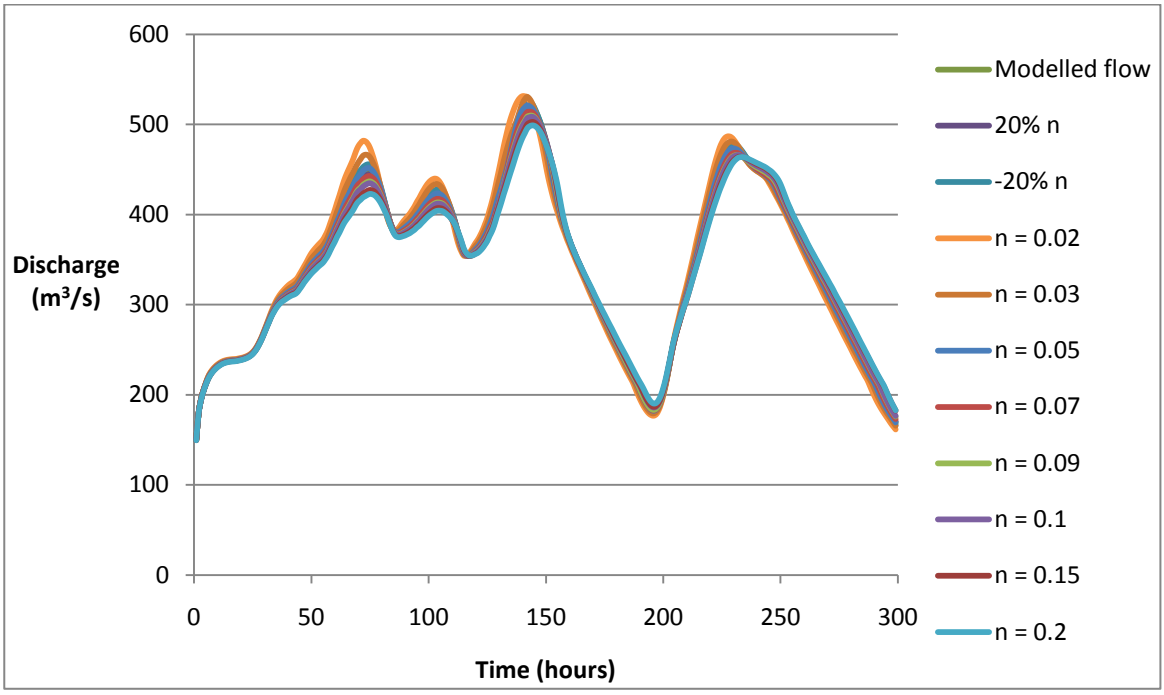

Figure 4.5 Discharge response to changes in floodplain Manning's *n* for all reaches in the model.

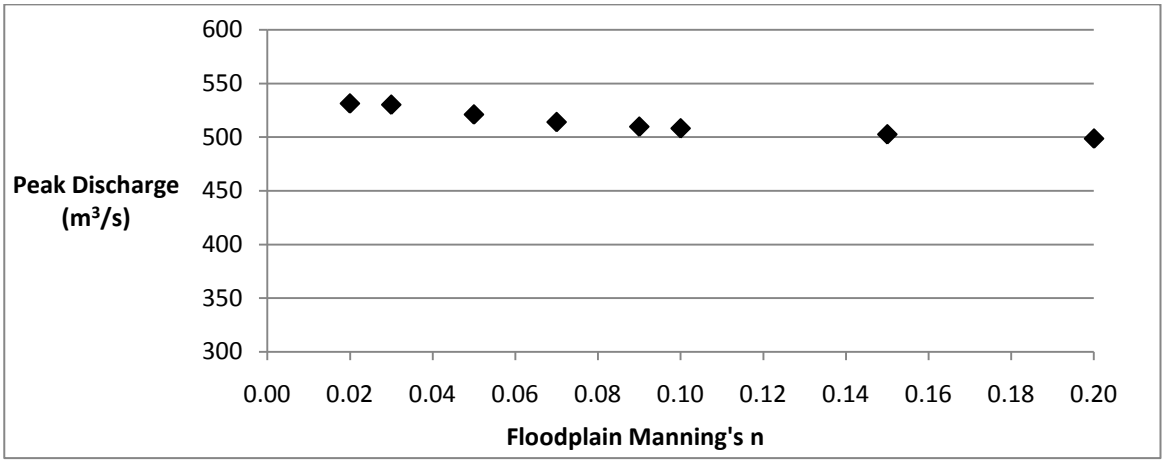

Figure 4.6 Peak discharge response to varying floodplain Manning's *n*.

Figures 4.7 and 4.8 indicate that varying only left bank floodplain roughness or right bank floodplain roughness alters discharge very slightly. The discharge hydrographs show that Manning's *n* for the left bank floodplain appears to have a slightly larger influence on discharge than right bank *n*, particularly at the peaks. Evidence for this is shown in Figure 4.9 where the left bank gives a range in discharge of 19 m^3/s compared to 11 m^3/s for the right bank. Table 4.3 shows that the sensitivity of the model to both left and right bank roughness changes is 0.00.

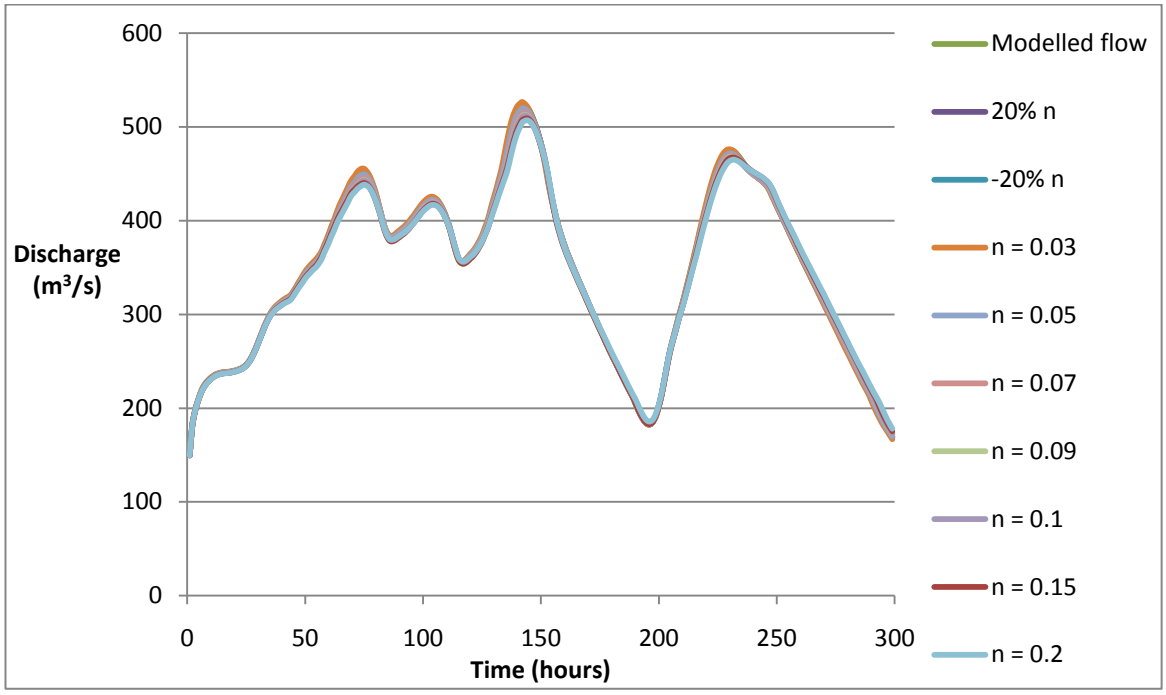

Figure 4.7 Discharge response to left bank floodplain changes in Manning's *n* for all reaches in the model.

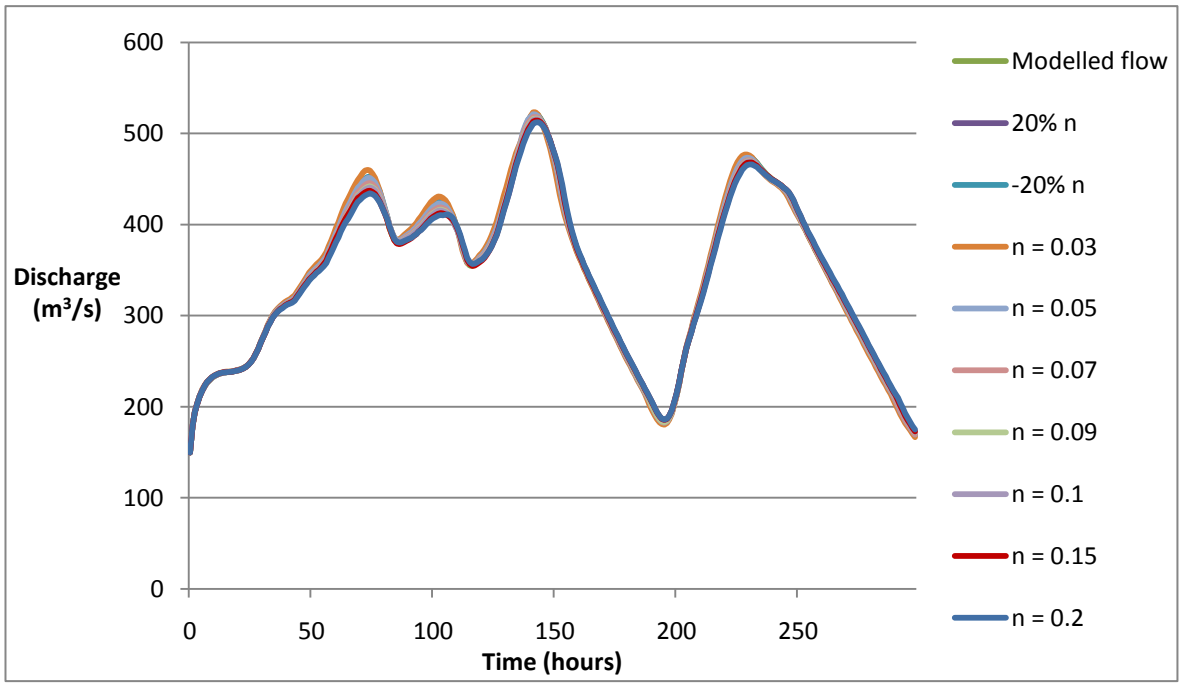

Figure 4.8 Discharge response to right bank floodplain changes in Manning's *n* for all reaches in the model.

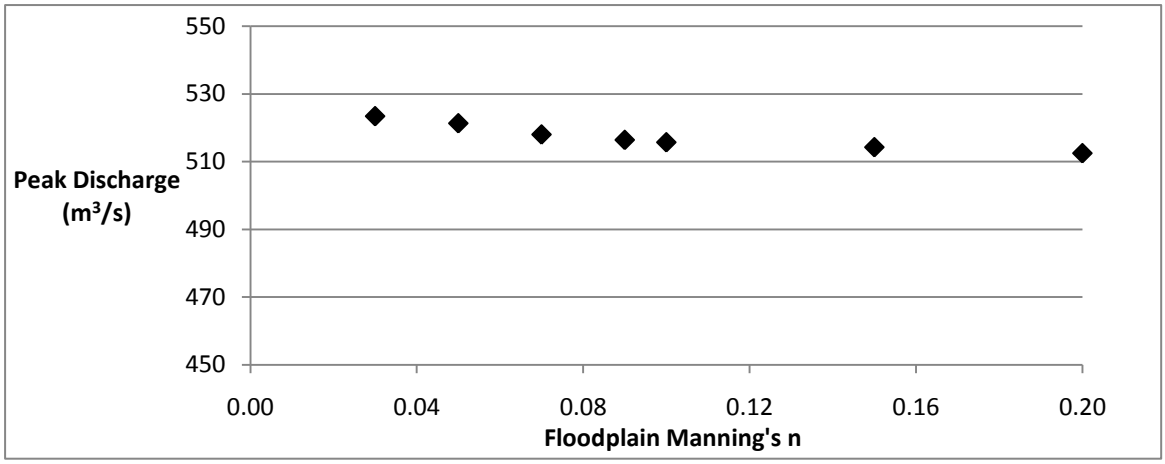

(a)

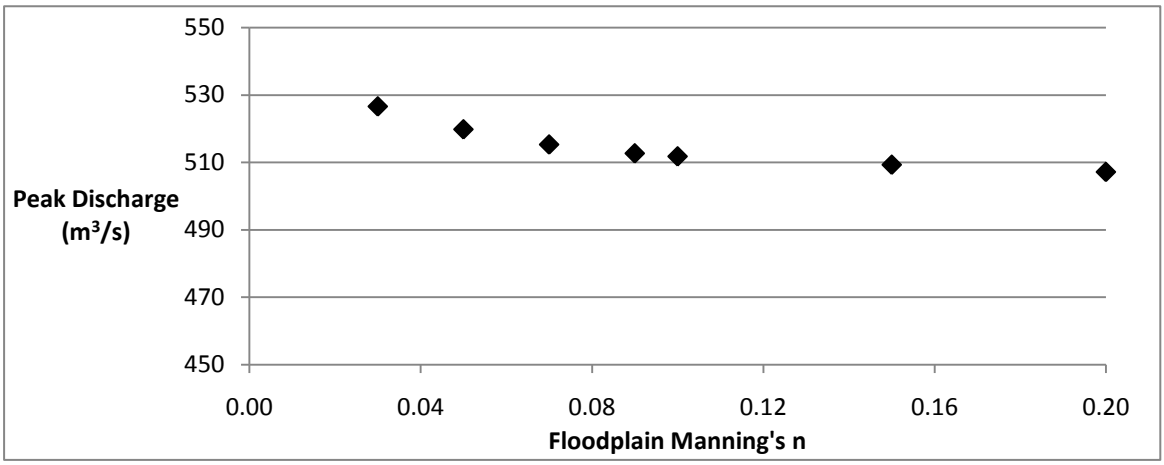

(b)

Figure 4.9 Peak discharge response to varying floodplain Manning's *n* for the left (a) and right (b) banks.

Manning's *n* for the tributaries

The influence of varying Manning's *n* within each of the three rivers on peak discharge was also assessed. Figure 4.10 shows the influence of varying Manning's *n* globally for each of the tributaries. Values for each of the tributaries were varied in turn, whilst all others remained unchanged. The discharge in the River Ouse is greatly affected by global changes in Manning's *n*, both reducing the peak and shifting the timing of the peaks. The River Swale and River Nidd responded to changes in global Manning's *n* but to a lesser extent. Figure 4.11 shows the influence of global *n* on the peak discharge for each of the tributaries. The peak discharges for the River Ouse had a much larger range than the other reaches; 174.3 m^3/s compared to 59.9 m^3/s and 19.0 m^3/s for the River Swale and River Nidd respectively.

Figure 4.12 shows the influence of varying Manning's *n* for the channel for each of the tributaries. The pattern is very similar to that of varying global *n* but the discharges are reduced slightly less for all tributaries. Figure 4.13 shows the influence of varying Manning's *n* for the floodplain for each of the tributaries. Only a very slight change in the discharge hydrograph is seen for the River Swale and River Nidd, with a slightly large change for the River Ouse. The model is very sensitive to changes in Manning's *n* values along the Ouse, with a calculated sensitivity of -0.4, but is not sensitive to changes in *n* along the Swale and Nidd (both 0.00) (Table 4.4).

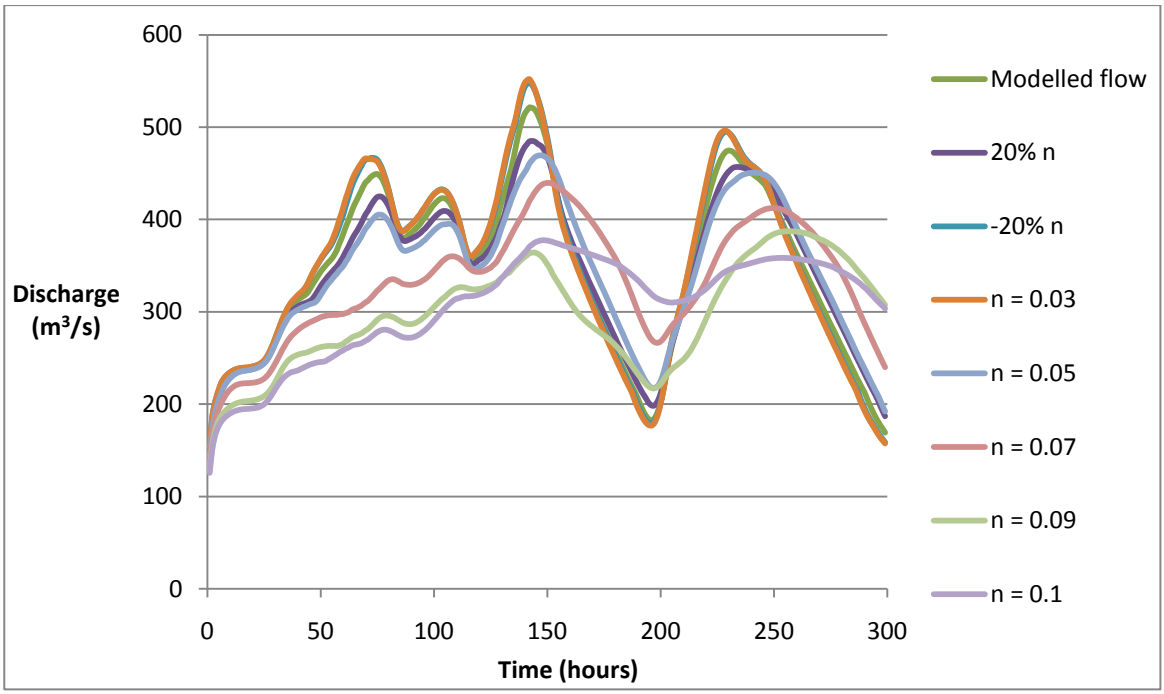

Figure 4.10 (a) Discharge response to changes in global Manning's *n* for the River Ouse.

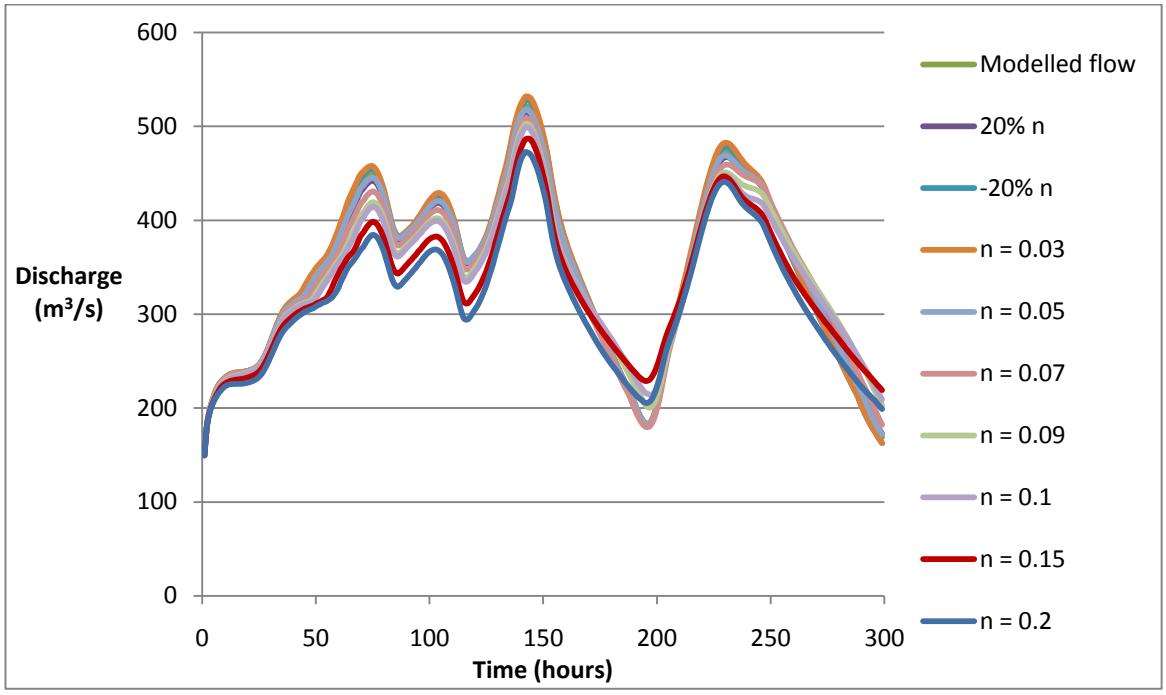

Figure 4.10 (b) Discharge response to changes in global Manning's *n* for the River Swale.

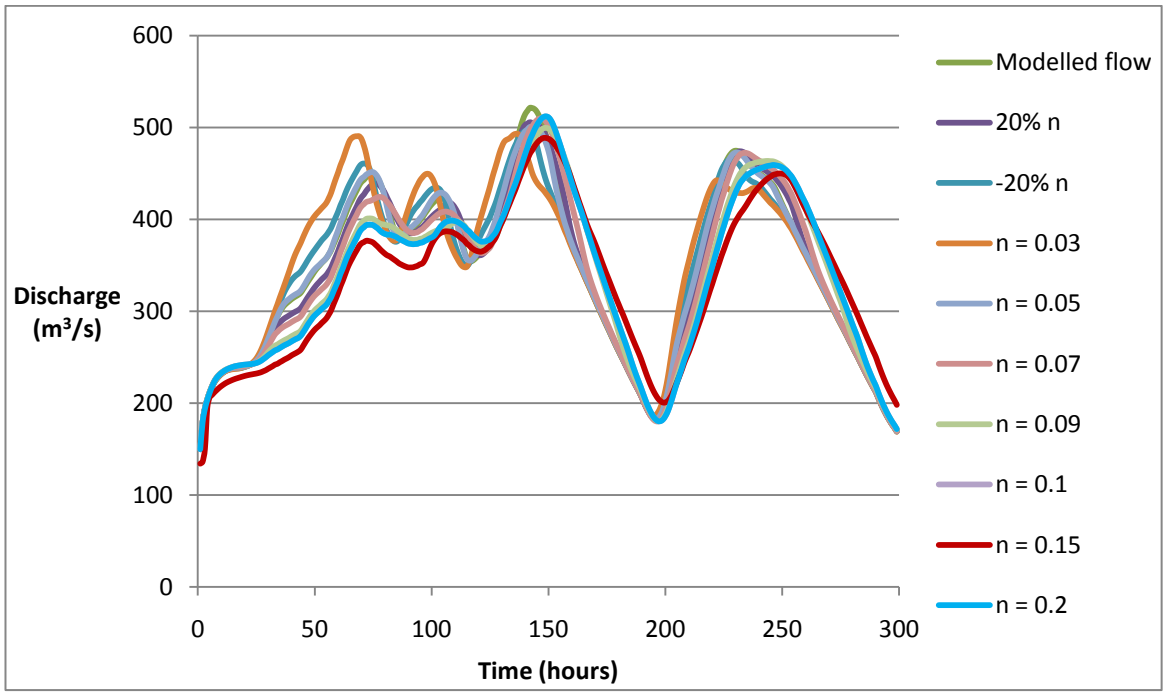

Figure 4.10 (c) Discharge response to changes in global Manning's *n* for the River Nidd.

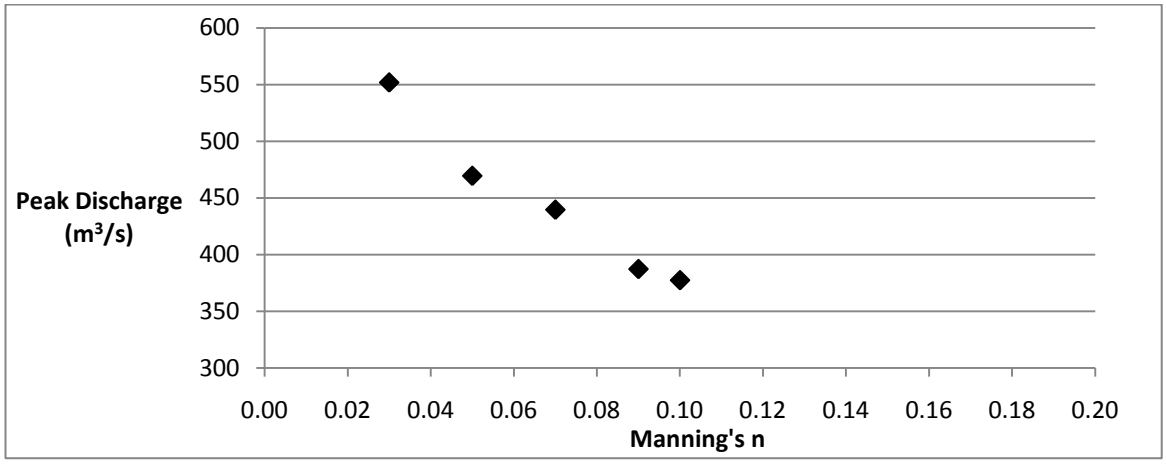

(a) Global Ouse *n* varied

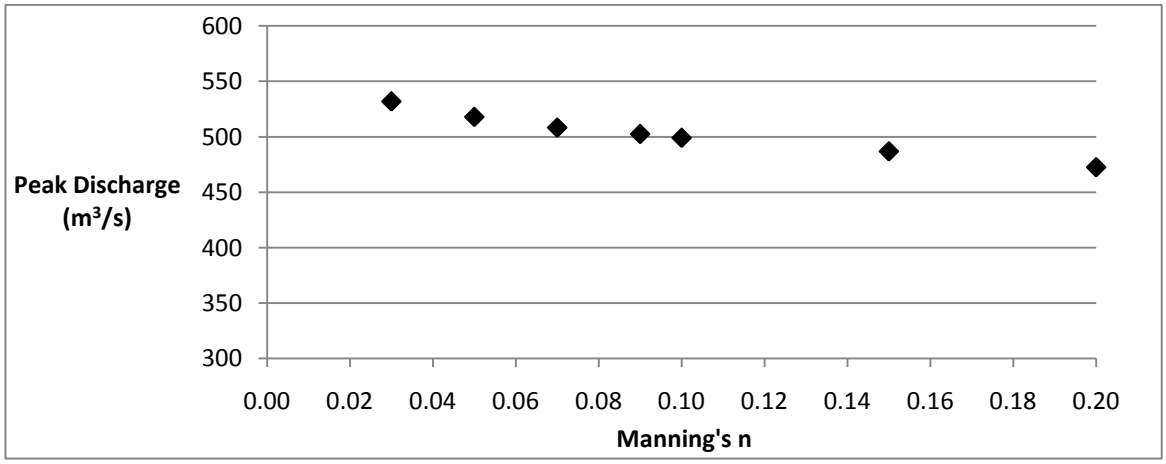

(b) Global Swale *n* varied

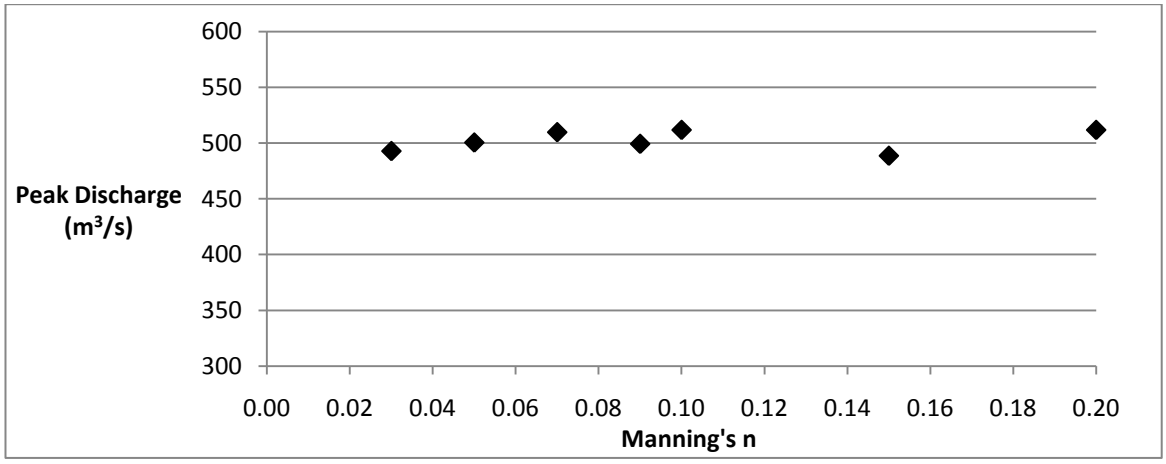

(c) Global Nidd *n* varied

Figure 4.11 Peak discharge response to varying global Manning's *n* in each of the three tributaries.

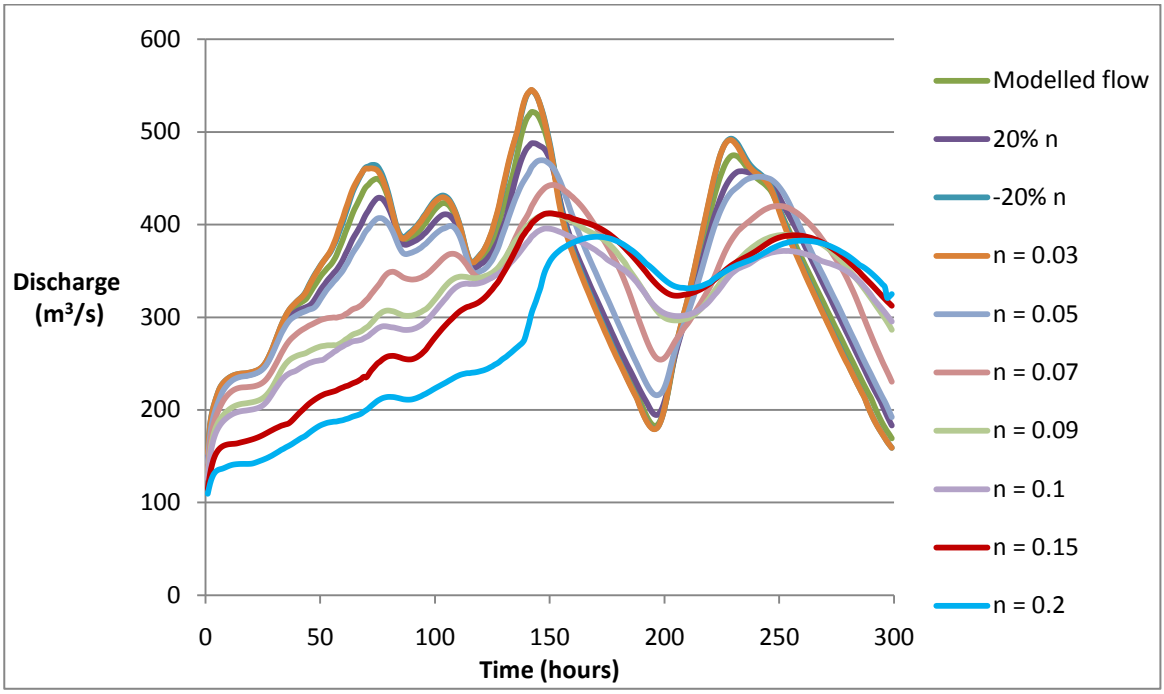

Figure 4.12 (a) Discharge response to changes in channel Manning's *n* for the River Ouse.

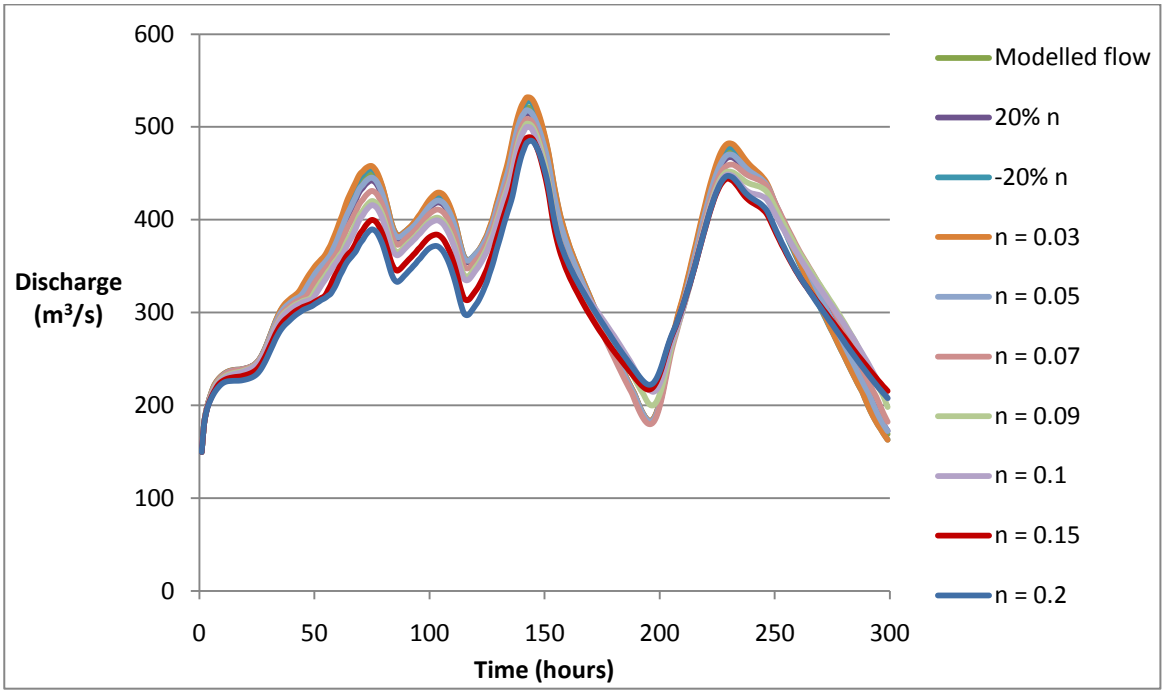

Figure 4.12 (b) Discharge response to changes in channel Manning's *n* for the River Swale.

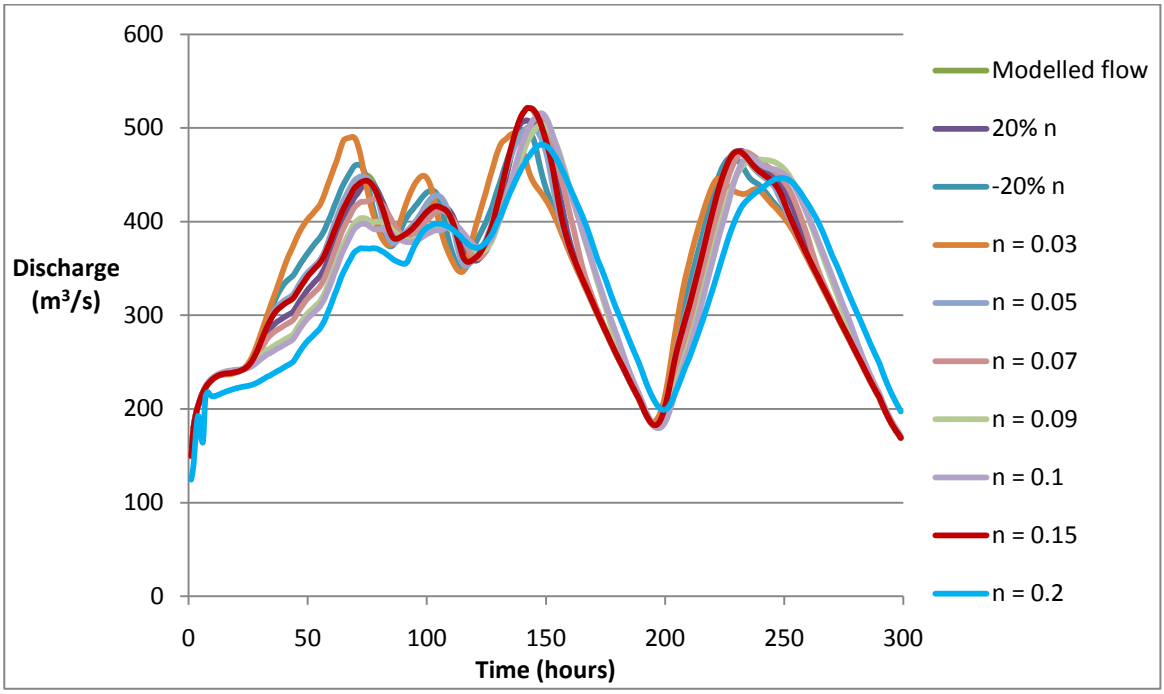

Figure 4.12 (c) Discharge response to changes in channel Manning's *n* for the River Nidd.

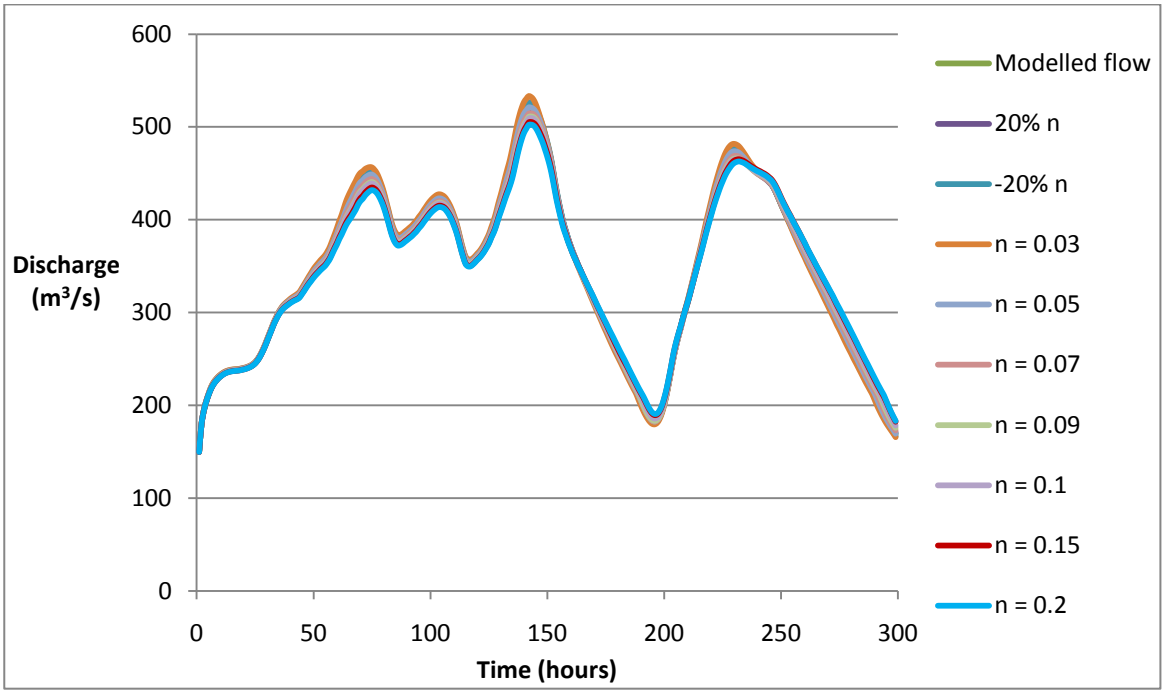

Figure 4.13 (a) Discharge response to changes in floodplain Manning's *n* for the River Ouse.

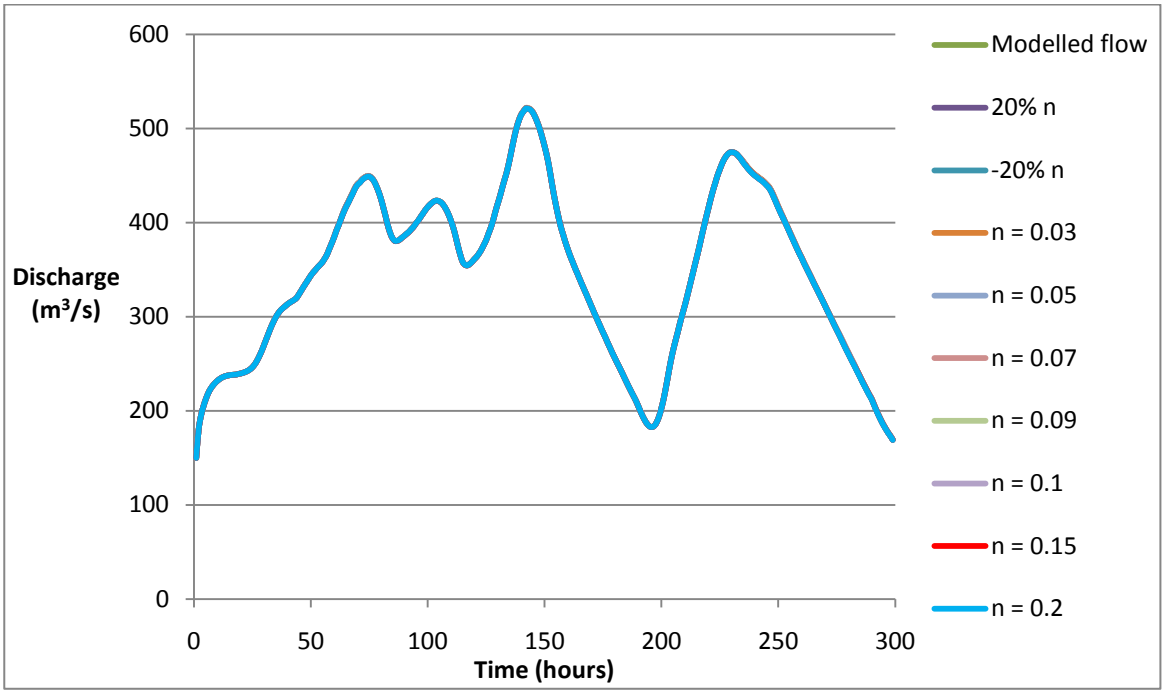

Figure 4.13 (b) Discharge response to changes in floodplain Manning's *n* for the River Swale. Variations to floodplain *n* did not change the hydrograph in these scenarios, thus all lines overlap on the graph.

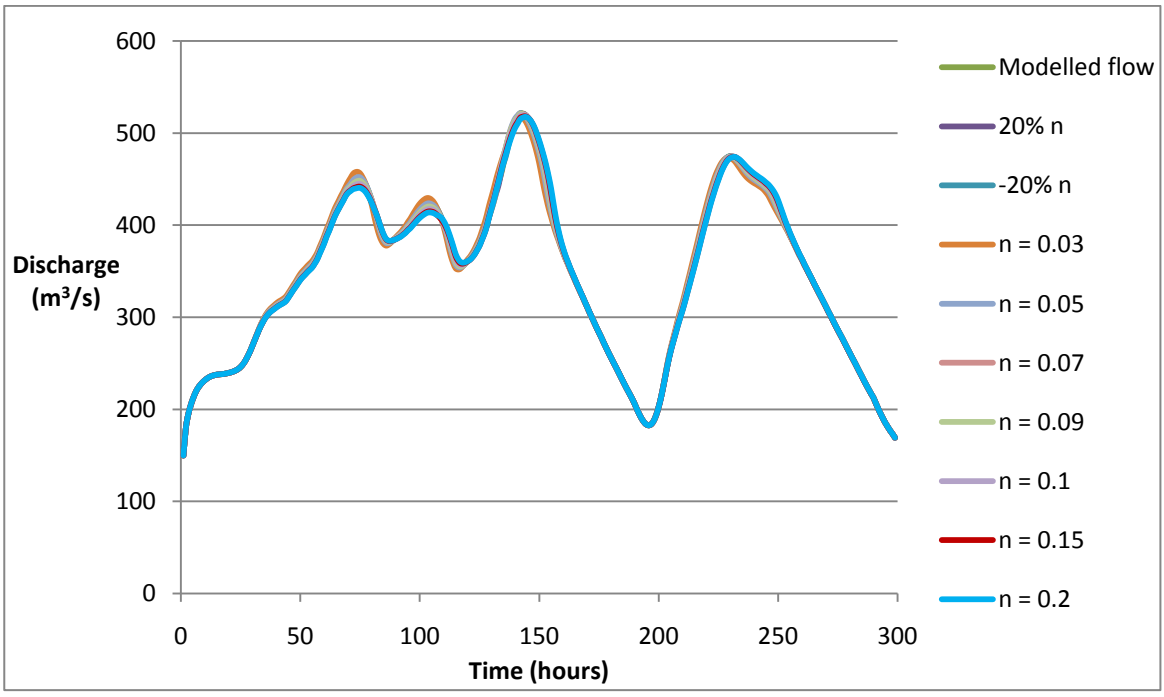

Figure 4.13 (c) Discharge response to changes in floodplain Manning's *n* for the River Nidd.

4.3.2 Discharge response to weir coefficient

This section explores the sensitivity of the model to the presence of weirs. As before, the output hydrograph for these simulations are compared to the original 'modelled flow'

returned after initial model building. Figure 4.14 shows that the whole shape of the hydrograph is affected by the introduction of Linton weir into the system whereas Cundall weir has little effect on the output hydrograph. Peak discharge is affected greatly by the presence of the weirs; discharge peaked at 521.4 m^3/s with the weirs compared to 629.8 m^3/s without weirs.

The weir coefficient used in the model had a small influence on discharge. The sensitivity of discharge to the weir coefficient varied with the weir in question. Figure 4.15 shows that the weir coefficient used for Linton weir had quite a large influence on discharge. The range in peak discharge was between 500.9 m^3/s to 539.1 m^3/s after increasing and decreasing the weir coefficient by 20%. Increasing the weir coefficient by 20% gave an R^2 of 0.98, compared to an R^2 of 0.97 after decreasing the weir coefficient by 20%. Increasing the weir coefficient by 20% showed an improved fit with the baseline ('modelled flow'). Table 4.5 shows that a higher weir coefficient value increased the mean peak timing delay to 2.5 hours, whilst a reduction in the weir coefficient value decreased mean peak timing delay to 1.5 hours.

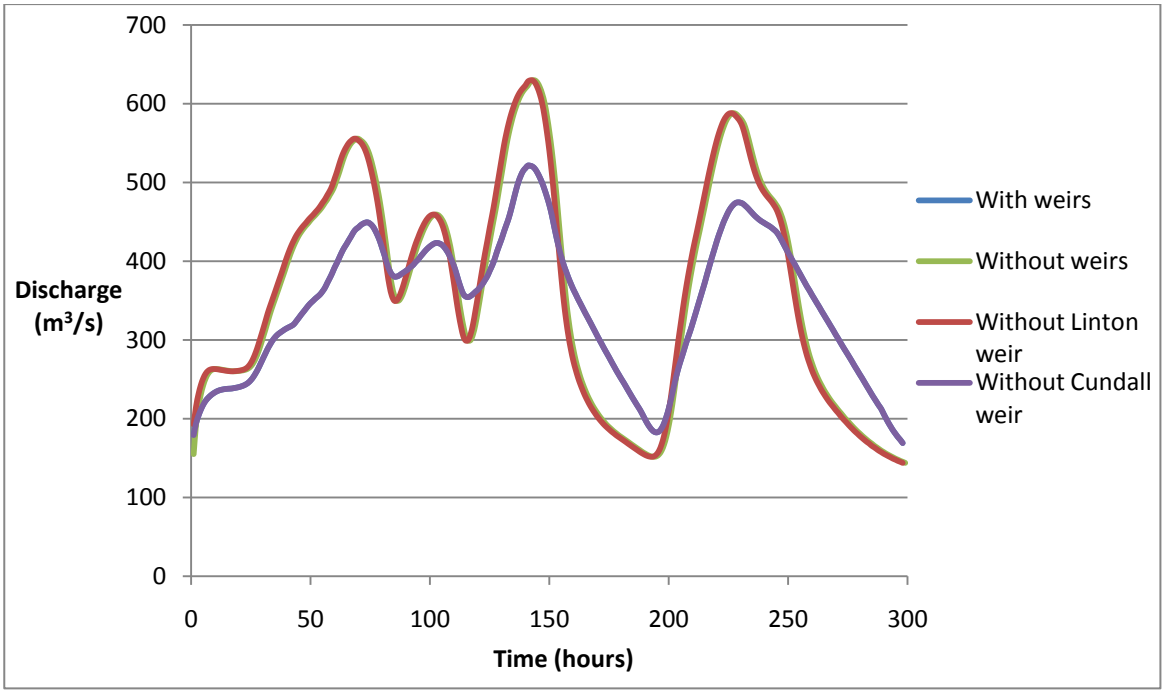

Figure 4.14 Effect of the weirs on the simulated hydrograph. The simulations 'with weirs', and 'without Cundall weir' overlap almost exactly. The simulations 'without weirs' and 'without Linton weir' also overlap almost exactly.

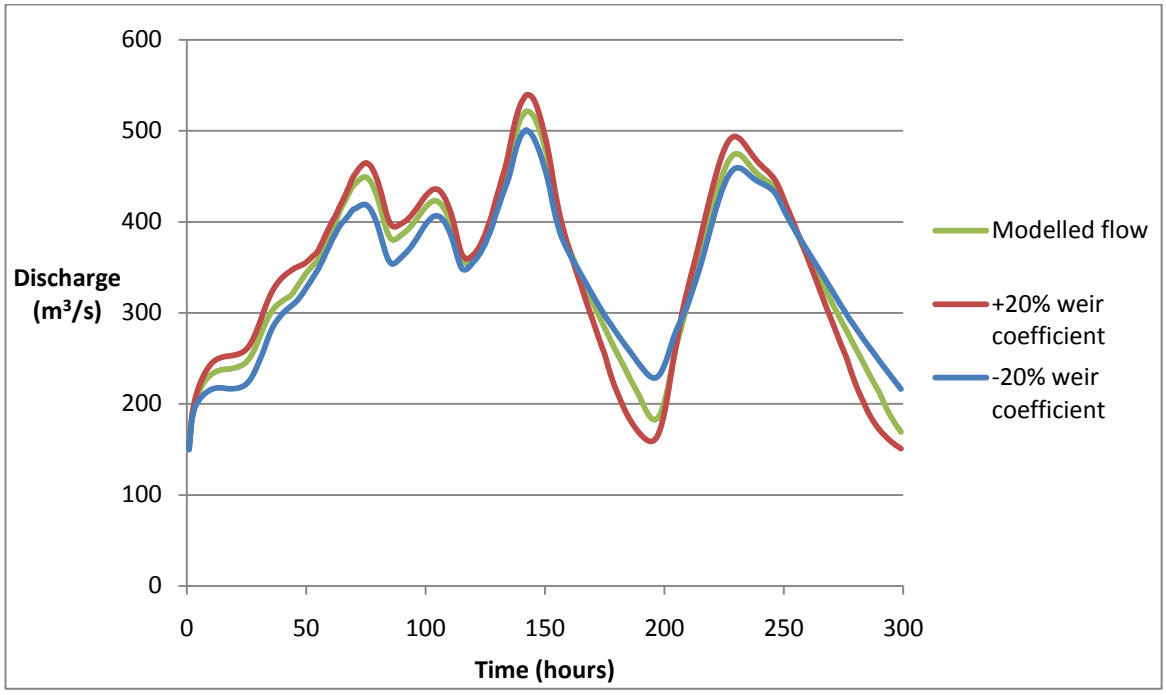

Figure 4.15 Effect of Linton weir coefficient on discharge.

Parameter	Peak No.	Peak Timing Delay (hr)	+ / - Time lag	Mean Peak Timing Delay (hr)
Weir coefficient +20% (Linton weir)	1	5	+	2.5
	2	1	+	
	3	2	+	
	4	2	-	
Weir coefficient -20% (Linton weir)	1	4	+	1.5
	2	1	+	
	3	1	+	
	4	0	+	
Weir coefficient +20% (Cundall weir)	1	5	+	2
	2	1	+	
	3	1	+	
	4	1	-	
Weir coefficient -20% (Cundall weir)	1	5	+	2
	2	1	+	
	3	1	+	
	4	1	-	

Table 4.5 Peak timing delay between the simulated and observed hydrographs after varying the weir coefficient by 20%. Timing delay was calculated for each of the four peaks in the hydrographs and the mean peak timing delay is displayed in the table. The lags in mean timing delay in relation to the modelled run (the baseline) are both positive and negative.

In comparison, the weir coefficient for Cundall weir had no effect on the discharge hydrograph. The R^2 value returned was the same after increasing and decreasing the weir coefficient (0.97), as the simulated discharge was only slightly affected. Similarly, Table 4.5 shows that the mean peak timing delay was not affected. The sensitivity of peak discharge to the Linton weir coefficient was calculated as 0.2 and to the Cundall weir coefficient as 0.0 (Table 4.4).

4.3.3 Discharge response to changing both inflow and Manning's *n*

Figures 4.16 (a) to (c) show that after increasing the inflow by 20% whilst also varying Manning's *n*, the discharge hydrographs do not change much in shape, but the peaks are approximately 50 m^3/s higher than when the original flow was used. The same pattern is shown, with discharge decreasing with increases in Manning's *n* (for global, channel and floodplain *n*). Similarly, Figures 4.17 (a) to (c) show that decreasing the inflow by 20% decreases the peak discharges by around 50 m^3/s, whilst the pattern remains the same. Figures 4.18 and 4.19 show that the changes in the inflow do not have a significant effect on the model as peak discharge still responds in the same way to Manning's *n*. Table 4.6 shows that increasing the inflow appears to increase the mean peak timing error. At a global value of $n = 0.03$ the mean timing error is 4.25 hours which increases to 27.5 hours at $n = 0.09$. In comparison a decrease in the inflow also increases the mean peak timing delay but to a lesser extent, from 3.5 hours at $n = 0.03$ to 18 hours at $n = 0.09$.

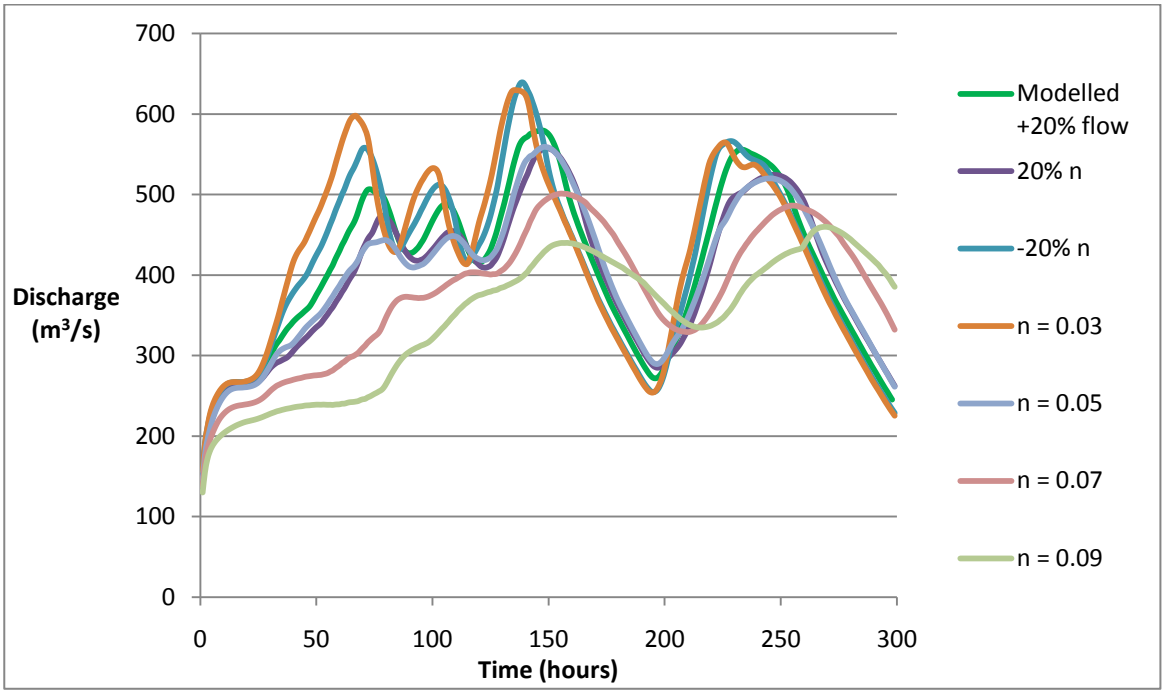

Figure 4.16 (a) Discharge response to a 20% increase in inflow and changes in global Manning's *n*.

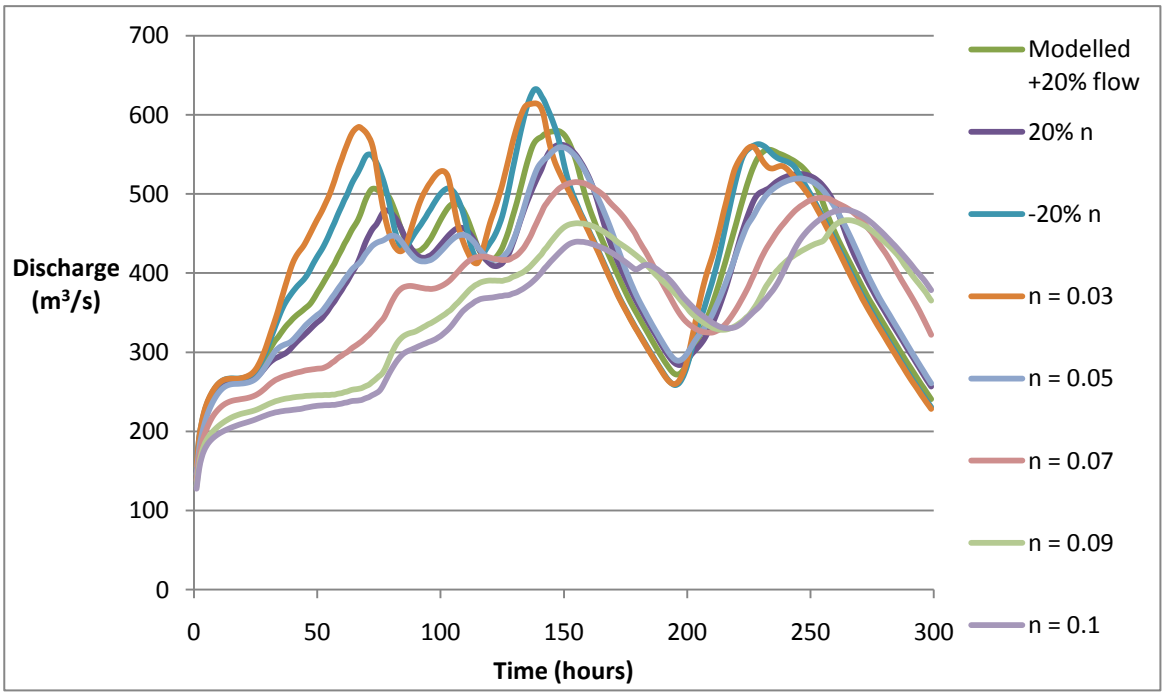

Figure 4.16 (b) Discharge response to a 20% increase in inflow and changes in channel Manning's *n*.

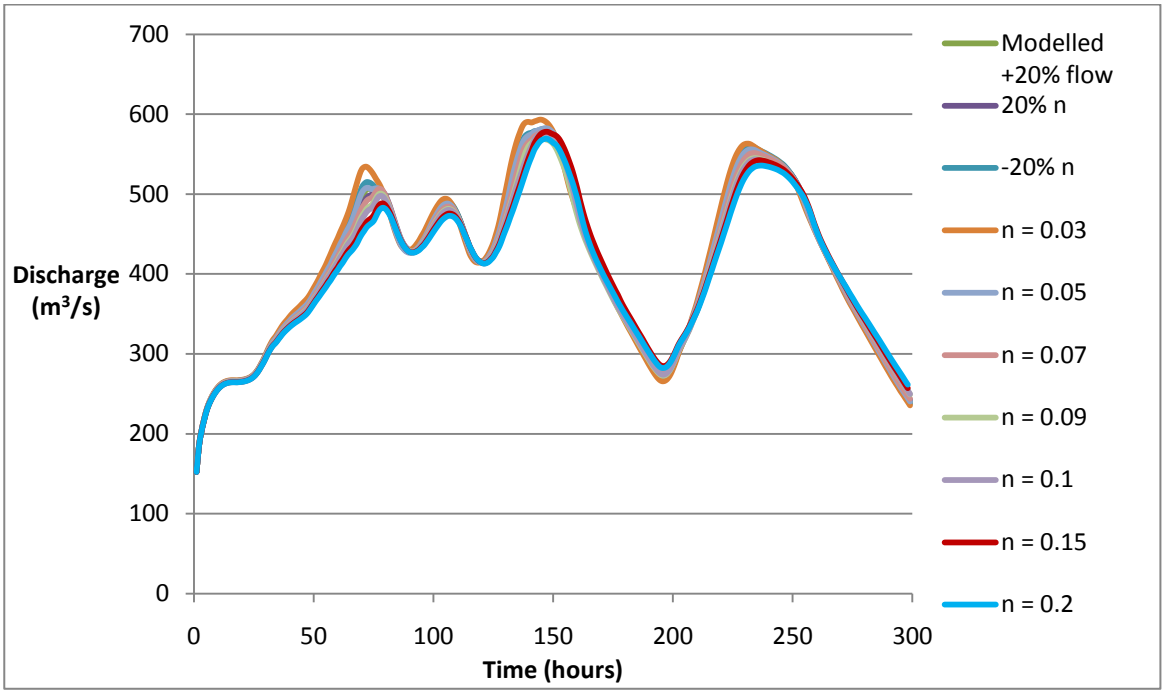

Figure 4.16 (c) Discharge response to a 20% increase in inflow and changes in floodplain Manning's *n*.

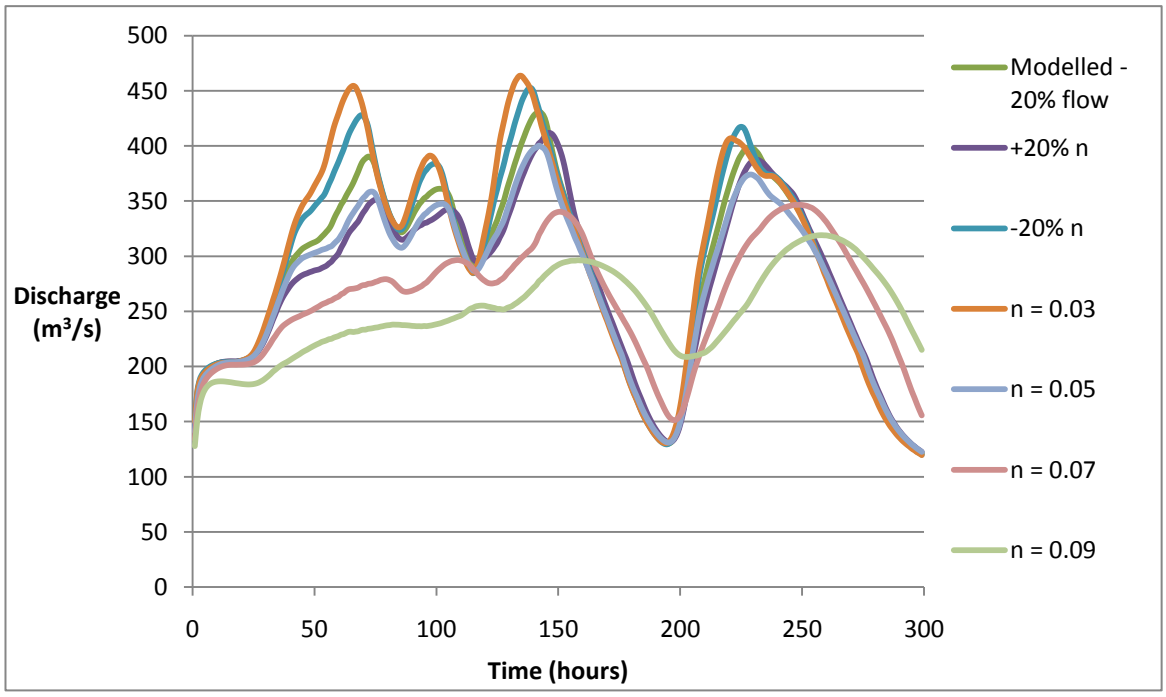

Figure 4.17 (a) Discharge response to a 20% decrease in inflow and changes in global Manning's *n*.

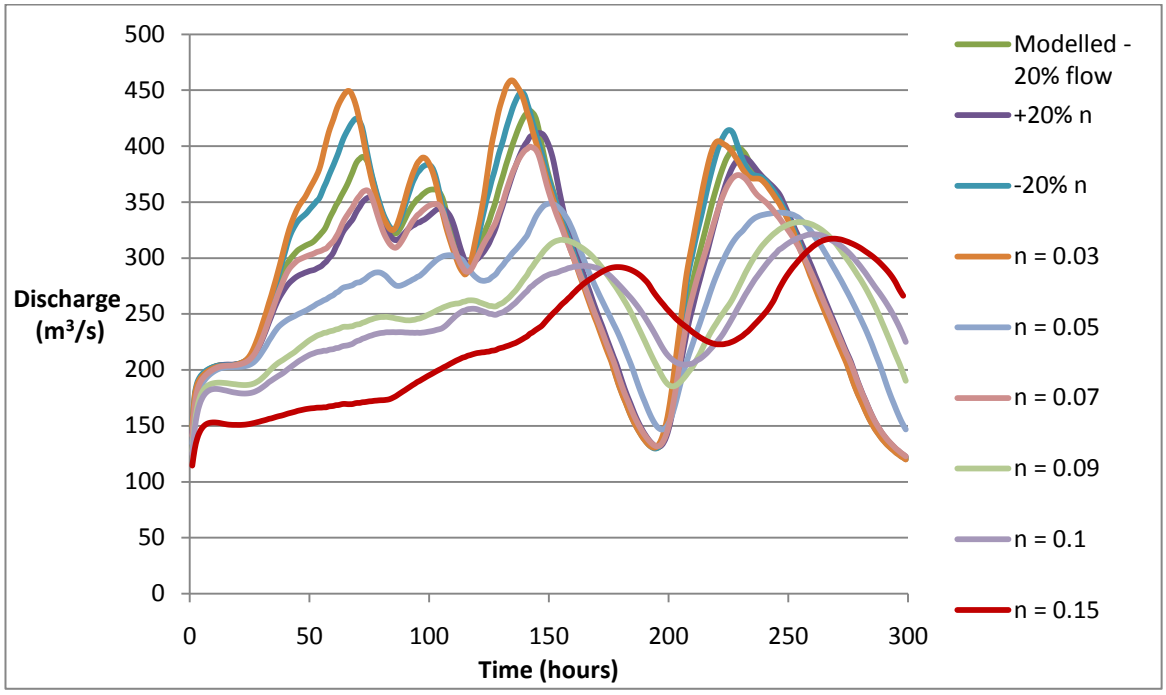

Figure 4.17 (b) Discharge response to a 20% decrease in inflow and changes in channel Manning's *n*.

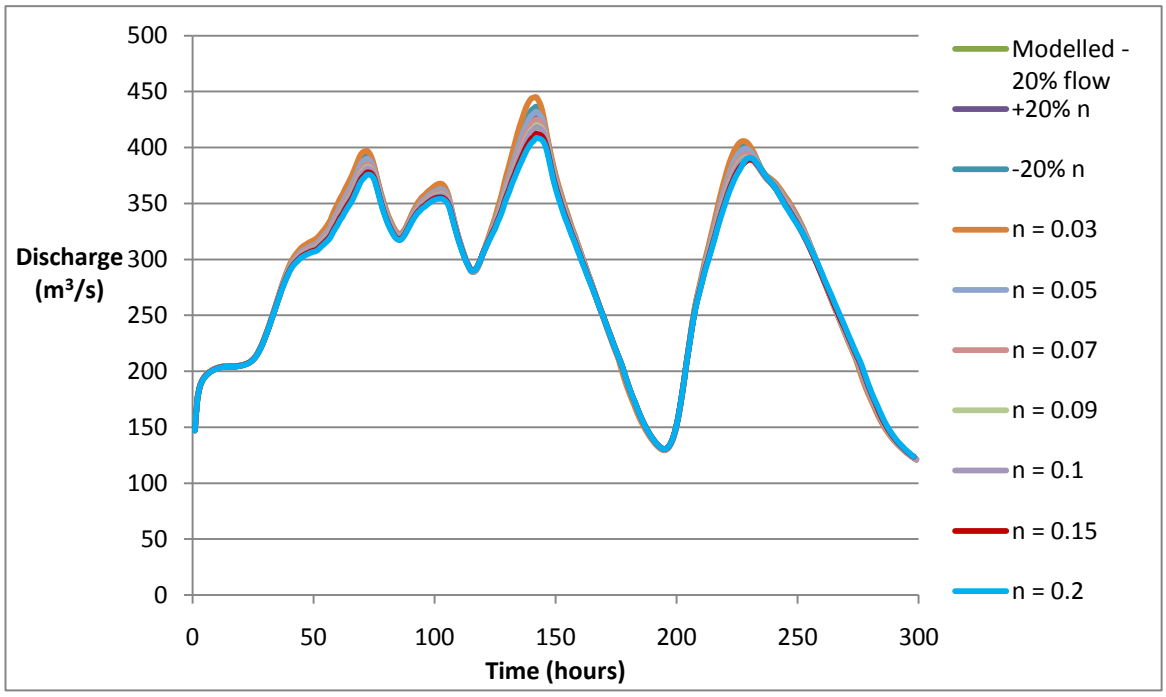

Figure 4.17 (c) Discharge response to a 20% decrease in inflow and changes in floodplain Manning's *n*.

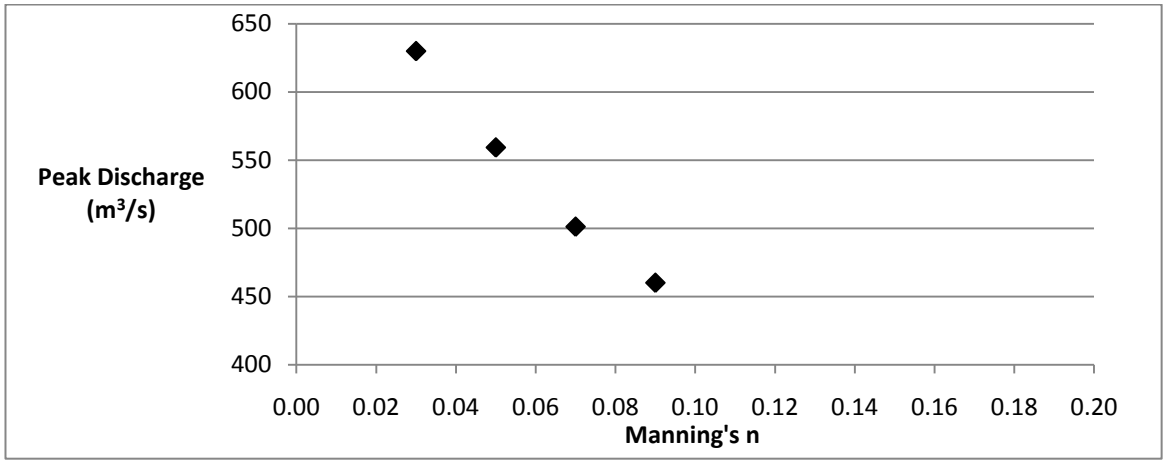

(a) Inflow increased by 20% and global *n* varied

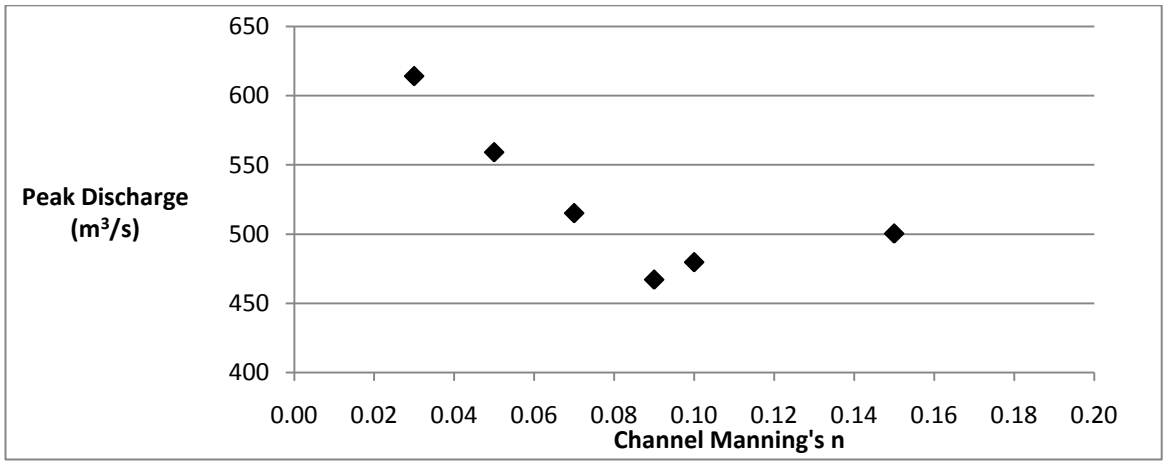

(b) Inflow increased by 20% and channel *n* varied

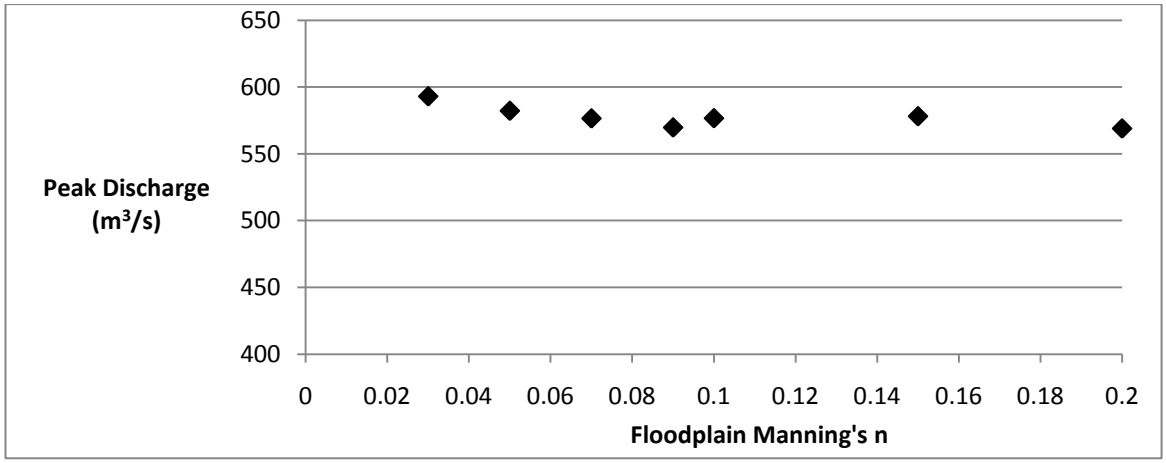

(c) Inflow increased by 20% and global floodplain *n* varied

Figure 4.18 Peak discharge response to a 20% increase in inflow and changes in Manning's *n*.

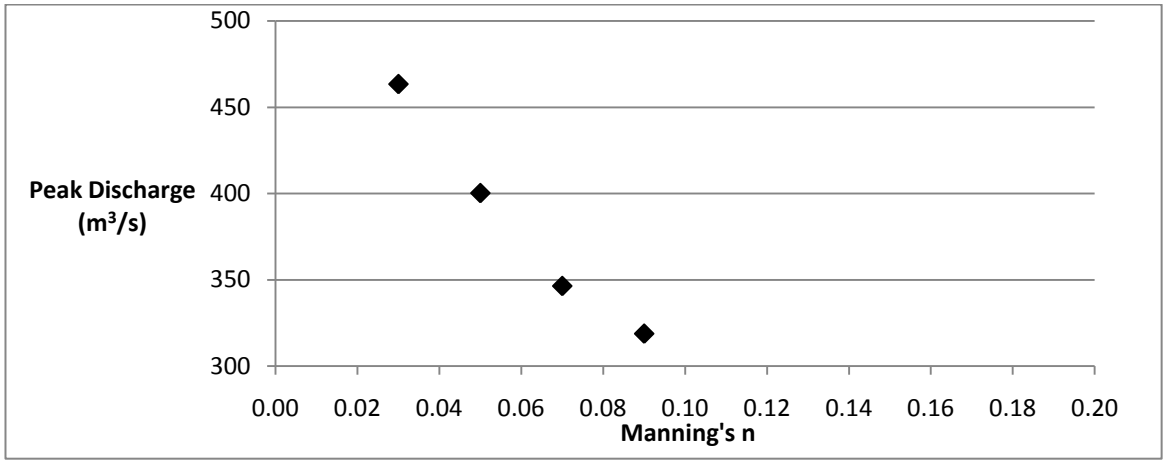

(a) Inflow decreased by 20% and global *n* varied

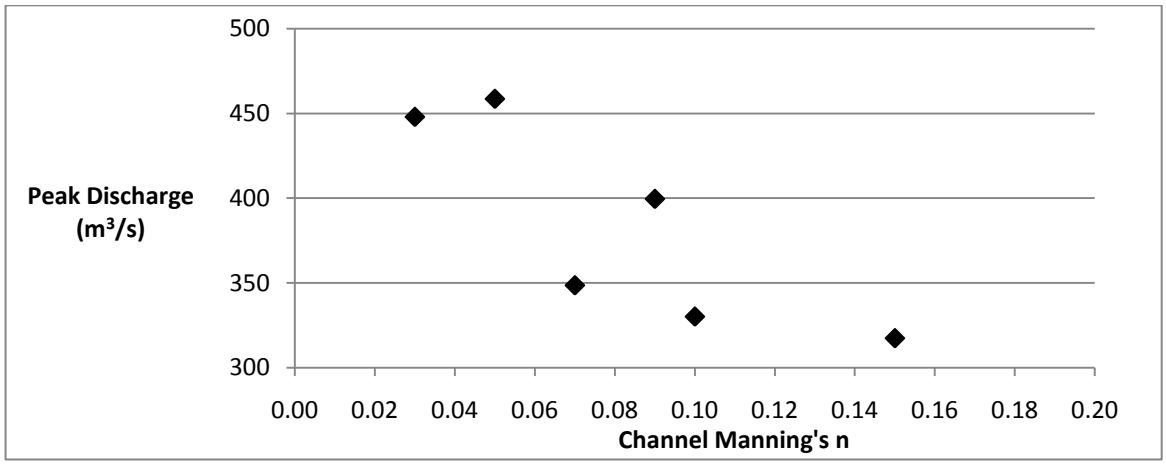

(b) Inflow decreased by 20% and channel *n* varied

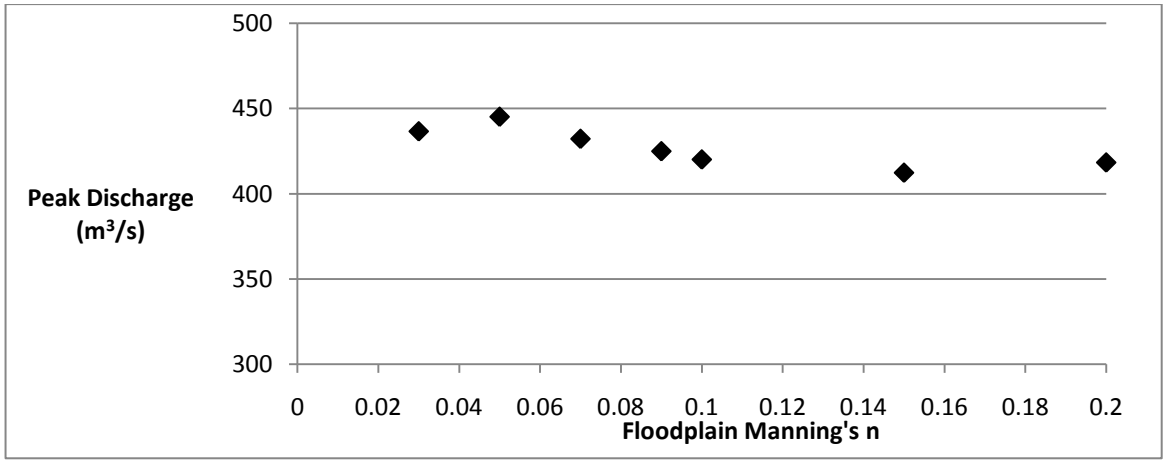

(c) Inflow decreased by 20% and floodplain *n* varied

Figure 4.19 Peak discharge response to a 20% decrease in inflow and changes in Manning's *n*.

	Inflow +20%	Inflow -20%
Variation	**Mean Peak Timing Delay (hr)**	**Mean Peak Timing Delay (hr)**
20% *n*	9.75	3
-20% *n*	1.5	3.5
***n* = 0.03**	4.25	3.5
***n* = 0.05**	9.75	1.75
***n* = 0.07**	18	10.75
***n* = 0.09**	27.5	18

Table 4.6 Peak timing delay between the simulated and observed hydrographs after increasing and decreasing inflow by 20% and varying Manning's *n* globally. Timing delay was calculated for each of the four peaks in the hydrographs. The lags in mean peak timing delay in relation to the modelled run are both positive and negative.

4.4 Results: model performance

Figure 4.20 shows that the initial output hydrograph simulated by the HEC-RAS model does not match very well with the observed hydrograph at Skelton. The peaks are slightly lower than the observed and the troughs much larger. The timing of the second and fourth peaks are good, but the other two peaks are slightly late. There appears to be some mass balance error as the total observed discharge is larger than the modelled discharge. This could result from expected overestimation of flow at gauging stations on the River Swale and River Nidd (see Section 4.6.2) or due to the removal of the input from the River Tutt. However, the latter is unlikely as the Tutt only contributes a very small discharge to the system. Calibrating the model should help to improve model prediction with regard to the observed data.

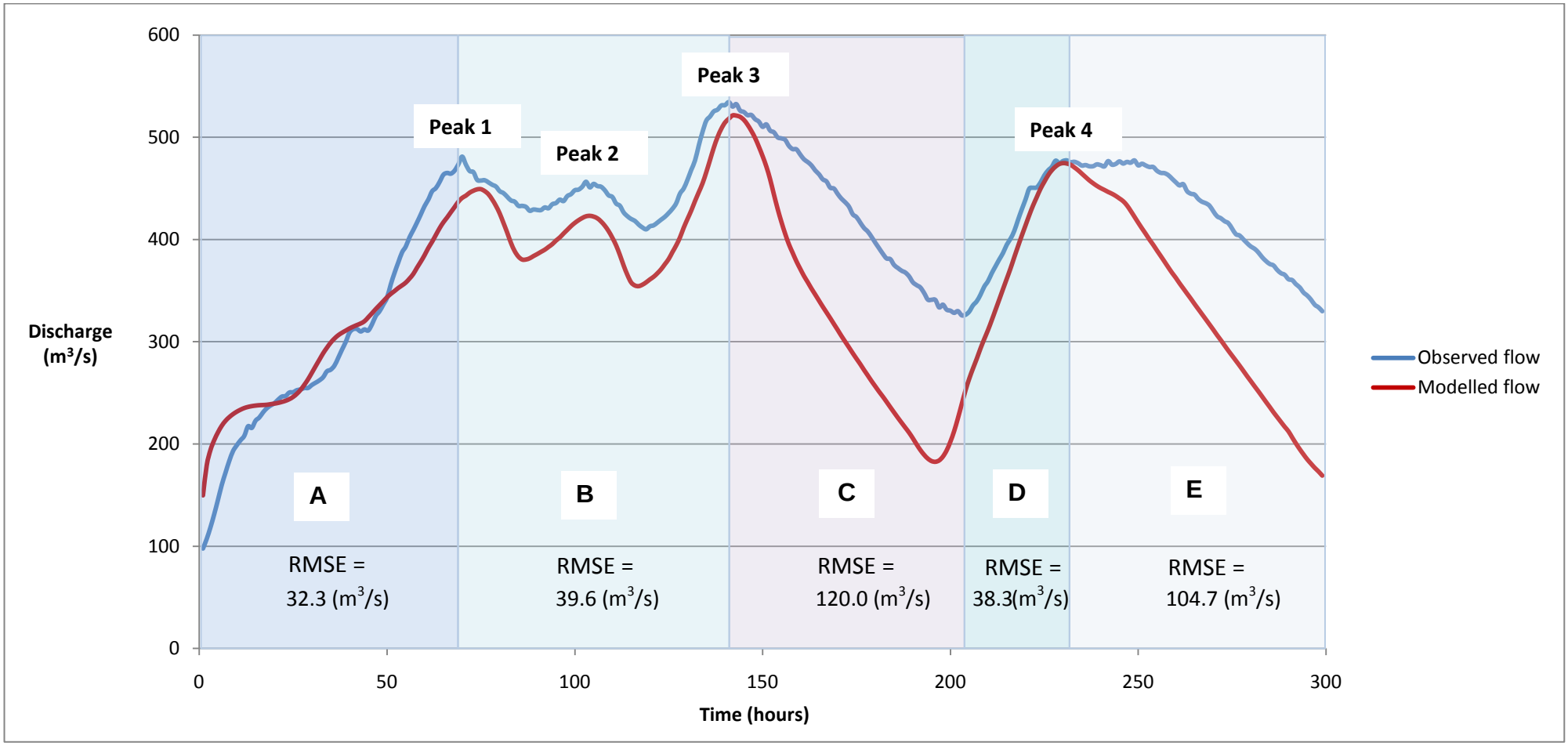

Figure 4.20 Observed hydrograph and the simulated hydrograph returned after initial model building, before calibration. The observed hydrograph data were obtained from the Environment Agency's flow gauging station at Skelton. RMSE was calculated for five sections of the original modelled and observed flow data. These were chosen to represent distinct sections of the hydrograph pattern.

4.4.1 Discharge response to Manning's *n*

Global *n*

Figure 4.21 shows that global changes in Manning's *n* affect the R^2 values produced; the highest *n* values appear to have high R^2 values. The best match is thus for *n* = 0.09, although this is not reflected visually by the hydrographs. Figure 4.22 shows that there is no clear relationship between Manning's *n* and Nash-Sutcliffe values. Figure 4.23 displays the expected trend in the percentage error in the peak; low values of Manning's *n* globally gave a small percentage error whilst high values gave a much larger error. For example, a global *n* of 0.03 had a peak error of 0.8% compared to a global *n* of 0.09 which had an error of -26.0%. Figure 4.24 shows this trend as a scatter plot. A value of 0.01 appears to be a threshold over which higher Manning's *n* values do not significantly increase the peak error.

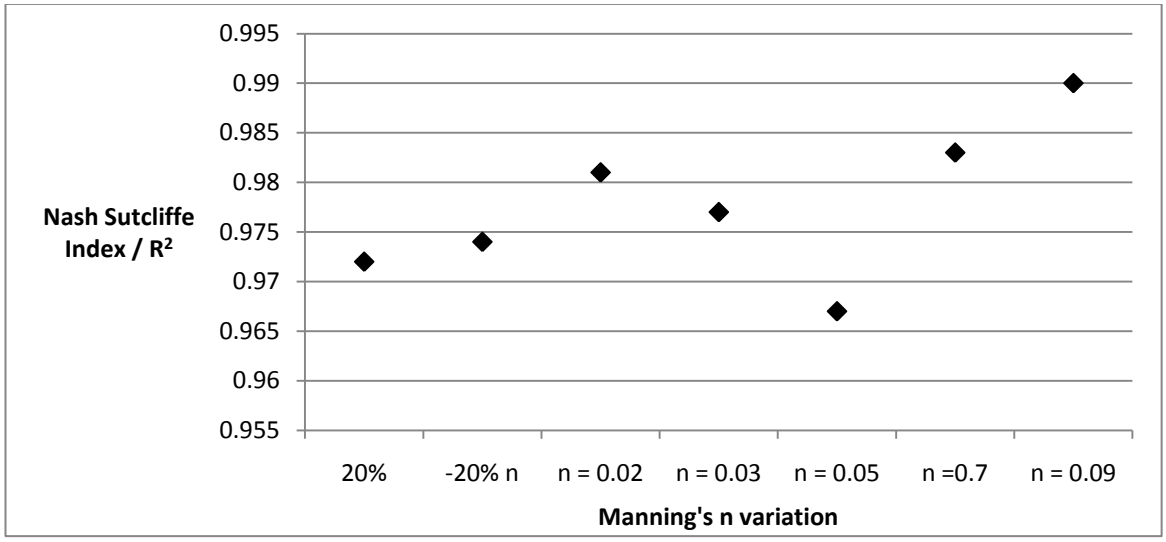

Figure 4.21 Nash-Sutcliffe values for varying global Manning's *n*. R^2 for the modelled flow was 0.97.

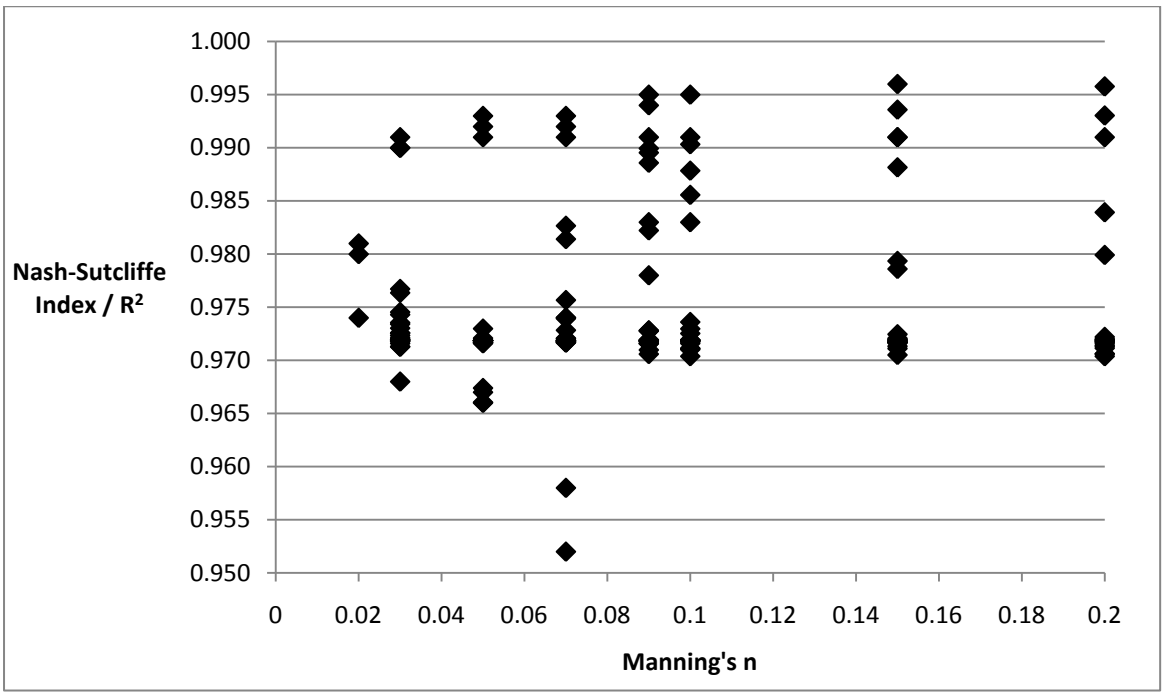

Figure 4.22 Nash-Sutcliffe values for each Manning's *n* value modelled.

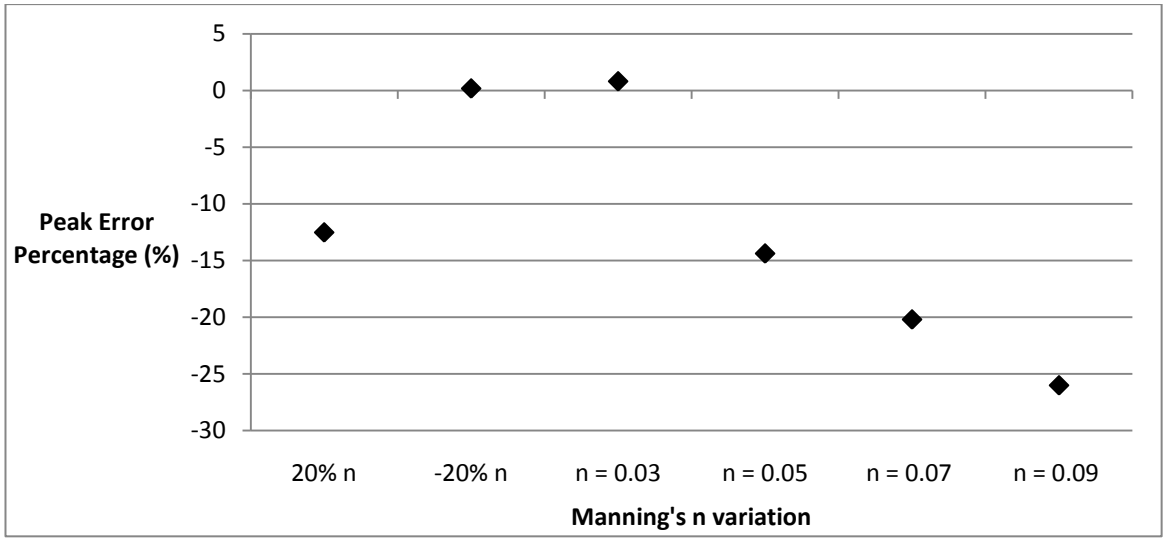

Figure 4.23 Percentage error in the peak of the simulated hydrograph compared to the observed hydrograph with changes in global Manning's *n*. Percentage error in the peak for the modelled flow was -2.4%.

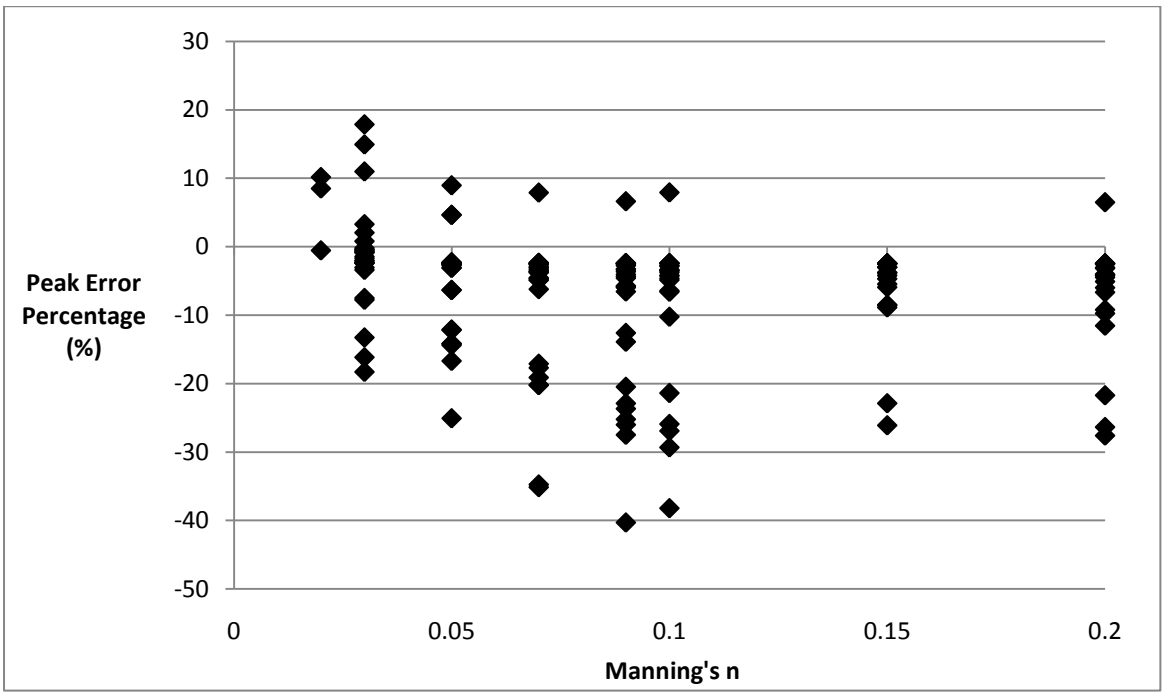

Figure 4.24 Percentage error in the peak for each of the Manning's *n* values modelled.

Table 4.7 (a) shows that RMSE also increases at higher Manning's *n* values. Figure 4.25 shows that simulations with low values of Manning's *n* have similar values for RMSE. As Manning's *n* increases over 0.07, RMSE increases and the range of values also increases from 70 m^3/s to 180 m^3/s. Figure 4.20 shows that RMSE is affected quite highly by large differences between the observed and simulated hydrographs. If the RMSE is calculated for sections of the hydrograph (Table 4.7 (b)), it is much smaller at around 30-40 m^3/s. The two main falling limbs of the hydrograph do not match well, which increases the overall RMSE recorded for the simulated hydrograph.

All Manning's *n*	RMSE (m^3/s)
Modelled flow	75.1
+20% *n*	75.0
-20% *n*	77.5
n = 0.03	82.6
n = 0.05	69.4
n = 0.07	96.0
n = 0.09	125.6

Section	RMSE (m^3/s)
A	32.3
B	39.6
C	120.0
D	38.4
E	104.7

Table 4.7 (a) RMSE of the simulated hydrograph compared to the observed hydrograph with changes in global Manning's *n*; (b) RMSE was also calculated for separate sections of the simulated vs observed hydrograph, shown in Figure 4.20.

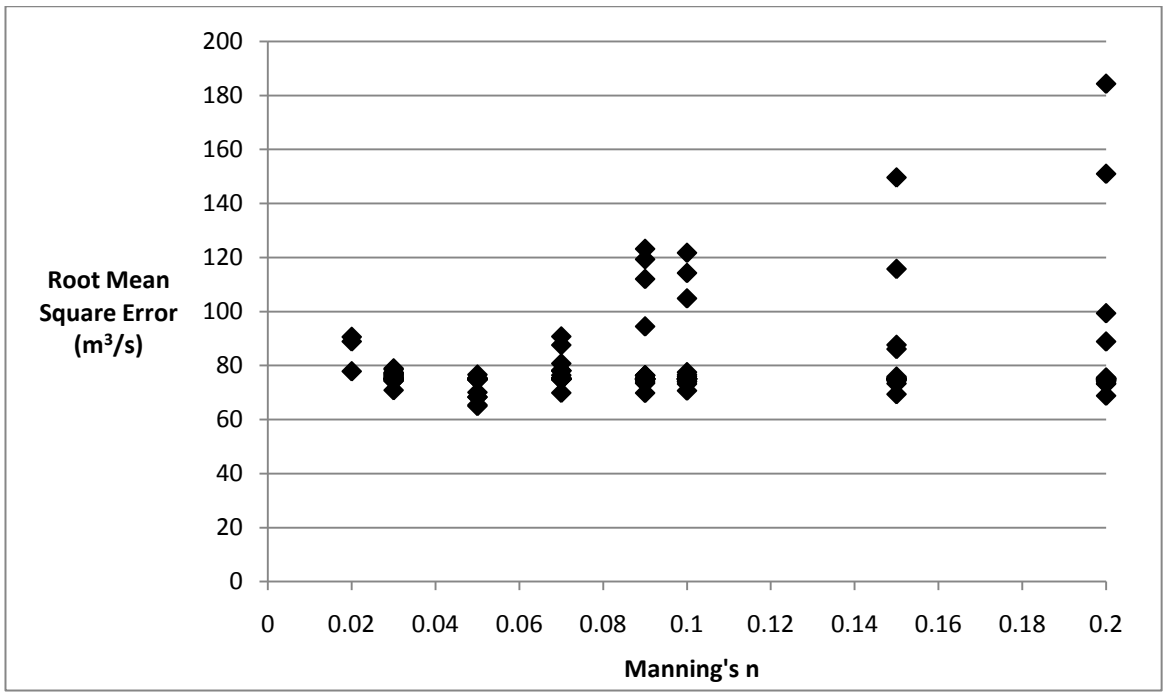

Figure 4.25 Root Mean Square Error for each of the Manning's *n* values modelled.

Figure 4.26 shows that the mean absolute error is lowest at a low Manning's *n* of 0.03 (38.4 m^3/s) and increases as Manning's *n* increases. Figure 4.27 shows this trend, with MAE increasing with *n*. As with Figure 4.25, an increase in the spread of the MAE values occurs above *n* = 0.07.

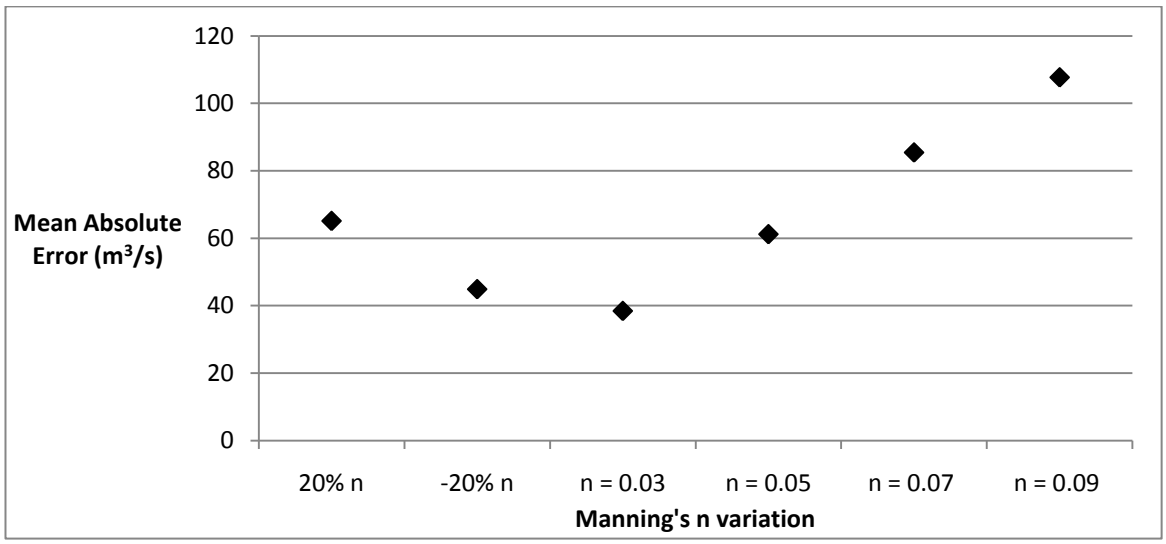

Figure 4.26 Mean absolute error values after varying global Manning's *n*.

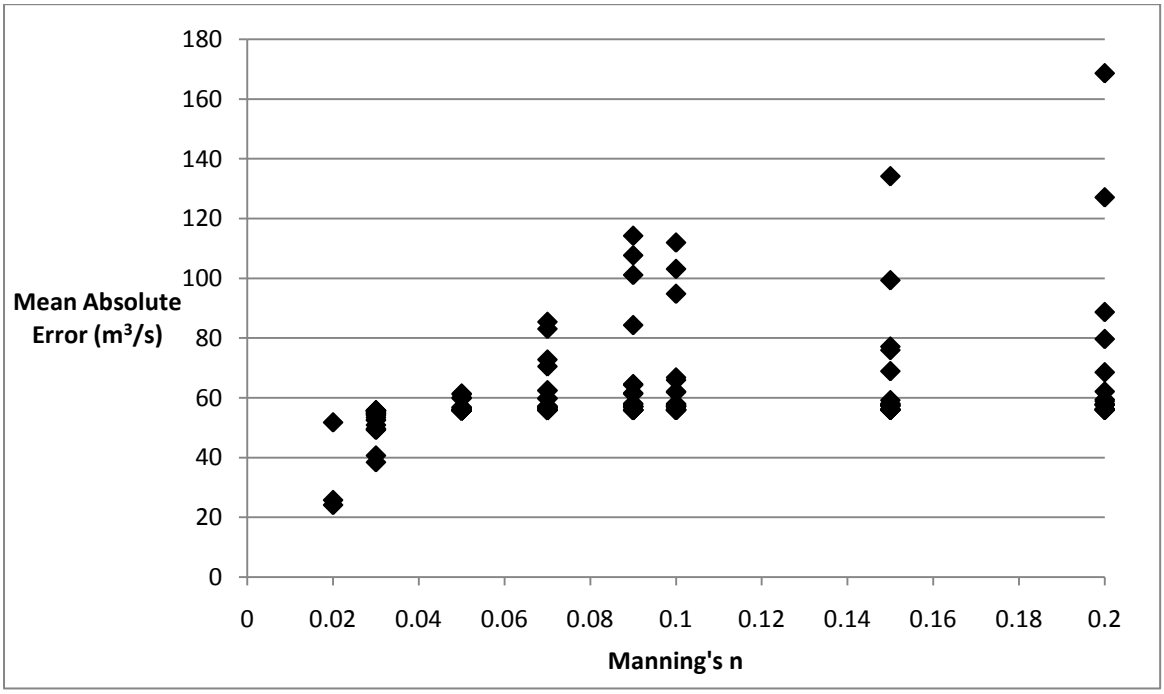

Figure 4.27 Mean absolute error values for each Manning's *n* value modelled.

Channel *n*

Table 4.8 shows that R^2 values for varying channel Manning's *n* are high for all the simulations. As channel *n* was increased, R^2 also increased, a trend shown with changes in global *n*. The percentage error in the peak ranges from -0.7% at a channel *n* of 0.03 to -26.4% at a value of 0.2. The peak error for channel *n* is slightly less than for global *n*. The RMSE values for channel *n* are very similar to that of global *n*, increasing from 81.9 m^3/s at *n* = 0.03 to 193.8 m^3/s at *n* = 0.2. MAE increases with channel *n*, from 40.7 m^3/s to 168.6 m^3/s at *n* = 0.2, values which are very similar to that of global *n*.

All channel *n*	R^2	PEP (%)	RMSE (m^3/s)	MAE (m^3/s)
+20% *n*	0.97	-11.4	74.9	64.2
-20% *n*	0.97	-0.7	76.6	45.6
n = 0.03	0.98	-0.7	81.9	40.7
n = 0.05	0.97	-14.2	69.8	61.4
n = 0.07	0.98	-20.2	92.4	83.1
n = 0.09	0.99	-23.7	118.0	101.1
n = 0.1	0.99	-26.9	128.1	111.9
n = 0.15	0.99	-26.1	157.4	134.1
n = 0.2	0.99	-26.4	193.8	168.6

Table 4.8 Nash-Sutcliffe indicies, percentage error in the peak, Root Mean Square Error and Mean Absolute Error values comparing the simulated hydrograph with the observed for varying channel Manning's *n*.

Floodplain *n*

Table 4.9 shows that R^2 values for varying floodplain Manning's *n* are very similar for all simulations. In contrast to global and channel *n*, R^2 appears to slightly decrease with increasing values for floodplain *n*, although the values are very similar. The peak error varies only slightly as the model is not very sensitive to Manning's *n* of the floodplain. The largest error of -6.7% is at *n* = 0.2. RMSE remains nearly constant for the floodplain changes in *n*, around 75 m^3/s, but shows a slight decrease with increasing floodplain *n*. The range of the MAE is a little larger, between 53.4 m^3/s at *n* = 0.03 and 59.4 m^3/s at *n* = 0.2, but compared to global and channel *n* varies only slightly as the model is not very sensitive to floodplain *n*. Table 4.10 shows that R^2 values for the left and right floodplain are the same.

All floodplain *n*	R^2	PEP (%)	RMSE (m^3/s)	MAE (m^3/s)
+20% *n*	0.97	-3.4	75.2	56.9
-20% *n*	0.97	-1.5	75.3	54.8
n =0.02	0.97	-	-	-
n = 0.03	0.97	-0.7	76.1	53.4
n = 0.05	0.97	-2.5	75.1	55.7
n = 0.07	0.97	-3.8	74.9	57.2
n = 0.09	0.97	-4.6	74.7	58.1
n = 0.1	0.97	-4.9	74.1	58.0
n = 0.15	0.97	-5.9	74.1	59.2
n = 0.2	0.97	-6.7	73.5	59.4

Table 4.9 Nash-Sutcliffe indicies, percentage error in the peak, Root Mean Square Error and Mean Absolute Error values comparing the simulated hydrograph with the observed for varying floodplain Manning's *n*.

All floodplain left	R^2
+20% *n*	0.97
-20% *n*	0.97
n =0.02	0.97
n = 0.03	0.97
n = 0.05	0.97
n = 0.07	0.97
n = 0.09	0.97
n = 0.1	0.97
n = 0.15	0.97

All floodplain right	R^2
+20% *n*	0.97
-20% *n*	0.97
n =0.02	0.97
n = 0.03	0.97
n = 0.05	0.97
n = 0.07	0.97
n = 0.09	0.97
n = 0.1	0.97
n = 0.15	0.97

Table 4.10 Nash-Sutcliffe values for varying Manning's *n* for the floodplain on the left and right sides of the river system.

Manning's *n* for the tributaries

Table 4.11 shows that global and channel changes in Manning's *n* along the River Ouse affected the R^2 values slightly, whilst floodplain *n* changes did not change R^2 values. Global and channel changes to Manning's *n* along the Swale also had an effect on R^2 whilst floodplain *n* did not. The R^2 values for the Nidd did not change with global, channel or floodplain *n* changes. Manning's *n* of the left and right floodplains in the system had no influence on R^2 values for each of the tributaries.

Global Ouse	**R^2**		**Global Swale**	**R^2**		**Global Nidd**	**R^2**
+20% *n*	0.97		+20% *n*	0.97		+20% *n*	0.97
-20% *n*	0.97		-20% *n*	0.97		-20% *n*	0.97
n = 0.03	0.97		*n* = 0.03	0.97		*n* = 0.03	0.97
n = 0.05	0.97		*n* = 0.05	0.97		*n* = 0.05	0.97
n = 0.07	0.98		*n* = 0.07	0.97		*n* = 0.07	0.97
n = 0.09	0.99		*n* = 0.09	0.97		*n* = 0.09	0.97
n = 0.1	0.99		*n* = 0.1	0.97		*n* = 0.1	0.97
-	-		*n* = 0.15	0.98		*n* = 0.15	0.97
-	-		*n* = 0.2	0.98		*n* = 0.2	0.97
Channel Ouse	**R^2**		**Channel Swale**	**R^2**		**Channel Nidd**	**R^2**
+20% *n*	0.97		+20% *n*	0.97		+20% *n*	0.97
-20% *n*	0.97		-20% *n*	0.97		-20% *n*	0.97
n = 0.03	0.97		*n* = 0.03	0.97		*n* = 0.03	0.97
n = 0.05	0.97		*n* = 0.05	0.97		*n* = 0.05	0.97
n = 0.07	0.97		*n* = 0.07	0.97		*n* = 0.07	0.97
n = 0.09	0.98		*n* = 0.09	0.97		*n* = 0.09	0.97
n = 0.1	0.99		*n* = 0.1	0.97		*n* = 0.1	0.97
n = 0.15	0.99		*n* = 0.15	0.98		*n* = 0.15	0.97
n = 0.2	0.99		*n* = 0.2	0.98		*n* = 0.2	0.97
Fplain Ouse	**R^2**		**Fplain Swale**	**R^2**		**Fplain Nidd**	**R^2**
+20% *n*	0.97		+20% *n*	0.97		+20% *n*	0.97
-20% *n*	0.97		-20% *n*	0.97		-20% *n*	0.97
n = 0.03	0.97		*n* = 0.03	0.97		*n* = 0.03	0.97
n = 0.05	0.97		*n* = 0.05	0.97		*n* = 0.05	0.97
n = 0.07	0.97		*n* = 0.07	0.97		*n* = 0.07	0.97
n = 0.09	0.97		*n* = 0.09	0.97		*n* = 0.09	0.97
n = 0.1	0.97		*n* = 0.1	0.97		*n* = 0.1	0.97
n = 0.15	0.97		*n* = 0.15	0.97		*n* = 0.15	0.97
n = 0.2	0.97		*n* = 0.2	0.97		*n* = 0.2	0.97
Fplain left Ouse	**R^2**		**Fplain left Swale**	**R^2**		**Fplain left Nidd**	**R^2**
+20% *n*	0.97		+20% *n*	0.97		+20% *n*	0.97
-20% *n*	0.97		-20% *n*	0.97		-20% *n*	0.97
n = 0.03	0.97		*n* = 0.03	0.97		*n* = 0.03	0.97
n = 0.05	0.97		*n* = 0.05	0.97		*n* = 0.05	0.97
n = 0.07	0.97		*n* = 0.07	0.97		*n* = 0.07	0.97
n = 0.09	0.97		*n* = 0.09	0.97		*n* = 0.09	0.97
n = 0.1	0.97		*n* = 0.1	0.97		*n* = 0.1	0.97
n = 0.15	0.97		*n* = 0.15	0.97		*n* = 0.15	0.97
n = 0.2	0.97		*n* = 0.2	0.97		*n* = 0.2	0.97

Fplain right Ouse	R^2		Fplain right Swale	R^2		Fplain right Nidd	R^2
+20% *n*	0.97		+20% *n*	0.97		+20% *n*	0.97
-20% *n*	0.97		-20% *n*	0.97		-20% *n*	0.97
n = 0.03	0.97		*n* = 0.03	0.97		*n* = 0.03	0.97
n = 0.05	0.97		*n* = 0.05	0.97		*n* = 0.05	0.97
n = 0.07	0.97		*n* = 0.07	0.97		*n* = 0.07	0.97
n = 0.09	0.97		*n* = 0.09	0.97		*n* = 0.09	0.97
n = 0.1	0.97		*n* = 0.1	0.97		*n* = 0.1	0.97
n = 0.15	0.97		*n* = 0.15	0.97		*n* = 0.15	0.97
n = 0.2	0.97		*n* = 0.2	0.97		*n* = 0.2	0.97

Table 4.11 Nash-Sutcliffe values for Manning's *n* variations in global, channel and floodplain *n* along the three tributaries.

4.4.2 Discharge response to changing both inflow and Manning's *n*

Table 4.12 shows that increasing the flow by 20% decreases the R^2 values for global *n* changes by approximately 0.14 (for *n* = +20%) compared to the original values with just Manning's *n* changes (Figure 4.21). The reductions to R^2 are exactly the same for with channel *n* changes as with global *n* changes. The smallest change is for floodplain *n* where R^2 decreased by 0.07 (for *n* = +20%) compared to the original value. In contrast, Table 4.12 also shows that decreasing the inflow by 20% increases the R^2 values for global changes. R^2 is increased by 0.02 for *n* = +20%. Similarly, decreasing the inflow increases the R^2 for channel *n*, and for floodplain *n* a large increase of 0.07 was produced.

+20% Inflow

All Manning's *n*	R^2
+20% *n*	0.84
-20% *n*	0.96
n = 0.03	0.97
n = 0.05	0.80
n = 0.07	0.96
n = 0.09	0.98

All channel *n*	R^2
+20% *n*	0.83
-20% *n*	0.95
n = 0.03	0.97
n = 0.05	0.80
n = 0.07	0.95
n = 0.09	0.98
n = 0.1	0.98
n = 0.15	0.99

All floodplain *n*	R^2
+20% *n*	0.90
-20% *n*	0.91
n = 0.03	0.93
n = 0.05	0.90
n = 0.07	0.89
n = 0.09	0.88
n = 0.1	0.88
n = 0.15	0.87
n = 0.2	0.85

-20% Inflow

All Manning's *n*	R^2
+20% *n*	0.99
-20% *n*	0.99
n = 0.03	0.99
n = 0.05	0.99
n = 0.07	0.99
n = 0.09	0.99

All channel *n*	R^2
+20% *n*	0.99
-20% *n*	0.99
n = 0.03	0.99
n = 0.05	0.99
n = 0.07	0.99
n = 0.09	0.99
n = 0.1	0.99
n = 0.15	0.99

All floodplain *n*	R^2
+20% *n*	0.99
-20% *n*	0.99
n = 0.03	0.99
n = 0.05	0.99
n = 0.07	0.99
n = 0.09	0.99
n = 0.1	0.99
n = 0.15	0.99
n = 0.2	0.99

Table 4.12 Nash-Sutcliffe calculated for each of the Manning's *n* values modelled with inflow increased and decreased by 20%.

4.5 Discussion

4.5.1 Discharge response to Manning's *n*

Global, channel and floodplain roughness

Figure 4.1 shows that variation in Manning's *n* globally across the whole model has a large influence on the modelled discharge output. Higher values of *n* decrease the discharge, attenuating the flood peak, and this makes sense because the capacity for flow is reduced due to turbulence at the boundary and physical obstructions caused by vegetation, so less water can pass in a given time (Fread, 1991; De Doncker *et al.*, 2009; McGahey *et al.*, 2009). The peak of the hydrograph is translated in time. This is because higher Manning's *n* values reduce the conveyance of water in the channel and across the floodplains, so the peak occurs later. Lower values of *n* have the opposite influence on discharge as the roughness coefficient is inversely proportional to the conveyance (Akanbi and Singh, 1997); discharge increases as friction is reduced. Figures 4.1 and 4.2 show that Manning's *n* has a large influence on discharge thus the sensitivity of the model to global *n* is high.

The sensitivity of the model to *n* may be higher if a smaller flood was modelled. Anderson *et al.* (2006) found that smaller floods were most sensitive to channel roughness (vegetation).

Channel *n* also has a large influence on discharge (Figures 4.3 and 4.4). The attenuation of peak discharge and delay of the hydrograph peak has been demonstrated in many investigations (Wollf and Burges, 1994; Woltenmade and Potter, 1994; Anderson *et al.*, 2006). Farahi *et al.* (2009) showed that roughness of the main channel had a large impact on model predictions. The conveyance of the water in the channel is slowed by high channel roughness values because the increased friction reduces the velocity. Changing channel *n* has the same impact as varying global *n*, reducing peak discharge with higher *n* values and skewing the hydrographs. Channel roughness is recognised as a major determinant of flood wave celerity and hydrograph skew (Anderson *et al.*, 2006). Varying Manning's *n* on the floodplain in the model does not have a large effect on discharge (Figures 4.5 and 4.6). This is because the flow is only affected by floodplain *n* when out-of-bank conditions occur. This pattern was also shown by Turner-Gillespie *et al.* (2003) who increased floodplain *n* from 0.055 to 0.07 producing a 3% decrease in peak discharge. Hall *et al.* (2005) found that although channel *n* dominated the sensitivity of their model, the sensitivity to floodplain *n* increased as floodplain width increased. Out-of-bank flows, and therefore roughness of the floodplains, are therefore important when investigating the use of floodplains to reduce flood risk.

Ouse, Swale and Nidd reaches

Varying Manning's *n* across the three reaches in the model produced very different impacts on peak discharge. The sensitivity of the model to Manning's *n* was quite high for the River Ouse, as with increasing *n* values the peak discharge decreased quite rapidly as shown for the whole model (Figure 4.11). This is because the topography for the River Ouse makes up a large proportion of the total in the model, thus changes in roughness along its reach will have the largest effect. The River Swale also showed sensitivity to changes in Manning's *n* (Figure 4.11) but not to the same extent as the River Ouse as it has a much smaller cross-sectional area. For both the River Ouse and the River Swale, a change in Manning's *n* globally and for the channel influenced output discharge, while changes in floodplain *n* had a very small or no influence. In comparison, the model showed no sensitivity to Manning's *n* changes for the River Nidd (Figure 4.11). This may

be due to the small cross-sectional area of the River Nidd in the model, but possibly because of instabilities found in the model. Decreasing the spacing between cross-sections by interpolation may aid this problem.

4.5.2 Discharge response to weir coefficient

Peak discharge is affected substantially by the weir structures because they provide an obstruction to flow (Rickard *et al.*, 2003). The channel capacity is reduced, thus less water is able to pass during a given amount of time. They cause more water to move out-of-banks as the capacity of the channel is reduced. Linton weir has the largest effect on flow movement because it has the largest cross-sectional area. Varying the weir coefficient for Linton weir had quite a significant influence on discharge (Figures 4.15). Increasing the weir coefficient increases peak discharge as the weir coefficient influences the resistance applied to the flow over the weir. As the River Ouse has a large cross-sectional area, the discharge is also large; hence Linton weir has a large impact on the dynamics of the flow. Peak timing delay increased with an increase in the weir coefficient as the velocity of the flow is reduced over the weir. Compared to Linton weir, the weir coefficient for Cundall weir had very little effect on modelled peak discharge. The channel of the River Nidd is a lot smaller than the River Ouse, thus the geometry of Cundall weir has a smaller impact on output discharge. For this reason the R^2 values and peak timing were also not affected.

4.6 Calibration

4.6.1 Calibration process

A critical phase when developing a hydraulic model is model calibration as this establishes confidence in the modelled outputs (Pappenberger *et al.*, 2007). The purpose of calibration is to match the modelled output to observed data. The observed data usually consist of information from river gauges, field observations and often local knowledge from residents (U. S. Army Corps of Engineers, 1993). It must be noted that the success of calibration relies on the quantity, quality and availability of input data (Janssen and Heuberger, 1995) and that even with known roughness data, a perfect match between the modelled output and the observed data should not be expected. The calibration process is also limited by the runtime of the model. Figure 4.28 illustrates the processes involved in calibration and determining whether a model is fit to use.

The standard procedure for calibration is to adjust one or more of the parameters until the model outputs give a satisfactory match to the observed data. Trial-and-error is often used to calibrate models by varying parameters until the model matches the observed data visually, but this approach suffers from great subjectivity. Hence, a systematic approach to calibration is needed to ensure the exactness and objectiveness of the results (Janssen and Heuberger, 1995). Calibration can be achieved by altering Manning's *n*, adjusting the expansion/contraction coefficients and modifying bridge geometries (U. S. Army Corps of Engineers, 1993). It is usually achieved by making most adjustments to Manning's *n*. It is recognised that there is uncertainty involved in the estimation of *n* as it is based on judgement. Burnham and Davies (1990) discussed a reliability scale on which most estimates lie: 0 (perfect knowledge of *n* values) to 1 (professional judgement without extensive field work). The US Army Corps of Engineers (1986) stated that "estimates by experienced hydraulic engineers commonly differ[…] by +- 20% at the same stream section" (cited U. S. Army Corps of Engineers, 1993: 33). When calibrating a model, varying Manning's *n* by + or -20% can thus be justified. In order to calibrate the HEC-RAS model Manning's *n* values were adjusted systematically up to 20% change. Manning's *n* for the River Ouse was varied independently to the River Swale and River Nidd which were grouped together as they had less effect on discharge in terms of Manning's *n*. The weir geometries were also varied to see the effect on discharge downstream. The sensitivity analysis showed that the HEC-RAS model is quite sensitive to Linton weir, thus the height and width parameters were varied during calibration. The Manning's *n* values used in the baseline model are the same as in the ISIS model. These *n* values had already been calibrated as part of the ISIS model building process.

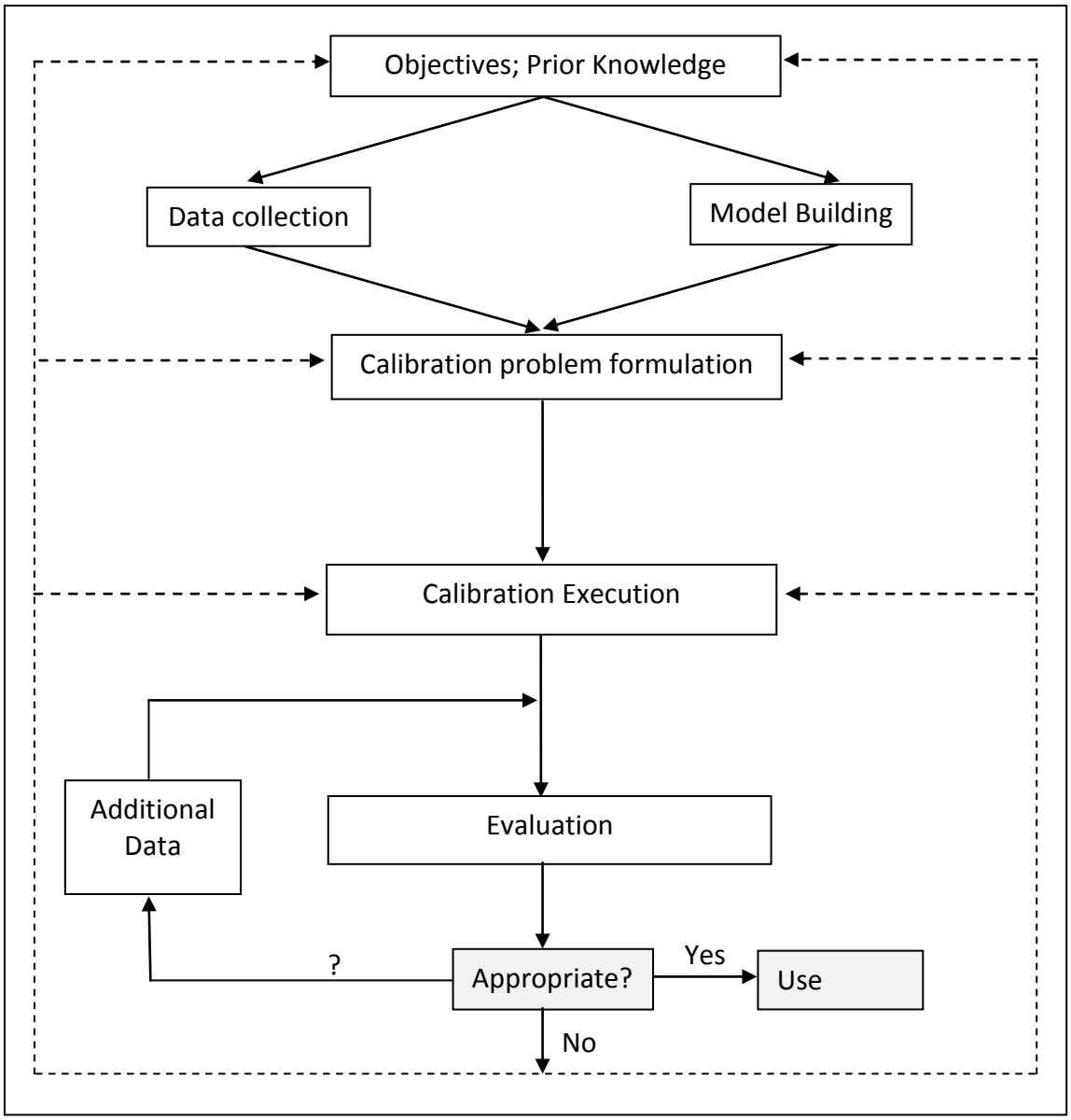

Figure 4.28 Stages involved in the calibration process of model building (Source: Janssen and Heuberger, 1995).

The sensitivity analysis was undertaken to check the model operation, assess model performance and identify important parameters. Following this it was recognised that the values for the Linton and Cundall weir coefficients had reverted back to the default values. These were changed back to the values specified by the ISIS model and the model run for the new weir coefficients (1.2 for Linton weir and 0.9 for Cundall weir). A difference of up to 30 m^3/s was experienced between the original weir coefficients and the new values hence the correction was important. All the runs computed during calibration and for the rest of the project use these values for the weir coefficients.

4.6.2 Calibration results

A summary of the simulated runs which showed the best fit with the observed data are presented in Table 4.13. Manning's *n* was varied systematically for each of the reaches. The two variations which provided the best results were:

Situation 1: reducing Manning's *n* globally by 20% (runs 1 to 5)

Situation 2: reducing Manning's *n* by 25% for the River Ouse and by 20% for the River Swale and River Nidd (runs 6 to 10).

These variations are shown in Figure 4.29. These two situations were then combined with changes in the weir geometries (Table 4.13), as this was believed to have a significant effect on the discharge hydrographs.

Run	Manning's *n*	Linton weir – width variation (m)	Linton weir – height variation (m)
1	Manning's *n* decreased globally by 20%	-	-
2		Increased 5m	-
3		Increased 5m	Decreased 5m
4		Decreased 1m	-
5		Decreased 9m	-
6	Manning's *n* for the Ouse decreased by 25%, *n* for the Nidd and Swale decreased by 20%	-	-
7		Increased 5m	-
8		Increased 5m	Decreased 5m
9		Decreased 1m	-
10		Decreased 9m	-

Table 4.13 Summary of the calibration runs. Manning's *n*, weir width and weir height were varied between runs. Runs 1-5 = situation 1; Runs 6-10 = situation 2.

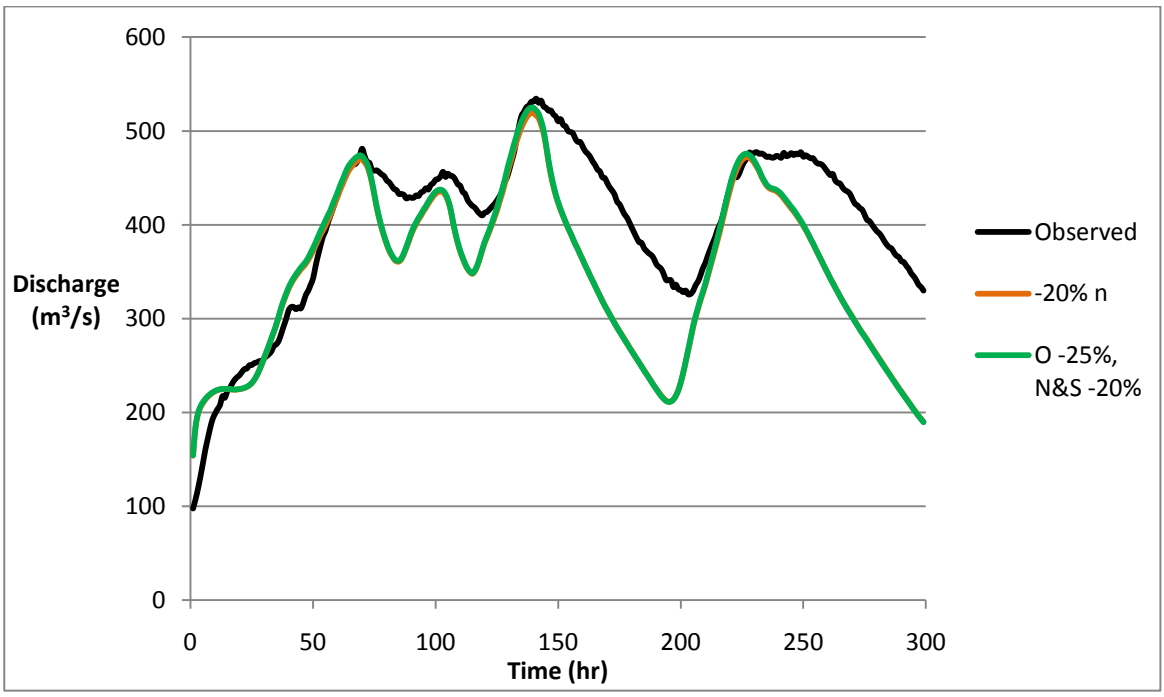

Figure 4.29 Varying Manning's *n* for calibration. Situation 1: Manning's *n* was decreased by 20% globally; Situation 2: Ouse *n* values were decreased by 25%, whilst the Nidd and Swale were decreased by 20%.

Table 4.14 shows that decreasing Manning's *n* by 20% globally in the model (Situation 1) appeared to have the most positive effect on the output hydrograph as it matched the observed data more readily than other changes. The runs in Situation 2 have higher R^2 values, showing a good match between observed and simulated, but the MAE, RMSE and peak timing error are higher than those of Situation 1. It must also be noted that varying Manning's *n* over 20% is unjustified as discussed earlier, thus Situation 1 was deemed to provide the best match. Figures 4.30 and 4.31 show visually that a larger variation in the discharge hydrographs is experienced with Situation 2.

	Run	P_O	P_S	R^2	PEP (%)	MAE (m^3/s)	RMSE (m^3/s)	Mean Peak Timing Delay (hr)
Situation 1	**1**	534.3	519.0	0.97	-2.9	52.9	75.3	2
	2	534.3	534.7	0.97	0.1	44.9	77.2	1.75
	3	534.3	534.7	0.97	0.1	44.9	77.2	1.75
	4	534.3	524.2	0.97	-1.9	51.4	75.5	2
	5	534.3	551.6	0.98	3.2	41.4	84.6	1.25
Situation 2	**6**	534.3	524.9	0.97	-1.8	51.4	75.3	2
	7	534.3	528.9	0.98	-1.0	53.4	85.1	2
	8	534.3	528.9	0.98	-1.0	53.3	84.8	2
	9	534.3	516.1	0.97	-3.4	55.3	76.6	2
	10	534.3	547.3	0.98	2.4	51.3	91.7	2.5

Table 4.14 Objective functions for calibration runs. P_o = observed peak discharge; P_s = simulated peak discharge.

Table 4.14 shows that run 1 gave fairly high values for PEP and MAE. The objective functions describing runs 2 and 3 are identical, showing that weir height has little effect on peak discharge as this is the only difference between the simulations (Table 4.14). Run 5 involved a large decrease in weir width which is deemed above reasonable limits for calibration, as the structure in the model no longer represents the observed geometry of the weir. However, this variation did decrease peak timing delay and give a high value for R^2. After analysing the hydrographs visually and quantitatively using the objective functions, run 4 was seen as the best match with the observed data. Run 4 has a fairly low MAE at 51.4 m^3/s, RMSE is one of the lowest at 75.5 m^3/s and the peak error only -1.9% (Table 4.14). Whilst the R^2 value is not the highest of all the runs, there is little difference between them. The simulated peak discharge for run 4 is only 10 m^3/s less than the observed. Both the peak discharge and peak timing are quite well matched for run 4, although the troughs do not match very well.

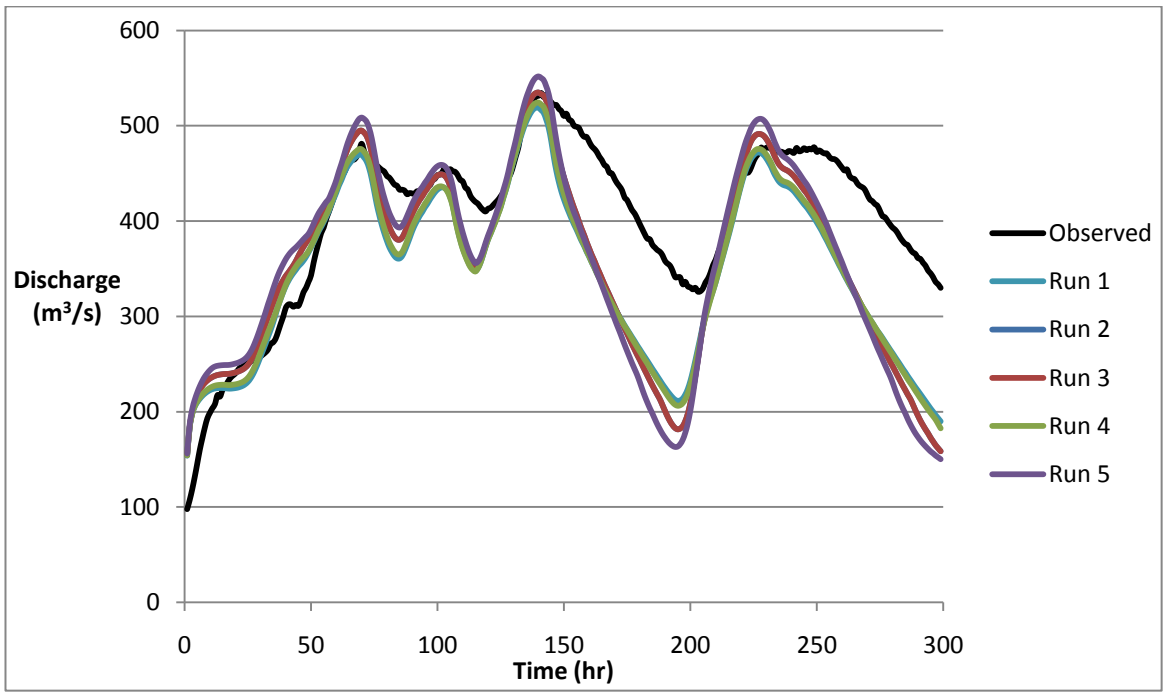

Figure 4.30 Manning's *n* decreased globally by 20% and the weir geometries changed differently in each run within Situation 1.

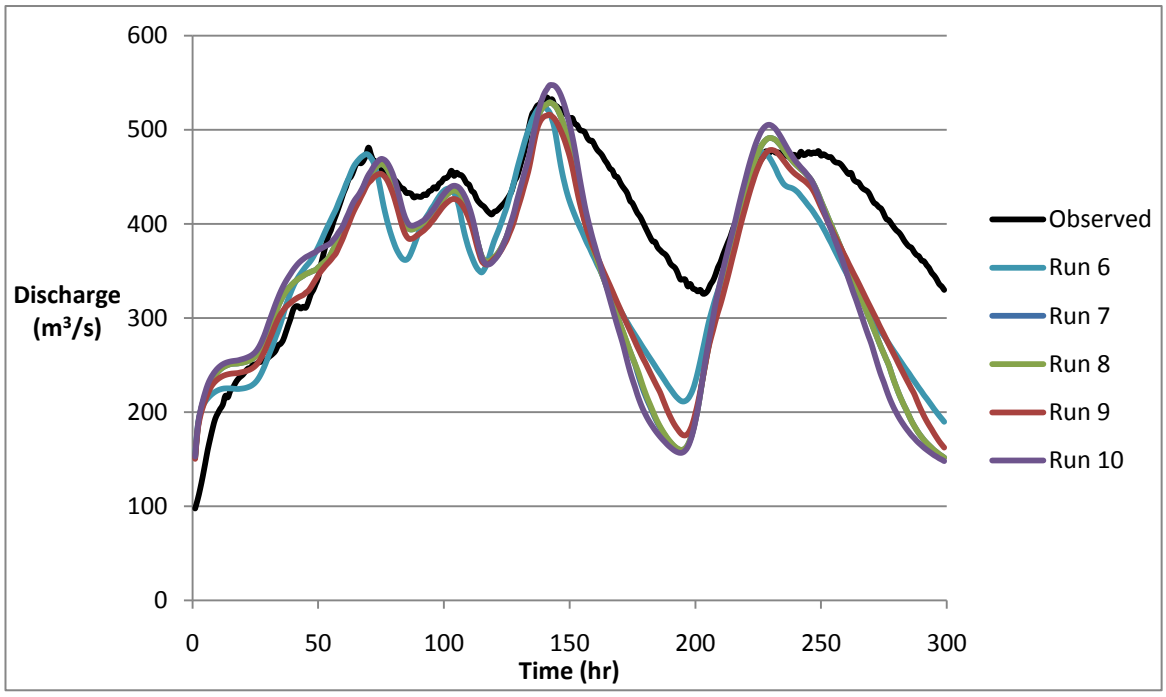

Figure 4.31 Manning's *n* of the River Ouse decreased globally by 25% and 20% for both the River Swale and River Nidd and the weir geometries changed differently in each run within Situation 2.

The problems of calibration must also be highlighted here. The calibration process relies on the reliability of the observed flow data for the River Ouse. The study had to assume that the observed data received were accurate for the 2000 flood event; however,

information from the Environment Agency (2010a) describes a number of problems with the gauging stations within the Ouse catchment. At Crakehill on the River Swale, high flows are thought to be overestimated due to drowning of the weir, and the rating is currently under review. Similarly, the high flows derived from a stage-discharge relationship at Hunsingore on the River Nidd are expected to be overestimated as found after the 2000 flood event. In contrast, the weir at Westwick is bypassed under extreme floods, therefore peaks may be underestimated. The stage data at Skelton, used for the downstream boundary condition of the model, were measured using an ultrasonic gauge and the data are believed to be accurate. These issues reduce the reliability of the observed data used for this study, and may suggest a reason why there is some variation between the simulated data and the flow data from the Ouse catchment. There were no internal records available to validate the results from this study.

Reductions in Manning's *n* were the main focus during calibration as the simulated discharge hydrograph needed to be increased slightly to match the observed data. In this situation a full calibration of the model was not possible due to a lack of data. If a longer modelling period were available, Manning's *n* could be varied at individual cross-sections in a systematic way. A satisfactory match between the modelled performance and the observed data allowed the model to be used for scenario analysis in the next stage of modelling.

4.7 Conclusion

The sensitivity analysis has shown that the HEC-RAS model is very sensitive to Manning's *n*, particularly to changes globally in the model and for the channel. High values of Manning's *n* attenuated the flood peak quite considerably and translated the hydrographs in time. The model is much less sensitive to Manning's *n* of the floodplains, a relationship shown by previous work (Yu and Lane, 2006a, 2006b). The HEC-RAS model is also sensitive to weir coefficients and changes in inflow, but to a much smaller extent. Manning's *n* was altered during the calibration process in order to improve the match of the simulated hydrograph to the observed. The correlation was improved by decreasing Manning's *n* by 20% and decreasing the width of Linton weir by 1 m. A systematic error remains between the observed and modelled flow which could result from issues with the flow data provided by the gauging stations used. The main error exists between the troughs of the observed and modelled hydrographs; however, this investigation is

primarily interested in the timing and magnitude of the flow peaks and the correlation between the two hydrographs is good at the peaks. Chapter Five will display the scenarios tested using the calibrated model.

Chapter Five

Simulation: Results

5.1 Introduction

This chapter presents the main findings of the modelling process. Section 5.2 illustrates the methods used for the main simulations presented in the results. Sections 5.3 to 5.5 present these results within the framework of the three research questions of the project. Section 5.6 summarises the main findings of the chapter.

5.2 Methodology

Four different model scenarios have been used throughout the simulation process. These are:

(1) *With levées* – current defences within the Ouse catchment are included in the model (the levées run nearly the full length of the Ouse)
(2) *Without levées* – the current defences are removed
(3) *Half height levées* – current defences are reduced to half their original height
(4) *Added height levées* – current defences are raised by 0.5 m

Each of the research questions explored below will discuss the simulations that were carried out using these four different scenarios.

5.2.1 Research Question 1 – In what way can the floodplain be used to reduce flood risk downstream?

In order to investigate research question 1, roughness characteristics within the model were varied. Understanding the interaction between channel and floodplain is required for assessing flood control strategies, particularly those using the floodplain (Ghavasieh *et al.*, 2006). Changing the roughness values within a model is a method frequently used to investigate the impact of both channel and floodplain roughness on reducing and delaying flood peaks (e.g. Wollf and Burges, 1994; Woltenmade and Potter, 1994; Blackwell and Maltby, 2005; Werner *et al.*, 2005; Ghavasieh *et al.*, 2006; Nisbet and Thomas, 2008).

The roughness values for the channel were set at between 0.02 and 0.1 (the specific values are shown in Table 5.2), a range that would capture any significant responses. The roughness values for the floodplain were set at between 0.03 and 0.3. Channel and floodplain were treated separately as the degree of roughness can vary quite

considerably between each (Nisbet and Thomas, 2008), and should be taken as separate parameters. The higher roughness values represent the establishment of woodland within the model, e.g. channel values of 0.1 and floodplain values of 0.3. Floodplain roughness of 0.3 is the upper limit for Manning's *n* and would require dense woodland with undergrowth and fallen trees (Nisbet and Thomas, 2008). This was the method used in the Ripon Multi-objective Project (MOP) recorded by Nisbet and Thomas (2008) to investigate the influence of introducing woodland to the catchment. Similarly, Nisbet (2004) used HEC-RAS to model three contrasting scenarios in terms of Manning's *n* for the Parrett catchment: (1) pasture; (2) broadleaved woodland on north bank; (3) woodland in centre of floodplain. The approaches of Nisbet (2004) and the Ripon MOP work were followed in this project but were applied further downstream within the Ouse catchment. In addition to varying roughness globally within the model, the floodplain roughness was varied along each of the tributaries independently to determine their effectiveness for water storage. Following this, the roughness variations were combined with each of the levée scenarios in order for the impact of levées in the system to be realised.

The influence of roughness within the model was quantified using the output hydrographs at Skelton from the model. Both the effect of channel and floodplain roughness on peak discharge and timing of the peak were assessed. These two parameters are used by floodplain modellers to understand the impact of possible flood control strategies on flows (e.g. Wollf and Burges, 1994; Ghavasieh *et al.*, 2006; Sholtes, 2009).

5.2.2 Research Question 2 – To what extent are land management signals impacted upon by flow attenuation?

In order to investigate research question 2, the link between the effect of blocking the upland grips and flow attenuation within the catchment was assessed. Beven *et al.* (2004) recognised that flow routing considerations might be important in how the peak response of a catchment is linked to local changes, such as flood risk. Lane (2006) acknowledged that upland environments are a good place to develop methods in order to adapt to climate change and its effects.

The Environment Agency (2010a) stated that grips are expected to have an influence at Westwick Weir gauge but no information on the exact effect of grips was available.

Therefore, hypothetical scenarios were developed in order to model the expected impact of blocking upland grips on the response of the catchment. Lane *et al.* (2003b) demonstrated that blocking grips reduces the connectivity of the hillslope to the drainage network, as water moves more slowly across the hillslope surface. After simulating blocked grips, travel time to the catchment outlet varied within the same area. It was suggested that blocking grips increases travel times, thus water is delivered more slowly through the catchment, reducing flood risk downstream (Lane *et al.*, 2003b). The potential of grip blocking to delay and attenuate floods was also recognised by the Environment Agency's (2000) moorland drainage study in Upper Wharfedale.

A number of *grip blocking scenarios* were developed in this study, in order to simulate the decreased runoff resulting from blocked grips as proposed in the literature:

- (1) The Ure input hydrograph was scaled (the discharge was multiplied by 1.01, 1.05, 1.10, 1.20, 1.25 and 1.50) to represent possible attenuation of the flood wave by reducing the peak of the hydrograph as a result of blocked grips. A range of percentages was used to see the largest hypothetical impact that grip blocking could have on the catchment. This was done by creating four pivot points or thresholds in time which coincided with the four peaks in the hydrograph (50 hr, 90 hr, 130 hr, 215 hr). 'If' functions were used to create a threshold for flow in order to scale the flow by removing water from the rising limb and adding it to the falling limb, acting like attenuation caused by blocked grips. It was ensured that mass was conserved after each calculation. In this way the shape of the hydrographs was altered in relation to the expected effects of upland grips. This hydrograph was then used as the upstream boundary condition for the River Ure.

- (2) The Ure input hydrograph was shifted by different timings (1 hr, 2 hr) to hypothetically represent the influence of blocking grips on the timing of the flood peak, creating a lag to the peak. This has the added effect of desynchronising the peak of the River Ure from the other tributaries, thus reducing the effects of flow augmentation which, where a large lateral inflow is present, can reduce the effects of attenuation (Lane and Thorne, 2007). Holden *et al.* (2004) recognised this effect to be important, as even if the flood peak is reduced from a tributary,

it may cause a delay to the peak so that it coincides with the peak of the main channel, causing an overall increase to the flood peak. This hydrograph was then used as the upstream boundary condition for the River Ure.

- (3) The above variations to the input hydrograph were combined so that both impacts of blocked grips could be seen on the downstream hydrograph. The scaled hydrograph from (1) was then shifted using the method from (2). This allowed different grip blocking scenarios in the Ure catchment to be modelled, showing the levels of attenuation and translation that could be produced using this land management technique. This hydrograph was then used as the upstream boundary condition for the River Ure. The impact of the grips on routing pathways downstream was then realised. The effect of this input hydrograph on peak discharges at different locations within the model was also assessed.

Only the Ure input hydrograph was altered with relation to the effect of blocked grips as it is recognised that the grips have the largest effect on the River Ure, and not the other tributaries (Environment Agency, 2010a). Once the changes to the Ure input hydrograph had been made, the new hydrographs were run with the 'with levées' scenario.

These grip-blocking scenarios are end members of possible grip blocking responses, so in practice the amount of attenuation and translation to the hydrograph is unlikely to be as large. This experimental approach serves as a guide to examine the scale of possible downstream consequences for peak flow as a result of grip blocking in upland catchments. The scaling and shifting of the hydrograph was used to hypothetically represent the influence of blocking grips on the system. Modelling by Lane *et al.* (2003) demonstrated that blocking grips can attenuate flows by as much as 2 hours, although this did assume a constant overland flow velocity and the location of grips does make a significant difference to the connectivity of the grips to the catchment outlet. It was thought that a shift in the hydrograph greater than 1 hour would be greatly overestimating the translation effect of blocking grips, as the main impact of grip blocking is attenuation, thus a 1 hour shift was mainly used. The large multiplications of the flow used in the scaling of the hydrograph were chosen to help highlight downstream changes to flow as a result of any propagation of the grip blocking signal. Therefore the

manipulation of the hydrographs exaggerates the effect of grip blocking on the hydrograph inputs in the headwaters.

5.2.3 Research Question 3 – Do flood levées aid the transmission of the upstream hydrograph?

In order to investigate research question 3, the combined influence of the blocked grips and the flood levées present in the model was assessed. It is expected that grip blocking results in the attenuation of flows within hillslopes, reducing flow peaks so that removing levées is a feasible flood management option (Environment Agency, 2000). Following levée removal, the frequency and duration of flooding would therefore increase behind the originally embanked area (Buijse *et al.*, 2002). This method follows that of Acreman *et al.* (2003), a study that also assessed the impact on floods of hypothetical changes to channel geometry by removing levées.

The changes to the input hydrograph with relation to blocked grips, as discussed in Section 5.2.2, were again used to address this research question. Firstly, the levées were removed and the model was run with all three variations to the hydrograph (scaled, shifted and scaled and shifted together). Secondly, the three different grip scenarios were combined with different roughness values within the model (for the channel and floodplain independently), whilst the levées were removed.

The above simulations were repeated for each of the different levée scenarios. The results obtained from running the model with the altered hydrographs and with the levées in place (as in research question 2) were compared to the results from the 'without levées' scenario in terms of effects on peak discharge and peak timing. The results were used to show how far the grip signal propagates downstream. The removal of defences from the model was used to illustrate whether or not the flood banks in the catchment translate the flood signal further downstream as inundation could be occurring further downstream. The flood bank geometry was then modified (levée scenarios 3 and 4) to see whether the signal is transmitted further downstream and has a bearing on magnitude and frequency of flood risk. It was expected that a higher flood bank would transmit the signal further. The peak flow and effect on peak timing under each of the modelled scenarios was calculated. A schematic illustrating the different variations carried out during simulations is shown in Figure 5.1.

Modelling different levée scenarios is a method used by Acreman *et al.* (2003) for the River Cherwell. They simulated extreme scenarios of levées and restored channels to show the maximum range of likely outcomes. Akanbi and Singh (1997) outlined possible future work involving the conversion of levées to temporary storage areas in order to reduce flood peaks. They recommended the use of different scenarios such as with levées, without levées and possible overtopping scenarios, the method deployed in this study. Akanbi and Singh (1997) recommended that these scenarios should be run for different flows, like the grip flows used here.

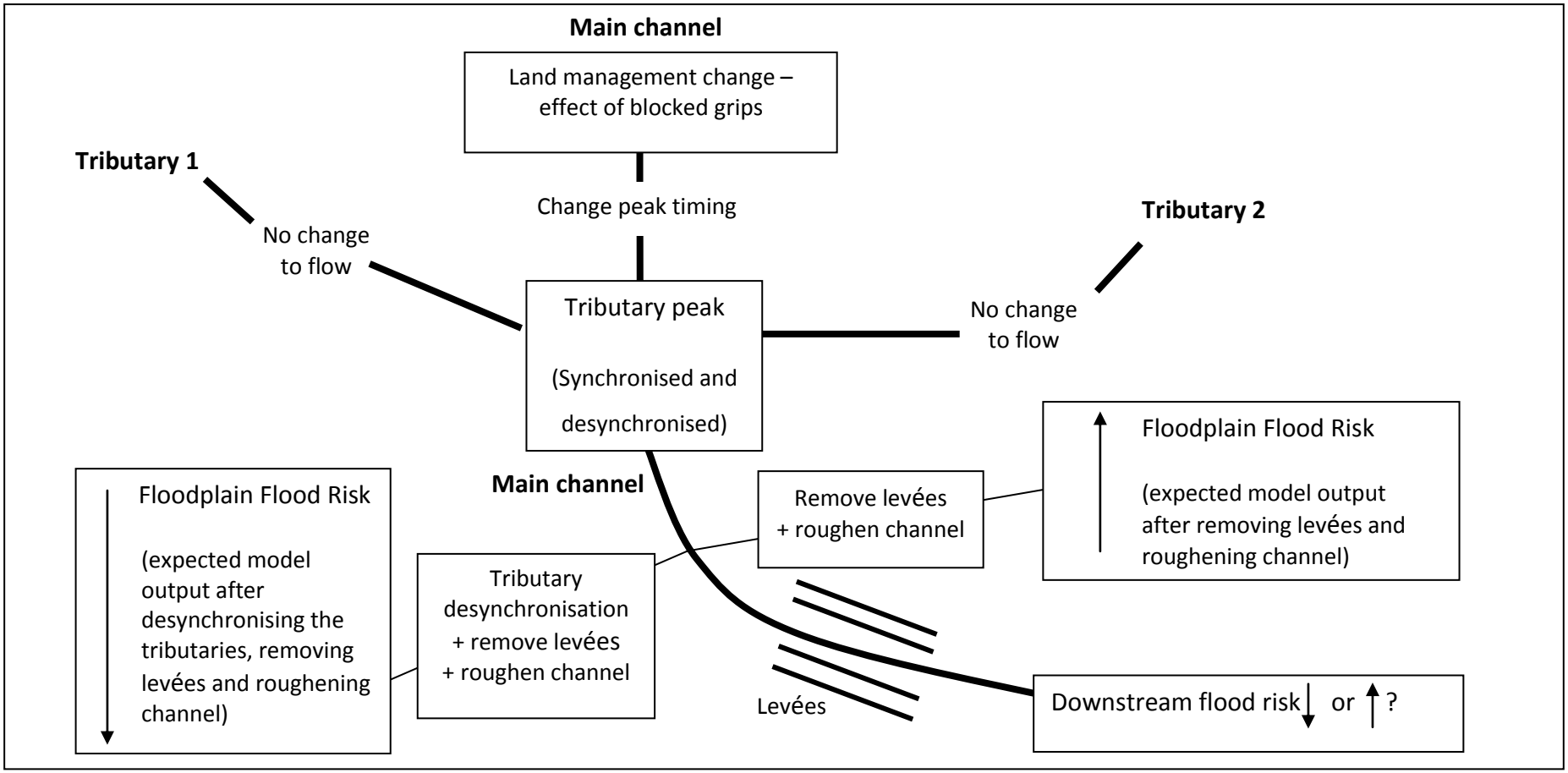

Figure 5.1 A schematic diagram of the whole system showing the possible outcomes for flood risk through model assessment. The system is constructed of three reaches which join upstream of the urban area. By modifying the main channel hydrograph, it will be possible to identify changes to the downstream hydrograph and how it affects floodplain flood risk.

5.3 Results: Research Question 1 – In what way can the floodplain be used to reduce flood risk downstream?

5.3.1 Initial hydrographs

In order to see whether a greater difference in discharge could be seen between the models, the output hydrographs at different cross-section locations were analysed (Figure 5.2). Figure 5.3 shows the initial output hydrographs at the downstream boundary at Skelton following model building. The hydrograph peaks at 524.2 m^3/s using the 'with levées' scenario. Once the levées were removed, the peak discharge reduced to 517.4 m^3/s, a reduction of 6.8 m^3/s. Figure 5.4 shows selected output hydrographs. Cross-sections 982 and 938 give the largest difference in peak discharge between the scenarios, at 11.5 m^3/s and 10.8 m^3/s respectively (Figure 5.5), although the difference in hydrograph shape is largest for cross-sections 955 and 938.

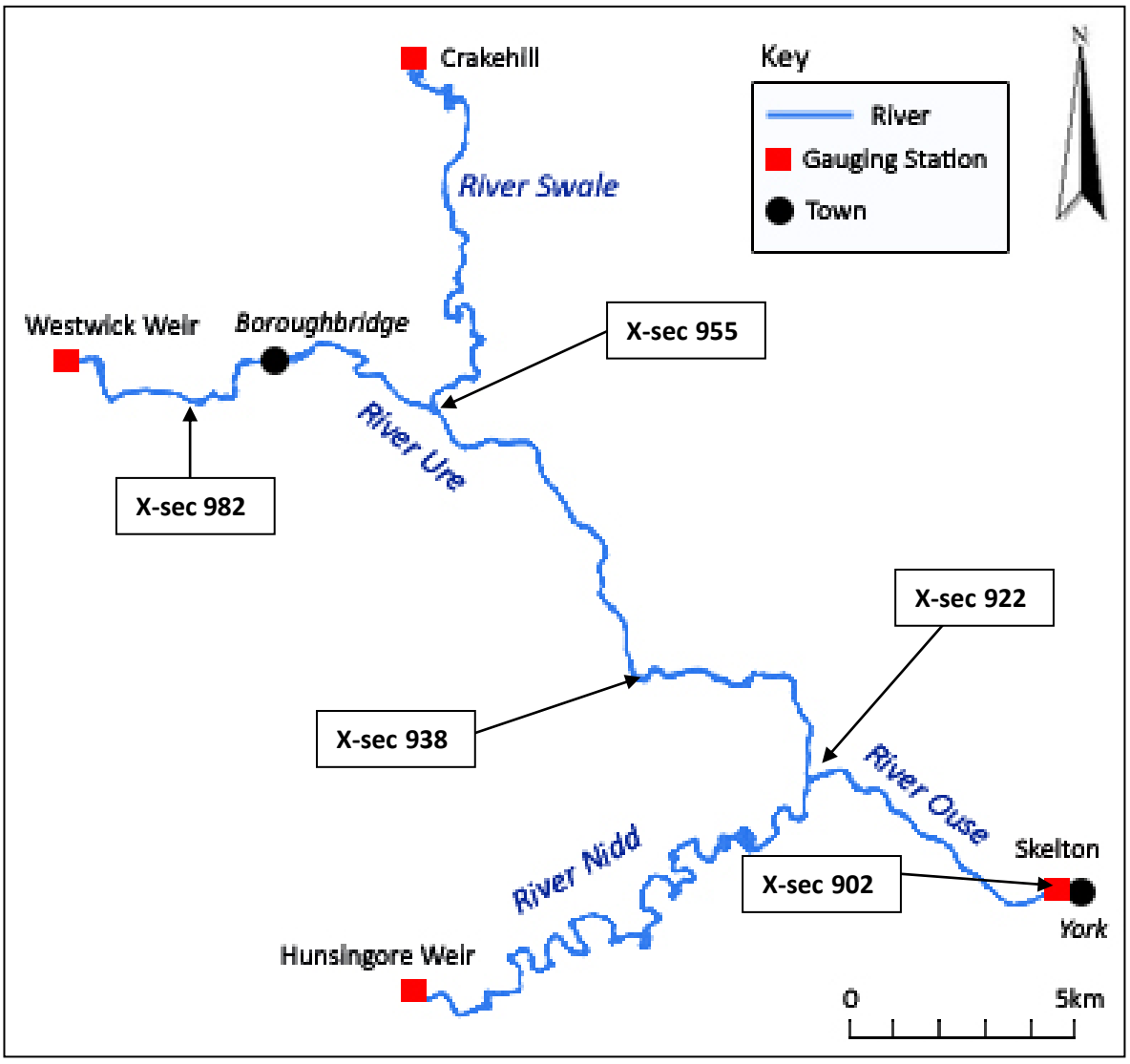

Figure 5.2 Locations of the cross-sections (x-sec) within the modelled reach that were used for flow analysis. These specific cross-sections were chosen for different reasons. Cross-section 982 is halfway between the top of the River Ouse and the confluence with the River Swale, thus any instabilities at the top of the model should not affect the results. Cross-section 955 is located just after the confluence of the River Swale and chosen in order to highlight the impact of the joining tributary on peak discharge. Cross-section 938 is halfway between the River Swale confluence and the River Nidd confluence. Cross-section 922 is just after the River Nidd confluence, and far enough from Linton weir that its effects on peak discharge should not be felt. Cross-section 902 marks the downstream boundary of the model.

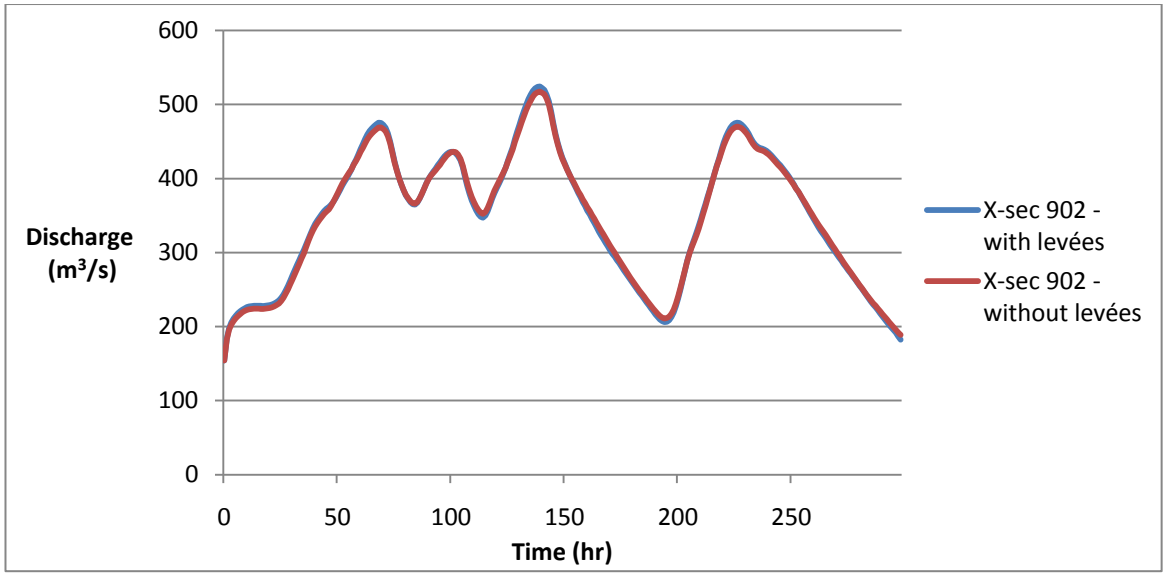

Figure 5.3 Output hydrograph at the downstream boundary for the original flow using the 'with levées' and 'without levées' scenarios. Cross-section 902 (x-sec) refers to the downstream boundary at Skelton.

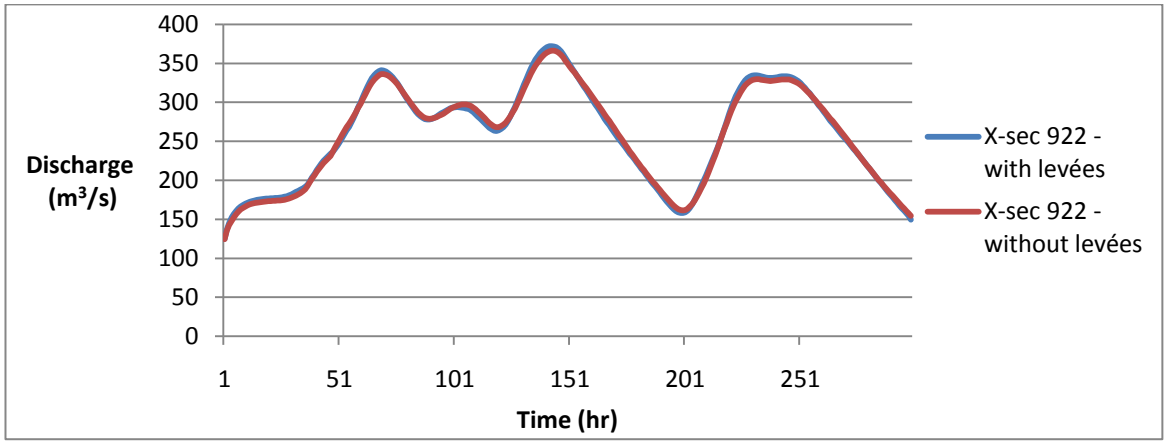

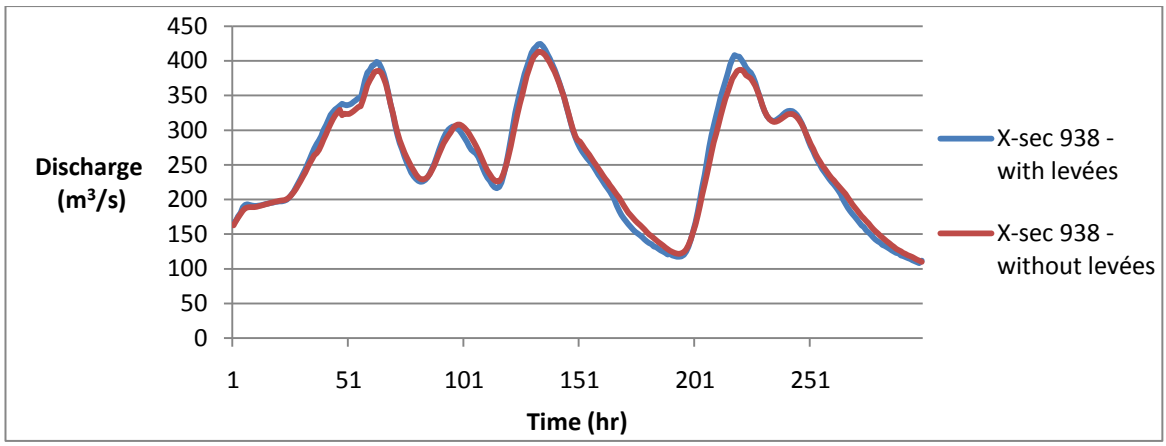

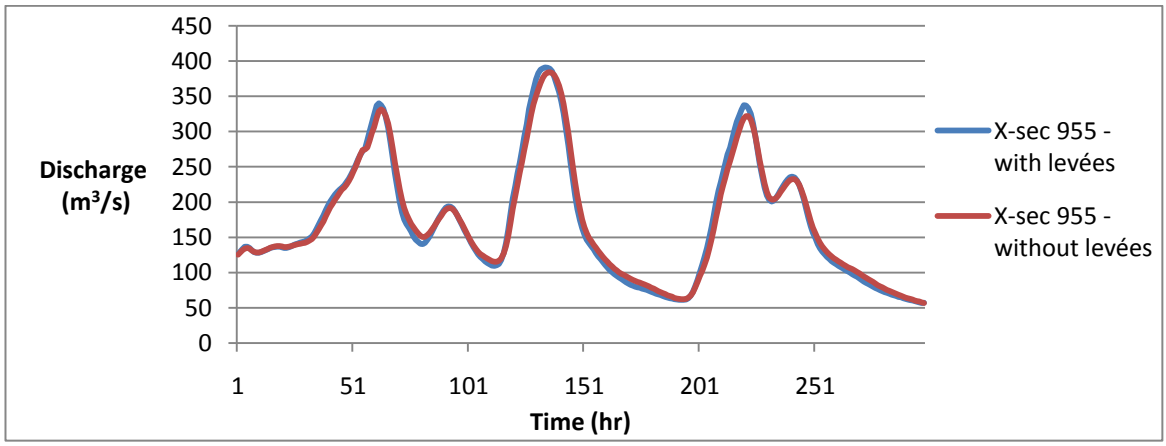

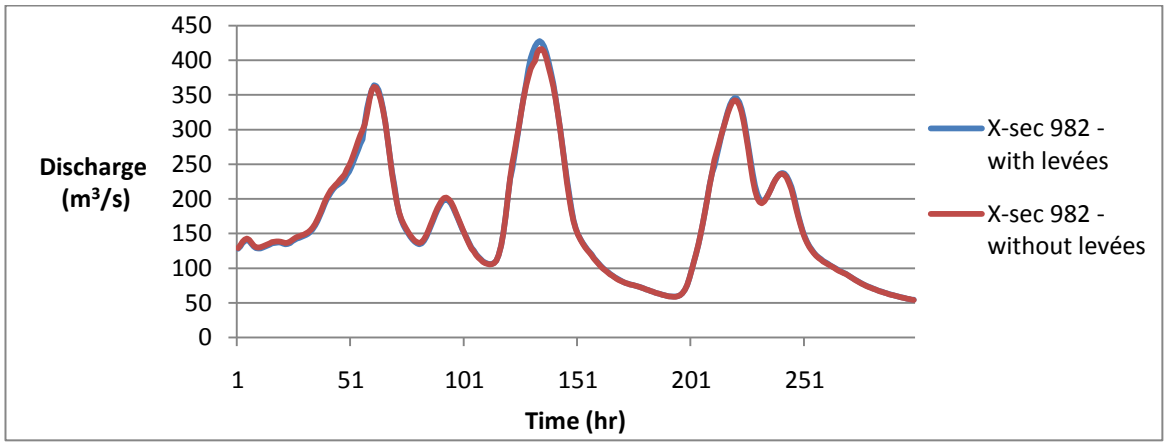

Figure 5.4 Output hydrographs at selected cross-sections in the model for the original flow using the 'with levées' and 'without levées' scenarios.

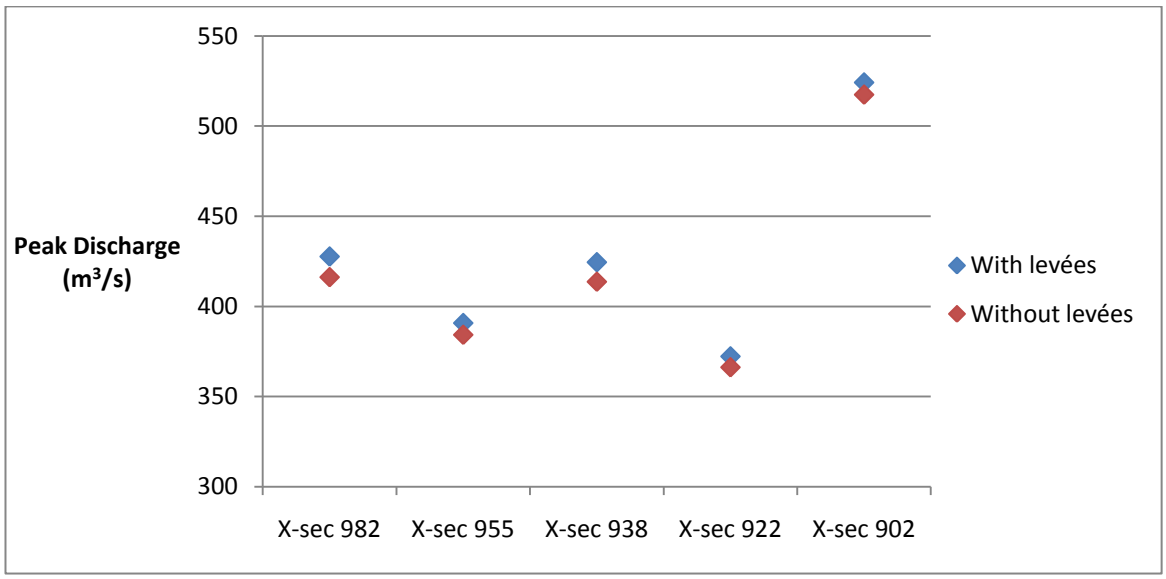

Figure 5.5 Difference in peak discharge between the scenarios for different cross-sections in the model. Cross-section locations are shown in Figure 5.2.

Figure 5.6 shows that the mean peak timing delay for the downstream boundary is 0.5 hours. Mean peak timing delay is greatest in the middle of the model, between 955 and 922, at 1.25 hours. At cross-section 982, near the beginning of the modelled reach, the mean peak timing delay is the lowest at 0.25 hours. Table 5.1 shows the statistics for peak discharge and peak timing delay for the cross-sections mentioned using both scenarios.

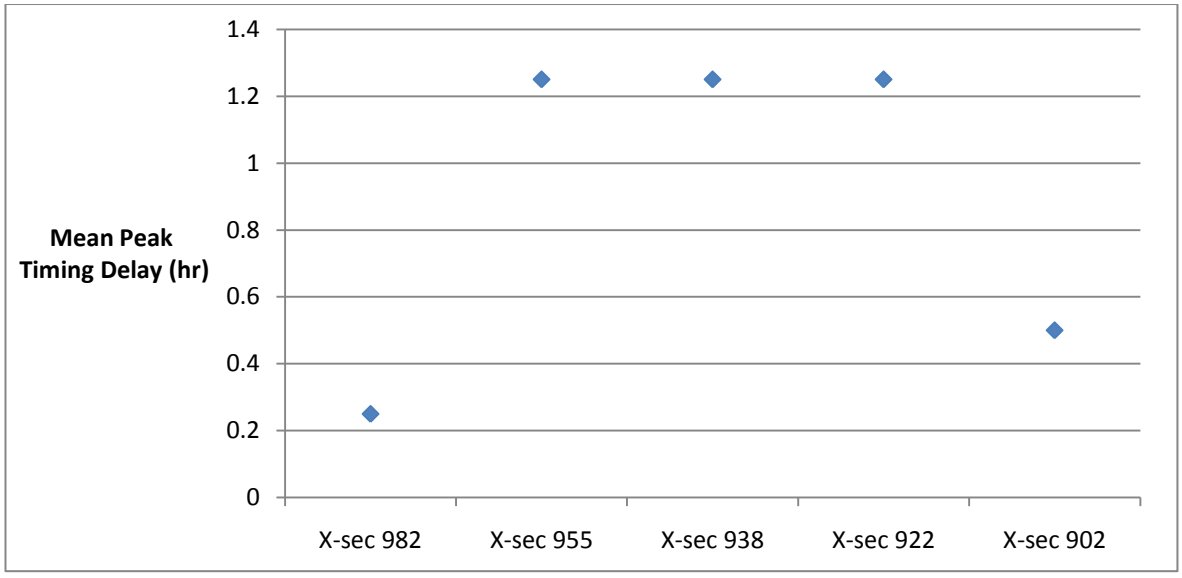

Figure 5.6 Difference in peak timing delay between the scenarios for different cross-sections in the model. The timing of the peak was averaged across each of four peaks in the hydrograph. Cross-section locations are shown in Figure 5.2.

Location	Peak Q (m^3/s)	dQ (m^3/s)	PEP (%)	Mean peak timing delay (hr)
With levées x-sec 982	427.6	11.5	-2.7	0.25
Without levées x-sec 982	416.2			
With levées x-sec 955	390.7	6.5	-1.7	1.25
Without levées x-sec 955	384.2			
With levées x-sec 938	424.5	10.8	-2.6	1.25
Without levées x-sec 938	413.6			
With levées x-sec 922	372.2	6.0	-1.6	1.25
Without levées x-sec 922	366.2			
With levées x-sec 902	524.2	6.8	-1.3	0.5
Without levées x-sec 902	517.4			

Table 5.1 Statistics for peak discharge and peak timing delay for the 'with levées' and 'without levées' scenarios for different cross-sections in the model. Cross-section locations are shown in Figure 5.2.

5.3.2 Varying Manning's *n* for all reaches

Figure 5.7 shows that Manning's *n* values for the channel have a large influence on the peak discharge recorded at the downstream boundary. For both scenarios, peak discharge reduces with increasing values of channel *n,* but the influence of Manning's *n* is lower at higher values. For the 'with levées' scenario, peak discharge is reduced from 585.3 m^3/s at n = 0.02 to 416.2 m^3/s at n = 0.1, a difference of 169.1 m^3/s. For the 'without levées' scenario, peak discharge is reduced by a larger margin, from 576.6 m^3/s at n = 0.02 to 396.0 m^3/s at n = 0.1, a difference of 180.6 m^3/s. Mostly the values for 'with levées' are higher than 'without levées', although at higher Manning's *n* values this trend becomes less.

A similar relationship between Manning's *n* values for the floodplain and peak discharge is shown for both scenarios (Figure 5.8). Peak discharge reduces with increasing floodplain *n* values but the trend is less linear: between n = 0.08 and 0.1 peak discharge actually increases slightly for both scenarios. The influence of floodplain *n* is not as strong as with channel *n*, reducing peak discharge from 518.2 m^3/s at n = 0.03 to 510.0 m^3/s at n = 0.3 with levées and from 516.1 m^3/s at n = 0.03 to 503.6 m^3/s at n = 0.3 without levées. The reduction in the peak discharge is slightly larger without levées.

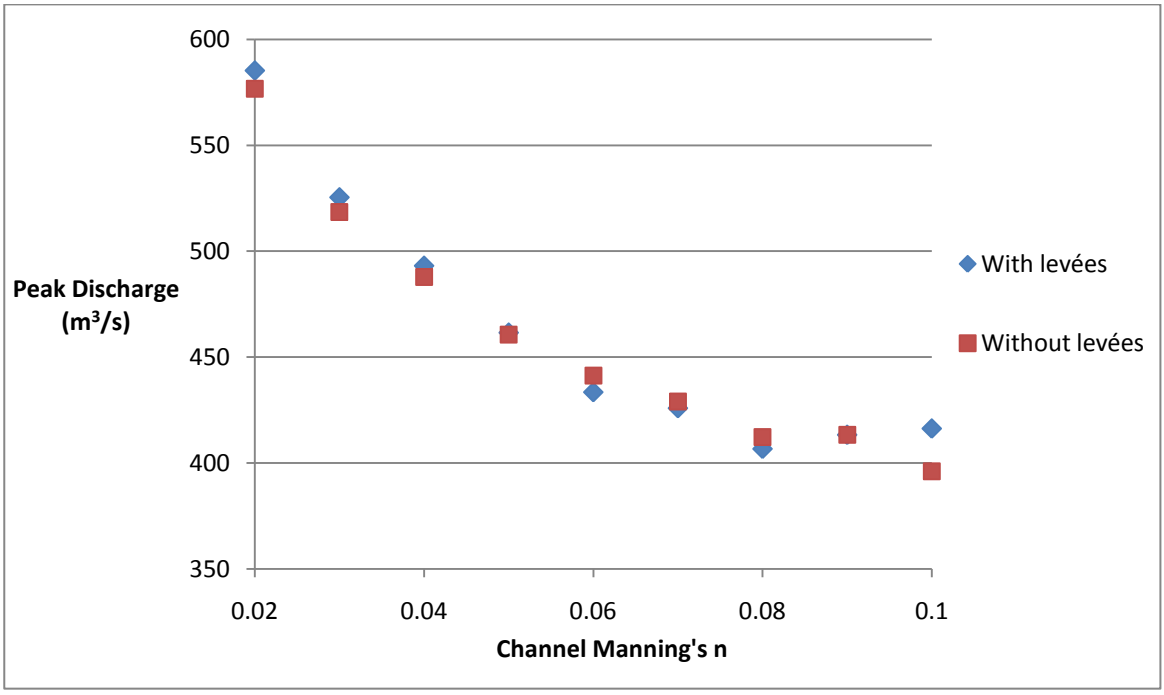

Figure 5.7 Change in peak discharge with relation to Manning's *n* values of the channel for the 'with levées' and 'without levées' scenarios.

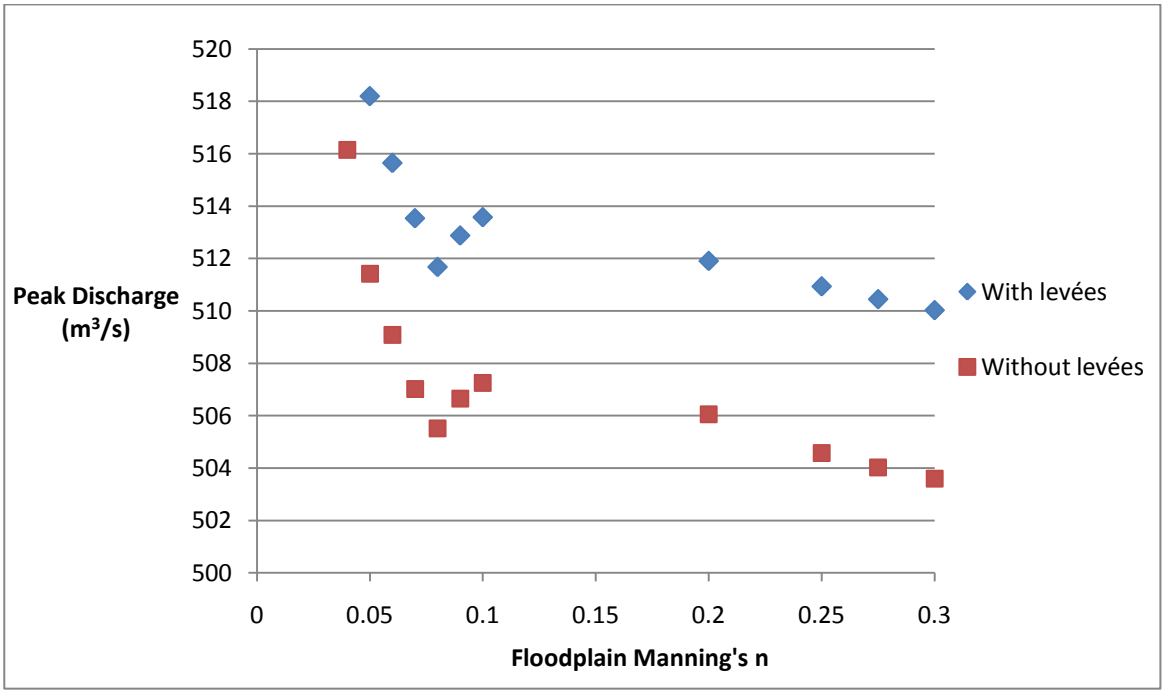

Figure 5.8 Change in peak discharge with relation to Manning's *n* values of the floodplain for the 'with levées' and 'without levées' scenarios.

In addition to varying channel and floodplain *n* independently, the effects were combined in Figures 5.9. Values for floodplain *n* were varied between 0.1 and 0.3 for each simulation and channel *n* remained constant at 0.08, 0.09 and 0.1. Peak discharge is

reduced with each combination, but the most by higher values of channel *n*. For the 'with levées' scenario, peak discharge is reduced by 17.8 m^3/s with channel *n* = 0.08, by 27.6 m^3/s with channel *n* = 0.09 and by 24.2 m^3/s with channel *n* = 0.1. For the 'without levées' scenario, peak discharge is reduced by 17.5 m^3/s with channel *n* = 0.08, by 22.6 m^3/s with channel *n* = 0.09 and by 23.7 m^3/s with channel *n* = 0.1. The reduction in the peak resulting from changes in Manning's *n* was larger with the levées.

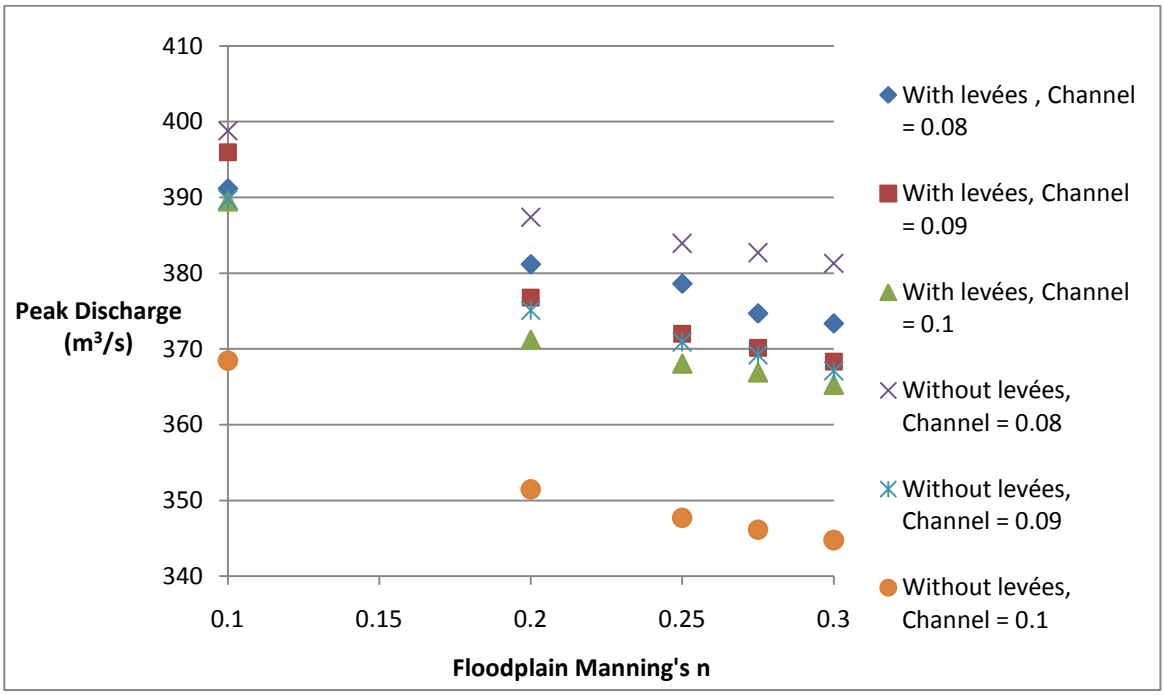

Figure 5.9 Change in peak discharge with relation to Manning's *n* values varied for both the channel and floodplain for the 'with levées' and 'without levées' scenarios. Manning's *n* values for the channel were fixed at 0.08, 0.09 and 0.1 whilst varied for the floodplain.

Figure 5.10 shows that the timing of the main peak in the hydrograph is shifted later with higher channel *n*. With low values for channel *n* the peak occurs much earlier than with the original Manning's *n* values. With levées the peak occurs 7 hours earlier with a channel *n* of 0.02 compared to 11 hours without the levées. High Manning's *n* values shift the timing of the peak much later: with levées the peak occurs 23 hours later with a channel *n* of 0.1, and 20 hours later without the levées. The timing of the peak appears to be primarily later without the levées. Floodplain *n* also has an influence on peak timing delay, but not to the same extent (Figure 5.11). Both scenarios display the same results, with the peak timing delay ranging from -1 hour at *n* = 0.03 (the peak occurred earlier than with the original values for Manning's *n* included in the model) to 2 hours at *n* =

0.09. Higher values for floodplain *n* do not have an influence on peak timing delay. The statistics for the simulations varying channel and floodplain *n* for the whole model are shown in Table 5.2.

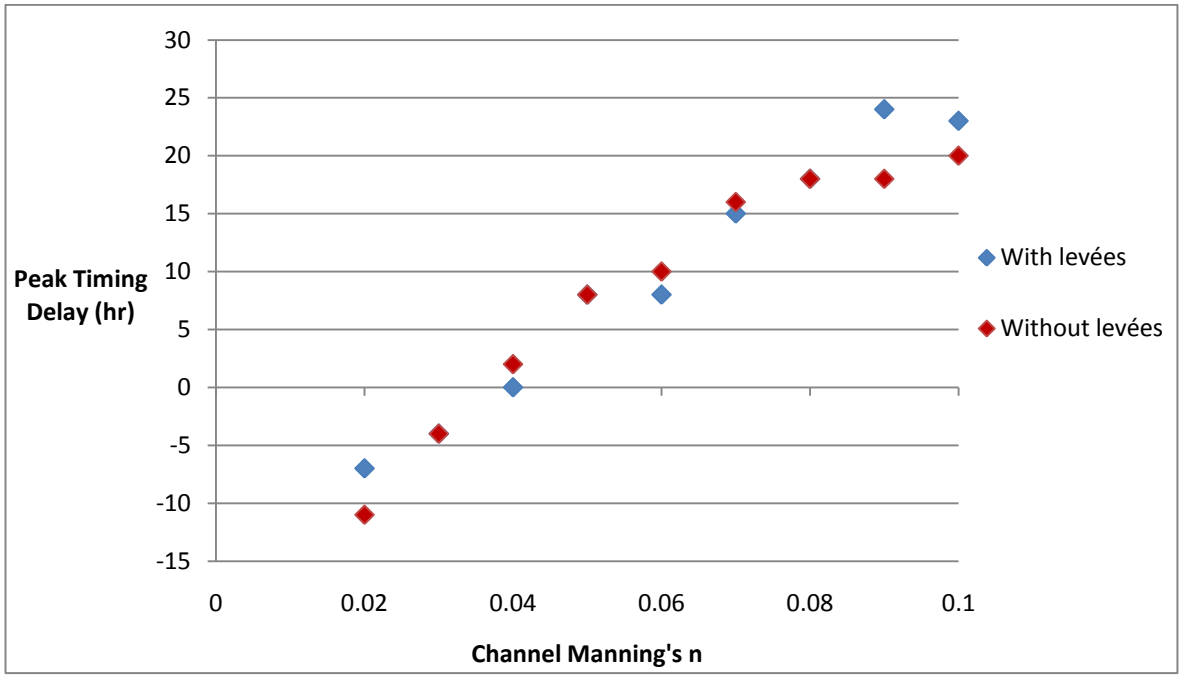

Figure 5.10 Change in peak timing delay with relation to Manning's *n* values of the channel for the 'with levées' and 'without levées' scenarios. The results use the original *n* values included in the model as the baseline, thus the negative values demonstrate that the peak occurred earlier than with the original values for Manning's *n*.

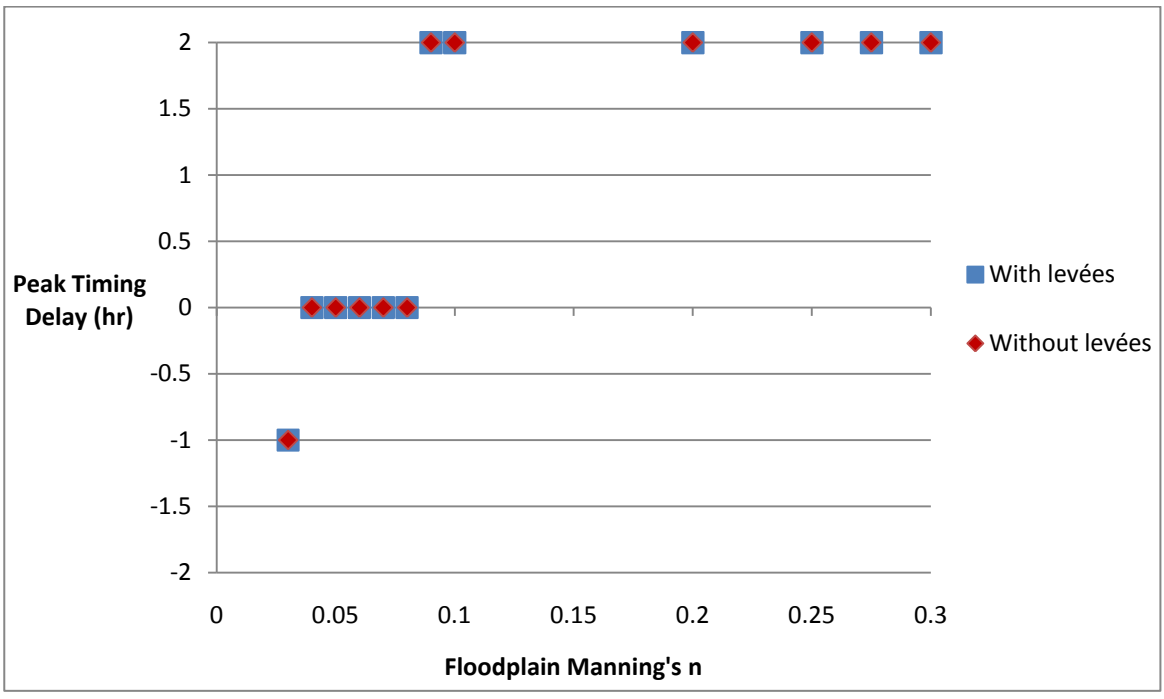

Figure 5.11 Change in peak timing delay with relation to Manning's *n* values of the floodplain for the 'with levées' and 'without levées' scenarios.

	With levées					Without levées				
Scenario	**Peak Q (m^3/s)**	**Peak timing (hr)**	**dQ (m^3/s)**	**dQ (%)**	**dt (hr)**	**Peak Q (m^3/s)**	**Peak timing (hr)**	**dQ (m^3/s)**	**dQ (%)**	**dt (hr)**
Baseline	**524.2**	**140**	**0.0**	**0.0**	**0**	**517.4**	**140**	**0.0**	**0.0**	**0**
Channel *n* = 0.02	585.3	133	61.1	-11.7	-7	576.6	129	59.2	-11.4	-11
Channel *n* = 0.03	525.4	136	1.2	-0.2	-4	518.6	136	1.1	-0.2	-4
Channel *n* = 0.04	493.1	140	-31.1	5.9	0	487.9	142	-29.6	5.7	2
Channel *n* = 0.05	461.5	148	-62.7	12.0	8	460.6	148	-56.9	11.0	8
Channel *n* = 0.06	433.4	148	-90.8	17.3	8	441.3	150	-76.2	14.7	10
Channel *n* = 0.07	425.8	155	-98.4	18.8	15	429.0	156	-88.5	17.1	16
Channel *n* = 0.08	406.6	158	-117.6	22.4	18	412.3	158	-105.2	20.3	18
Channel *n* = 0.09	413.2	164	-111.0	21.2	24	413.3	158	-104.2	20.1	18
Channel *n* = 0.1	416.2	163	-108.0	20.6	23	396.0	160	-121.4	23.5	20
Floodplain *n* = 0.03	529.6	139	5.5	-1.0	-1	522.2	139	4.7	-0.9	-1
Floodplain *n* = 0.04	523.2	139	-1.0	0.2	-1	516.1	140	-1.3	0.3	0
Floodplain *n* = 0.05	518.2	140	-6.0	1.1	0	511.4	140	-6.0	1.2	0
Floodplain *n* = 0.06	515.7	140	-8.5	1.6	0	509.1	140	-8.4	1.6	0
Floodplain *n* = 0.07	513.5	140	-10.7	2.0	0	507.0	140	-10.4	2.0	0
Floodplain *n* = 0.08	511.7	140	-12.5	2.4	0	505.5	140	-11.9	2.3	0
Floodplain *n* = 0.09	512.9	142	-11.3	2.2	2	506.7	142	-10.8	2.1	2
Floodplain *n* = 0.1	513.6	142	-10.6	2.0	2	507.3	142	-10.2	2.0	2
Floodplain *n* = 0.2	511.9	142	-12.3	2.3	2	506.1	142	-11.4	2.2	2
Floodplain *n* = 0.25	510.9	142	-13.3	2.5	2	504.6	142	-12.9	2.5	2
Floodplain *n* = 0.275	510.5	142	-13.7	2.6	2	504.0	142	-13.4	2.6	2
Floodplain *n* = 0.3	510.0	142	-14.2	2.7	2	503.6	142	-13.8	2.7	2
C = 0.08, fplain = 0.1	391.2	158	-133.0	25.4	18	398.8	158	-118.7	22.9	18
C = 0.08, fplain = 0.2	381.2	165	-143.0	27.3	25	387.4	165	-130.1	25.1	25

	With levées					Without levées				
Scenario	**Peak Q (m^3/s)**	**Peak timing (hr)**	**dQ (m^3/s)**	**dQ (%)**	**dt (hr)**	**Peak Q (m^3/s)**	**Peak timing (hr)**	**dQ (m^3/s)**	**dQ (%)**	**dt (hr)**
C = 0.08, fplain = 0.25	378.6	166	-145.6	27.8	26	383.9	165	-133.5	25.8	25
C = 0.08, fplain = 0.275	374.7	165	-149.5	28.5	25	382.7	165	-134.7	26.0	25
C = 0.08, fplain = 0.3	373.4	165	-150.8	28.8	25	381.3	165	-136.1	26.3	25
C = 0.09, fplain = 0.1	396.0	167	-128.2	24.5	27	389.7	165	-127.7	24.7	25
C = 0.09, fplain = 0.2	376.8	171	-147.4	28.1	31	375.1	170	-142.4	27.5	30
C = 0.09, fplain = 0.25	372.0	171	-152.2	29.0	31	370.9	170	-146.5	28.3	30
C = 0.09, fplain = 0.275	370.1	172	-154.1	29.4	32	369.2	170	-148.2	28.6	30
C = 0.09, fplain = 0.3	368.3	172	-155.9	29.7	32	367.1	174	-150.4	29.1	34
C = 0.1, fplain = 0.1	389.5	168	-134.7	25.7	28	368.5	164	-149.0	28.8	24
C = 0.1, fplain = 0.2	371.2	175	-153.0	29.2	35	351.5	172	-166.0	32.1	32
C = 0.1, fplain = 0.25	368.1	175	-156.1	29.8	35	347.7	173	-169.7	32.8	33
C = 0.1, fplain = 0.275	366.9	175	-157.3	30.0	35	346.1	174	-171.3	33.1	34
C = 0.1, fplain = 0.3	365.3	175	-158.9	30.3	35	344.8	174	-172.7	33.4	34

Table 5.2 Peak discharge and peak timing results for simulations using the 'with levées' scenario. The baseline is the results returned from the original 'modelled flow' after initial model building. The results are compared to this baseline.

5.3.3 Varying Manning's *n* for the River Ouse

Figure 5.12 shows that variations in Manning's *n* values for the Ouse channel have a large influence on the peak discharge of the model. With levées, peak discharge reduces nearly linearly from 546.3 m^3/s at *n* = 0.02 to 411.1 m^3/s at *n* = 0.1. Without levées, peak discharge reduces from 538.6 m^3/s at *n* = 0.02 to 392.0 m^3/s at *n* = 0.1. The reduction in peak discharge is larger without the levées. The reduction in peak discharge is 34.0 m^3/s less than for varying channel roughness for the whole model. The difference in peak discharge between the scenarios gradually increases towards high *n* values, as the gradient for the 'without levées' scenario is steeper. As with varying the floodplain roughness for the whole model, increasing Manning's *n* values for the Ouse floodplain decreases peak discharge gradually. In contrast to the whole model, Figure 5.13 shows a regular reduction in peak discharge with increasing Manning's *n* on the floodplain.

The effects of varying channel and floodplain *n* were also combined in Figure 5.14. The same three simulations were run as with the roughness variations in Figure 5.10 for the whole model. With levées, peak discharge is reduced by 21.1 m^3/s with a channel of 0.08, by 20.5 m^3/s with a channel *n* of 0.09 and by 35.0 m^3/s with a channel *n* of 0.1. Without levées, peak discharge is reduced by 21.7 m^3/s with a channel *n* of 0.08, by 25.5 m^3/s with a channel *n* of 0.09 and by 29.4 m^3/s with a channel *n* of 0.1. In contrast with the whole model, the reductions in peak discharge are mainly highest without the levées.

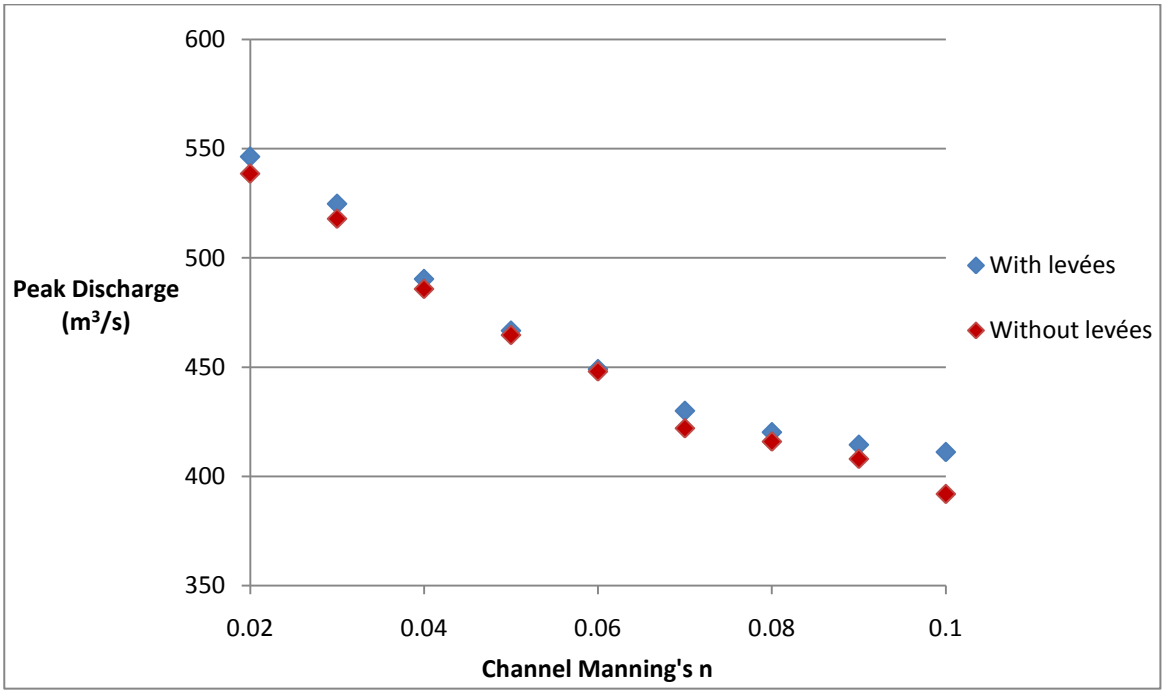

Figure 5.12 Change in peak discharge with relation to Manning's *n* values of the Ouse channel for the 'with levées' and 'without levées' scenarios.

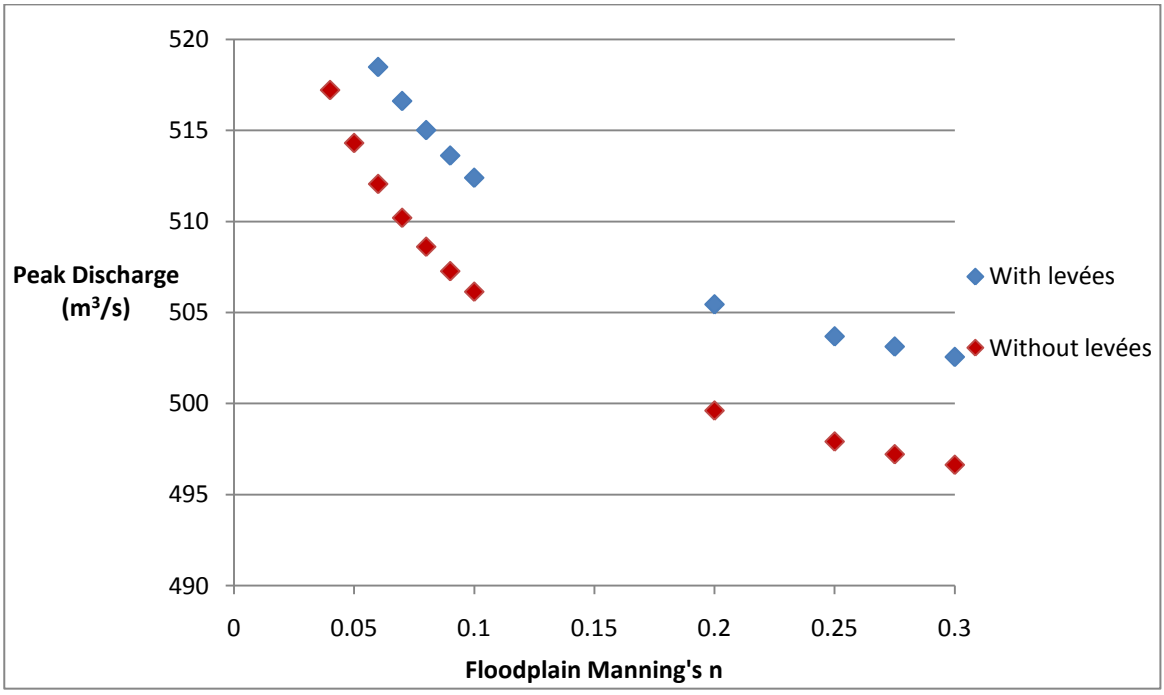

Figure 5.13 Change in peak discharge with relation to Manning's *n* values of the Ouse floodplain for the 'with levées' and 'without levées' scenarios.

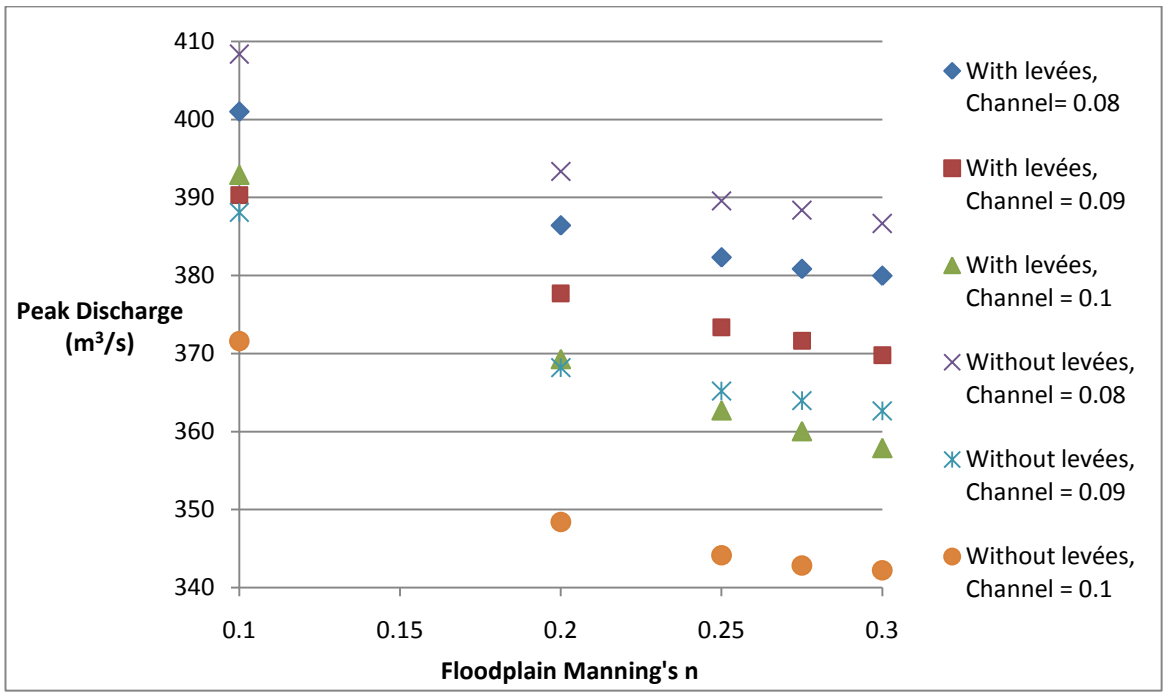

Figure 5.14 Change in peak discharge with relation to Manning's *n* values varied for both the channel and floodplain for the 'with levées' and 'without levées' scenarios. Manning's *n* values for the channel were fixed at 0.08, 0.09 and 0.1 whilst varied for the floodplain.

Figure 5.15 shows the influence of Manning's *n* values for the Ouse channel on the timing of the main peak. With levées, the delay in peak timing delay increases from 0 hours at *n* = 0.02 to 6 hours at *n* = 0.08 but, unlike the trend for the whole model, reduces to 5 hours at *n* = 0.1. Without the levées the same trend is shown, but rising to 8 hours at *n* = 0.08 and falling to 4 hours at *n* = 0.1. Therefore channel Manning's *n* has a greater influence on peak timing delay in the 'without levées' scenario. Figure 5.16 shows that varying the Ouse floodplain *n* does not affect the timing of the peak for the 'without levées' scenario. In contrast, the peak occurs 1 hour earlier with the levées with a floodplain *n* of between 0.25 and 0.3. The statistics for the simulations varying channel and floodplain *n* for the Ouse are shown in Table 5.3.

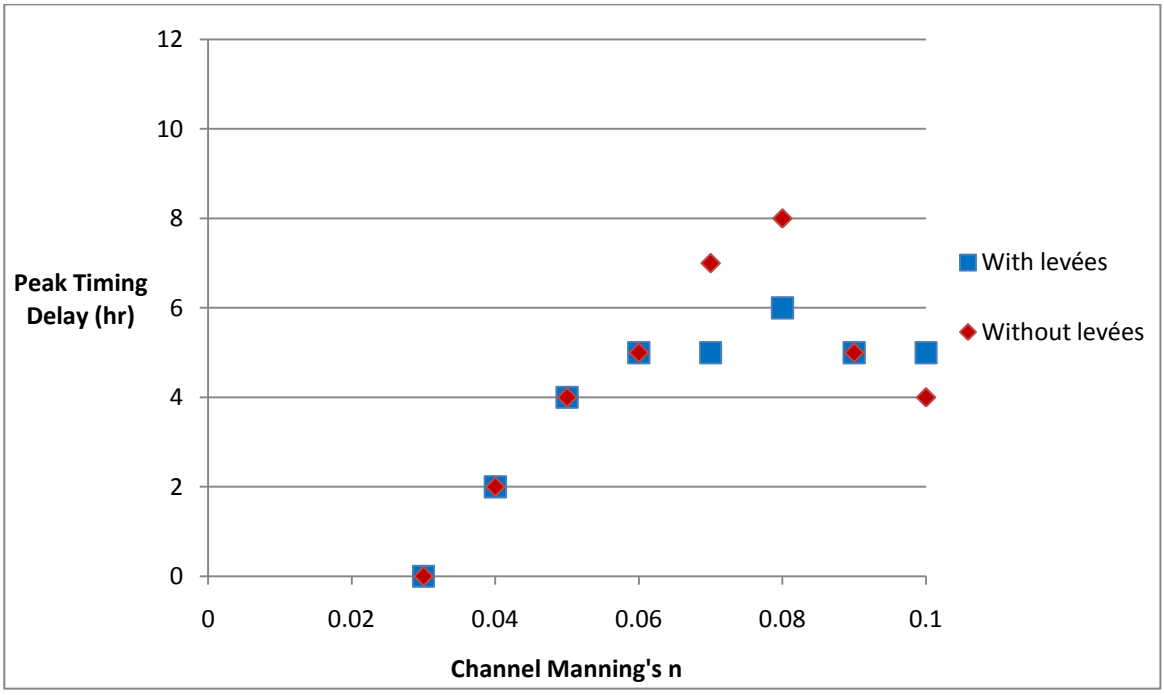

Figure 5.15 Change in peak timing delay with relation to Manning's *n* values of the Ouse channel for the 'with levées' and 'without levées' scenarios.

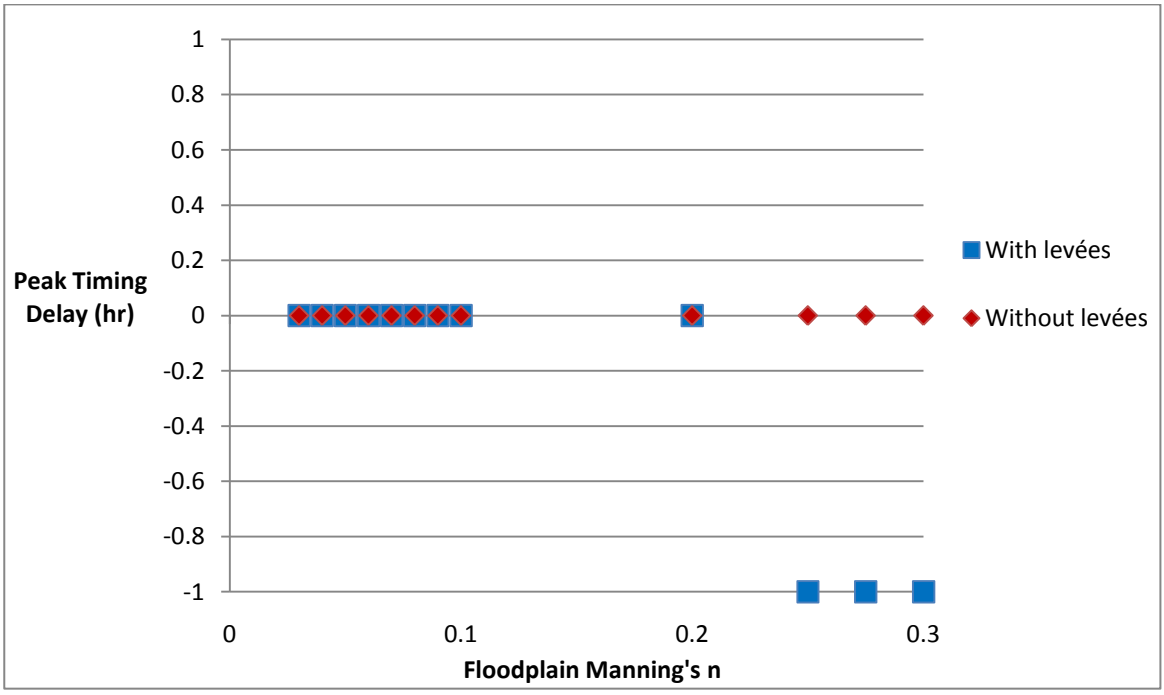

Figure 5.16 Change in peak timing delay with relation to Manning's *n* values of the Ouse floodplain for the 'with levées' and 'without levées' scenarios.

	With levées					Without levées				
Scenario	**Peak Q (m^3/s)**	**Peak timing (hr)**	**dQ (m^3/s)**	**dQ (%)**	**dt (hr)**	**Peak Q (m^3/s)**	**Peak timing (hr)**	**dQ (m^3/s)**	**dQ (%)**	**dt (hr)**
Baseline	**524.2**	**140**	**0.0**	**0.0**	**0**	**517.4**	**140.0**	**0.0**	**0.0**	**0**
Channel *n* = 0.02	546.3	139	22.1	-4.2	-1	538.6	139.0	21.1	-4.1	-1
Channel *n* = 0.03	524.8	140	0.6	-0.1	0	517.9	140.0	0.5	-0.1	0
Channel *n* = 0.04	490.4	142	-33.8	6.5	2	485.8	142.0	-31.6	6.1	2
Channel *n* = 0.05	466.7	144	-57.5	11.0	4	464.7	144.0	-52.7	10.2	4
Channel *n* = 0.06	449.1	145	-75.1	14.3	5	448.1	145.0	-69.4	13.4	5
Channel *n* = 0.07	430.0	145	-94.2	18.0	5	422.1	147.0	-95.4	18.4	7
Channel *n* = 0.08	420.2	146	-104.0	19.8	6	416.0	148.0	-101.5	19.6	8
Channel *n* = 0.09	414.5	145	-109.7	20.9	5	408.0	145.0	-109.4	21.1	5
Channel *n* = 0.1	411.1	145	-113.1	21.6	5	392.0	144.0	-125.4	24.2	4
Floodplain *n* = 0.03	527.9	140	3.7	-0.7	0	520.8	140.0	3.4	-0.7	0
Floodplain *n* = 0.04	524.1	140	-0.1	0.0	0	517.2	140.0	-0.2	0.0	0
Floodplain *n* = 0.05	521.1	140	-3.1	0.6	0	514.3	140.0	-3.1	0.6	0
Floodplain *n* = 0.06	518.5	140	-5.7	1.1	0	512.1	140.0	-5.4	1.0	0
Floodplain *n* = 0.07	516.6	140	-7.6	1.4	0	510.2	140.0	-7.2	1.4	0
Floodplain *n* = 0.08	515.0	140	-9.2	1.8	0	508.6	140.0	-8.8	1.7	0
Floodplain *n* = 0.09	513.6	140	-10.6	2.0	0	507.3	140.0	-10.2	2.0	0
Floodplain *n* = 0.1	512.4	140	-11.8	2.3	0	506.1	140.0	-11.3	2.2	0
Floodplain *n* = 0.2	505.4	140	-18.8	3.6	0	499.6	140.0	-17.8	3.5	0
Floodplain *n* = 0.25	503.7	139	-20.5	3.9	-1	497.9	140.0	-19.5	3.8	0
Floodplain *n* = 0.275	503.1	139	-21.1	4.0	-1	497.2	140.0	-20.2	3.9	0
Floodplain *n* = 0.3	502.6	139	-21.6	4.1	-1	496.6	140.0	-20.8	4.0	0
C = 0.08, fplain = 0.1	401.0	144	-123.2	23.5	4	408.4	145.0	-109.1	21.1	5
C = 0.08, fplain = 0.2	386.4	144	-137.8	26.3	4	393.4	148.0	-124.1	24.0	8

	With levées					Without levées				
Scenario	**Peak Q (m^3/s)**	**Peak timing (hr)**	**dQ (m^3/s)**	**dQ (%)**	**dt (hr)**	**Peak Q (m^3/s)**	**Peak timing (hr)**	**dQ (m^3/s)**	**dQ (%)**	**dt (hr)**
C = 0.08, fplain = 0.25	382.3	144	-141.9	27.1	4	389.6	148.0	-127.9	24.7	8
C = 0.08, fplain = 0.275	380.8	144	-143.4	27.4	4	388.4	148.0	-129.1	25.0	8
C = 0.08, fplain = 0.3	380.0	142	-144.2	27.5	2	386.7	148.0	-130.8	25.3	8
C = 0.09, fplain = 0.1	390.3	148	-133.9	25.5	8	388.1	145.0	-129.3	25.0	5
C = 0.09, fplain = 0.2	377.7	148	-146.5	27.9	8	368.2	148.0	-149.3	28.9	8
C = 0.09, fplain = 0.25	373.4	148	-150.8	28.8	8	365.2	148.0	-152.2	29.4	8
C = 0.09, fplain = 0.275	371.6	150	-152.6	29.1	10	364.0	148.0	-153.5	29.7	8
C = 0.09, fplain = 0.3	369.8	148	-154.4	29.5	8	362.7	148.0	-154.8	29.9	8
C = 0.1, fplain = 0.1	392.9	148	-131.3	25.0	8	371.6	144.0	-145.9	28.2	4
C = 0.1, fplain = 0.2	369.3	148	-154.9	29.6	8	348.4	145.0	-169.0	32.7	5
C = 0.1, fplain = 0.25	362.7	150	-161.5	30.8	10	344.1	145.0	-173.3	33.5	5
C = 0.1, fplain = 0.275	360.1	150	-164.1	31.3	10	342.8	145.0	-174.6	33.7	5
C = 0.1, fplain = 0.3	357.9	150	-166.3	31.7	10	342.2	145.0	-175.2	33.9	5

Table 5.3 Peak discharge and peak timing results for simulations using the 'with levées' scenario for the River Ouse. The baseline is the results returned from the original 'modelled flow' after initial model building. The results are compared to this baseline.

5.3.4 Varying Manning's *n* for the River Swale

Figure 5.17 shows that, although varying Manning's *n* values for the Swale channel does have an influence on peak discharge, it is not very strong. With the levées, peak discharge reduces from 530.6 m^3/s at *n* = 0.02 to 489.6 m^3/s at *n* = 0.1, a reduction of 41 m^3/s. Without the levées, peak discharge reduces from 523.6 m^3/s at *n* = 0.02 to 482.5 m^3/s at *n* = 0.1, a reduction of 41.1 m^3/s which is larger than with the levées. However, these reductions to peak discharge are much lower than those caused by changes to the whole model and to the River Ure. For each of the changes to Manning's *n*, the peak discharge recorded is higher with the levées. Figure 5.18 shows that floodplain *n* of the Swale only has a very small effect on peak discharge, reducing it by only 0.1 m^3/s both with and without levées. The difference in peak discharge between the scenarios is around 7 m^3/s.

Figures 5.19 and 5.20 show these changes in terms of their effect on peak timing. For both scenarios, peak timing delay is only changed by channel *n* of the Swale at 0.02, for which the hydrograph peak occurs an hour earlier than with the original Manning's *n* values. As with the Ouse floodplain, changes to the Swale floodplain do not affect peak timing delay for either scenario. The statistics for the simulations varying channel and floodplain *n* for the Swale are shown in Table 5.4.

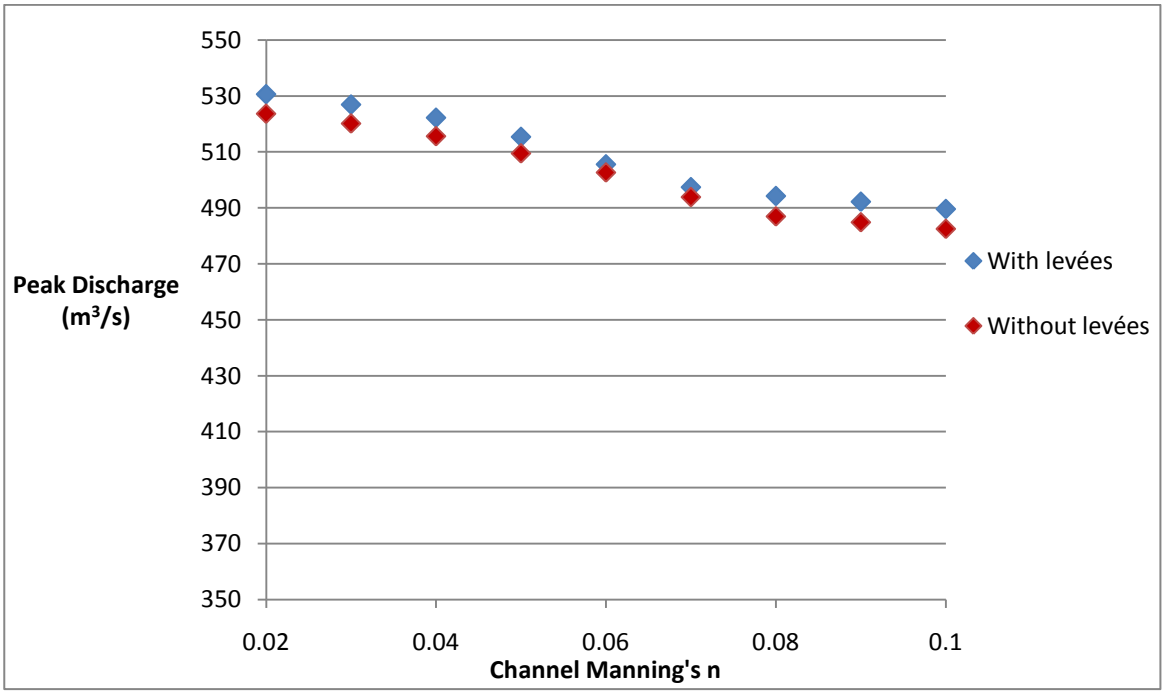

Figure 5.17 Change in peak discharge with relation to Manning's *n* values of the Swale channel for the 'with levées' and 'without levées' scenarios.

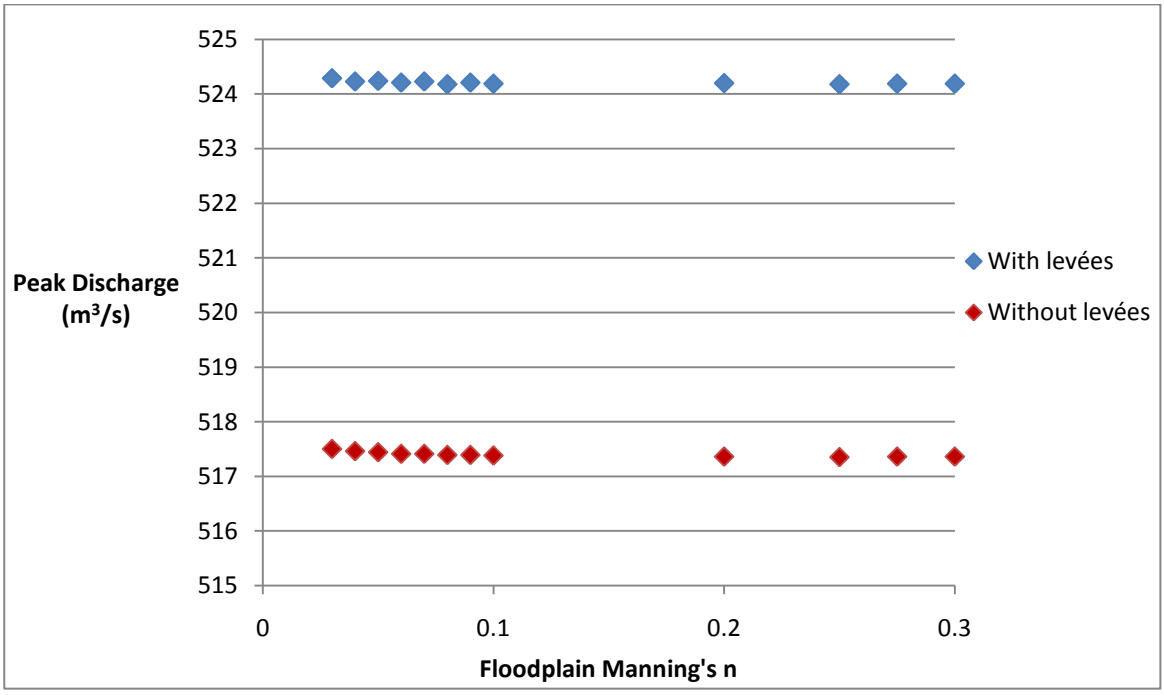

Figure 5.18 Change in peak discharge with relation to Manning's *n* values of the Swale floodplain for the 'with levées' and 'without levées' scenarios.

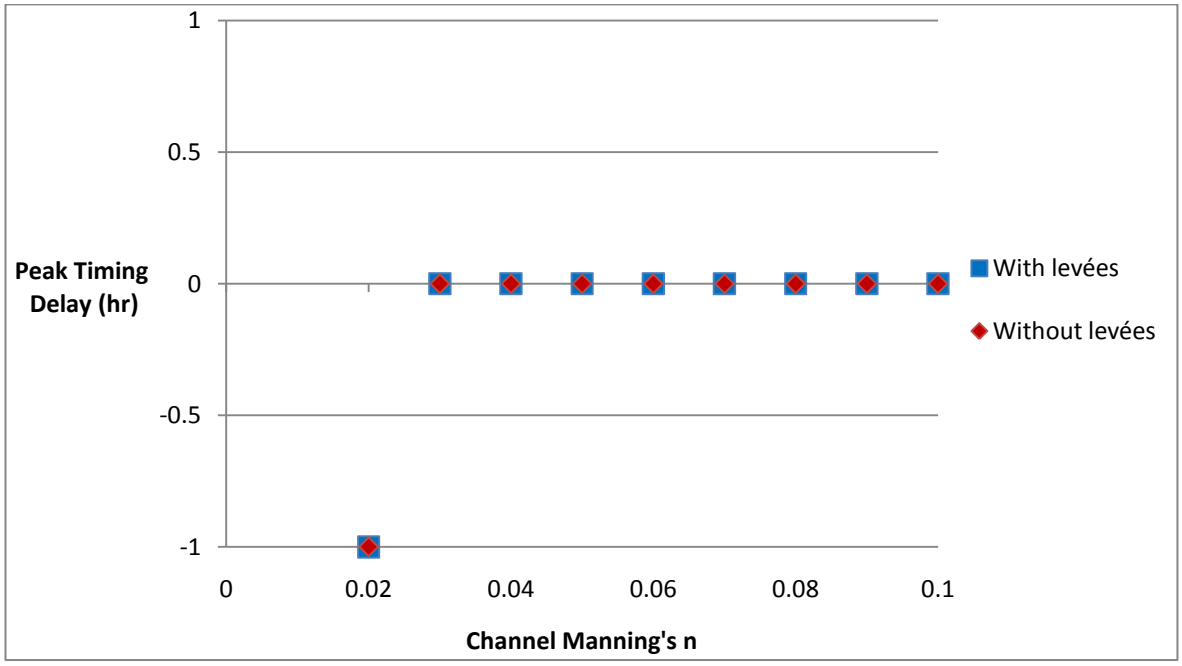

Figure 5.19 Change in peak timing delay with relation to Manning's *n* values of the Swale channel for the 'with levées' and 'without levées' scenarios.

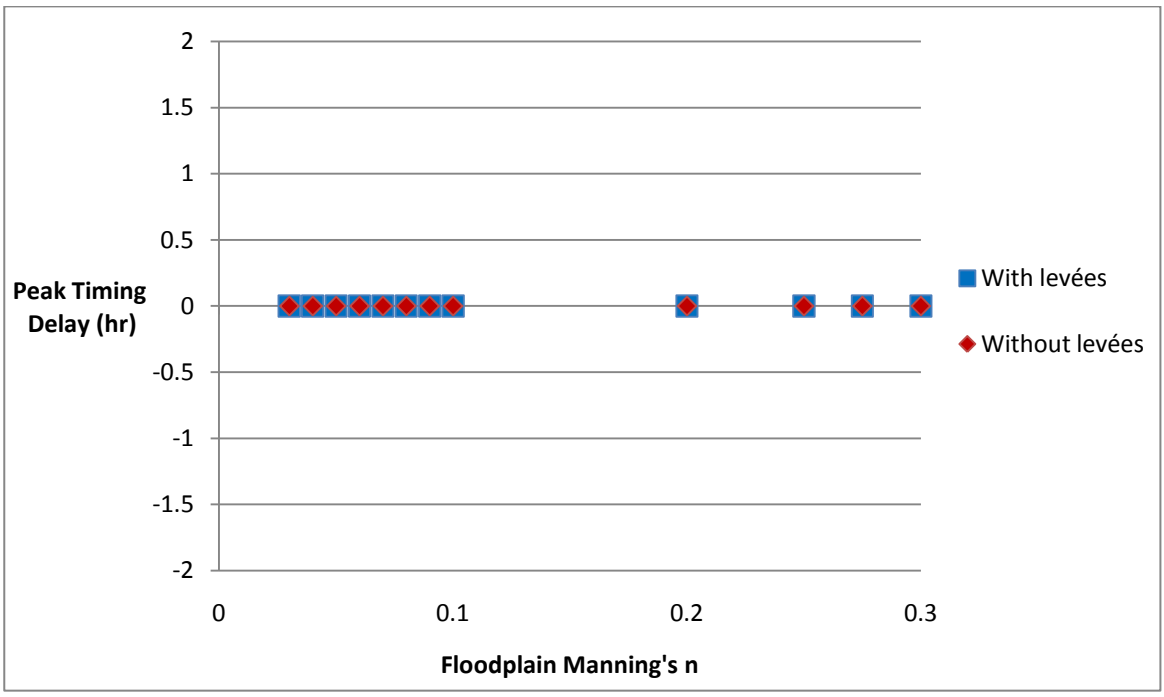

Figure 5.20 Change in peak timing delay with relation to Manning's *n* values of the Swale floodplain for the 'with levées' and 'without levées' scenarios.

	With levées					Without levées				
Scenario	**Peak Q (m^3/s)**	**Peak timing (hr)**	**dQ (m^3/s)**	**dQ (%)**	**dt (hr)**	**Peak Q (m^3/s)**	**Peak timing (hr)**	**dQ (m^3/s)**	**dQ (%)**	**dt (hr)**
Baseline	**524.2**	**140**	**0.0**	**0.0**	**0**	**517.4**	**140**	**0.0**	**0.0**	**0**
Channel *n* = 0.02	530.6	139	6.4	-1.2	-1	523.6	139	6.2	-1.2	-1
Channel *n* = 0.03	526.9	140	2.7	-0.5	0	520.2	140	2.7	-0.5	0
Channel *n* = 0.04	522.2	140	-2.0	0.4	0	515.6	140	-1.8	0.4	0
Channel *n* = 0.05	515.4	140	-8.8	1.7	0	509.5	140	-8.0	1.5	0
Channel *n* = 0.06	505.6	140	-18.6	3.6	0	502.7	140	-14.8	2.9	0
Channel *n* = 0.07	497.4	140	-26.8	5.1	0	493.9	140	-23.6	4.6	0
Channel *n* = 0.08	494.3	140	-29.9	5.7	0	487.0	140	-30.5	5.9	0
Channel *n* = 0.09	492.3	140	-31.9	6.1	0	484.9	140	-32.6	6.3	0
Channel *n* = 0.1	489.6	140	-34.6	6.6	0	482.5	140	-34.9	6.8	0
Floodplain *n* = 0.03	524.3	140	0.1	0.0	0	517.5	140	0.1	0.0	0
Floodplain *n* = 0.04	524.2	140	0.0	0.0	0	517.5	140	0.0	0.0	0
Floodplain *n* = 0.05	524.2	140	0.1	0.0	0	517.4	140	0.0	0.0	0
Floodplain *n* = 0.06	524.2	140	0.0	0.0	0	517.4	140	0.0	0.0	0
Floodplain *n* = 0.07	524.2	140	0.0	0.0	0	517.4	140	0.0	0.0	0
Floodplain *n* = 0.08	524.2	140	0.0	0.0	0	517.4	140	-0.1	0.0	0
Floodplain *n* = 0.09	524.2	140	0.0	0.0	0	517.4	140	-0.1	0.0	0
Floodplain *n* = 0.1	524.2	140	0.0	0.0	0	517.4	140	-0.1	0.0	0
Floodplain *n* = 0.2	524.2	140	0.0	0.0	0	517.4	140	-0.1	0.0	0
Floodplain *n* = 0.25	524.2	140	0.0	0.0	0	517.4	140	-0.1	0.0	0
Floodplain *n* = 0.275	524.2	140	0.0	0.0	0	517.4	140	-0.1	0.0	0
Floodplain *n* = 0.3	524.2	140	0.0	0.0	0	517.4	140	-0.1	0.0	0

Table 5.4 Peak discharge and peak timing results for simulations using the 'with levées' scenario for the River Swale. The baseline is the results returned from the original 'modelled flow' after initial model building. The results are compared to this baseline.

5.3.5 Varying Manning's *n* for the River Nidd

Figure 5.21 shows the relationship between Manning's *n* for the Nidd channel and peak discharge. Peak discharge does not gradually fall as with the other tributaries, rising and falling between 552.8 m^3/s at *n* = 0.02 and 514.1 m^3/s at *n* = 0.1 with levées and 544.9 m^3/s at *n* = 0.02 and 507.3 m^3/s at *n* = 0.1 without levées. The same pattern is seen in both scenarios though peak discharge for each simulation is higher with the levées. The reduction in peak discharge caused by varying channel *n* is larger with the levées at 38.7 m^3/s compared to 37.7 m^3/s without levées. Compared to the other tributaries, the reduction in peak discharge is smallest for the River Nidd. Figure 5.22 shows that varying floodplain *n* for the Nidd appears to give the opposite trend to the other tributaries: peak discharge increases with Manning's *n*, although at lower *n* values the peak discharge falls. The same pattern is seen for both scenarios, with peak discharge around 6 m^3/s lower without the levées.

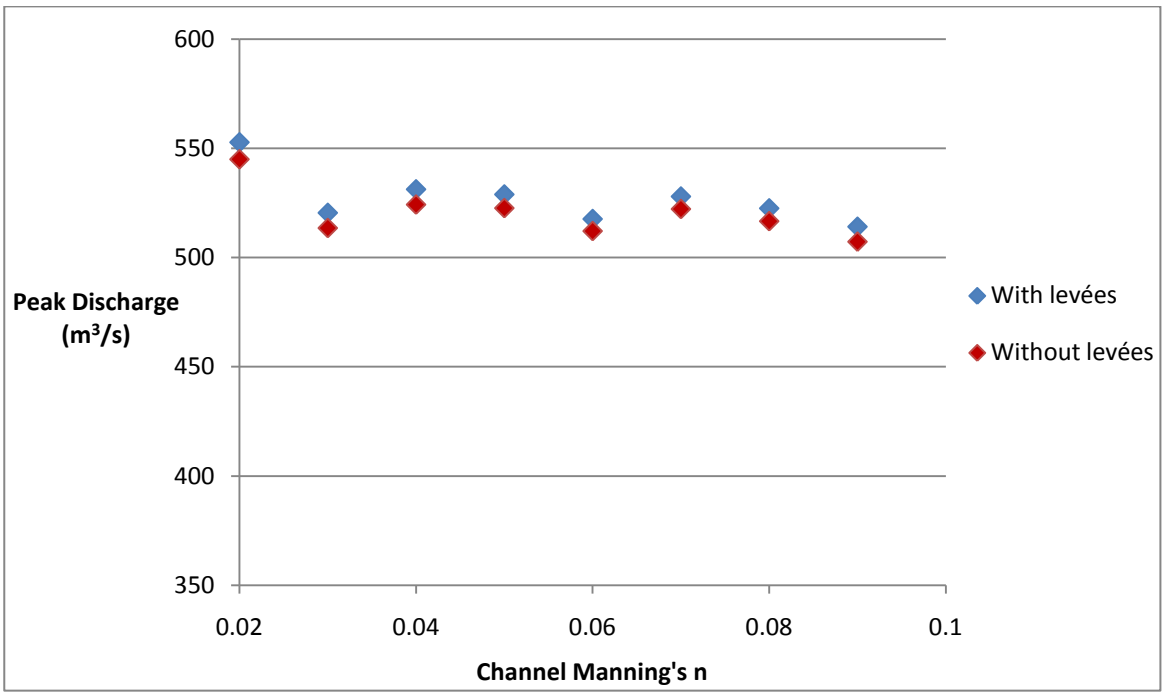

Figure 5.21 Change in peak discharge with relation to Manning's *n* values of the Nidd channel for the 'with levées' and 'without levées' scenarios.

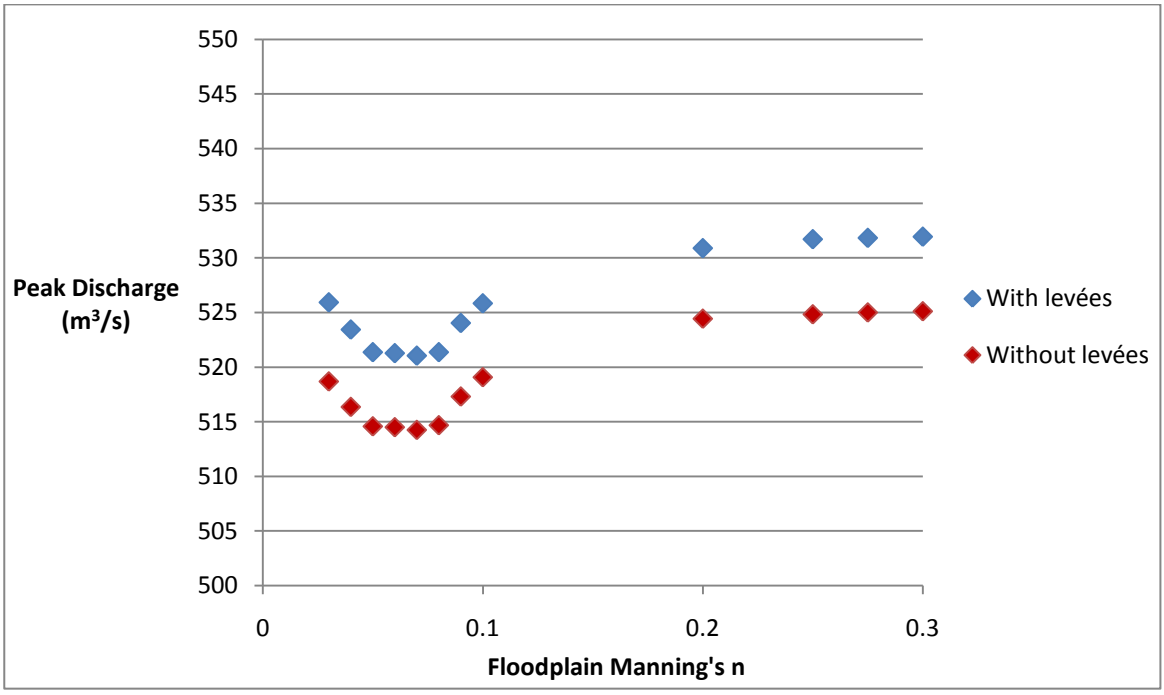

Figure 5.22 Change in peak discharge with relation to Manning's *n* values of the Nidd floodplain for the 'with levées' and 'without levées' scenarios.

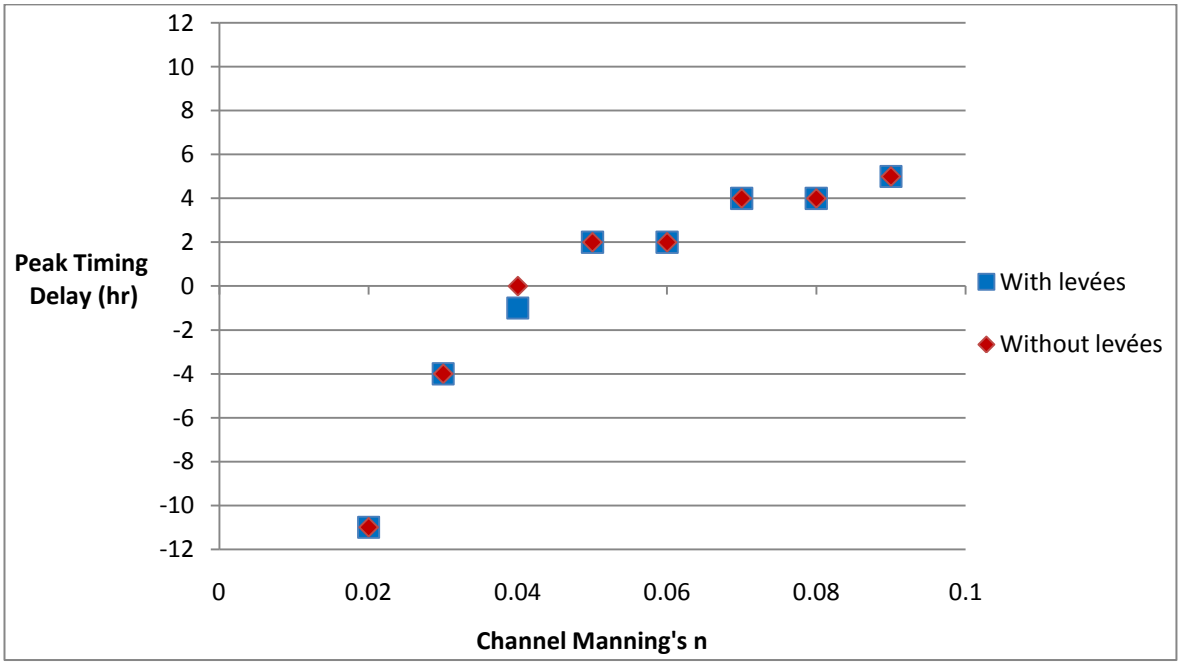

Figure 5.23 Change in peak timing delay with relation to Manning's *n* values of the Nidd channel for the 'with levées' and 'without levées' scenarios.

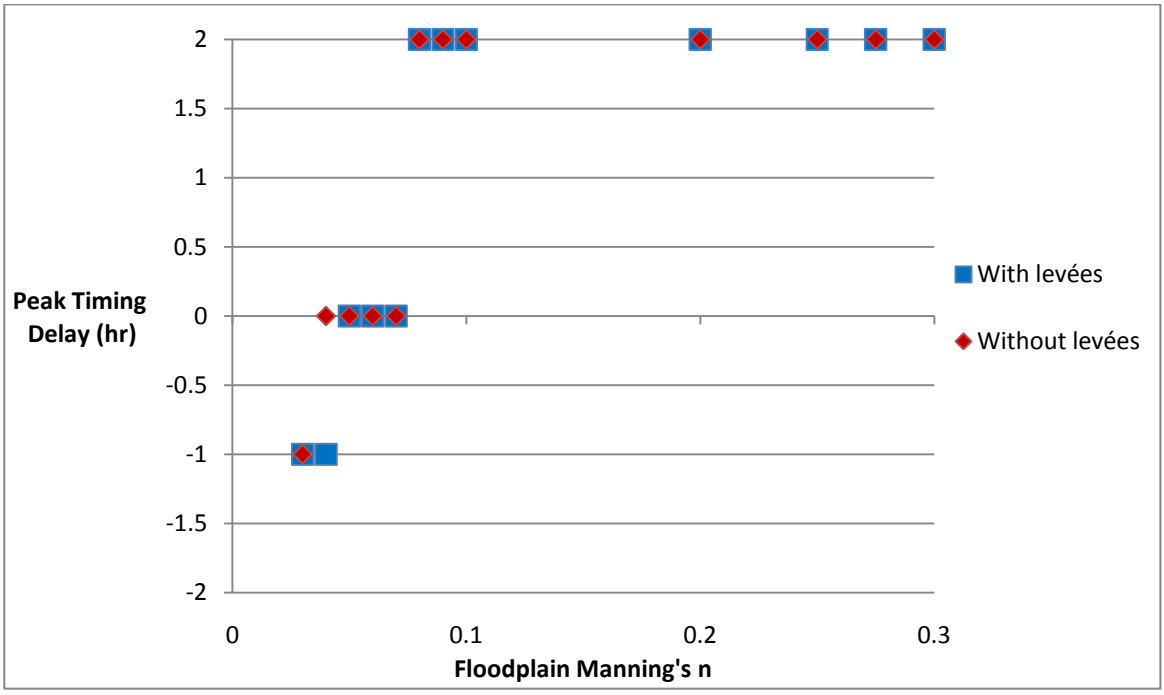

Figure 5.24 Change in peak timing delay with relation to Manning's *n* values of the Nidd floodplain for the 'with levées' and 'without levées' scenarios.

Figure 5.23 shows that varying channel *n* has a large effect on peak timing delay, particularly at lower values for Manning's *n*. The influence on peak timing delay reduces rapidly, as at *n* = 0.02 the peak is shifted 11 hours earlier whilst at *n* = 0.03 the peak is shifted by 4 hours. At higher values for channel *n*, the peak is shifted later: the peak occurs 5 hours later at *n* = 0.09. This trend is shown for both scenarios.

In comparison to the Ouse and Swale, varying floodplain *n* of the Nidd appears to have a larger influence on peak timing delay (Figure 5.24). At *n* = 0.03 (or *n* = 0.04 with levées) the peak is shifted earlier by 1 hour whilst at *n* = 0.08 the peak is 2 hours later. Higher values for floodplain *n* do not increase the timing delay further. The statistics for the simulations varying channel and floodplain *n* for the Swale are shown in Table 5.5. Table 5.6 shows the peak discharge and peak timing statistics for each of the three tributaries to aid comparison.

	With levées					Without levées				
Scenario	**Peak Q (m^3/s)**	**Peak timing (hr)**	**dQ (m^3/s)**	**dQ (%)**	**dt (hr)**	**Peak Q (m^3/s)**	**Peak timing (hr)**	**dQ (m^3/s)**	**dQ (%)**	**dt (hr)**
Baseline	**524.2**	**140**	**0.0**	**0.0**	**0**	**517.4**	**140**	**0.0**	**0.0**	**0**
Channel *n* = 0.02	552.8	129	28.6	-5.5	-11	544.9	129	27.5	-5.3	-11
Channel *n* = 0.03	520.5	136	-3.7	0.7	-4	513.5	136	-3.9	0.8	-4
Channel *n* = 0.04	531.2	139	7.0	-1.3	-1	524.2	140	6.8	-1.3	0
Channel *n* = 0.05	528.9	142	4.7	-0.9	2	522.6	142	5.2	-1.0	2
Channel *n* = 0.06	517.6	142	-6.6	1.3	2	512.1	142	-5.3	1.0	2
Channel *n* = 0.07	528.0	144	3.8	-0.7	4	522.2	144	4.8	-0.9	4
Channel *n* = 0.08	522.5	144	-1.7	0.3	4	516.6	144	-0.8	0.2	4
Channel *n* = 0.09	514.1	145	-10.1	1.9	5	507.3	145	-10.2	2.0	5
Floodplain *n* = 0.03	525.9	139	1.7	-0.3	-1	518.7	139	1.2	-0.2	-1
Floodplain *n* = 0.04	523.4	139	-0.8	0.1	-1	516.4	140	-1.1	0.2	0
Floodplain *n* = 0.05	521.4	140	-2.8	0.5	0	514.6	140	-2.9	0.6	0
Floodplain *n* = 0.06	521.3	140	-2.9	0.6	0	514.5	140	-3.0	0.6	0
Floodplain *n* = 0.07	521.0	140	-3.2	0.6	0	514.2	140	-3.2	0.6	0
Floodplain *n* = 0.08	521.4	142	-2.8	0.5	2	514.7	142	-2.8	0.5	2
Floodplain *n* = 0.09	524.0	142	-0.2	0.0	2	517.3	142	-0.1	0.0	2
Floodplain *n* = 0.1	525.8	142	1.6	-0.3	2	519.1	142	1.6	-0.3	2
Floodplain *n* = 0.2	530.9	142	6.7	-1.3	2	524.4	142	7.0	-1.4	2
Floodplain *n* = 0.25	531.7	142	7.5	-1.4	2	524.8	142	7.4	-1.4	2
Floodplain *n* = 0.275	531.8	142	7.6	-1.5	2	525.0	142	7.6	-1.5	2
Floodplain *n* = 0.3	531.9	142	7.7	-1.5	2	525.1	142	7.7	-1.5	2

Table 5.5 Peak discharge and peak timing results for simulations using the 'with levées' scenario for the River Nidd. The baseline is the results returned from the original 'modelled flow' after initial model building. The results are compared to this baseline.

Scenario	With levées			With levées			Without levées			Without levées		
	Peak Q (m^3/s)			Peak timing (hr)			Peak Q (m^3/s)			Peak timing (hr)		
	Ouse	Swale	Nidd	Ouse	Swale	Nidd	Ouse	Swale	Nidd	Ouse	Swale	Nidd
Channel *n* = 0.02	546.3	530.6	552.8	139	139	129	538.6	523.6	544.9	139	139	129
Channel *n* = 0.03	524.8	526.9	520.5	140	140	136	517.9	520.2	513.5	140	140	136
Channel *n* = 0.04	490.4	522.2	531.2	142	140	139	485.8	515.6	524.2	142	140	140
Channel *n* = 0.05	466.7	515.4	528.9	144	140	142	464.7	509.5	522.6	144	140	142
Channel *n* = 0.06	449.1	505.6	517.6	145	140	142	448.1	502.7	512.1	145	140	142
Channel *n* = 0.07	430.0	497.4	528.0	145	140	144	422.1	493.9	522.2	147	140	144
Channel *n* = 0.08	420.2	494.3	522.5	146	140	144	416.0	487.0	516.6	148	140	144
Channel *n* = 0.09	414.5	492.3	514.1	145	140	145	408.0	484.9	507.3	145	140	145
Channel *n* = 0.1	411.1	489.6	-	145	140	-	392.0	482.5	-	144	140	-
Floodplain *n* = 0.03	527.9	524.3	525.9	140	140	139	520.8	517.5	518.7	140	140	139
Floodplain *n* = 0.04	524.1	524.2	523.4	140	140	139	517.2	517.5	516.4	140	140	140
Floodplain *n* = 0.05	521.1	524.2	521.4	140	140	140	514.3	517.4	514.6	140	140	140
Floodplain *n* = 0.06	518.5	524.2	521.3	140	140	140	512.1	517.4	514.5	140	140	140
Floodplain *n* = 0.07	516.6	524.2	521.0	140	140	140	510.2	517.4	514.2	140	140	140
Floodplain *n* = 0.08	515.0	524.2	521.4	140	140	142	508.6	517.4	514.7	140	140	142
Floodplain *n* = 0.09	513.6	524.2	524.0	140	140	142	507.3	517.4	517.3	140	140	142
Floodplain *n* = 0.1	512.4	524.2	525.8	140	140	142	506.1	517.4	519.1	140	140	142
Floodplain *n* = 0.2	505.4	524.2	530.9	140	140	142	499.6	517.4	524.4	140	140	142
Floodplain *n* = 0.25	503.7	524.2	531.7	139	140	142	497.9	517.4	524.8	140	140	142
Floodplain *n* = 0.275	503.1	524.2	531.8	139	140	142	497.2	517.4	525.0	140	140	142
Floodplain *n* = 0.3	502.6	524.2	531.9	139	140	142	496.6	517.4	525.1	140	140	142

Table 5.6 Comparison of the results for the three tributaries using the 'with levées' scenario. There are no values for the River Nidd using a channel *n* of 0.1 due to instabilities in the model at such a high Manning's *n* value.

5.3.6 Four levée scenarios

For this section, each of the scenarios was tested in terms of the influence of Manning's *n* on peak discharge and peak timing along the River Ouse. Figure 5.25 shows the discharges for each of the four levée scenarios before Manning's *n* was varied. The hydrographs are very similar, but do show a difference in peak discharge values and in the minimum values of the troughs on the hydrographs. Figure 5.25(b) shows that the highest peak discharge is attained with the levées in place, at 524.2 m^3/s. Under the half height scenario, peak discharge is reduced slightly to 523.2 m^3/s, and further to 517.4 m^3/s when the levées were removed completely. In the final scenario the levées were elevated by 0.5 m, reducing peak discharge to 520.5 m^3/s.

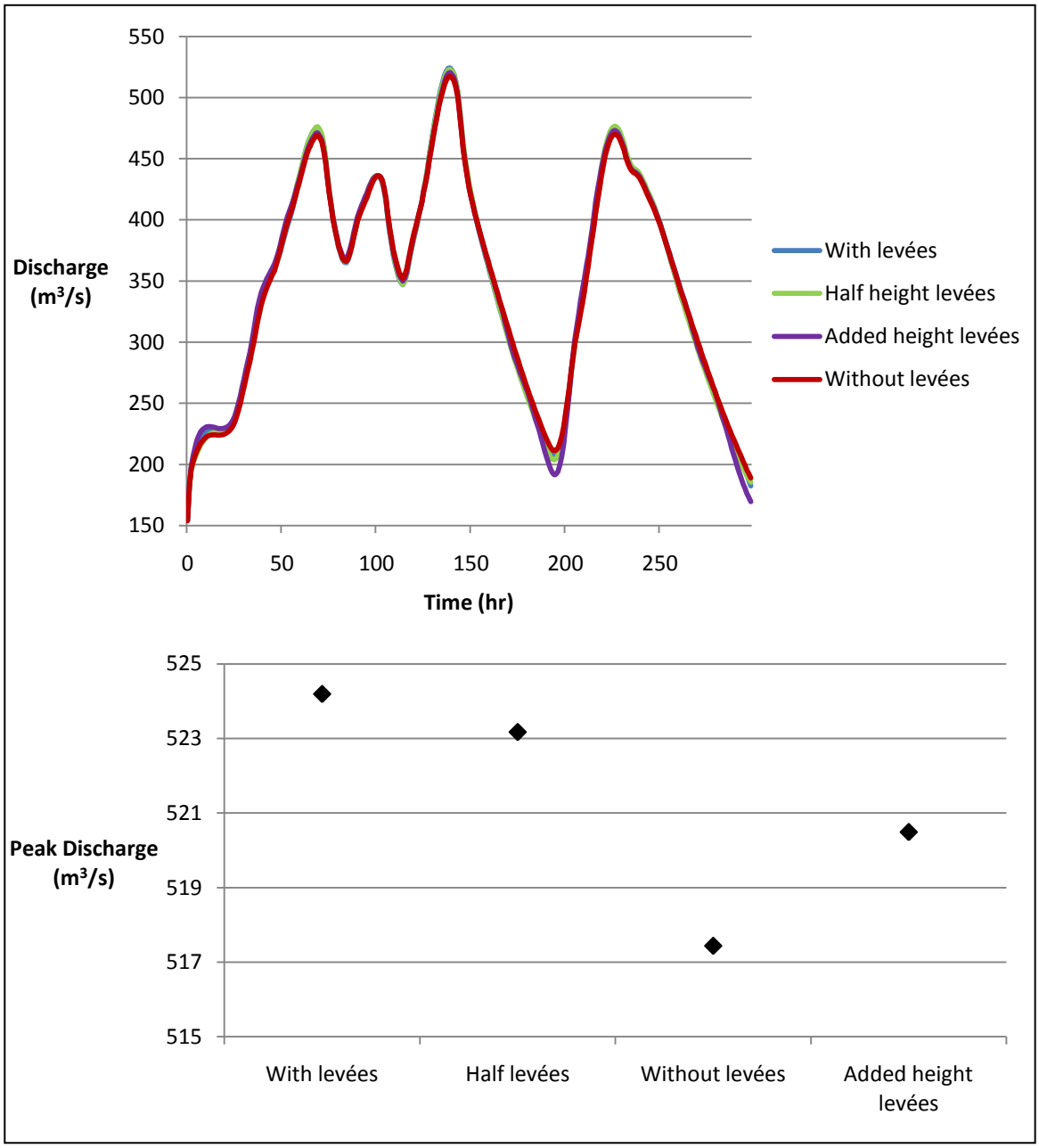

Figure 5.25 (a) Output hydrographs for each of the four levée scenarios using the original input hydrographs; (b) Peak discharges at the downstream boundary of the model (cross-section 902) for each of the four levée scenarios.

Figure 5.26 shows the effect of varying Manning's *n* for the channel on peak discharge for each of the four scenarios. The 'with levées' scenario generally has the highest values for peak discharge, although there appears to be an anomaly at *n* = 0.08 for the 'added height' scenario. The 'half height' scenario lies between the 'with levées' and 'without levées' scenarios, though the values are closer to the 'with levées' scenario. The lowest values for peak discharge are recorded using the 'without levées' scenario, falling to 392.0

m^3/s at n = 0.1. This scenario appears to be most affected by channel n values in terms of peak discharge.

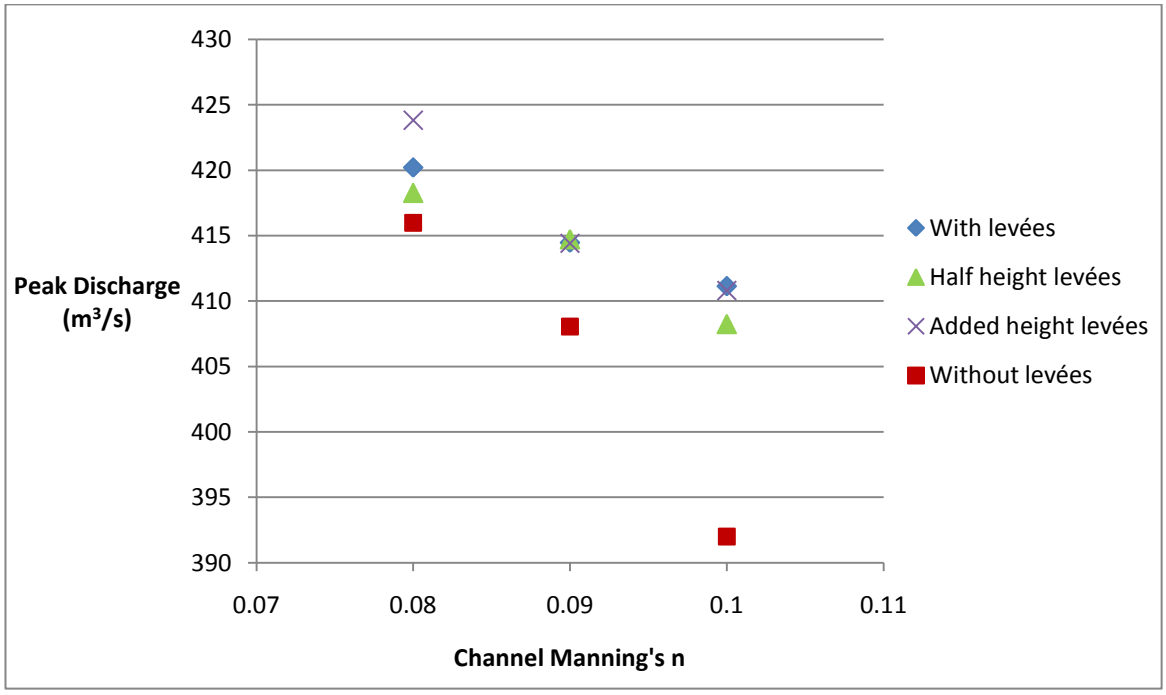

Figure 5.26 Change in peak discharge with relation to Manning's *n* values of the channel for all four levée scenarios.

Figure 5.27 shows the effect of varying Manning's n for the floodplain on peak discharge for each of the four scenarios tested. The pattern is clearer than for channel n: peak discharge is reduced in each scenario by around the same amount, with the 'with levées' scenario producing the highest values for peak discharge, followed by the 'half height levées', 'added height levées' and finally 'without levées' scenarios. Values range from 512.4 m^3/s at n = 0.1 to 502.6 m^3/s at n = 0.3 with the levées compared to 506.1 m^3/s at n = 0.1 and 496.6 m^3/s at n = 0.3 without levées. Table 5.7 gives the peak discharge recorded for each scenario with the changes in channel and floodplain n. The statistics for the simulations varying channel and floodplain n for the 'half height levées' and 'added height levées' scenarios are shown in Tables 5.8 and 5.9.

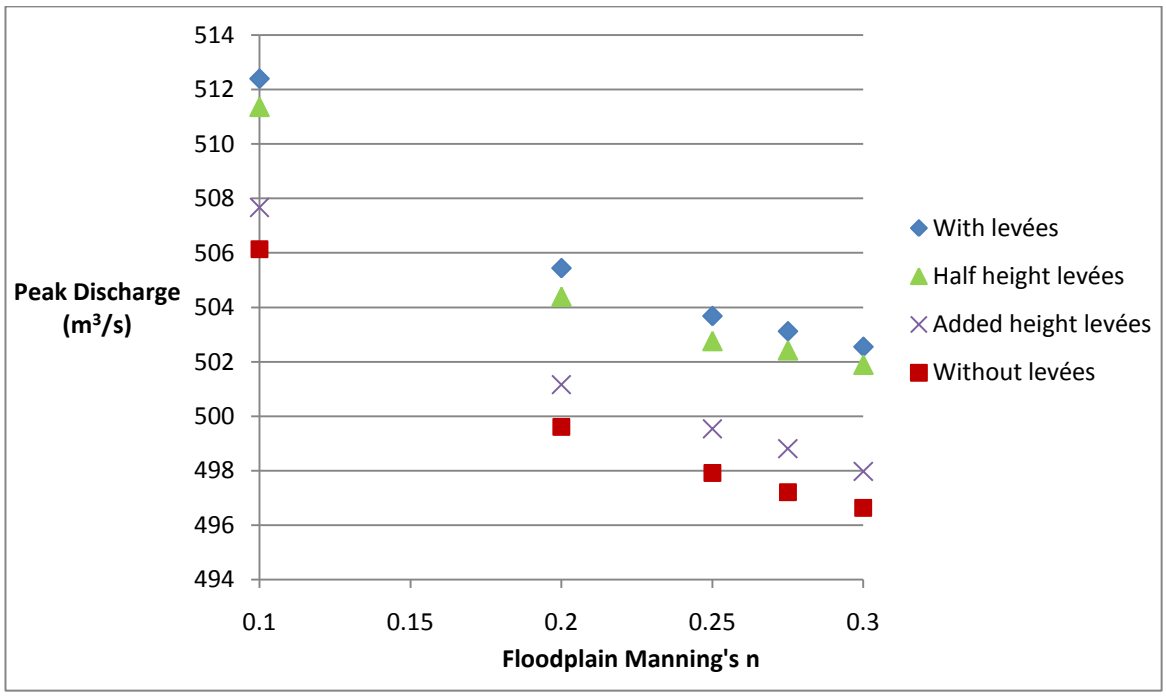

Figure 5.27 Change in peak discharge with relation to Manning's *n* values of the floodplain for all four levée scenarios.

	Peak Discharge (m^3/s)			
Manning's *n*	**With levées**	**Half height levées**	**Added height levées**	**Without levées**
Channel *n* = 0.08	420.2	418.3	423.8	416.0
Channel *n* = 0.09	414.5	414.7	414.4	408.0
Channel *n* = 0.1	411.1	408.2	410.8	392.0
Floodplain *n* = 0.1	512.4	511.4	507.7	506.1
Floodplain *n* = 0.2	505.4	504.4	501.2	499.6
Floodplain *n* = 0.25	503.7	502.8	499.5	497.9
Floodplain *n* = 0.275	503.1	502.4	498.8	497.2
Floodplain *n* = 0.3	502.6	501.9	498.0	496.6

Table 5.7 Statistics for each of the four levée scenarios showing change in peak discharge after varying both Manning's *n* for the channel and floodplain.

Scenario	Peak Q (m^3/s)	Peak timing (hr)	dQ (m^3/s)	dQ (%)	dt (hr)
Baseline	**523.17**	**140**	**0.00**	**0.00**	**0**
Channel *n* = 0.08	418.28	148	-104.89	20.05	8
Channel *n* = 0.09	414.73	146	-108.44	20.73	6
Channel *n* = 0.1	408.24	144	-114.93	21.97	4
Floodplain *n* = 0.1	511.36	140	-11.81	2.26	0
Floodplain *n* = 0.2	504.39	140	-18.78	3.59	0
Floodplain *n* = 0.25	502.76	140	-20.41	3.90	0
Floodplain *n* = 0.275	502.42	140	-20.75	3.97	0
Floodplain *n* = 0.3	501.89	140	-21.28	4.07	0

Table 5.8 Statistics for each simulation varying both Manning's *n* for the channel and floodplain using the 'half height levées' scenario.

Scenario	Peak Q (m^3/s)	Peak timing (hr)	dQ (m^3/s)	dQ (%)	dt (hr)
Baseline	**520.5**	**140**	**0.0**	**0.0**	**0**
Channel *n* = 0.08	423.8	148	-96.7	18.6	8
Channel *n* = 0.09	414.4	146	-106.1	20.4	6
Channel *n* = 0.1	410.8	144	-109.7	21.1	4
Floodplain *n* = 0.1	507.7	140	-12.8	2.5	0
Floodplain *n* = 0.2	501.2	140	-19.3	3.7	0
Floodplain *n* = 0.25	499.5	140	-21.0	4.0	0
Floodplain *n* = 0.275	498.8	140	-21.7	4.2	0
Floodplain *n* = 0.3	498.0	140	-22.5	4.3	0

Table 5.9 Statistics for each simulation varying both Manning's *n* for the channel and floodplain using the 'added height levées' scenario.

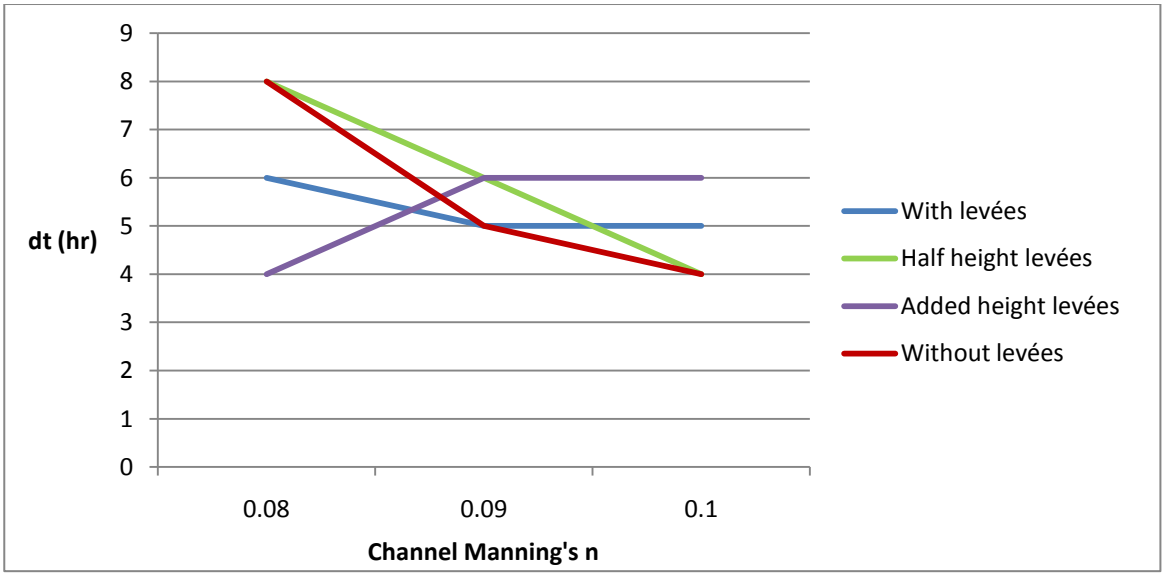

Figure 5.28 Change in peak timing delay from the original timing with relation to Manning's *n* values of the channel for all four levée scenarios.

Figure 5.28 shows the effect of changing Manning's *n* of the channel on the change in peak timing delay. There is no clear relationship, though the spread in values appears larger at channel *n* = 0.08 compared to *n* = 0.1. The change in peak timing delay with *n* is also larger for the 'half height' and 'without levées' scenarios compared to the other scenarios. Figure 5.29 shows that all of the scenarios, except for 'with levées' do not change the timing of the flood. The 'with levées' scenario peaks an hour earlier for floodplain *n* values of 0.25 and 0.3. The statistics for peak timing delay using each of the scenarios are shown in Table 5.10. Appendix Two shows the hydrographs produced after varying Manning's *n* for each of the levée scenarios.

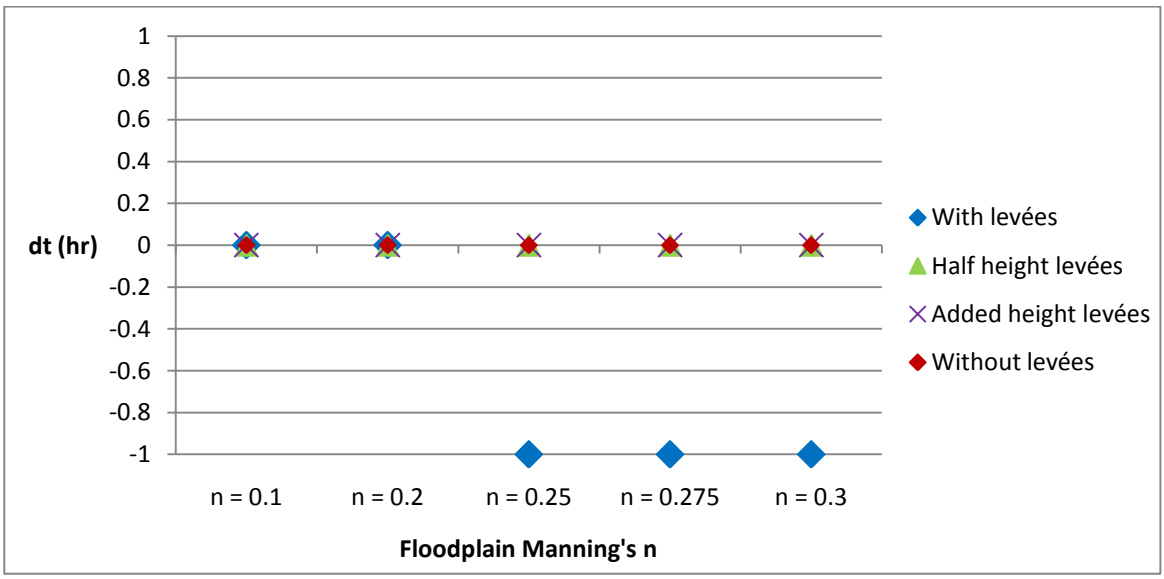

Figure 5.29 Change in peak timing delay with relation to Manning's *n* values of the floodplain for all four levée scenarios. The peak timing delay for the 'half', 'added' and 'without' levées scenarios is 0 hr.

Scenario	dt (hr) With levées	dt (hr) Half height levées	dt (hr) Without levées	dt (hr) Added height levées
Channel *n* = 0.08	6	8	8	4
Channel *n* = 0.09	5	6	5	6
Channel *n* = 0.1	5	4	4	6
Floodplain *n* = 0.1	0	0	0	0
Floodplain *n* = 0.2	0	0	0	0
Floodplain *n* = 0.25	-1	0	0	0
Floodplain *n* = 0.275	-1	0	0	0
Floodplain *n* = 0.3	-1	0	0	0

Table 5.10 Statistics for each of the four levée scenarios showing change in peak timing delay after varying both Manning's *n* for the channel and floodplain.

5.4 Research Question 2 – To what extent are land management signals impacted upon by flow attenuation?

5.4.1 Grip blocking scenarios

Figure 5.30 displays the different changes to the River Ouse input hydrographs that were used to simulate the expected effect of grip blocking. Essentially, the hydrographs were stretched in order to represent the possible attenuation of the flood peak created by grip blocking. The hydrographs were multiplied by 1.01, 1.05, 1.10, 1.20, 1.25 and 1.50 initially and then shifted in time by 1 and 2 hours to represent the possible influence of blocking grips on the timing of the flood peak. These two modifications to the hydrograph were then combined in order to model the attenuation and translation observed from different levels of grip blocking.

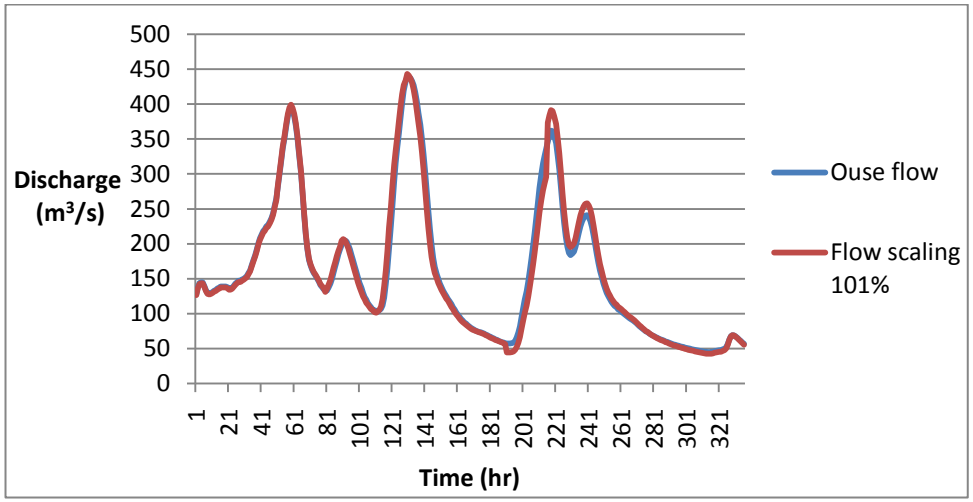
Discharge (m³/s)
500
450
400
350
300
250
200
150
100
50
0
1
21
41
61
81
101
121
141
161
181
201
221
241
261
281
301
321
Time (hr)
Ouse flow
Flow scaling 101%

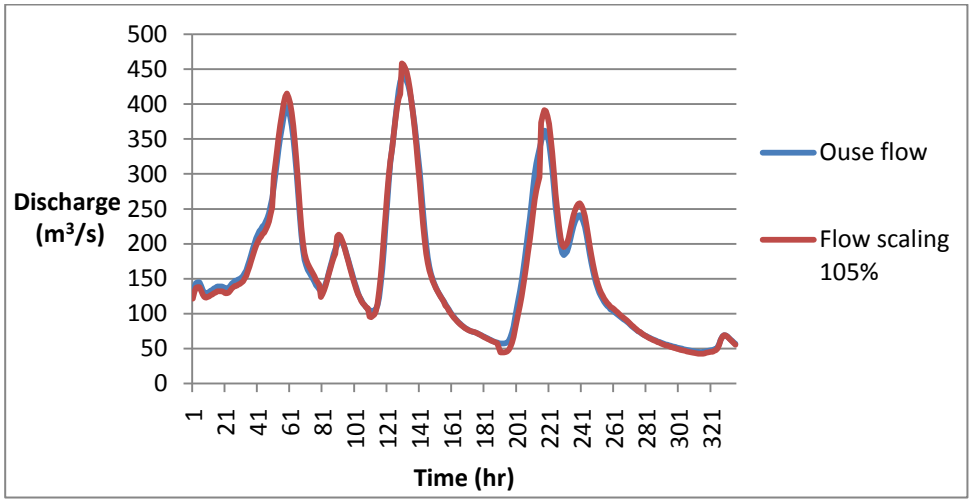
Discharge (m³/s)
500
450
400
350
300
250
200
150
100
50
0
1
21
41
61
81
101
121
141
161
181
201
221
241
261
281
301
321
Time (hr)
Ouse flow
Flow scaling 105%

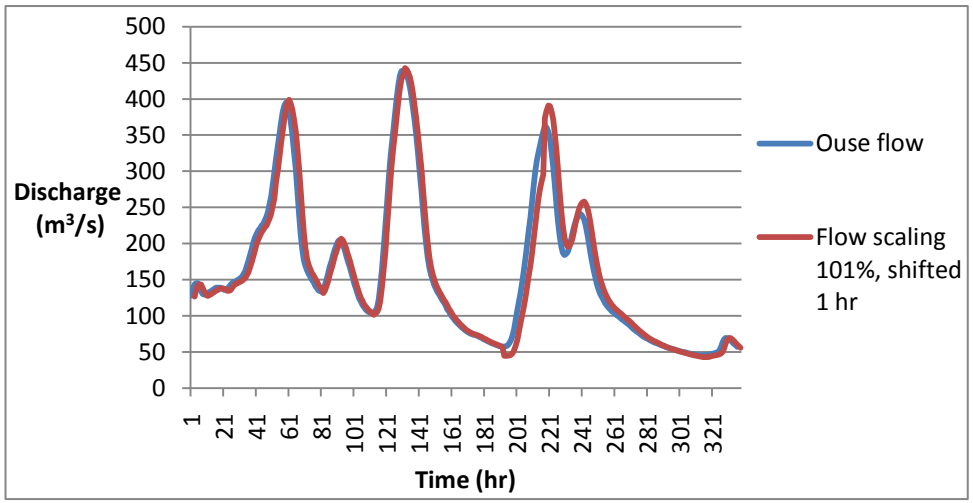
Discharge (m³/s)
500
450
400
350
300
250
200
150
100
50
0
1
21
41
61
81
101
121
141
161
181
201
221
241
261
281
301
321
Time (hr)
Ouse flow
Flow scaling 101%, shifted 1 hr

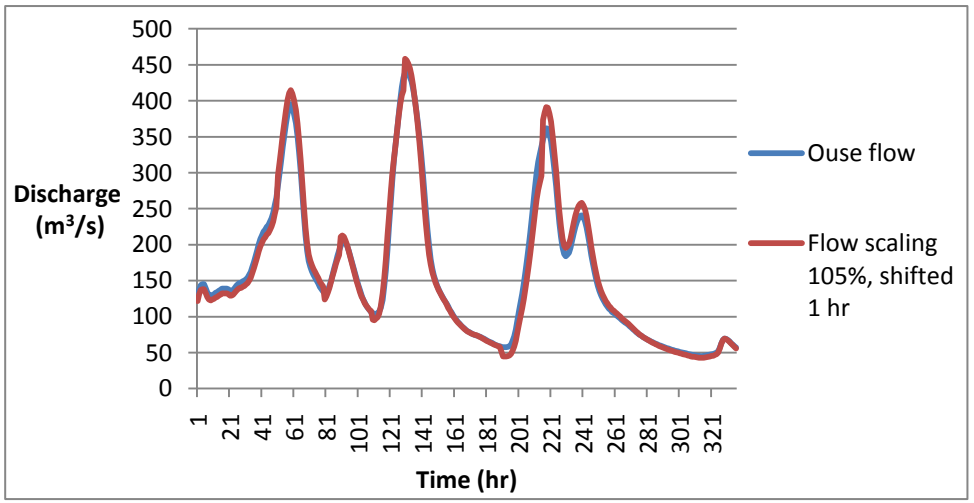
Discharge (m³/s)
500
450
400
350
300
250
200
150
100
50
0
1
21
41
61
81
101
121
141
161
181
201
221
241
261
281
301
321
Time (hr)
Ouse flow
Flow scaling 105%, shifted 1 hr

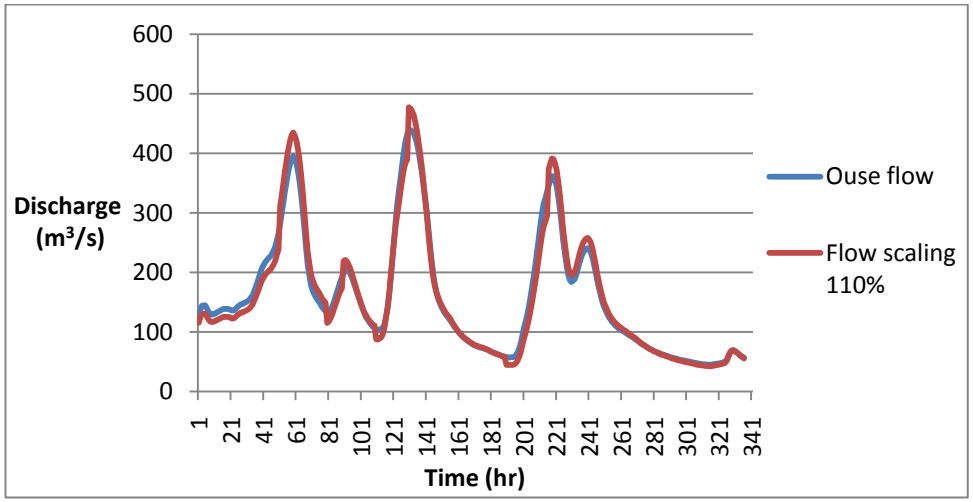
Discharge (m³/s)
600
500
400
300
200
100
0
1 21 41 61 81 101 121 141 161 181 201 221 241 261 281 301 321 341
Time (hr)
Ouse flow
Flow scaling 110%

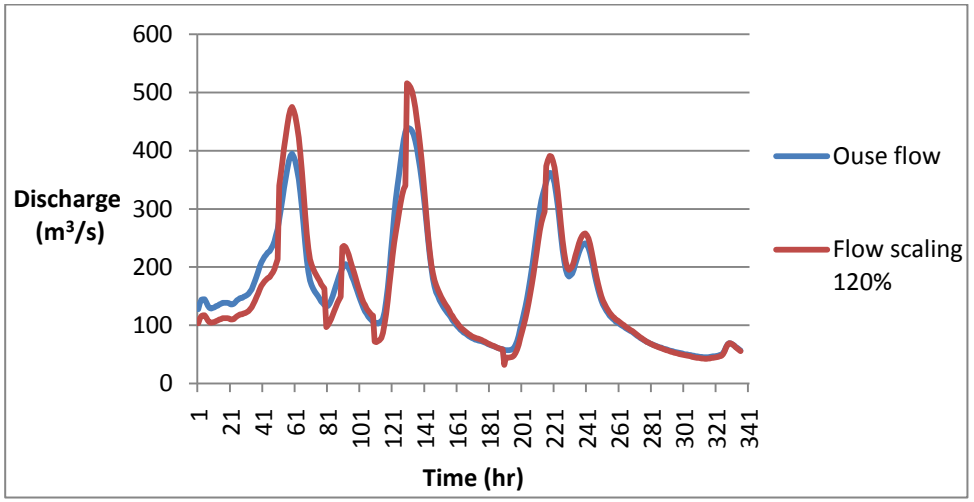
Discharge (m³/s)
600
500
400
300
200
100
0
1 21 41 61 81 101 121 141 161 181 201 221 241 261 281 301 321 341
Time (hr)
Ouse flow
Flow scaling 120%

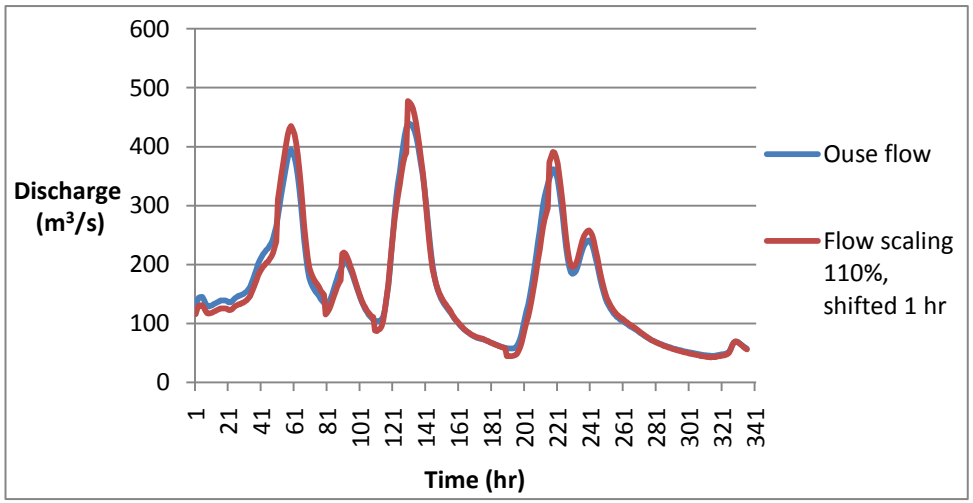
Discharge (m³/s)
600
500
400
300
200
100
0
1 21 41 61 81 101 121 141 161 181 201 221 241 261 281 301 321 341
Time (hr)
Ouse flow
Flow scaling 110%, shifted 1 hr

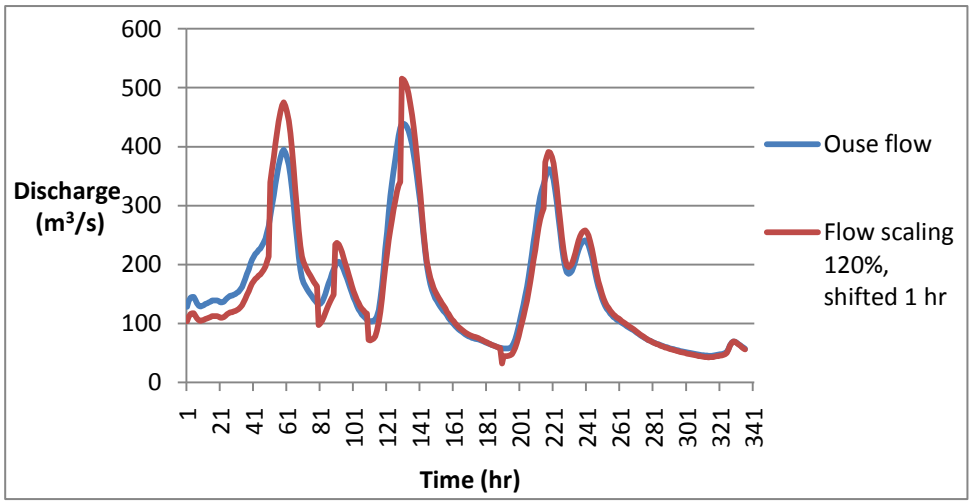
Discharge (m³/s)
600
500
400
300
200
100
0
1 21 41 61 81 101 121 141 161 181 201 221 241 261 281 301 321 341
Time (hr)
Ouse flow
Flow scaling 120%, shifted 1 hr

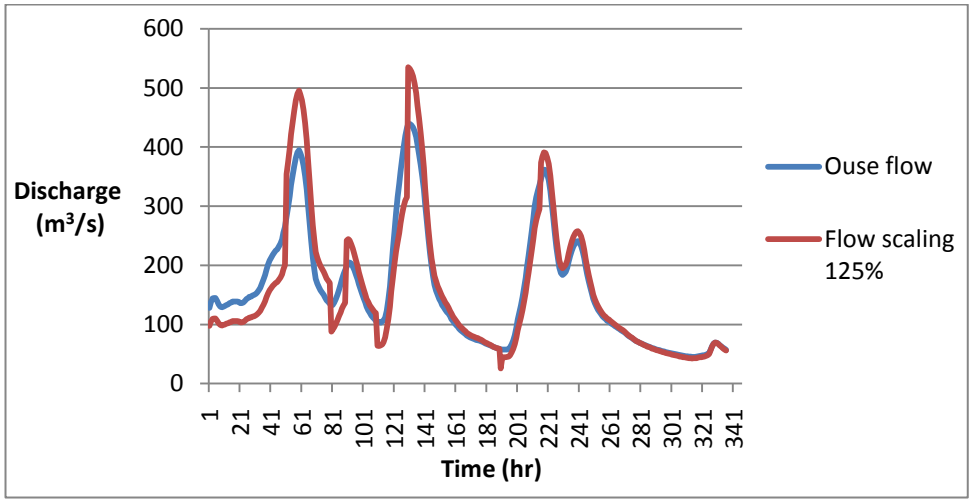

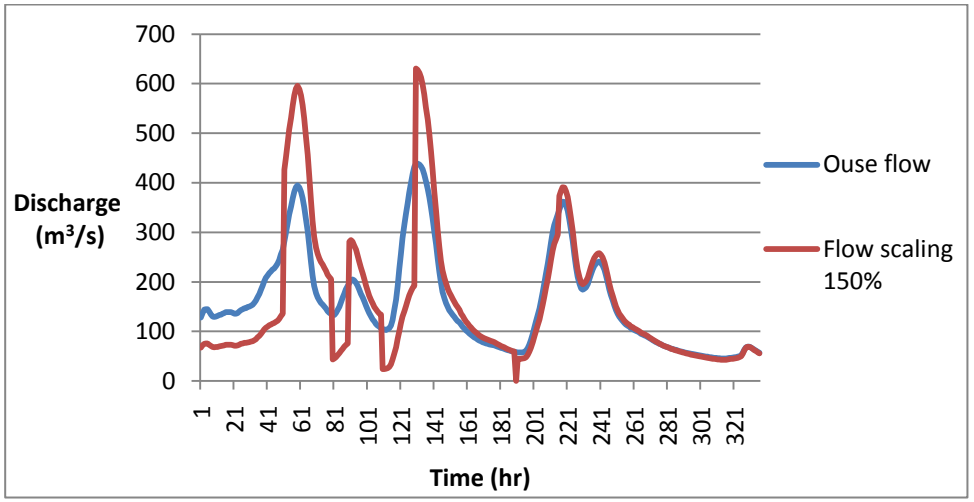

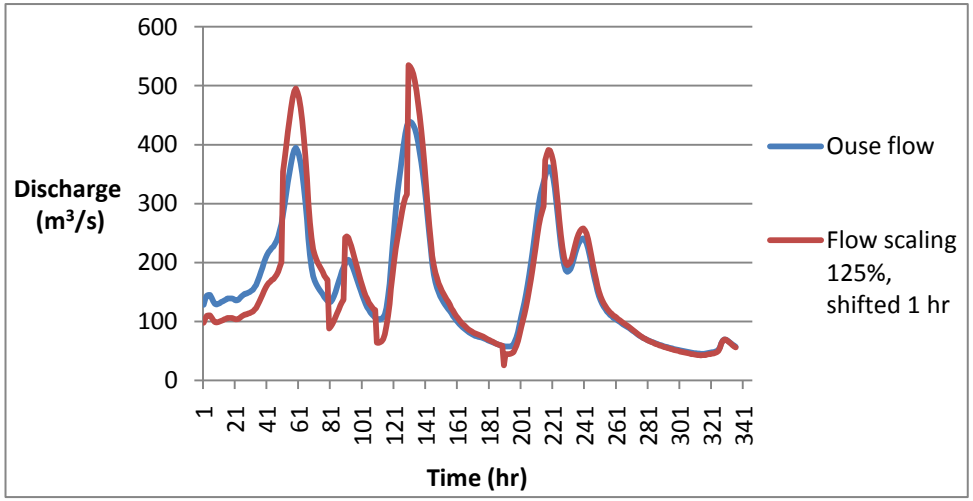

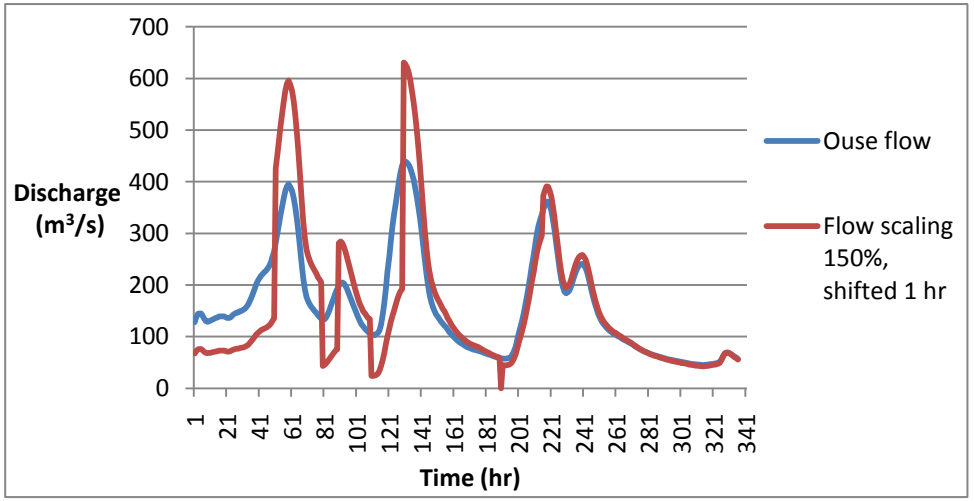

Figure 5.30 Ouse input hydrograph scaled by 1.01, 1.05, 1.10, 1.20, 1.25 and 1.50 and subsequently shifted by 1 hour.

5.4.2 Effect on output hydrographs – with levées

Flow scaled

Figure 5.31 shows that after scaling the hydrographs, peak discharge changes quite dramatically under the 'with levées' scenario. With a scaling of 101%, peak discharge rises from 524.2 m^3/s under the original flow to 526.2 m^3/s. But, for higher scalings, the peak flow falls.

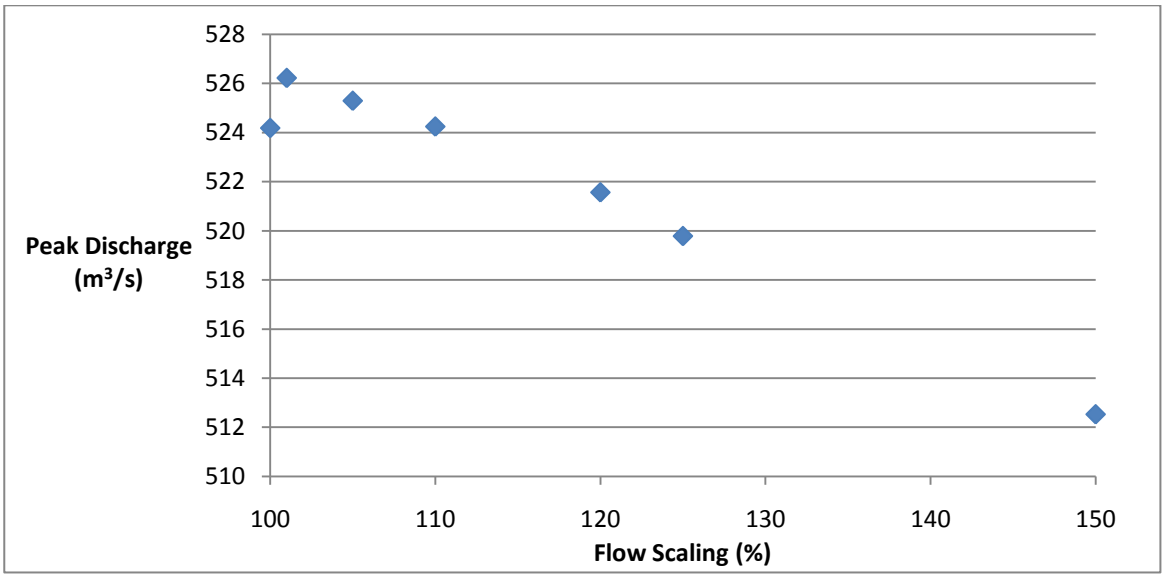

Figure 5.31 Effect of the scaled flow on peak discharge for the 'with levées' scenario. The value at 100% is the peak discharge with the original input hydrograph for the River Ure.

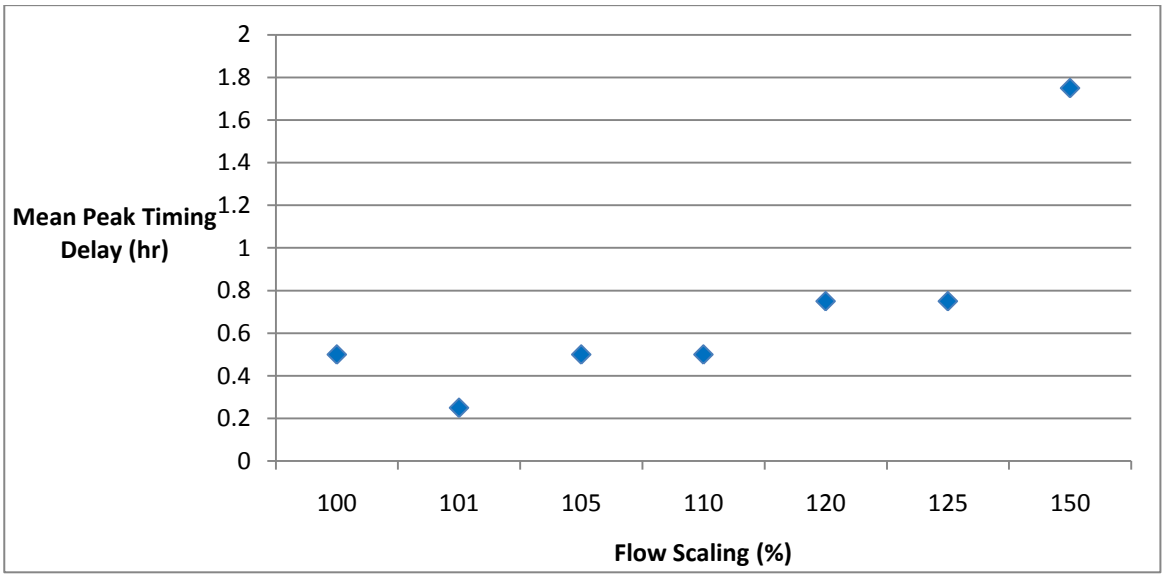

Figure 5.32 Peak timing delay in relation to each scaled flow under the 'with levées' scenario. The peak timing was averaged across each of the four peaks in the hydrograph.

Figure 5.32 illustrates that as the scaling of the flow increases, so too does the peak timing delay. Peak timing delay increases gradually with each variation, increasing from 0.25 hr at 101% to 1.75 hr at 150%. The same delay in peak timing was shown for a scaling of 105% and 110% (0.5 hr) as well as 120% and 125% (0.75 hr).

Flow scaled – different cross-section locations

Figure 5.33 shows that the peak discharges recorded at each cross-section are quite different for each scaled flow. The peak discharges recorded at the downstream boundary (cross-section 902) lie within a small range, with the scaling of 150% producing the lowest value. At the other locations however, the pattern reverses and the flows with a larger scaling produce higher peak discharges than those with a smaller scaling. Also to note is that at cross-section 982 the difference in peak discharge between the flows is large, ranging from 565.6 m^3/s (scaled by 150%) to 425.2 m^3/s (scaled by 101%). This difference reduces with distance downstream. The lowest peak discharges are recorded at cross-section 922.

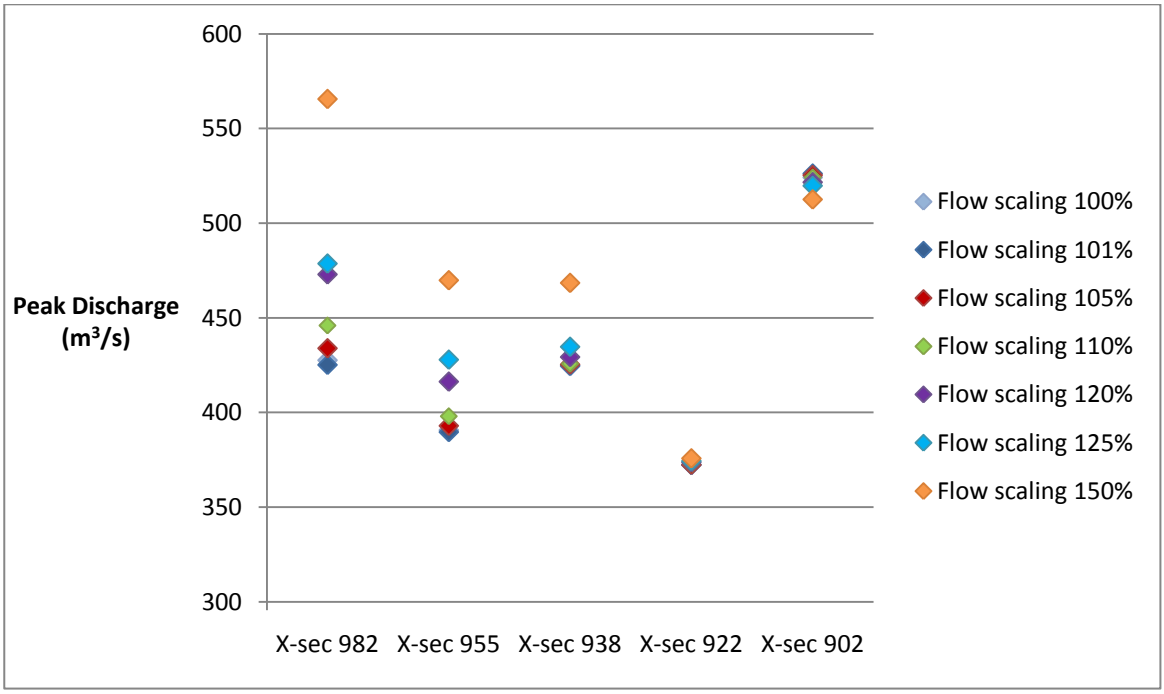

Figure 5.33 Peak discharge at selected cross section locations using the 'with levées' scenario for each of the scaled flows. The cross-section locations are from upstream to downstream in the reach (left to right on the graph). Cross-section locations are shown in Figure 5.2.

Flow shifted

After shifting the hydrograph in time peak discharge is reduced. Peak discharge reduces from 524.2 m^3/s with the original flow to 522.1 m^3/s with a 1 hour shift and 519.6 m^3/s with a 2 hour shift. The difference in peak discharge from the original value after 1 hour shift is 2.1 m^3/s and 4.6 m^3/s after 2 hours.

Flow scaled and shifted

Figure 5.34 shows that peak discharge reduces from 524.0 m^3/s to 507.9 m^3/s after scaling the flow by 101% to 150% combined with a shift in the hydrograph of 1 hour. The reduction in peak discharge is quite gradual but becomes steeper with increased scaling. The peak discharge after scaling by 101% and shifting the flow is 2.2 m^3/s lower than after scaling the flow alone. The peak discharge after scaling by 150% and shifting the flow is 4.6 m^3/s lower than after scaling the flow alone. The overall reduction in peak discharge after both scaling and shifting the flow is 16.1 m^3/s, compared to 13.7 m^3/s after only scaling the flow.

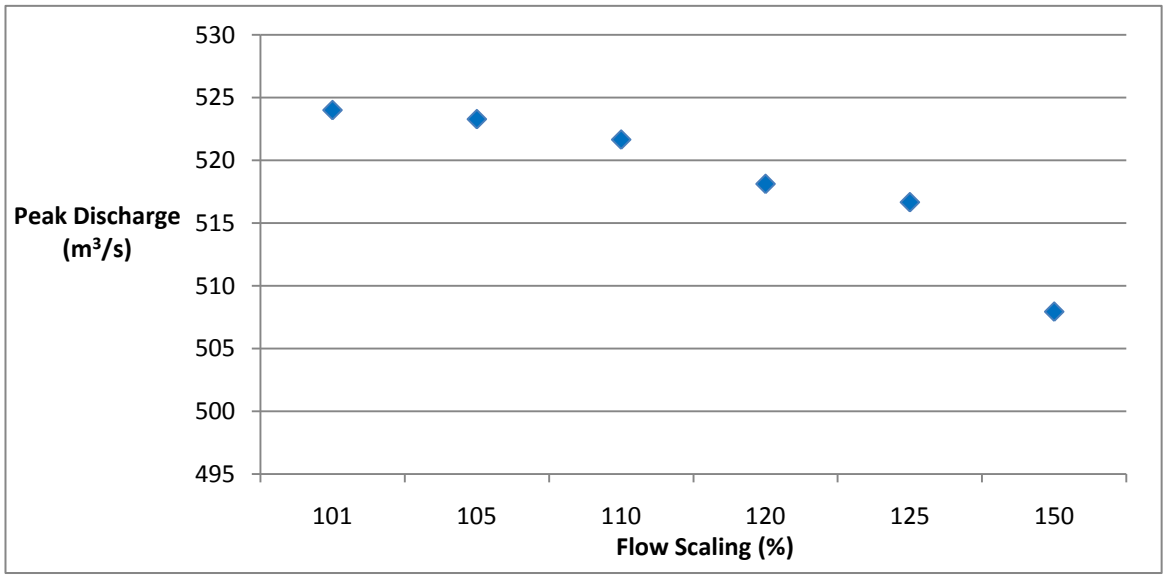

Figure 5.34 Change in peak discharge after scaling and shifting the flow using the 'with levées' scenario. In addition to the scaling, flow has been shifted by 1 hr.

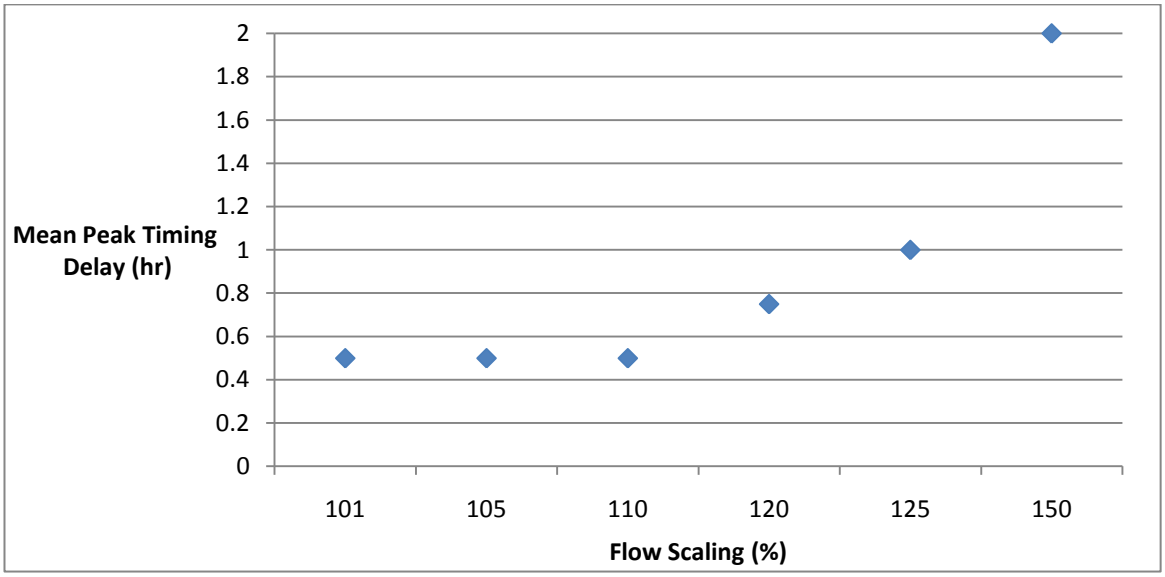

Figure 5.35 Change in peak timing delay after scaling and shifting the flow using the 'with levées' scenario. The peak timing was averaged across each of the four peaks in the hydrograph. In addition to the scaling, flow has been shifted by 1 hr.

Figure 5.35 shows that the peak timing delay after both scaling and shifting the flow is higher for all changes to the flow, compared to only scaling the flow. Here the peak timing delay ranges from 0.5 hr to 2 hr, compared to a range of between 0.25 hr and 1.75 hr for the scaled flow. Table 5.11 shows the statistics for each of the variations to the input hydrograph.

Flow scaling (%)	**101**	**105**	**110**	**120**	**125**	**150**
Peak discharge (m^3/s)	526.2	525.3	524.3	521.6	519.8	512.5
Shifted flow (hr)	**1**	**2**				
Peak discharge (m^3/s)	522.1	519.6				
Flow scaled and shifted	**Flow scaling 101%, 1 hr shift**	**Flow scaling 105%, 1 hr shift**	**Flow scaling 110%, 1 hr shift**	**Flow scaling 120%, 1 hr shift**	**Flow scaling 125%, 1 hr shift**	**Flow scaling 150%, 1 hr shift**
Peak discharge (m^3/s)	524.0	523.3	521.6	518.1	516.7	507.9

Table 5.11 Statistics for each variation to the input hydrograph: (1) scaled; (2) shifted; (3) scaled and shifted; using the 'with levées' scenario.

Flow scaled and shifted – different cross-section locations

Figure 5.36 shows similar results to Figure 5.33. At all locations, except for the downstream boundary (cross-section 902), the flows scaled by a larger percentage produce higher peak discharges than those scaled by a small percentage. At the downstream boundary the range in peak discharge between the flows is larger than that produced after scaling the flow: the difference is 13.7 m^3/s after the flow is scaled compared to 16.1 m^3/s after the flow is scaled and shifted. However, the range is about the same at cross-section 982 as with scaling the flow. As well as the larger range at the downstream boundary, the values are also smaller than after just scaling the flow. For example scaling the flow by 150% produced a peak discharge of 512.5 m^3/s, whilst scaling (150%) and shifting the flow produced a peak discharge of 507.9 m^3/s.

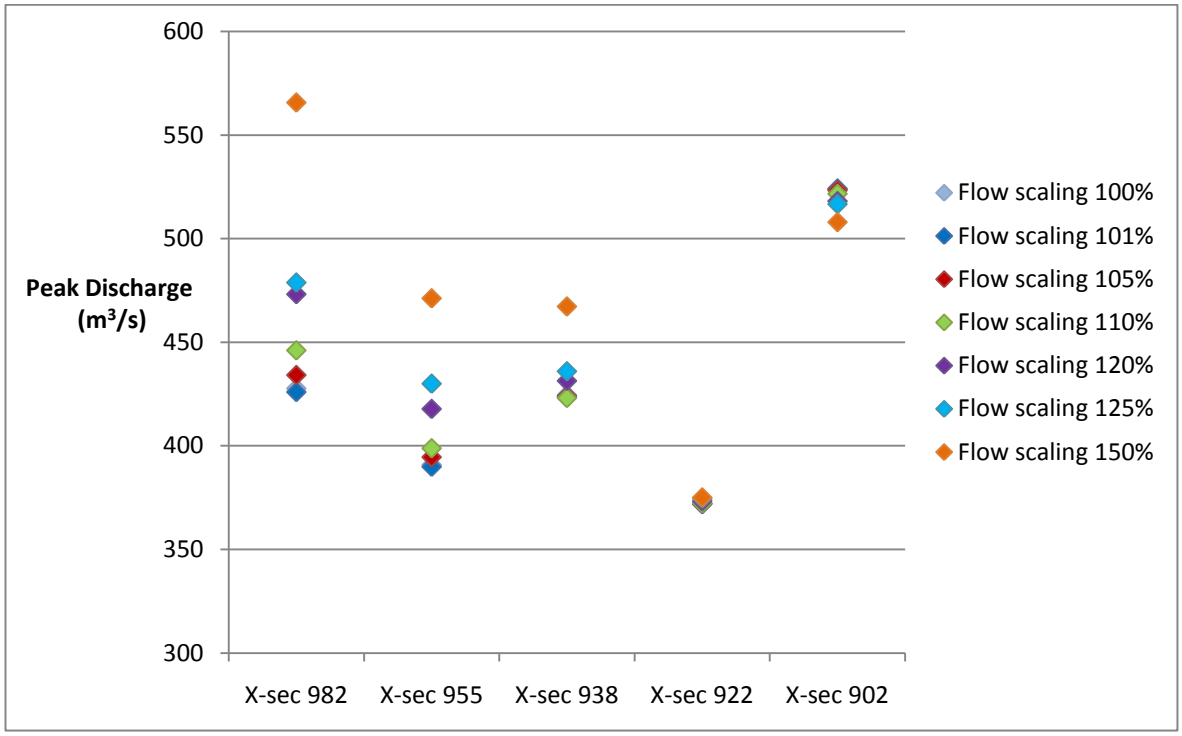

Figure 5.36 Peak discharge at selected cross section locations using the 'with levées' scenario for each of the scaled and shifted flows. In addition to the scaling, flow has been shifted by 1 hr. Cross-section locations are shown in Figure 5.2.

5.5 Research Question 3 – Do flood levées aid the transmission of the upstream hydrograph?

5.5.1 Effect on output hydrographs – without levées

Flow scaled

Figure 5.37 shows that after removing the levées and scaling the flow, peak discharge reduces with the same trend as with the levées. Peak discharge reduces with increased scaling of the flow from 519.3 m^3/s at 101% to 507.5 m^3/s at 150%. The values for peak discharge for the 'without levées' scenario are about 7 m^3/s less than with the levées.

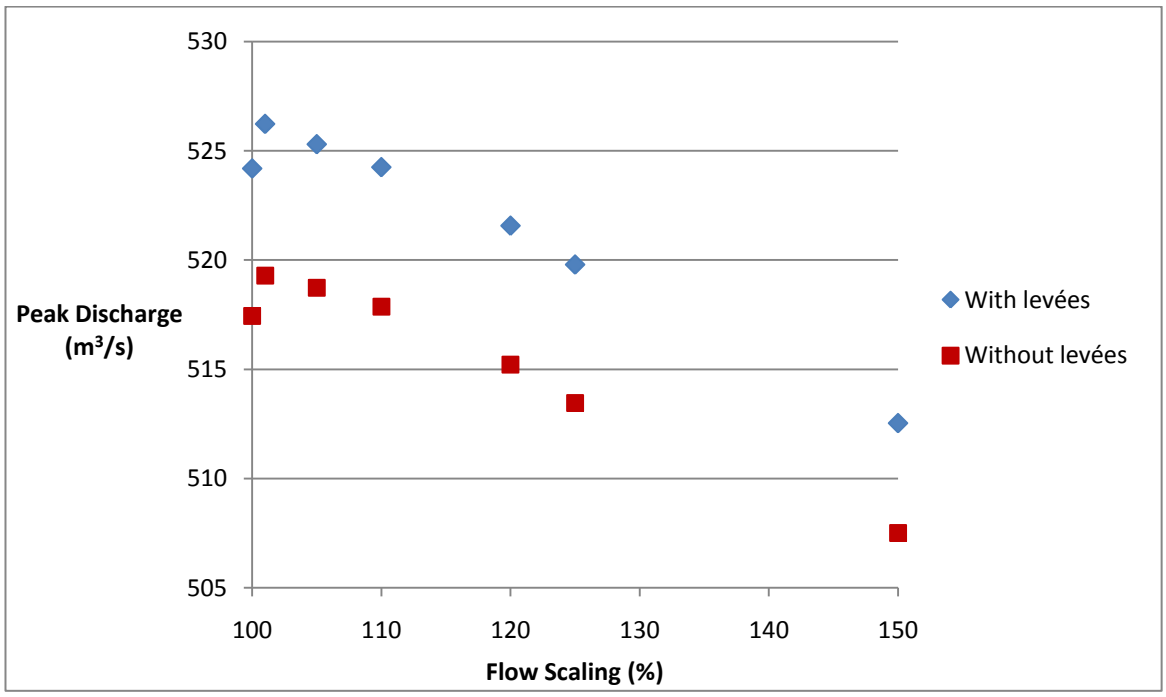

Figure 5.37 Effect of the scaled flow on peak discharge for the 'with levées' and 'without levées' scenarios. The value at a flow scaling of 100% is the original peak discharge with the normal hydrograph for the River Ure.

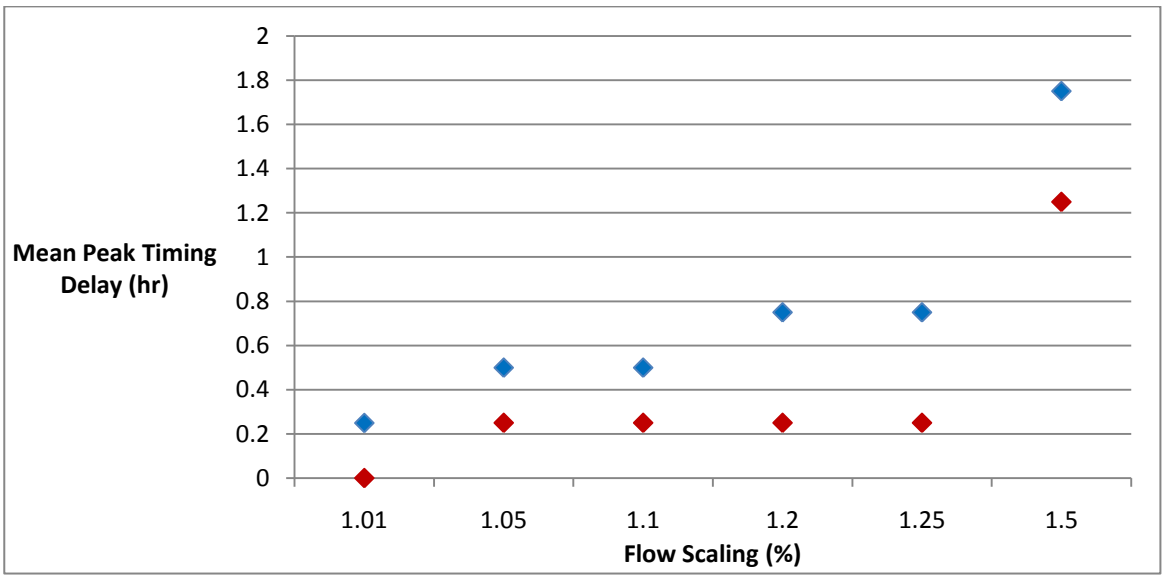

Figure 5.38 Peak timing delay in relation to each scaled flow under the 'with levées' and 'without levées' scenarios.

Figure 5.38 shows a similar pattern in peak timing delay after the levées were removed: as the flow is scaled, peak timing delay increases from 0 hr at 101% to 1.25 hr at 150%. The delay in peak timing is higher with the levées in place. There is little change to peak timing delay without the levées until the flow is scaled by 150%.

Flow scaled – different cross-section locations

Figure 5.39 shows a very similar pattern to that produced 'with levées'. However, the overall peak discharge has been reduced at all locations. The peak discharge at the downstream boundary ranges from 519.3 m^3/s at 101% to 507.5 m^3/s at 150%. In comparison, the corresponding range in peak discharge with the levées was 526.2 m^3/s to 512.5 m^3/s. The peak discharge recorded at cross-section 982 without the levées has reduced for all the flows, ranging from 547.6 m^3/s for 101% and 418.4 m^3/s for 150% compared to 565.6 m^3/s and 425.2 m^3/s with the levées.

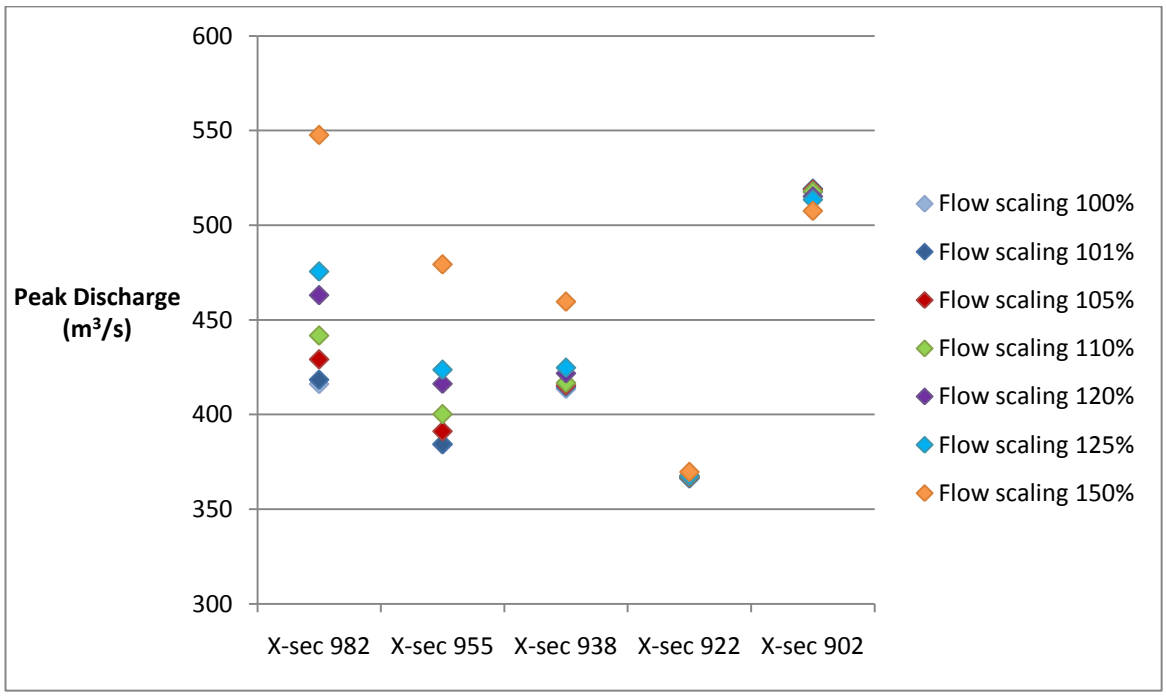

Figure 5.39 Peak discharge at selected cross section locations using the 'without levées' scenario for each of the scaled flows. The cross-section locations are from upstream to downstream in the reach (left to right on the graph). Cross-section locations are shown in Figure 5.2.

Flow shifted

Shifting the hydrograph in time reduces peak discharge with a negative linear correlation, the same relationship as with the levée scenarios. Peak discharge reduces from 517.4 m^3/s with the original flow to 515.1 m^3/s with a 1 hour shift and 512.4 m^3/s with a 2 hour shift. After shifting the hydrograph by 2 hours whilst removing the levées, the peak discharge is reduced by 9.7 m^3/s compared to that with the levées present. The difference in peak discharge from the original value with a 1 hour shift is 2.3 m^3/s and 5.1 m^3/s after 2 hours, a larger difference than with the levées.

Flow scaled and shifted

Figure 5.40 shows that peak discharge reduces from 517.3 m^3/s to 503.0 m^3/s after scaling the flow by 101% to 150% combined with a shift in the hydrograph of 1 hour. The shape of the graph is the same as with the levées, becoming steeper with increased scaling. The overall reduction in peak discharge after both scaling and shifting the flow is 14.3 m^3/s, compared to 11.8 m^3/s after only scaling the flow.

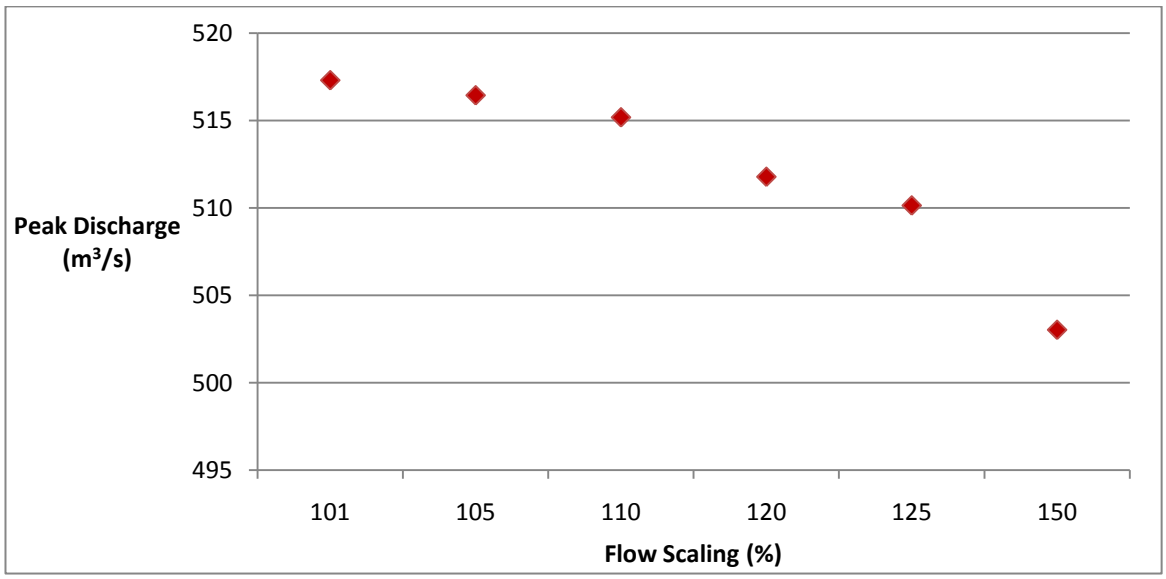

Figure 5.40 Change in peak discharge after scaling and shifting the flow using the 'without levées' scenario. In addition to the scaling, flow has been shifted by 1 hr.

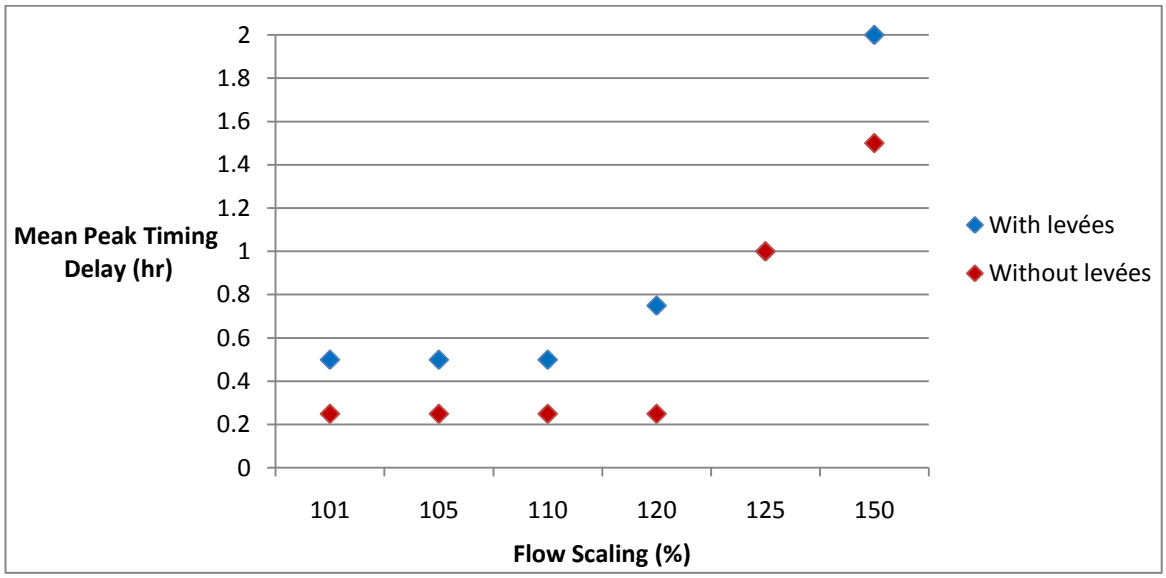

Figure 5.41 Change in peak timing delay after scaling and shifting the flow using the 'without levées' scenario. In addition to the scaling, flow has been shifted by 1 hr.

Comparison of Figure 5.35 and 5.41 shows that for the 'without levées' scenario, the delay in peak timing has increased after both scaling and shifting the flow, compared to just scaling the flow. After scaling the flow, the peak timing delay ranged from 0 hr to 1.25 hr. After scaling and shifting the flow, the range is between 0.25 hr and 1.5 hr. It also shows that the peak timing delay is longer by about 0.25 hr with the levées. Table 5.12 shows the statistics for each of the variations to the input hydrograph.

With levées

Flow scaling (%)	**101**	**105**	**110**	**120**	**125**	**150**
Peak Discharge (m^3/s)	526.2	525.3	524.3	521.6	519.8	512.5
Shifted flow (hr)	**1**	**2**				
Peak Discharge (m^3/s)	522.1	519.6				
Flow scaled and shifted	**Flow scaling 101%, 1 hr shift**	**Flow scaling 105%, 1 hr shift**	**Flow scaling 110%, 1 hr shift**	**Flow scaling 120%, 1 hr shift**	**Flow scaling 125%, 1 hr shift**	**Flow scaling 150%, 1 hr shift**
Peak Discharge (m^3/s)	524.0	523.3	521.6	518.1	516.7	507.9

Without levées

Flow scaling (%)	**101**	**105**	**110**	**120**	**125**	**150**
Peak Discharge (m^3/s)	519.3	518.7	517.9	515.2	513.5	507.5
Shifted flow (hr)	**1**	**2**				
Peak Discharge (m^3/s)	515.1	512.4				
Flow scaled and shifted	**Flow scaling 101%, 1 hr shift**	**Flow scaling 105%, 1 hr shift**	**Flow scaling 110%, 1 hr shift**	**Flow scaling 120%, 1 hr shift**	**Flow scaling 125%, 1 hr shift**	**Flow scaling 150%, 1 hr shift**
Peak Discharge (m^3/s)	517.3	516.4	515.2	511.8	510.1	503.0

Half height levées

Flow scaling (%)	**101**	**105**	**110**	**120**	**125**	**150**
Peak Discharge (m^3/s)	525.1	524.4	522.9	519.7	518.2	510.9
Shifted flow (hr)	**1**	**2**				
Peak Discharge (m^3/s)	520.6	517.8				
Flow scaled and shifted	**Flow scaling 101%, 1 hr shift**	**Flow scaling 105%, 1 hr shift**	**Flow scaling 110%, 1 hr shift**	**Flow scaling 120%, 1 hr shift**	**Flow scaling 125%, 1 hr shift**	**Flow scaling 150%, 1 hr shift**
Peak Discharge (m^3/s)	523.2	521.8	520.1	516.6	514.3	505.7

Added height levées

Flow scaling (%)	**101**	**105**	**110**	**120**	**125**	**150**
Peak Discharge (m^3/s)	521.9	521.5	519.8	517.1	516.1	508.3
Shifted flow (hr)	**1**	**2**				
Peak Discharge (m^3/s)	517.8	514.4				
Flow scaled and shifted	**Flow scaling 101%, 1 hr shift**	**Flow scaling 105%, 1 hr shift**	**Flow scaling 110%, 1 hr shift**	**Flow scaling 120%, 1 hr shift**	**Flow scaling 125%, 1 hr shift**	**Flow scaling 150%, 1 hr shift**
Peak Discharge (m^3/s)	520.2	518.8	517.4	513.8	512.5	503.1

Table 5.12 Statistics for each variation to the input hydrograph: (1) scaled; (2) shifted; (3) scaled and shifted under each scenario.

Flow scaled and shifted – different cross-section locations

Figure 5.42 shows similar results to those produced after only scaling the flow. The peak discharges recorded at the downstream boundary range from 517.3 m^3/s at 101% to 503.0 m^3/s at 150%. Using the 'with levées' scenario and both scaling and shifting the flow gave a range of 524.0 m^3/s and 507.9 m^3/s which is higher than when the levées were taken out. Figure 5.43 shows that the difference in peak discharge between the scenarios is largest at cross-sections 955 and 982. The difference is smallest at cross-section 902, between 5 m^3/s and 7 m^3/s.

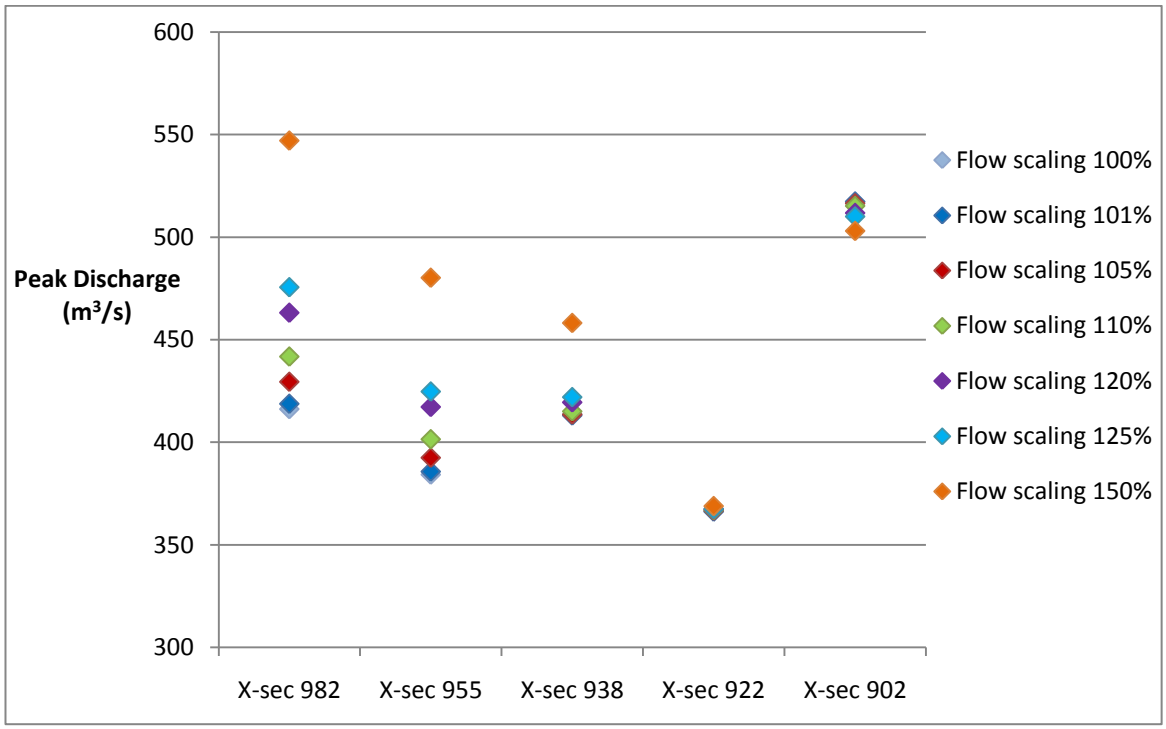

Figure 5.42 Peak discharge at selected cross section locations using the 'without levées' scenario for each of the scaled and shifted flows. In addition to the scaling, flow has been shifted by 1 hr. Cross-section locations are shown in Figure 5.2.

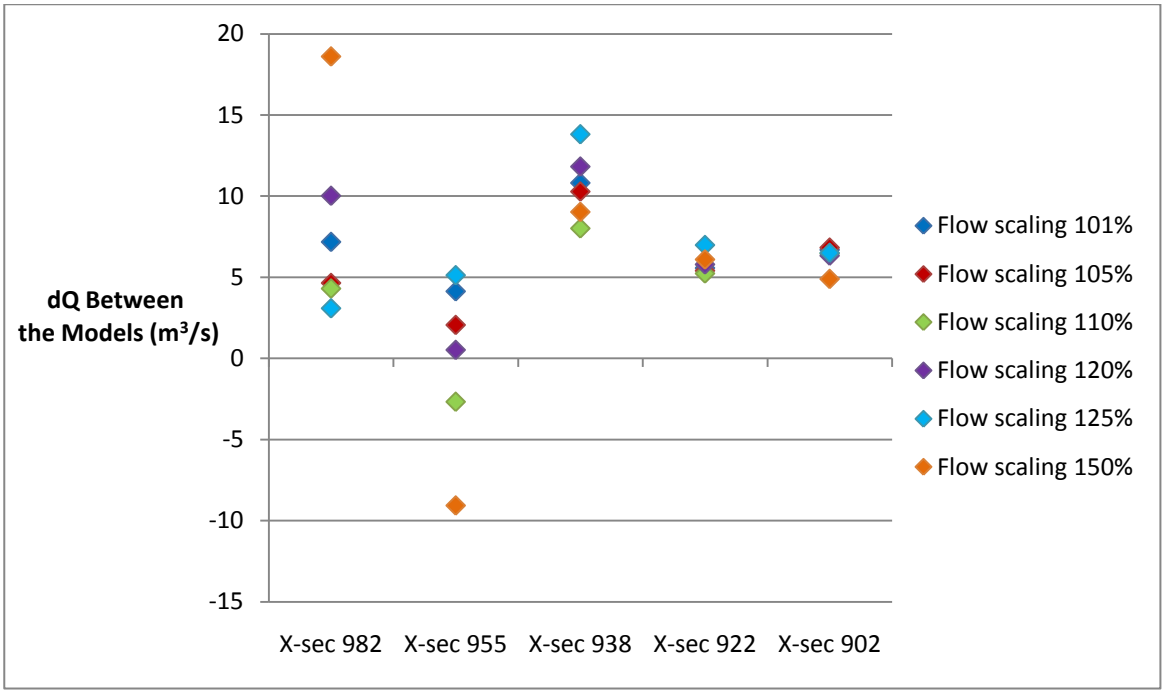

Figure 5.43 Difference in peak discharge between the 'with levées' and 'without levées' scenarios at selected cross section locations for each of the scaled and shifted flows. In addition to the scaling, flow has been shifted by 1 hr. Cross-section locations are shown in Figure 5.2.

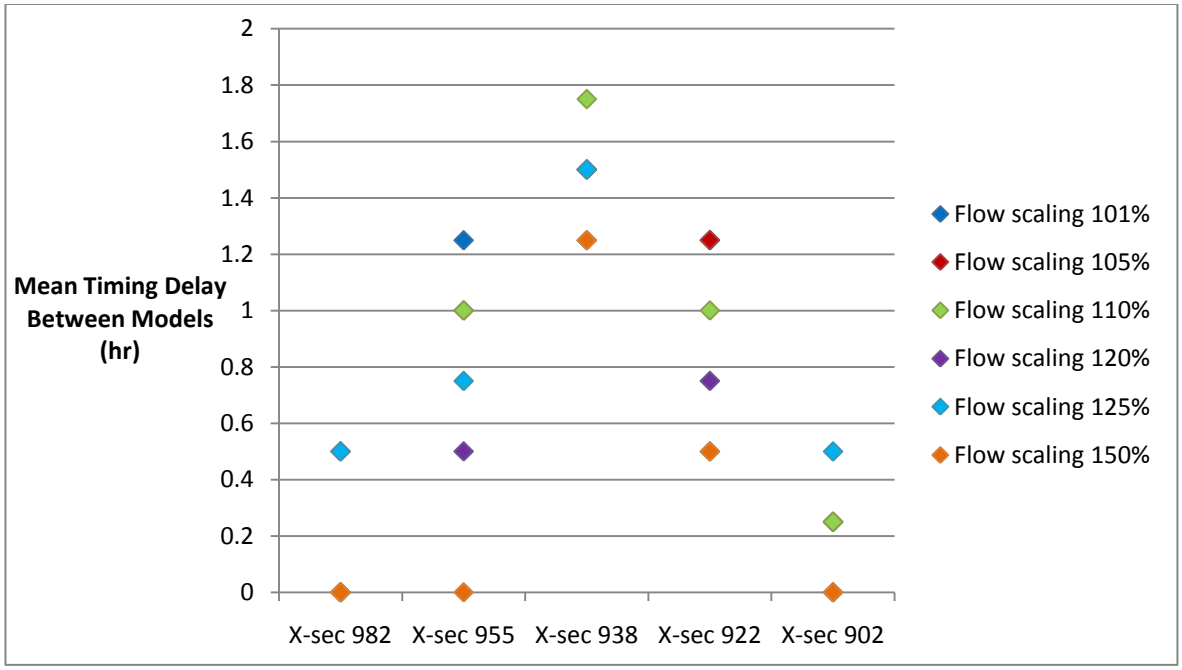

Figure 5.44 Difference in peak timing delay between the 'with levées' and 'without levées' scenarios at selected cross section locations for each of the scaled and shifted flows. The peak timing was averaged across each of the four peaks in the hydrograph. In addition to the scaling, flow has been shifted by 1 hr. Cross-section locations are shown in Figure 5.2.

Figure 5.44 shows that the difference in peak timing between the scenarios is highest for all of the flows at cross section 938. There is little difference in peak timing between the scenarios and flows at cross-section 902. The difference between the models is smallest for the 150% flow.

5.5.2 Effect on output hydrographs – half levées and added height levées

Flow scaled

Figure 5.45 shows the 'half height' scenario follows the same trend as the other scenarios, with peak discharge reducing gradually as the degree of flow scaling increases. Peak discharge reduces from 525.1 m^3/s at 101% to 510.9 m^3/s at 150%. These values are around 1.5 m^3/s lower than for the 'with levées' scenario but 5.0 m^3/s higher than without the levées. Peak discharge reduces in the same way for the 'added height' scenario, from 519.3 m^3/s to 508.3 m^3/s. These values lie between the 'half height' and 'without levées' scenarios.

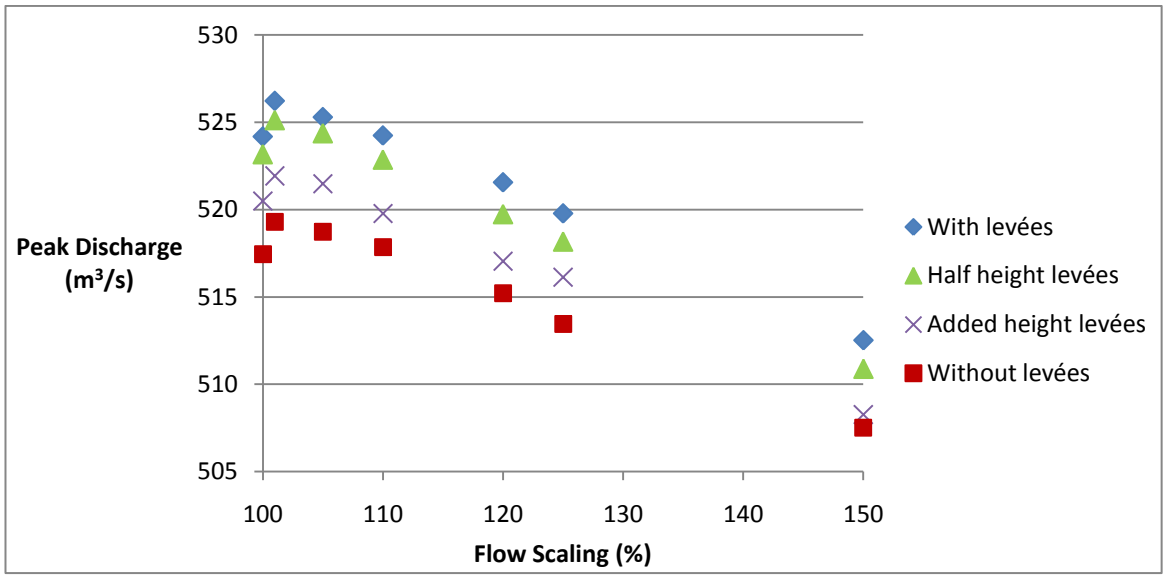

Figure 5.45 The effect of the scaled flow on peak discharge for all levée scenarios. The value at a flow scaling of 100% is the original peak discharge with the normal hydrograph for the River Ouse under each of the scenarios.

Flow shifted

Figure 5.46 shows that the same relationship is produced for the 'half height levées' scenario as described previously with and without the levées present. After shifting the timing of the input hydrograph, the peak discharge reduces from 523.2 m^3/s with the

original flow to 520.6 m^3/s with a 1 hour shift and 517.8 m^3/s with a 2 hour shift. These values are around 1.5 m^3/s lower than for the 'with levées' scenario but 5 m^3/s higher than without the levées. The 'added height levées' scenario also produces a similar pattern after the shift in timing to the input hydrograph. The peak reduces from 520.5 m^3/s with the original flow to 517.8 m^3/s with a 1 hour shift and 514.4 m^3/s with a 2 hour shift. These values lie between the 'half height' and 'without levées' scenarios. Figure 5.46 illustrates that peak discharge is reduced by around the same amount in all of the scenarios after shifting the timing of the hydrograph.

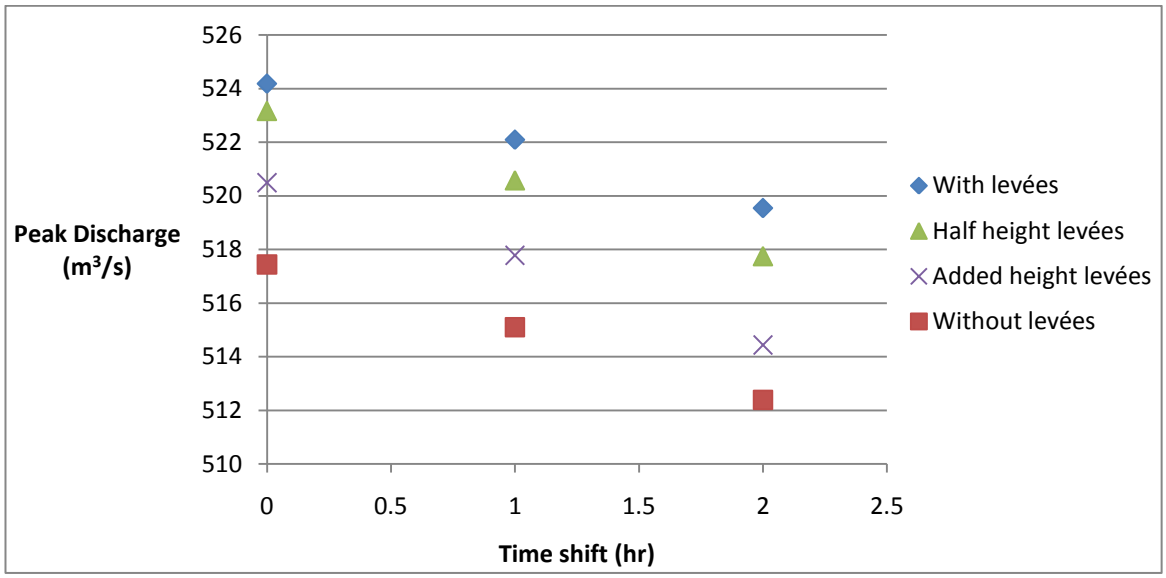

Figure 5.46 Change in peak discharge with each shift to the flow using the 'half height levées' and 'added height levées' scenarios.

Figure 5.47 shows that the difference in peak discharge from the original value after a 1 hour shift for the half height scenario is 2.6 m^3/s and 5.4 m^3/s after 2 hours. For the 'added height levées' scenario, these values are 2.7 m^3/s and 6.1 m^3/s. Overall, the change in peak discharge as a result of shifting the hydrograph is highest for the 'added height scenario' and subsequently 'half height', 'without levées' and 'with levées' scenarios.

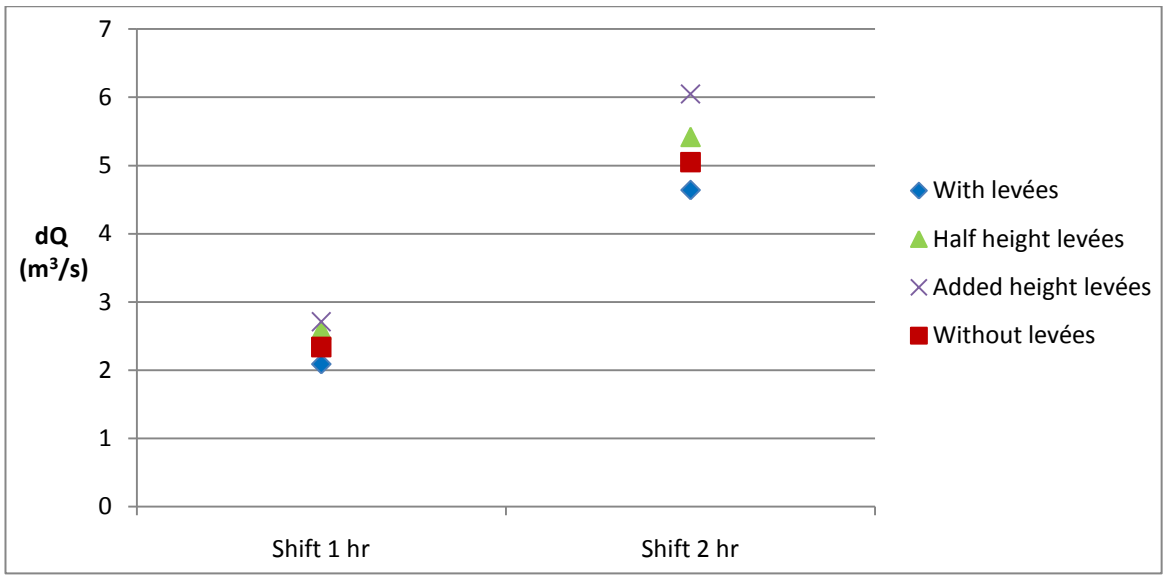

Figure 5.47 Change in peak discharge from the original peak discharge after shifting the flow using the 'half height levées' and 'added height levées' scenarios.

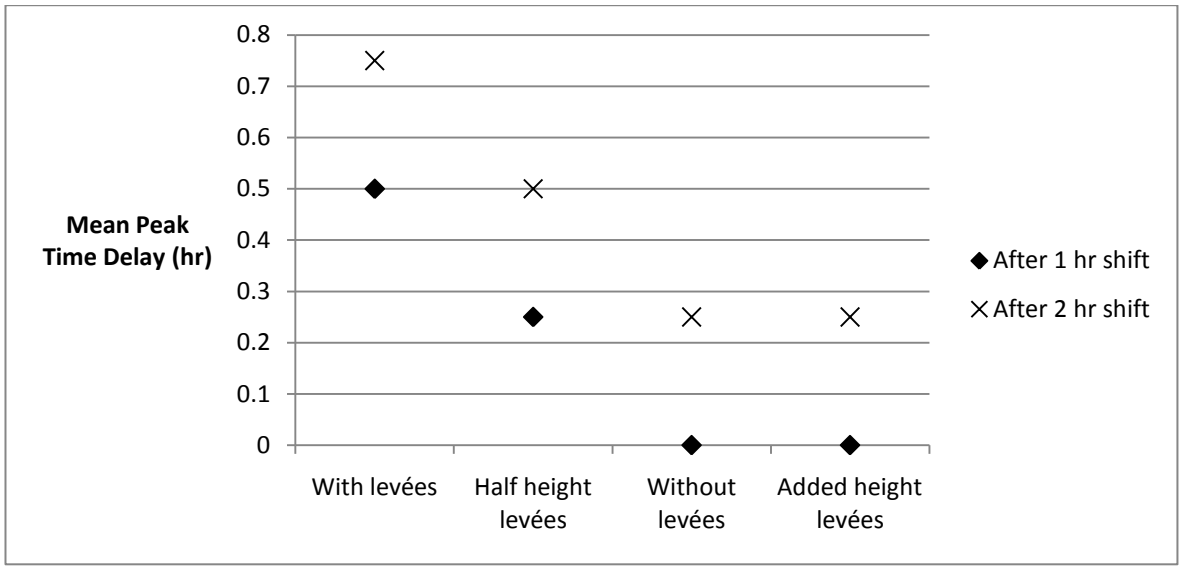

Figure 5.48 Change in peak timing delay after shifting the flow for each of the four levée scenarios.

Figure 5.48 shows that peak timing delay is affected in the same way for each scenario after shifting the hydrograph by 1 hour and 2 hours. Peak timing delay is affected most with the levées included in the model: the peak timing delay is 0.5 hr with a shift of 1 hour and 0.75 hr after a shift of 2 hours. The 'half height' scenario is also influenced by the shift in the hydrograph but to a lesser extent. The peak is delayed by 0.25 hr after a 1 hour shift and 0.5 hr after a 2 hour shift. The 'without levées' and 'added height levées' scenarios respond in the same way: there is no delay in peak timing.

Flow scaled and shifted

Figure 5.49 shows that peak discharge for the 'half height' scenario reduces from 523.2 m^3/s to 505.7 m^3/s after scaling the flow by 101% to 150% combined with a shift in the hydrograph of 1 hour. Peak discharge for the 'added height' scenario reduces from 520.2 m^3/s to 503.1 m^3/s. The same pattern is seen as with scaling the flow only: 'with levées' produced the highest discharges, then the 'half height', 'added height' and 'without levées' scenarios. Scaling and shifting the flow reduces the peak discharge by a larger amount than scaling or shifting the flow alone. The 'without levées' and 'added height' levées scenarios produce the lowest discharges. Appendix Three shows the hydrographs produced after scaling and shifting the flow for each of the levée scenarios.

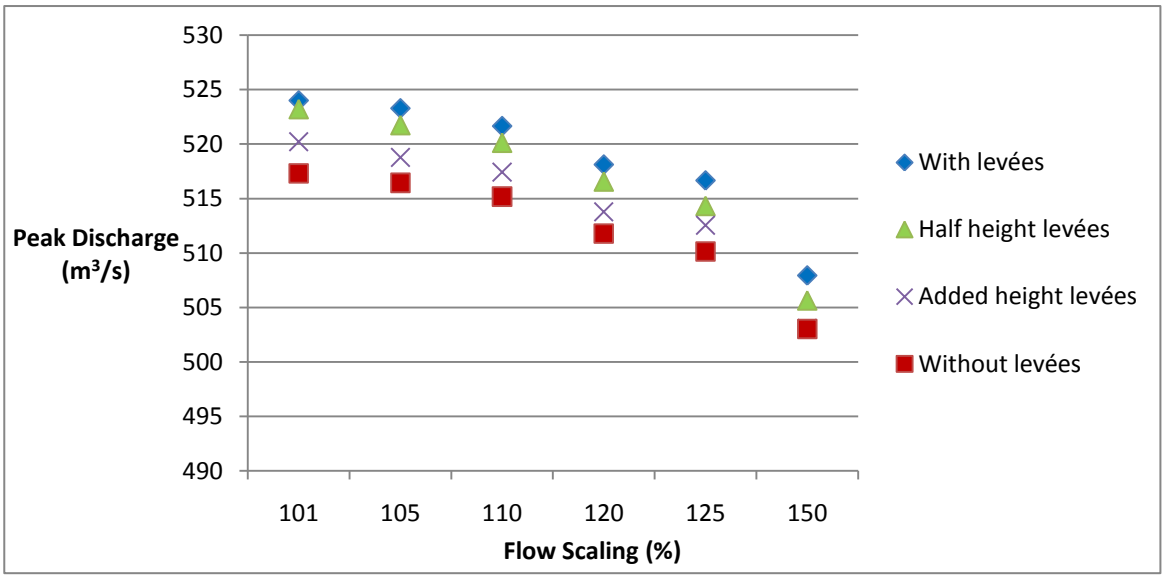

Figure 5.49 Change in peak discharge after scaling and shifting the flow using the 'half height levées' and 'added height levées' scenarios. In addition to the scaling, flow has been shifted by 1 hr.

5.5.3 Effect on hydrograph with changes to roughness – with levées

Figure 5.50 shows that peak discharge is reduced for each flow after varying Manning's *n* for the channel. Peak discharge is reduced as the flow is scaled but also as Manning's *n* is increased. Peak discharge ranges from 420.4 m^3/s with a 101% scaled and shifted flow (*n* = 0.08) to 396.5 m^3/s with a 150% scaled and shifted flow (*n* = 0.09). The values at *n* = 0.1 for the flows between 110% and 150% appear too high as it would be expected that peak discharge would continue to decrease with increased Manning's *n* and scaling.

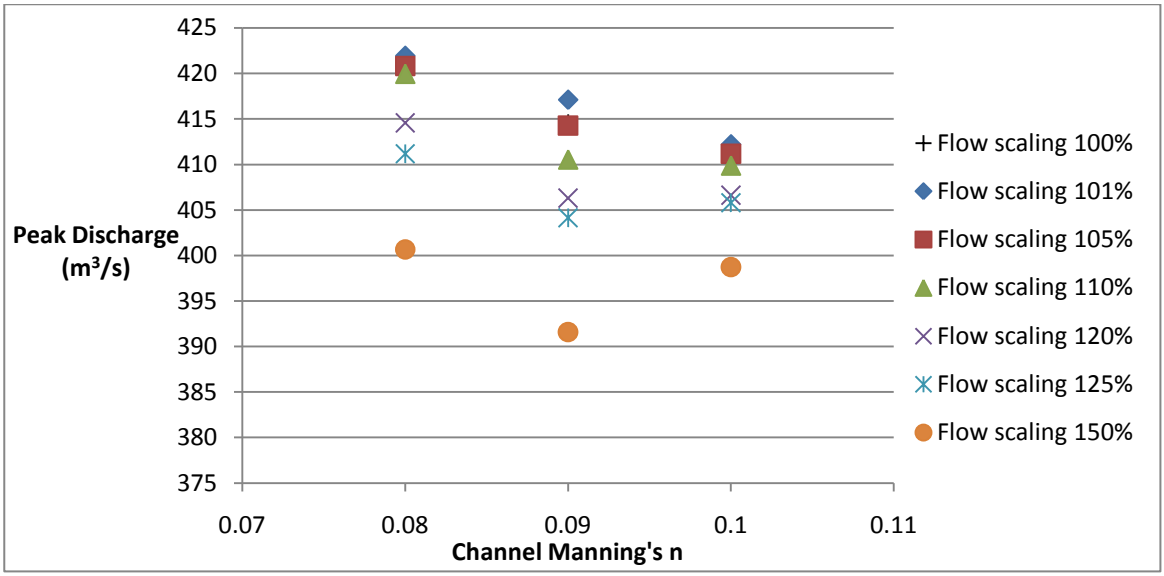

Figure 5.50 Change in peak discharge with channel Manning's *n* for each of the scaled and shifted flows using the 'with levées' scenario. In addition to the scaling, flow has been shifted by 1 hr.

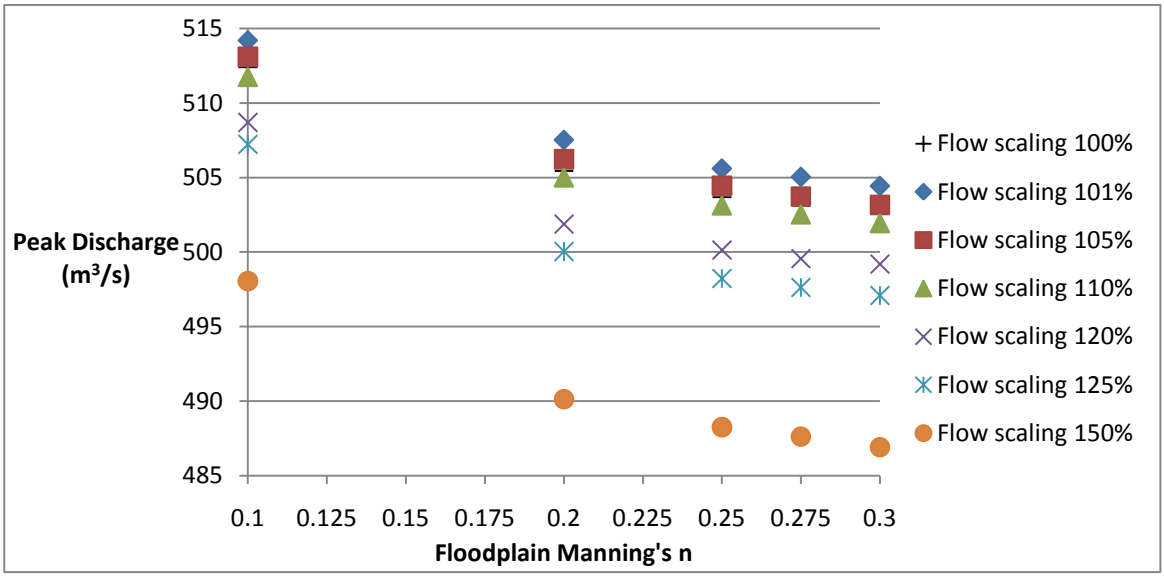

Figure 5.51 Change in peak discharge with floodplain Manning's *n* for each of the scaled and shifted flows using the 'with levées' scenario. In addition to the scaling, flow has been shifted by 1 hr.

Figure 5.51 shows that peak discharge is also reduced for each flow after varying Manning's *n* for the floodplain. With a floodplain *n* of 0.1, peak discharge ranges from 512.2 m^3/s (flow scaled by 101%) to 493.8 m^3/s (flow scaled by 150%). With a floodplain *n* of 0.3, peak discharge ranges from 502.3 m^3/s (flow scaled by 101%) to 483.1 m^3/s (flow scaled by 150%). Table 5.13 displays the values for peak discharge produced after

conducting simulations using the 'with levées' scenario and varying both Manning's *n* and flow scaling.

Manning's *n* / Flow Scaling (%)	101	105	110	120	125	150
Channel *n* = 0.08	420.4	418.5	417.5	411.5	409.1	399.5
Channel *n* = 0.09	413.8	410.7	407.5	404.3	402.8	389.0
Channel *n* = 0.1	409.9	409.2	407.8	404.9	404.2	396.5
Floodplain *n* = 0.1	512.2	511.0	509.4	505.7	504.1	493.8
Floodplain *n* = 0.2	505.3	504.1	502.5	499.2	496.7	486.3
Floodplain *n* = 0.25	503.5	502.5	500.9	497.3	495.1	484.4
Floodplain *n* = 0.275	502.9	501.8	500.2	496.8	494.4	483.7
Floodplain *n* = 0.3	502.3	501.3	499.7	496.2	493.9	483.1

Table 5.13 Statistics for each simulation varying both Manning's *n* for the channel and floodplain and flow (scaled and shifted) using the 'with levées' scenario. In addition to the scaling, flow has been shifted by 1 hr.

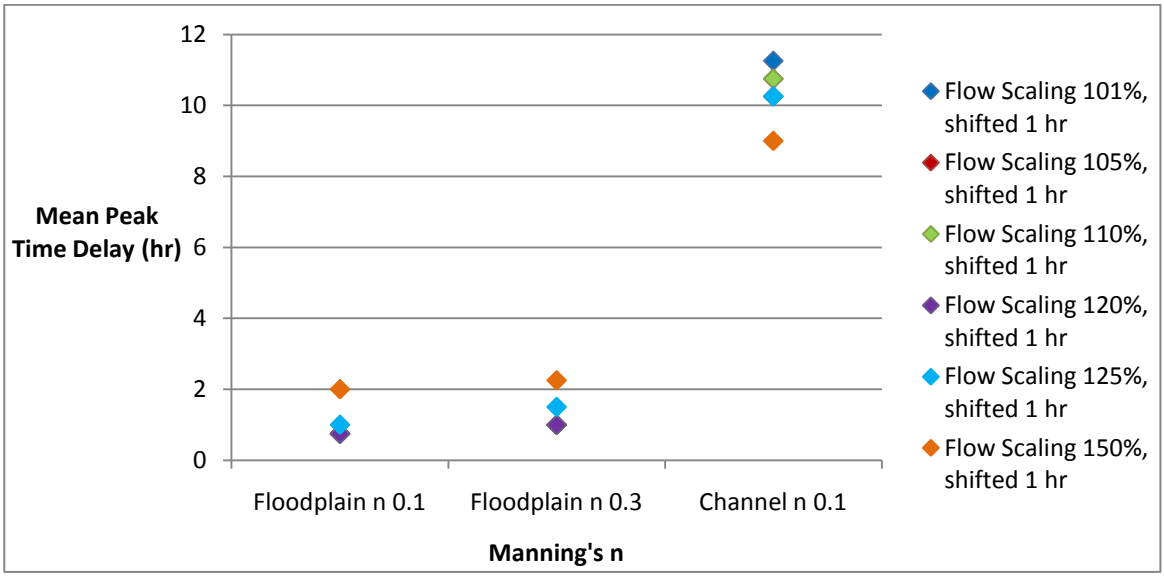

Figure 5.52 Change in peak timing delay with Manning's *n* for each of the scaled and shifted flows using the 'with levées' scenario. All other Manning's n values in these simulations were not changed from the values input into the original model.

Figure 5.52 shows that the delay in peak timing after varying floodplain *n* to 0.1 is highest for the flow scaled by 150%, at 2 hours. A lag of around 1.5 hours is produced for the

other flows. In contrast to this, when channel *n* was increased to 0.1, the flow scaled by 150% gave the smallest delay in peak timing of 9 hours, compared to the flow scaled by 101% which had a timing lag of 11.25 hours. A much higher delay in peak timing is created for all of the flows when varying channel *n*, compared to floodplain *n*.

5.5.4 Effect on hydrograph with changes to roughness – without levées

Figure 5.53 shows that all of the values produced for Manning's *n* values of 0.08 and 0.09 are 7 m^3/s less than the 'with levées' scenario. The simulations using channel Manning's *n* of 0.1 produce lower peak discharges than the other *n* values. This is as expected, unlike in Figure 5.50 using the 'with levées' scenario. There is a large difference in peak discharge for different channel *n* values, between 413.6 m^3/s and 391.4 m^3/s for the flow scaled by 101% and between 398.9 m^3/s and 376.8 m^3/s for the flow scaled by 150%.

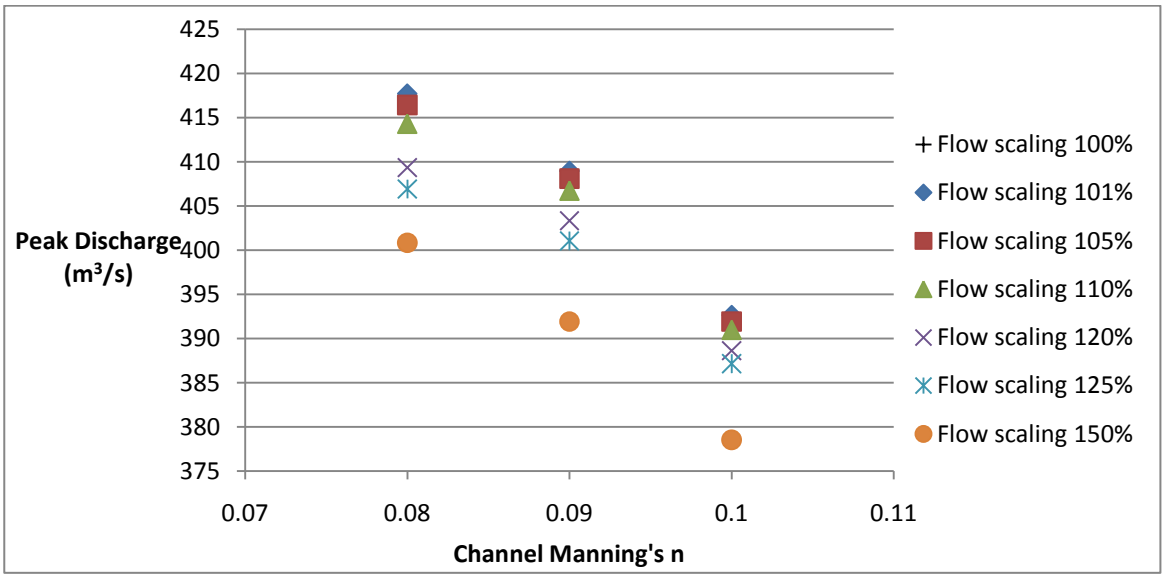

Figure 5.53 Change in peak discharge with channel Manning's *n* for each of the scaled and shifted flows using the 'without levées' scenario. In addition to the scaling, flow has been shifted by 1 hr.

Figure 5.54 shows that the difference between the flows after varying Manning's *n* for the floodplain is larger than with the levées. Peak discharge reduces with increasing *n,* with a difference of around 16 m^3/s between the 101% and 150% scaled flows at each of the Manning's *n* values. With a floodplain *n* of 0.1, peak discharge ranges from 506 m^3/s (flow scaled by 101%) to 489.7 m^3/s (flow scaled by 150%). With a floodplain *n* of 0.3, peak discharge ranges from 496.4 m^3/s (flow scaled by 101%) to 479.4 m^3/s (flow scaled by

150%). Table 5.14 displays the values for peak discharge produced after conducting simulations using the 'without levées' scenario and varying both Manning's *n* and flow.

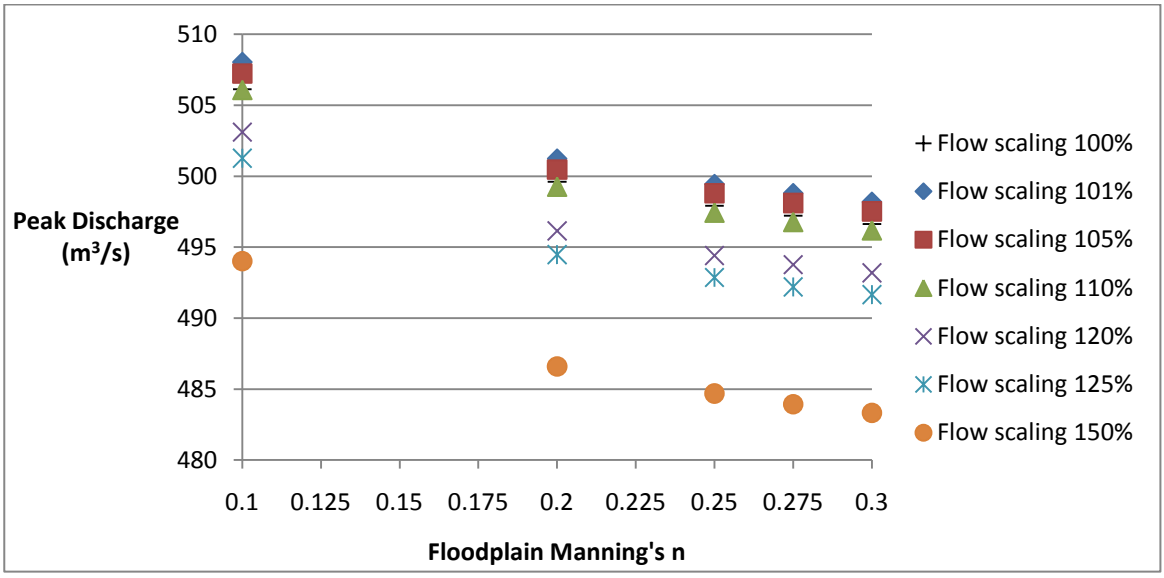

Figure 5.54 Change in peak discharge with floodplain Manning's *n* for each of the scaled and shifted flows using the 'without levées' scenario. In addition to the scaling, flow has been shifted by 1 hr.

Manning's *n* / Flow Scaling (%)	101	105	110	120	125	150
Channel *n* = 0.08	415.1	413.6	411.4	406.5	404.0	398.9
Channel *n* = 0.09	407.3	406.3	404.9	401.2	398.8	390.6
Channel *n* = 0.1	391.4	390.7	389.7	387.3	385.7	376.8
Floodplain *n* = 0.1	506.0	505.0	503.6	500.0	498.0	489.7
Floodplain *n* = 0.2	499.4	498.4	496.9	493.3	491.2	482.5
Floodplain *n* = 0.25	497.6	496.7	495.2	491.5	489.7	480.7
Floodplain *n* = 0.275	497.0	495.9	494.5	490.8	489.1	480.0
Floodplain *n* = 0.3	496.4	495.4	493.9	490.3	488.5	479.4

Table 5.14 Statistics for each simulation varying both Manning's *n* for the channel and floodplain and flow (scaled and shifted) using the 'without levées' scenario. In addition to the scaling, flow has been shifted by 1 hr.

Figure 5.55 shows that after removing the levées, the influence of both Manning's *n* and the grip flows on the delay in peak timing is not as strong. The largest change in peak timing delay was produced for the 150% scaled and shifted flow, ranging from 1.5 hr with

a floodplain *n* of 0.1 to 9.75 hr with a channel *n* of 0.1. In contrast to the 'with levées' scenario, the 150% scaled and shifted flow gave the highest delay in peak timing for all three simulations shown.

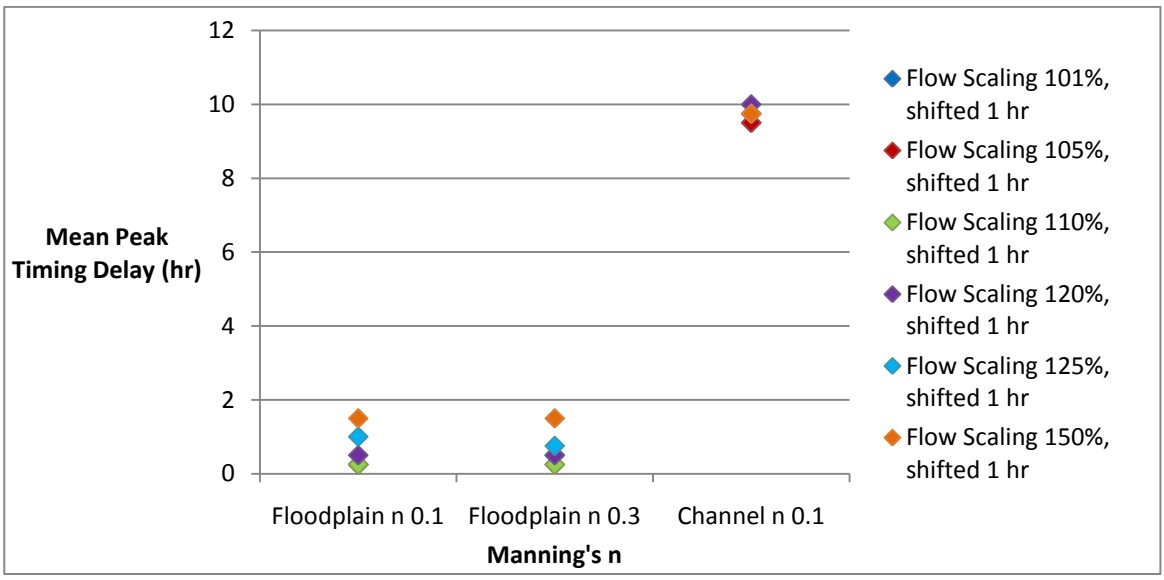

Figure 5.55 Change in peak timing delay with Manning's *n* for each of the scaled and shifted flows using the 'without levées' scenario. All other Manning's n values in these simulations were not changed from the values input into the original model.

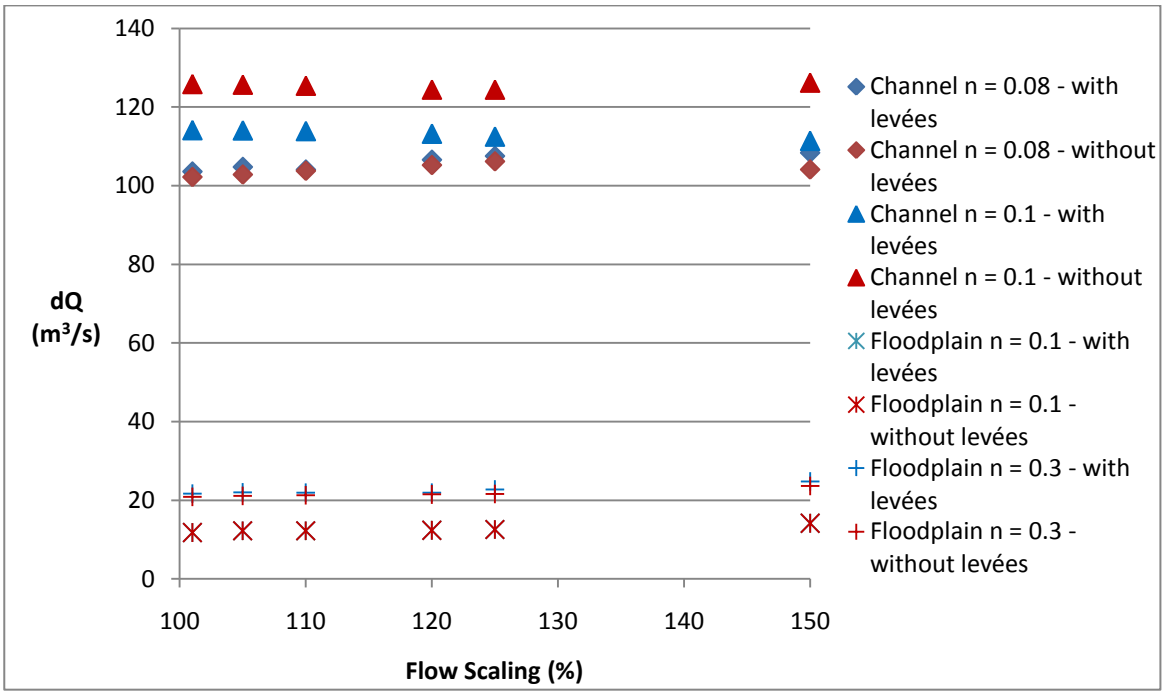

Figure 5.56 Comparing the change in peak discharge for the 'with levées' and 'without levées' scenarios after varying both Manning's *n* for the channel and floodplain and scaling and shifting the flow with original Manning's *n* values. In addition to the scaling, flow has been shifted by 1 hr.

Figure 5.56 and Table 5.15 show that both Manning's *n* and the flows have a large influence on peak discharge. The difference in peak discharge from original values is largest for variations involving channel *n*, as would be expected, and is 100 m^3/s to 130 m^3/s. The difference in peak discharge is much smaller for variations using floodplain *n*, and is 10 m^3/s to 25 m^3/s. The difference in peak discharge reduces as Manning's *n* values are decreased. In all the cases, the 'with levées' scenario gives a higher difference in peak discharge except when channel *n* was set to 0.1. For all of the simulations, the change in peak discharge increases very slightly as the flow is scaled.

	Manning's *n* / Flow Scaling (%)	**101**	**105**	**110**	**120**	**125**	**150**
With levées	**Channel *n* = 0.08**	103.6	104.8	104.1	106.6	107.6	108.4
	Channel *n*= 0.1	114.1	114.1	113.9	113.2	112.5	111.4
	Floodplain *n* = 0.1	11.8	12.2	12.3	12.4	12.5	14.1
	Floodplain *n* = 0.3	21.7	22.0	21.9	21.9	22.7	24.8

	Manning's *n* / Flow Scaling (%)	**101**	**105**	**110**	**120**	**125**	**150**
Without levées	**Channel *n* = 0.08**	102.2	102.8	103.8	105.3	106.2	104.1
	Channel *n*= 0.1	125.9	125.7	125.4	124.5	124.4	126.2
	Floodplain *n* = 0.1	11.3	11.4	11.6	11.7	12.2	13.3
	Floodplain *n* = 0.3	20.9	21.1	21.3	21.5	21.6	23.7

Table 5.15 Statistics for each simulation varying both Manning's *n* for the channel and floodplain and flow (scaled and shifted) using the 'with levées' and 'without levées' scenarios. In addition to the scaling, flow has been shifted by 1 hr.

5.5.5 Effect on hydrograph with changes to roughness – half levées

Figure 5.57 shows a similar trend to that of the 'with levées' scenario, with the peak discharge at Manning's *n* of 0.1 being higher than expected (looking at the trend shown in Figure 5.57). Peak discharge ranges from 419.7 m^3/s to 410.1 m^3/s for the 101% scaled and shifted flow and between 400.4 m^3/s and 395.8 m^3/s for the 150% scaled and shifted flow. Overall peak discharges for the 'half height levées' scenario are about 1 m^3/s less than the 'with levées' scenario and 20 m^3/s larger than 'without levées'.

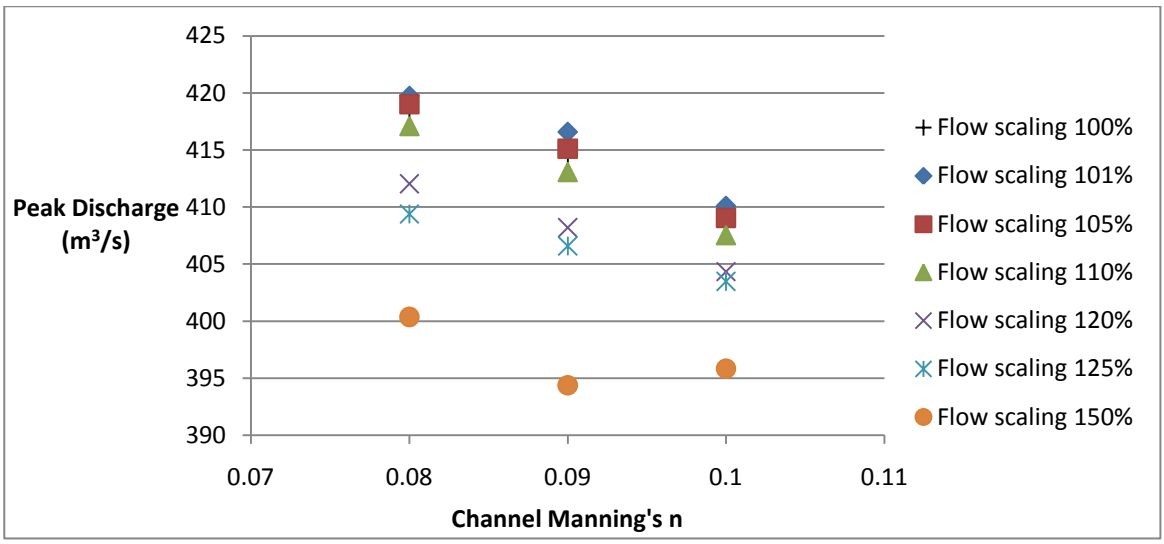

Figure 5.57 Change in peak discharge with channel Manning's *n* for each of the scaled and shifted flows using the 'half height levées' scenario. In addition to the scaling, flow has been shifted by 1 hr.

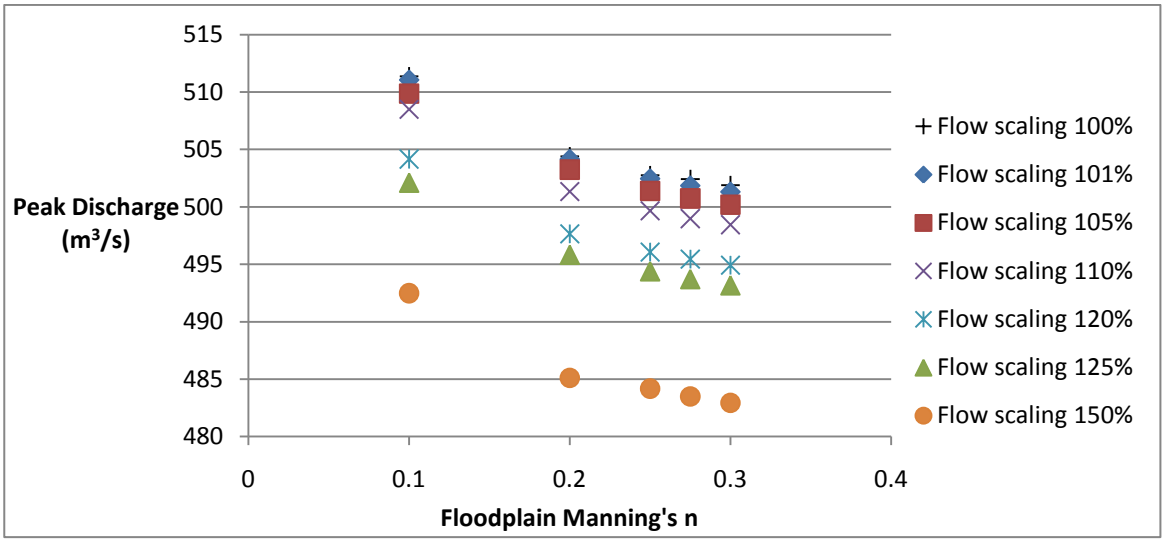

Figure 5.58 Change in peak discharge with floodplain Manning's *n* for each of the scaled and shifted flows using the 'half height levées' scenario. In addition to the scaling, flow has been shifted by 1 hr.

Figure 5.58 shows that peak discharge decreases with increasing floodplain roughness, with a difference of around 19 m^3/s between the 101% and 150% scaled and shifted flows at each of the Manning's *n* values. With a floodplain *n* of 0.1, peak discharge ranges from 511.1 m^3/s for the 101% scaled and shifted flow to 492.5 m^3/s for the 150% scaled and shifted flow. With a floodplain *n* of 0.3, peak discharge ranges from 501.3 m^3/s for the 101% scaled and shifted flow to 482.9 m^3/s for the 150% scaled and shifted flow. As with Figure 5.57, the peak discharges for the 'half height levées' scenario are about 1 m^3/s less

than the 'with levées' scenario and 20 m^3/s larger than 'without levées'. Table 5.16 displays the values for peak discharge produced after conducting simulations using the 'half height levées' scenario and varying both Manning's *n* and flow.

Manning's *n* / Flow Scaling (%)	**101**	**105**	**110**	**120**	**125**	**150**
Channel *n* = 0.08	419.7	419.0	417.1	412.0	409.4	400.4
Channel *n* = 0.09	416.6	415.1	413.1	408.2	406.6	394.4
Channel *n* = 0.1	410.1	409.1	407.5	404.3	403.5	395.8
Floodplain *n* = 0.1	511.1	509.9	508.5	504.2	502.1	492.5
Floodplain *n* = 0.2	504.2	503.2	501.3	497.7	495.8	485.1
Floodplain *n* = 0.25	502.5	501.4	499.7	496.1	494.4	484.2
Floodplain *n* = 0.275	501.8	500.7	499.0	495.5	493.7	483.5
Floodplain *n* = 0.3	501.3	500.2	498.5	494.9	493.2	482.9

Table 5.16 Statistics for each simulation varying both Manning's *n* for the channel and floodplain and flow (scaled and shifted) using the 'half height levées' scenario. In addition to the scaling, flow has been shifted by 1 hr.

5.5.6 Effect on hydrograph with changes to roughness – added height levées

Figure 5.59 shows that the 'added height levées' scenario gives similar results to that of the 'half height levées' scenario, although peak discharges are slightly higher for the 'added height levées' scenario. Peak discharge ranges from 423.6 m^3/s to 410.9 m^3/s for the flow scaled by 101% and between 398.7 m^3/s and 396.4 m^3/s for the flow scaled by 150%. Overall peak discharge for the 'added height levées' scenario is approximately the same as for the 'with levées' scenario and 20 m^3/s larger than the 'without levées' scenario.

Figure 5.60 shows that peak discharge decreases with increasing floodplain roughness, with a difference of around 19 m^3/s between the 101% and 150% scaled and shifted flows at each of the Manning's *n* values. This is the same amount shown using the 'half height levées' scenario. With a floodplain *n* of 0.1, peak discharge ranges from 507.4 m^3/s for the 101% scaled and shifted flow to 488.5 m^3/s for the 150% scaled and shifted flow. With a

floodplain *n* of 0.3, peak discharge ranges from 497.8 m^3/s for the 101% scaled and shifted flow to 479.0 m^3/s for the 150% scaled and shifted flow. Table 5.17 displays the values for peak discharge produced after conducting simulations using the 'added height levées' scenario and varying both Manning's *n* and flow.

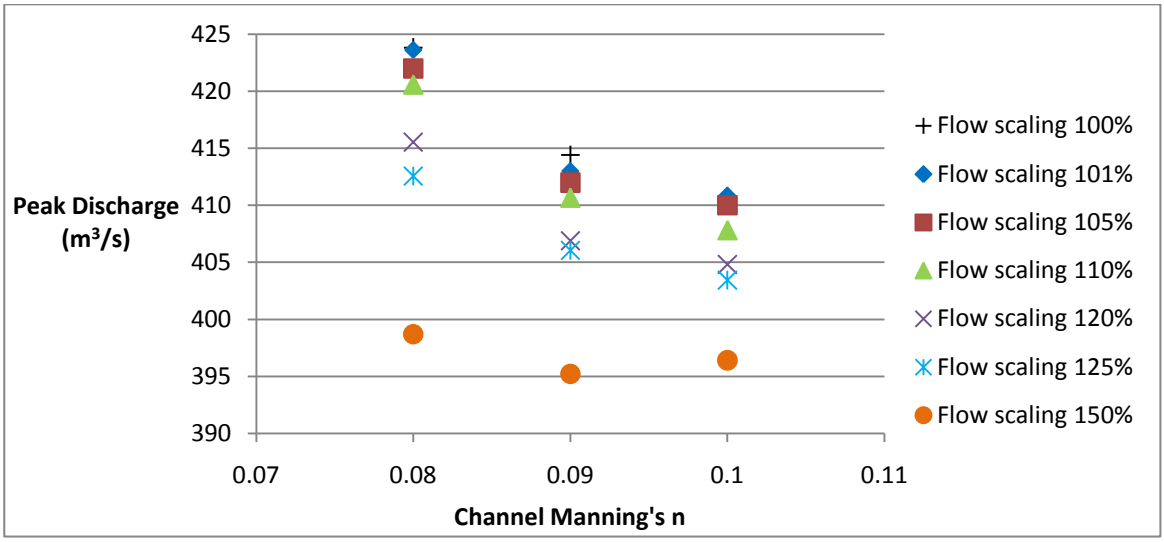

Figure 5.59 Change in peak discharge with channel Manning's *n* for each of the scaled and shifted flows using the 'added height levées' scenario. In addition to the scaling, flow has been shifted by 1 hr.

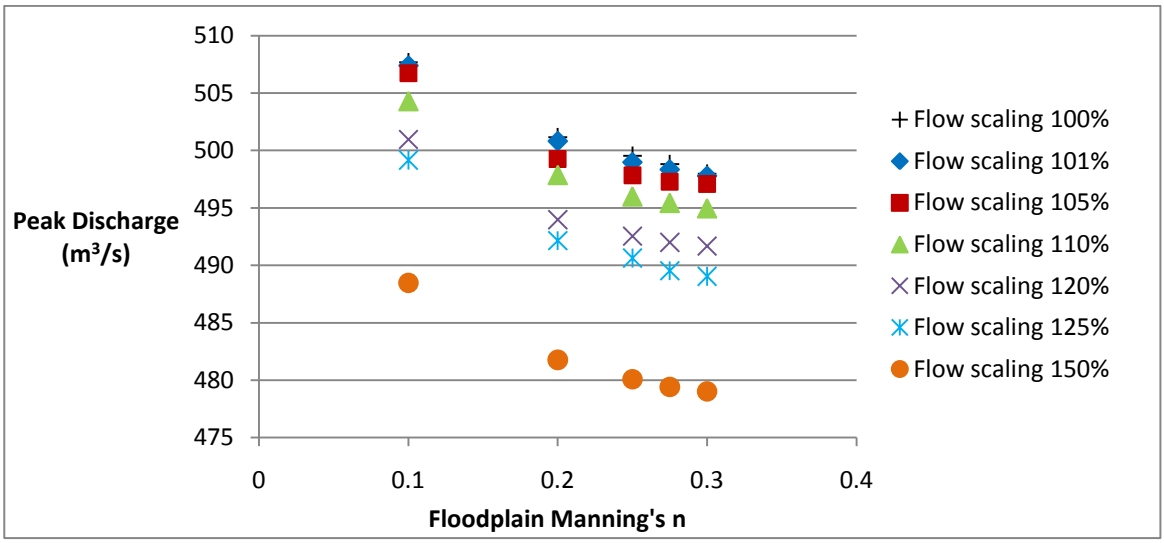

Figure 5.60 Change in peak discharge with floodplain Manning's *n* for each of the scaled and shifted flows using the 'added height levées' scenario. In addition to the scaling, flow has been shifted by 1 hr.

Manning's *n* / Flow Scaling (%)	100	105	110	120	125	150
Channel *n* = 0.08	423.6	422.0	420.6	415.5	412.6	398.7
Channel *n* = 0.09	413.0	412.0	410.7	406.9	406.1	395.2
Channel *n* = 0.1	410.9	410.0	407.8	404.8	403.4	396.4
Floodplain *n* = 0.1	507.4	506.7	504.3	501.0	499.2	488.5
Floodplain *n* = 0.2	500.8	499.3	497.9	494.0	492.2	481.8
Floodplain *n* = 0.25	499.0	497.8	496.0	492.5	490.6	480.1
Floodplain *n* = 0.275	498.4	497.3	495.5	492.0	489.5	479.4
Floodplain *n* = 0.3	497.8	497.1	495.0	491.7	489.0	479.0

Table 5.17 Statistics for each simulation varying both Manning's *n* for the channel and floodplain and flow (scaled and shifted) using the 'added height levées' scenario. In addition to the scaling, flow has been shifted by 1 hr.

5.5.7 Influence of the changes on peak discharge

Figure 5.61 illustrates how the different simulations conducted affect peak discharge recorded at the downstream boundary of the model. Scaling the flow by 101% for the 'with levées' scenario (1) gives a peak discharge of 526.2 m^3/s compared to 519.3 m^3/s for the 'without levées' scenario, a difference of 6.9 m^3/s. Shifting the flow by 1 hour (2) decreases the peak discharge slightly more for both scenarios, to 522.1 m^3/s with the levées and 515.1 m^3/s without the levées. Using the 101% scaled and shifted flow (3) increased the peak discharge to 524.0 m^3/s with the levées and 517.3 m^3/s without the levées. A Manning's *n* of 0.1 for the floodplain (4) reduces the peak discharge to 512.4 m^3/s with the levées and 506.1 m^3/s without. Using this value for floodplain *n* and the 101% scaled and shifted flow (5) gives a discharge of 514.2 m^3/s with the levées and 508.0 m^3/s without the levées. Increasing the floodplain *n* value to 0.3 (6) decreases the peak discharge to 502.6 m^3/s with the levées and 496.6 m^3/s without. Adding the scaled and shifted flow (7) increases the peak discharge to 504.4 m^3/s with the levées and 498.2 m^3/s without. Peak discharge reduces overall due to the increased value for floodplain Manning's *n*. Using a Manning's *n* value of 0.1 for the channel (8) decreases the peak discharge even more to 411.1 m^3/s with the levées and 392.0 m^3/s without. Adding the

scaled and shifted flow (9) increases the peak discharge very slightly to 411.6 m^3/s with the levées and 392.7 m^3/s without.

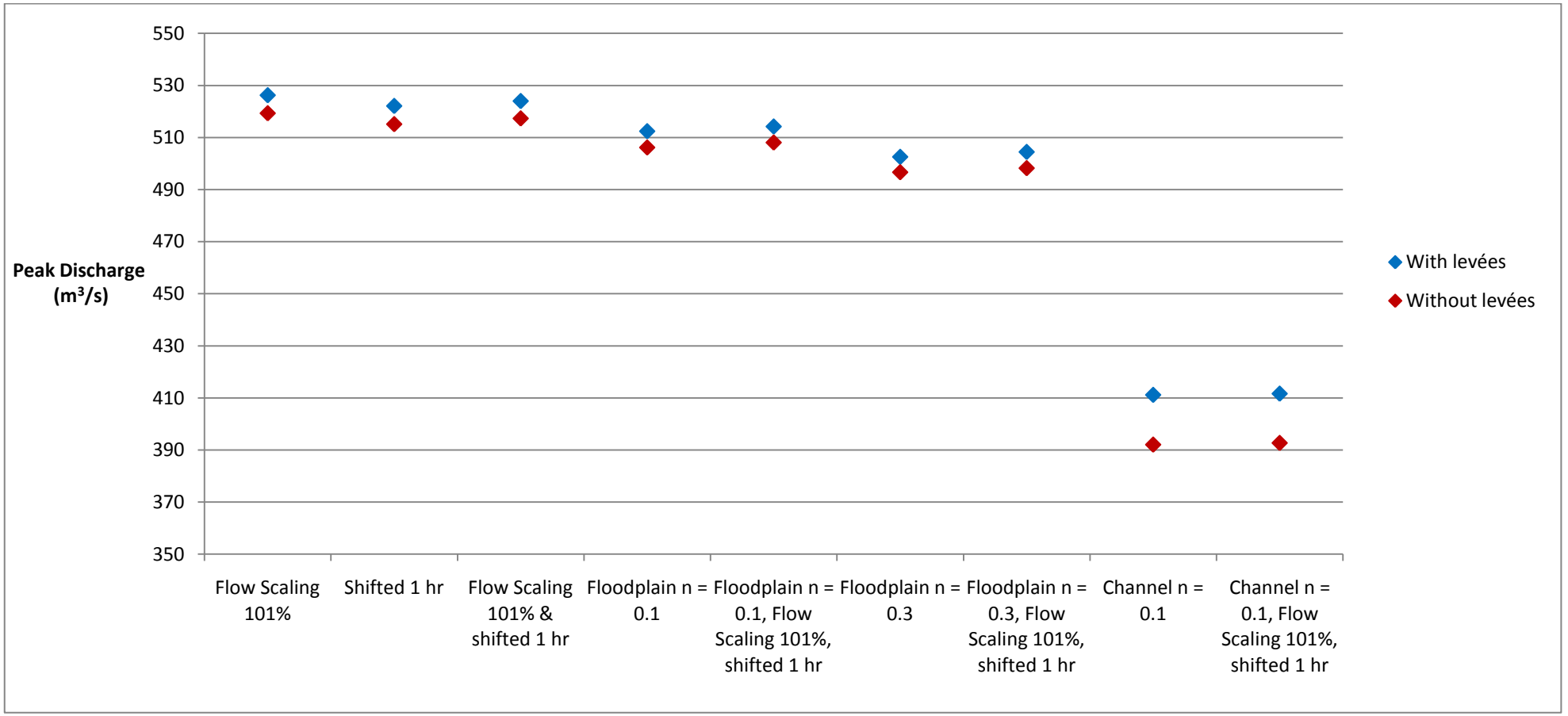

Figure 5.61 Comparing the peak discharge for each variation using the 'with levées' and 'without levées' scenarios. (1) scaling the flow by 101%; (2) shifting the flow by 1 hour; (3) scaling the flow by 101% and shifting the flow by 1 hour; (4) original flow used with a floodplain *n* of 0.1; (5) floodplain *n* of 0.1 and scaling the flow by 101% and shifting the flow by 1 hour; (6) original flow used with a floodplain *n* of 0.3; (7) floodplain *n* of 0.3 and scaling the flow by 101% and shifting the flow by 1 hour; (8) original flow used with a channel *n* of 0.1; (9) channel *n* of 0.1 and scaling the flow by 101% and shifting the flow by 1 hour.

Figure 5.62 illustrates the changes to peak discharge as a result of the flow scaled by 110%. Scaling the flow by 110% (1) for the 'with levées' scenario gives a peak discharge of 524.2 m^3/s compared to 517.9 m^3/s without the levées. This is a reduction of approximately 2 m^3/s compared to the scaling of 101%. With the 110% scaled and shifted flow (3), peak discharge reduced by another 2 m^3/s compared to Figure 5.61, decreasing to 521.6 m^3/s with the levées and 515.2 m^3/s without the levées. After combining the floodplain *n* of 0.1 and the 110% scaled and shifted flow (5), discharge is reduced to 511.8 m^3/s with the levées and 506.1 m^3/s without the levées. This is a decrease of 2 m^3/s from using the 101% scaled and shifted flow. Increasing the floodplain *n* value to 0.3 and using the 10% scaled and shifted flow (7) gives peak discharges of 501.9 m^3/s with the levées and 496.2 m^3/s without the levées. This is a reduction of approximately 2 m^3/s from using the 101% scaled and shifted flow. Using a channel *n* value of 0.1 and using the 110% scaled and shifted flow (9) gives peak discharges of 406.5 m^3/s with the levées and 391.0 m^3/s without. This is a reduction of 5 m^3/s with the levées and 2 m^3/s without the levées.

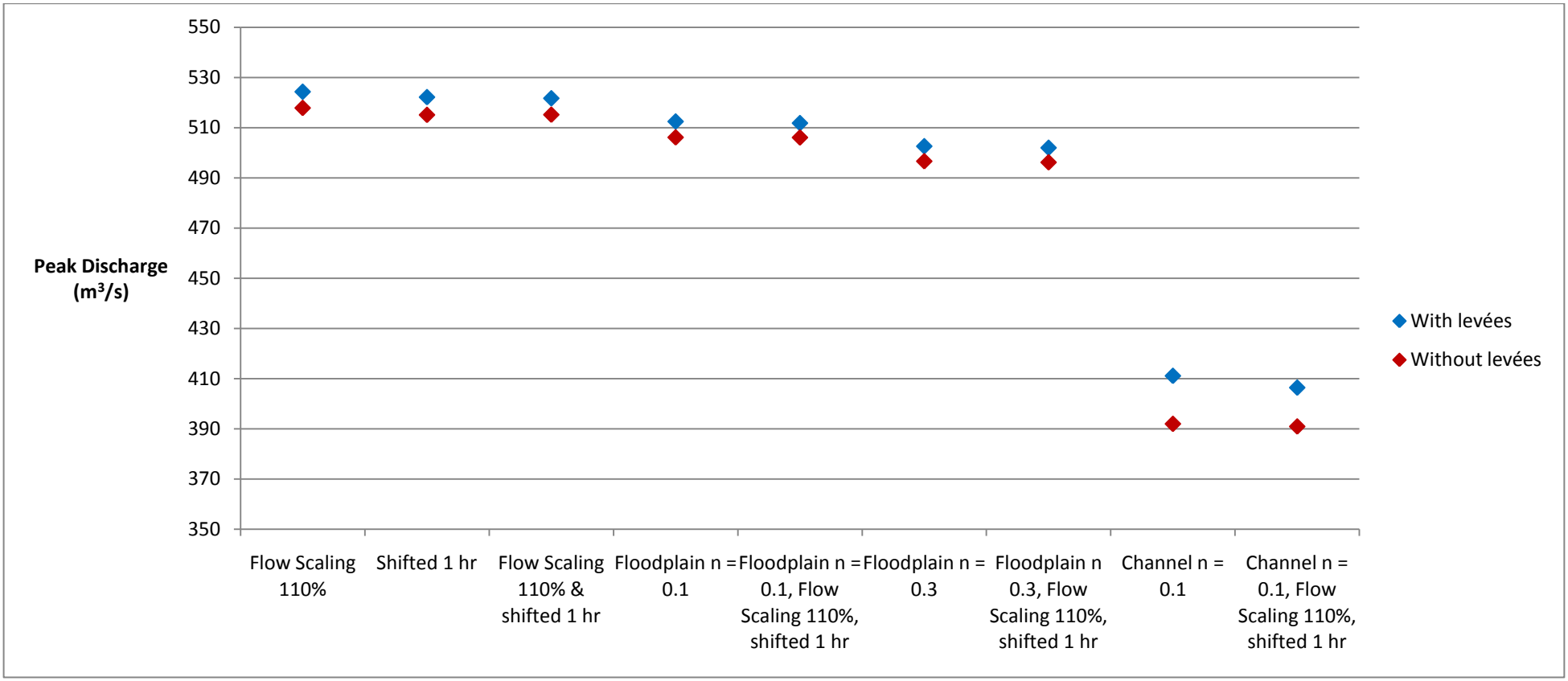

Figure 5.62 Comparing the peak discharge for each variation using the 'with levées' and 'without levées' scenarios. (1) scaling the flow by 110%; (2) shifting the flow by 1 hour; (3) scaling the flow by 110% and shifting the flow by 1 hour; (4) original flow used with a floodplain *n* of 0.1; (5) floodplain *n* of 0.1 and scaling the flow by 110% and shifting the flow by 1 hour; (6) original flow used with a floodplain *n* of 0.3; (7) floodplain *n* of 0.3 and scaling the flow by 110% and shifting the flow by 1 hour; (8) original flow used with a channel *n* of 0.1; (9) channel *n* of 0.1 and scaling the flow by 110% and shifting the flow by 1 hour.

Figure 5.63 shows that scaling the flow by 150% (1) reduces the peak discharge quite considerably, to 522.1 m^3/s with levées and 507.5 m^3/s without levées. Using the 150% scaled and shifted flow (3) reduces the discharge further to 507.9 m^3/s with levées and 503.0 m^3/s without levées. Combining a change in Manning's *n* of the floodplain to 0.1 and the 150% scaled and shifted flow (5) reduces the peak discharge to 498.1 m^3/s with the levées and 494.0 m^3/s without. In comparison to using the same value for Manning's *n* and 101% scaled and shifted flow, this is a reduction of 16.2 m^3/s and 14.0 m^3/s with and without the levées, respectively. Increasing the floodplain *n* value to 0.3 and using the 150% scaled and shifted flow (7) gives peak discharges of 486.9 m^3/s with the levées and 483.3 m^3/s without the levées. This is a reduction of approximately 15 m^3/s and 13 m^3/s from using the 110% scaled and shifted flow. Using a channel *n* value of 0.1 and using the 150% scaled and shifted flow (9) gives peak discharges of 398.7 m^3/s with the levées and 378.5 m^3/s without. This is a reduction of 7.7 m^3/s with the levées and 12.4 m^3/s with the levées from using the 110% scaled and shifted flow. Appendix Four shows the hydrographs produced for each of the variations presented in Figures 5.61 to 5.63.

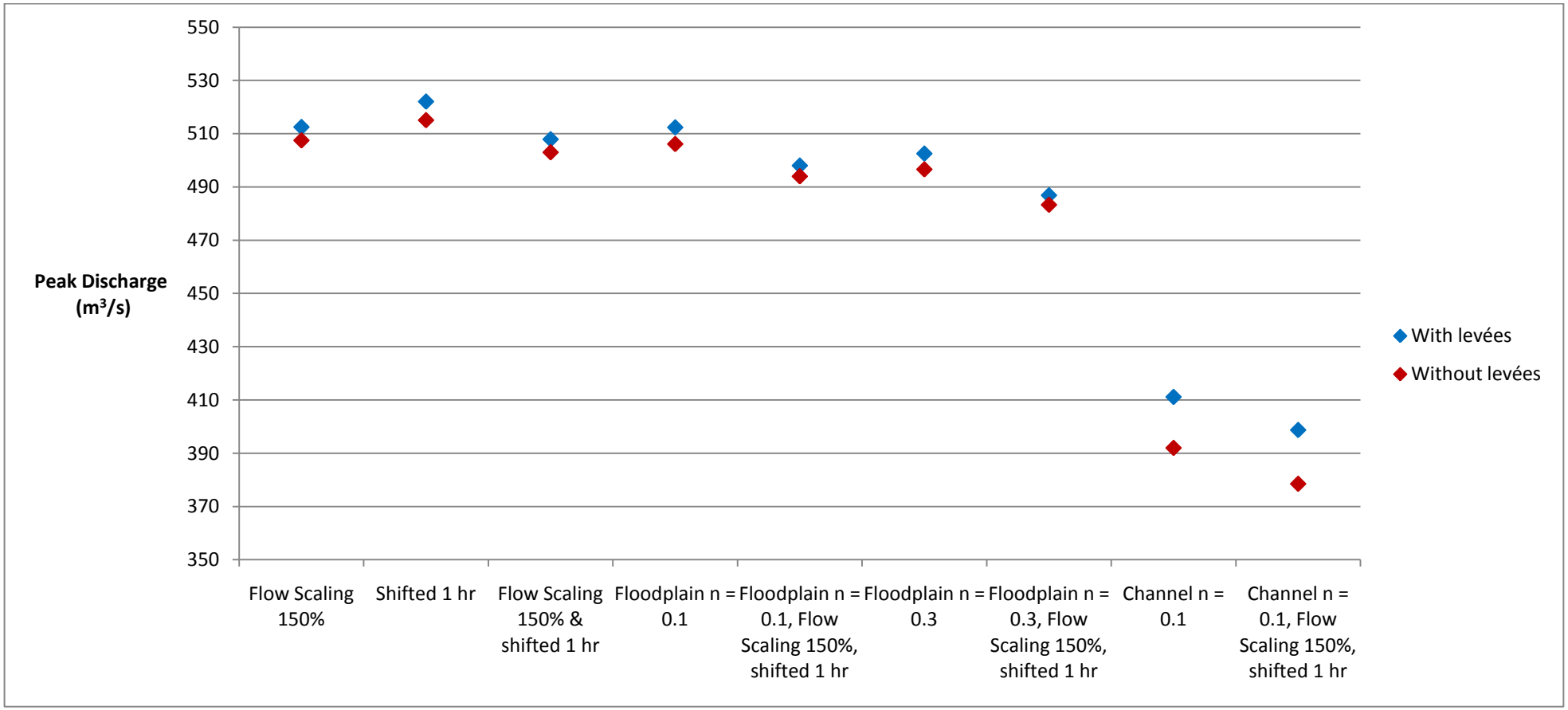

Figure 5.63 Comparing the peak discharge for each variation using the 'with levées' and 'without levées' scenarios. (1) scaling the flow by 150%; (2) shifting the flow by 1 hour; (3) scaling the flow by 150% and shifting the flow by 1 hour; (4) original flow used with a floodplain *n* of 0.1; (5) floodplain *n* of 0.1 and scaling the flow by 150% and shifting the flow by 1 hour; (6) original flow used with a floodplain *n* of 0.3; (7) floodplain *n* of 0.3 and scaling the flow by 150% and shifting the flow by 1 hour; (8) original flow used with a channel *n* of 0.1; (9) channel *n* of 0.1 and scaling the flow by 150% and shifting the flow by 1 hour.

5.5.8 Comparison of the four levée scenarios

Figures 5.64 and 5.65 summarise the different simulations carried out for each of the four scenarios. Figure 5.64 shows that channel *n* has the biggest influence on peak discharge in each of the scenarios. Shifting the input hydrograph by 1 and 2 hours reduced the peak discharge more than did the 101% scaled and shifted flow. However, the 150% scaled and shifted flow decreased the peak discharge by a larger degree.

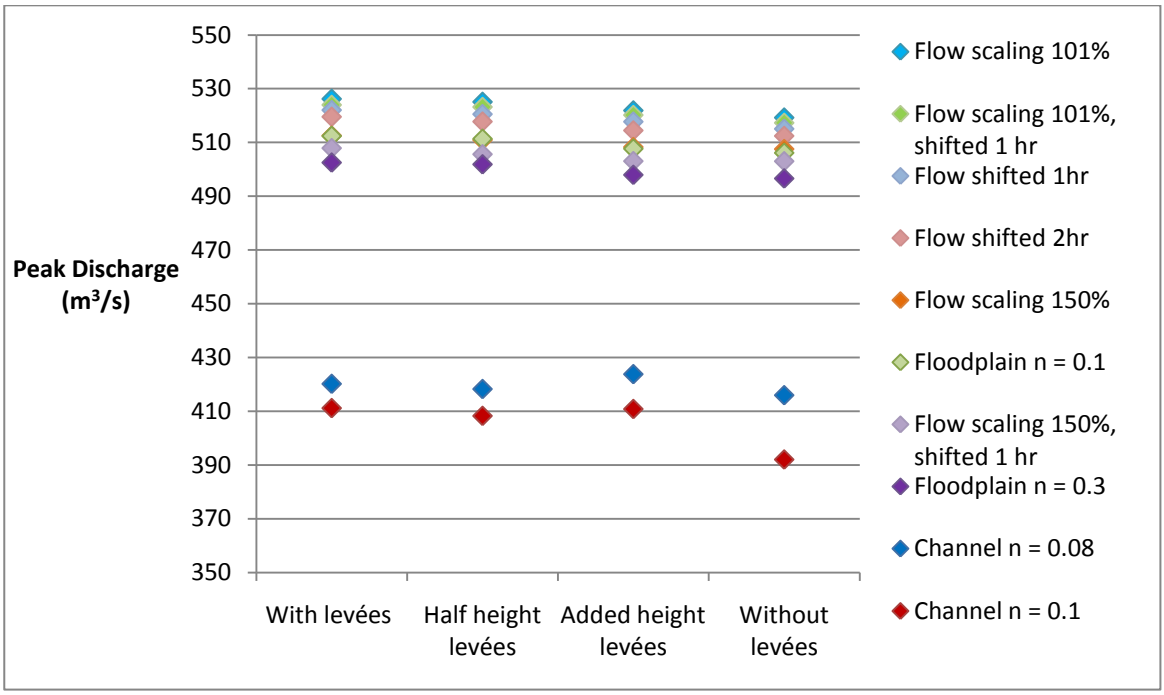

Figure 5.64 Comparisons of the effects of varying (1) Manning's *n*; (2) scaled flow; (3) shifted flow; and (4) scaled and shifted flow for each of the levée scenarios.

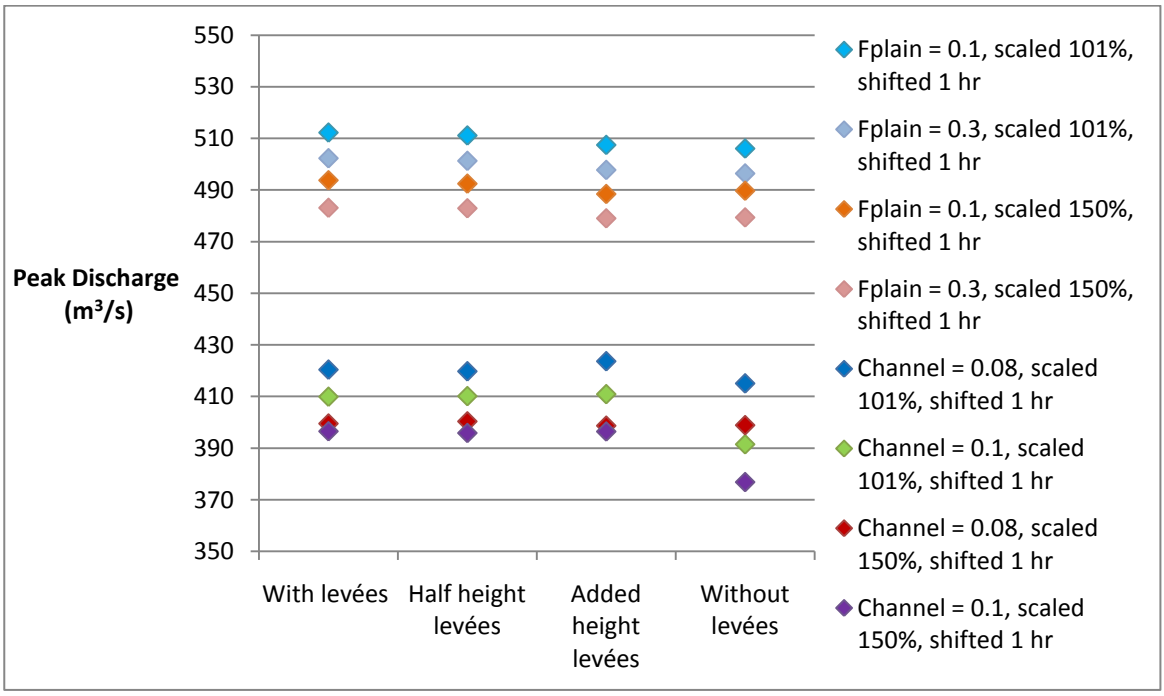

Figure 5.65 Comparisons of the effects of varying Manning's *n* and the scaled and shifted flows for each of the levée scenarios.

Figure 5.65 shows the peak discharge output from the model when the variations to Manning's *n* were used with the scaled and shifted flows. All of the simulations involving floodplain *n* showed the same trend, with peak discharge decreasing gradually between scenarios. The highest peak discharges were seen using the 'with levées' scenario, followed by 'half height', 'added height', and 'without levées' scenarios. Setting the floodplain *n* to 0.1 and using the scaled and shifted 101% flow reduced the peak discharge by the least amount. Changing the Manning's *n* of the channel had a different effect. Peak discharge reduced in the same way between scenarios as described using the floodplain *n*, but peak discharge was highest for all the simulations using the 'added height levées' scenario. Peak discharge was reduced the most across all simulations using the 'without levées' scenario.

5.6 Conclusion

This chapter has shown that varying levée height does have an impact on the peak discharge recorded. Removing the levées completely reduces peak discharge by the greatest amount. The model is very sensitive to channel Manning's *n*, reducing peak discharge dramatically as Manning's *n* increases, but changes in floodplain *n* reduce peak discharge to a lesser extent. Scaling and shifting the flow in order to simulate the effects

of blocked grips reduces peak discharge. Combined the scaling and shifting of the flow with the removal of levées and increases in channel Manning's *n* has the most impact on peak discharge reduction. Peak timing is delayed more with the levées in place than without the levées included in the model. This result was unexpected and will be discussed further in Chapter Six.

Chapter Six

Simulation: Discussion

6.1 Introduction

Following the presentation of the results of the HEC-RAS modelling in Chapter Five, Chapter Six discusses the results with reference to current knowledge in flood management and the findings of previous relevant studies. As with Chapter Five, this chapter uses the framework of the three research questions. Section 6.2 illustrates how removing levées can aid flood risk reduction. Section 6.3 discusses the interaction between signals from grip blocking and flow attenuation, whilst Section 6.4 assesses the impact of levées on the propagation of the upstream hydrograph. The implications for flood management are concluded in Section 6.5.

6.2 Research Question 1 – In what way can the floodplain be used to reduce flood risk downstream?

Table 6.1 summarises the main results from the HEC-RAS modelling. The simulations are based on the York flood event of 2000 and therefore the values discussed are with reference to this sized event. Peak discharge reduces by 1.3% after removing the levées, demonstrating that restoring the connection between channel and floodplain alone only has a small influence in terms of reducing flood risk (Lane and Thorne, 2007; Sholtes, 2009). Although the reduction is minimal, the result confirms the understanding in the literature that by storing flood water on the floodplain, this water no longer contributes to flood volumes and flood risk is reduced (Blackwell and Maltby, 2005). In Chapter One flood risk was defined as:

Risk = probability x exposure x consequence

Lowering the peak discharge was the focus of this study because this will reduce the probability of the hazard occurring and reduce exposure to it. Larger reductions in peak discharge were found at upstream cross-sections in the model (2.8% at cross-section 982 and 2.6% at cross-section 938 – Table 6.1), suggesting that the positive impact of removing the levées, in terms of decreasing the flood peak, is dissipated as the flood wave propagates downstream. However, Leopold (1994) suggested that even a fairly small reduction in the flood peak resulting from the removal of levées could be highly effective for reducing losses, although this depends on the relationship between discharge and inundation downstream.

			Peak reduction (%)			
			With levées	Half height levées	Added height levées	Without levées
RQ1	Original flow – x-sec 902		-	0.2	0.7	1.3
	Original flow – x-sec 982		-	-	-	2.8
	Original flow – x-sec 938		-	-	-	2.6
	Channel *n* = 0.1	All tributaries	25.9	28.4	27.6	32.4
		Ouse	28.0	-	-	33.7
		Swale	7.1	-	-	8.6
	(*n* = 0.09 here as 0.1 unstable)	Nidd	2.0	-	-	3.3
	Floodplain *n* = 0.3	All tributaries	4.3	4.4	5.3	5.6
		Ouse	4.3	-	-	5.6
		Swale	0.0	-	-	1.3
		Nidd	1.5	-	-	0.2
RQ2/RQ3	Flow Scaling 150%		2.3	2.6	3.1	3.33
	Shifted 1 hr		0.4	0.7	1.2	1.8
	Flow Scaling 150%, shifted 1 hr		3.2	3.7	4.2	4.2
RQ3	Channel *n* =0.08	Flow Scaling 101%, shifted 1 hr	24.7	24.9	23.8	26.3
		Flow Scaling 150%, shifted 1 hr	31.2	30.9	31.5	31.4
	Channel *n* = 0.1	Flow Scaling 101%, shifted 1 hr	27.9	27.8	27.6	33.9
		Flow Scaling 150%, shifted 1 hr	32.2	32.4	32.2	39.1
	Floodplain *n* = 0.1	Flow Scaling 101%, shifted 1 hr	2.3	2.6	3.3	3.6
		Flow Scaling 150%, shifted 1 hr	6.2	6.4	7.3	7.0
	Floodplain *n* = 0.3	Flow Scaling 101%, shifted 1 hr	4.4	4.6	5.3	5.6
		Flow Scaling 150%, shifted 1 hr	8.5	8.5	9.4	9.4

Table 6.1 Peak reductions after varying Manning's *n*, levée height and flow in relation to each of the research questions. The percentage change in peak reduction is relative to the original modelled output with the levées included in the model. No data are included in the table under research question 1 (with levées) as these are the baselines for the comparisons.

Once the levées were removed, the peak occurred 0.5 hours later than with the levées in place (Table 6.2). This trend matches the current understanding of flood water storage; storage of water on the floodplain where conveyance is slower reduces the velocity of flow thus translating the flood hydrograph (Morris *et al.*, 2003). However, the focus of levée removal is usually the reduction of peak discharge rather than the timing of the flood peak (Akanbi and Singh, 1997; Acreman *et al.*, 2003). The peak timing is delayed less at the downstream boundary than at upstream cross-section locations, where the peak is delayed by 1.25 hours (Table 6.2), due to the suggested dissipating effects of the large distances involved in the Ouse system.

			Peak timing delay (hr)	
			With levées	Without levées
RQ1	Original flow – x-sec 902		-	0.5
	Original flow – x-sec 922-955		-	1.25
	Channel *n* = 0.1	All tributaries	23	20
		Ouse	5	4
		Swale	0	0
	(*n* = 0.09 here as 0.1 unstable)	Nidd	5	5
	Floodplain *n* =0.3	All tributaries	2	2
		Ouse	0	0
		Swale	0	0
		Nidd	2	2
RQ2/RQ3	Flow Scaling 150%		1.75	1.25
	Flow Scaling 150%, shifted 1 hr		2	1.5
RQ3	Channel *n* = 0.1	Flow Scaling 150%, shifted 1 hr	9	9.75
	Floodplain *n* = 0.3	Flow Scaling 150%, shifted 1 hr	2	1.5

Table 6.2 Peak timing delay after varying Manning's *n*, levée height and flow in relation to each of the research questions. The change in peak timing is relative to the original modelled output

with the levées included in the model. No data are included in the table under research question 1 (with levées) as these are the baselines for the comparisons.

Reducing thevlevées to half their original height caused the peak discharge to decrease by 0.2% (Table 6.1). Although this is a very small change it illustrates how changing the geometry of the levées in the system can vary the propagation of the flood peak downstream. Increasing the height of the levées by an extra 0.5 m reduced the peak discharge by 0.7% (Table 6.1). The extra height of the levées does not increase peak discharge as might be expected. These results are complex and relate to the floodplains having two effects:

(a) storage (i.e. taking water off the hydrograph) – beneficial close to York

(b) slowing flow (attenuation) – beneficial upstream

The reduction in peak discharge by both lowering and raising levée height can be explained by two counteracting processes (Figure 6.1). First, when the levée height is reduced, more water is transferred onto the floodplain and the transfer occurs earlier, causing an increase in attenuation. Second, increasing the height of the levées retains more water in the channel so less attenuation occurs. But, crucially, increasing the levée height increases the likelihood that only the peak of the flow is taken off. Storage is also used later, countering the effects of the decreased attenuation. Thus, when levée height is increased storage dominates over attenuation. The results imply that both increasing and decreasing levée height could decrease peak discharge.

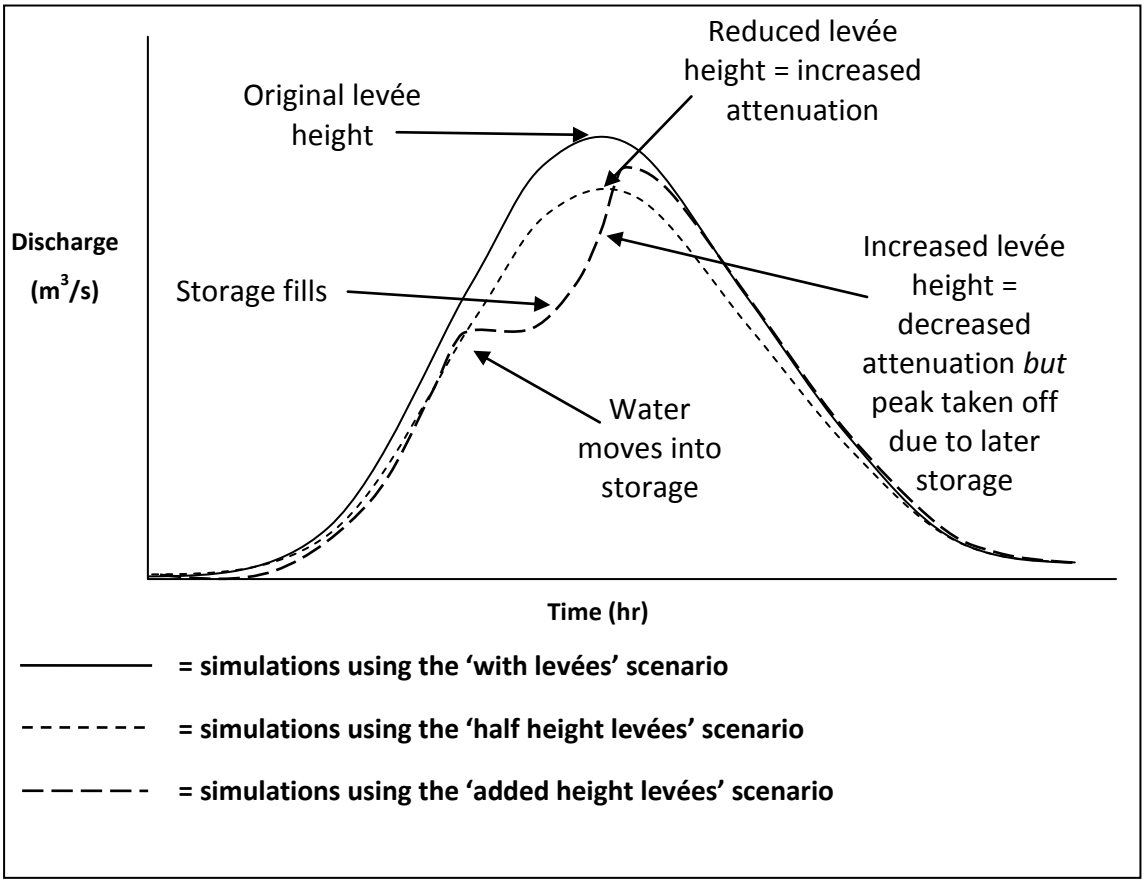

Figure 6.1 Effect of raising and reducing levée heights in the system on the flood hydrograph.

6.2.1 Varying Manning's *n* for the levée scenarios

Table 6.1 shows the influence of Manning's *n* on the system, under each levée scenario. By varying channel *n* values for each of the levée scenarios it was possible to demonstrate which scenario had the greatest potential to reduce flooding downstream at York. Increasing Manning's *n* values for the channel to 0.1 reduces peak discharge quite dramatically for both scenarios; by 25.9% with levées and by 32.4% without levées (Table 6.1). This is expected, as a higher Manning's *n* value for the channel slows the flow, increases water levels and the water flux to the floodplain, allowing floodplain roughness to exert a greater influence on peak discharge and travel times (Hunter *et al.*, 2006). Peak discharge is reduced more without the levées as the restored connection between channel and floodplain allows water to move freely onto the floodplain, and thus more water is affected by floodplain roughness (Hunter *et al.*, 2006). The same process explains why reducing the levées to half height with a channel roughness of 0.1 reduces the peak discharge by 28.4%, which is larger than with the original levée height (Table 6.1). Raising the height of the levées and applying a channel *n* of 0.1 reduces the peak discharge by 27.6%, which is less than when using the half height levées (Table 6.1). This may result

from swamping of the model (where the modelled water surface elevation exceeds the input topography elevation) due to the high volume of water in the channel. At very high Manning's *n* values, attenuation becomes dominant for all levée heights, especially the lower levée heights. As illustrated in Figure 5.1 and described by Morris *et al.* (2003), floodplain inundation increases when the levées are removed and channel *n* is increased, whilst downstream flood risk is alleviated. However, increasing floodplain roughness is preferred to channel roughness as it can be achieved more easily. It must be noted that an increase in channel roughness to 0.1 may not be deliverable because increases in Manning's *n* tend to be hard to achieve in very large rivers such as the Ouse (Chow, 1959).

Modelling the effect of floodplain vegetation by increasing Manning's *n* to 0.3 reduces peak discharge but to a lesser extent, as the model is most sensitive to channel roughness (Chapter Four). The peak is reduced by 4.3% with levées and 5.6% without levées (Table 6.1). This shows the effectiveness of removing the levées, as floodplain roughness exerts more friction on the flow, increasing attenuation. The reduction of peak discharge after removing the levées again suggests that restoring the channel-floodplain connection is crucial for the aim of reducing flood peaks in the Ouse system. Reducing the levées to half height, with an increase in floodplain *n* to 0.3, reduces peak discharge by 4.4%, a small amount more than with the levées, as the attenuation effects are greater (Table 6.1). Raising the levées reduced the peak discharge by quite a large amount, 5.3% (Table 6.1). Using a high floodplain roughness does reduce peak discharge, but for the Ouse catchment these levels are not as high as some previous studies. For example, Woltenmade and Potter (1994) increased floodplain roughness to 0.064 and peak discharge reduced by up to 21%. However, the results are similar to those of Turner-Gillespie *et al.* (2003) where increases of floodplain roughness to 0.07 decreased peak discharge by 3%, very similar to this study (with floodplain *n* of 0.07, a reduction of 2.07% was produced with levées, and 3.38% without the levées). The reduction in peak discharge caused by Manning's *n* depends on catchment and floodplain characteristics. In contrast to the majority of the literature, the smaller reductions in peak discharge found here may be a result of the high magnitude and duration of the 2000 event modelled; Archer (1989) showed that attenuation effects of Manning's *n* diminish at high flow peaks and volumes. Many previous studies have focused on small to moderate floods, where for example Diehl (1990) showed that peak discharge was reduced by up to 27%. Although

the reduction in peak discharge is smaller than reported in some studies, the results illustrate that increasing floodplain roughness upstream could be an effective method for reducing flood peaks at York, but may be more valuable for small to moderate floods. However, using storage areas can achieve the same reduction in the flood peak over a short distance and thus is a more accessible method for reducing flood risk at York (Hornberger *et al.*, 1998). In addition, it is easier for flood engineers to manage discrete interventions such as storage areas (Lane *et al.*, 2007). Increasing channel roughness *and* floodplain roughness may be the most beneficial method of varying Manning's *n* to aid the reduction of peak discharges.

Peak timing is delayed by increasing channel *n* as conveyance is decreased, showing that the flood wave is sensitive to roughness (Hunter *et al.*, 2006). It was expected that by removing the levées the availability of the floodplains for storage would increase the translation of the flood wave (Morris *et al.*, 2004). However, contrary to reports in the literature, the peak occurs later with the levées in the system than without (Table 6.2). Without the levées the peak occurs earlier, which may be caused because, once the flows are attenuated by removing the levées, the effects of other processes (increases in Manning's *n* and grip changes) are also decreased. As the relationship between channel Manning's *n* and peak timing delay is unclear, the earlier timing of peak discharge may also suggest that, contrary to the suggestions in the literature, for large systems such as the Ouse, the translation effect (delay of the flood peak) expected as a result of using floodplains for storage (Leopold, 1994; McCartney and Naden, 1995; Whiting and Pomeranets, 1997; Hornberger *et al.*, 1998; Pepper *et al.*, 1998; Morris *et al.*, 2004; Blackwell and Maltby, 2005) is dissipated within the system. The peak occurs earlier with lower values of channel *n* as friction is reduced, thus conveyance is increased (Lane *et al.*, 2007). Increases in floodplain *n* increased peak timing delay (Table 6.2) but much less than for channel *n,* as the model is much less sensitive to floodplain roughness (Chapter Four). However, Anderson *et al.* (2006) recognised that the influence of floodplain roughness on flood wave timing varies with flood magnitude. So, crucially, the effectiveness of an intervention depends on the size of a flood. Thus, modelling of a smaller event than the 2000 event may show a larger delay in peak timing. Further investigation is needed in order to draw conclusions here in terms of lag times resulting from changes to Manning's *n* for each levée scenario.

6.2.2 Varying Manning's *n* for the Rivers Ouse, Swale and Nidd

The large reductions in peak discharge associated with increasing Manning's *n* for the River Ouse result from the high sensitivity of the model to the roughness of this reach. As the Ouse is the longest and widest reach in the model, its topography has the greatest effect on discharge. After increasing channel *n* to 0.1 for the River Ouse, peak discharge is reduced by 27.5% with the levées, showing that increasing Manning's *n* for this reach can dramatically decrease peak discharges at York (Table 6.1). A greater reduction in peak discharge of 33.7% is demonstrated by removing the levées (Table 6.1). The same reductions in peak discharge are found for the Ouse reach as with the whole model when floodplain roughness is increased to 0.3, suggesting that the topography of the River Ouse has a strong control on the flow in the entire catchment. Channel roughness of the Ouse has a greater influence on peak timing with the defences in place as the peak is delayed more than without the levées included (Table 6.2). This finding is contrary to that of Hunter *et al.* (2006) who stated that increasing channel roughness increases travel times of the peak. In addition, the finding that peak discharge is delayed more with levees is contrary to that of Nisbet and Broadmeadow (2003) and Thomas and Nisbet (2007) who suggested that storage on the floodplain should increase the time to the peak, thus the removal of defences enhances the translation of the flood peak as a result of the roughened channel. The opposite result found in this study may be due to the dissipating effects of such a large river system (as explained in Section 6.2.1). Floodplain roughness for the River Ouse does not affect peak timing as the model is not very sensitive to floodplain roughness (Table 6.2).

Increasing channel *n* of the Swale to 0.1 decreases the peak discharge but only by 7.1%, much less than the River Ouse (Table 6.1). This suggests that although channel roughness of the Swale does affect flow, its influence is not very strong because its cross-sectional area is much smaller than that of the Ouse. Removing the levées reduces the peak discharge further by 8.6% (Table 6.1), again illustrating that the levées have an impact on flow in the system (Buijse *et al.,* 2002; Acreman *et al.,* 2003). With the levées present, increasing floodplain roughness to 0.3 does not affect peak discharge, whilst removing the levées reduces the peak discharge by 1.3% (Table 6.1). Thus, varying roughness in the Swale is a less effective method for reducing flow at York than varying that of the Ouse.

The results for the Nidd may have been affected by small instabilities present along this reach in the model. Peak discharge does not decrease gradually with increasing Manning's *n* for the Nidd channel. Most instabilities were removed by increasing the density of cross-sections along the Nidd (Chapter Three). However, the model remained unstable when computing high Manning's *n* values along the Nidd reach. Increasing channel *n* to 0.1 decreased peak discharge by 2.0% with the levées and 3.3% without levées (Table 6.1) showing that channel roughness does influence peak discharge, as with the Ouse and Swale, but to a much smaller extent. The large influence of roughness on peak discharges and peak timing delay along the Nidd must be viewed with caution as the Nidd demonstrated the smallest sensitivity to roughness in Chapter Four.

6.3 Research Question 2 – To what extent are land management signals impacted upon by flow attenuation?

This section explores the impact of the scaled flows on the Ouse system with the current defences in place. For the levée scenarios, using a high level of scaling (120% to 150%) reduces the peak discharge by a small amount. The scaling of the hydrographs was designed to represent the attenuation of the flood peak expected from blocking grips upstream (Environment Agency, 2000). Scaling the flow by 150% (an extreme level of scaling) reduces the peak discharge by 2.3% (Table 6.1). When running the scaled hydrographs, the peak discharge recorded at each cross-section within the model varies quite considerably. Figure 5.33 shows that the peak discharges at cross-section 982 lie within a wide range of values indicating that the scaled flows have a large influence on the attenuation created within the model. However, further downstream the attenuation reduces, which suggests that the impact of scaled flows (and thus land use signals) dissipates as the flood wave travels downstream. With the levées in place, scaling the flow also increases peak timing delay (Table 6.2).

In addition to scaling the hydrographs in order to represent possible attenuation of the flood wave resulting from blocked grips, the hydrographs were also shifted in time to represent the expected delay in the peak caused by blocking grips. These two manipulations of the hydrograph were then combined to create the scaled and shifted hydrographs, representing the hypothetical effect of the grips. Table 6.1 shows that after scaling the flow by 150% and shifting the hydrograph by one hour, peak discharge is reduced by 3.2%. Therefore, by blocking grips there is some potential to reduce peak

discharges in the Ouse catchment with the current defences in place. However, the reduction in peak discharge is quite small. The scaled and shifted flow hydrographs reduce the peak discharge further than solely scaling the flow. Peak timing delay of the flood wave increases up to 2 hours (Table 6.2), again demonstrating that hypothetical grip blocking scenarios have the potential to both attenuate and translate flood waves along the River Ouse. In contrast, Lane *et al.* (2003b) found that blocking grips reduces travel times of water in the system. Modelling the expected influence of blocked grips in the Ouse catchment has demonstrated that their impact on flow is noticeable downstream despite intervening attenuation effects. However, even with the extreme levels of scaling tested here, the effects are not that significant.

6.4 Research Question 3 – Do flood levées aid the transmission of the upstream hydrograph?

6.4.1 Scaling the flow and varying levée heights

This section explores the impact of the scaled flows on the Ouse system after raising and reducing the height of the levées. Once the hydrographs were scaled, peak discharge was reduced more with the levées removed from the model, by 3.3% compared to 2.3% with the levées (Table 6.1). Figure 5.40 demonstrates that there is more sensitivity of peak discharge to scaling with the levées, suggesting that levées do make the grip effect more noticeable. However, the small reduction in peak discharge shows that the influence of the levées is not large. Peak discharge is higher with the levées, suggesting that the levées do transmit the flood signal further downstream to York because they reduce floodplain attenuation.

Similarly, Acreman *et al.* (2003) observed a large increase in peak flow as a result of levées. With a higher level of flow scaling, the change in discharge with levées is larger than without levées because the input flow has a larger influence on downstream recorded flow when the flow is contained with the levées (Acreman *et al.*, 2003). Similarly to research question 2, peak discharge reduces towards the downstream end of the model as flow is scaled with the levées, with the exception of the values at cross-section 902. As the values at the downstream boundary (cross-section 902) are higher, this again suggests that the impact of the scaled flow is dissipated as the flood wave propagates downstream. Once the levées were removed, peak discharges reduces at all locations in

the model when using the scaled flow hydrographs. This reduction in peak discharge again confirms that the levées along the River Ouse do influence the flood wave travelling to York; reconnecting the channel with the floodplain increases attenuation and reduces the grip blocking signal.

Peak timing is earlier without the levées (Table 6.2), as recognised earlier, and may be caused because a smaller volume of water is in contact with the channel, thus Mannning's *n* has less effect, so travel times can increase. Peak timing delay is increased with scaling of the flow (Figure 5.46) showing that blocking grips has the potential to increase travel times (as shown by Environment Agency (2000) and Lane *et al.* (2003a), although this is most effective at high levels of scaling.

6.4.2 Scaling and shifting the flow and varying levée heights

For each of the levée scenarios, the peak discharge reduces as scaling of the scaled and shifted flow is increased. Peak discharge reduces the least with the levées included, by 3.2% (Table 6.1), suggesting that the levées must channelise the flow, preventing the available floodplains from attenuating the flow (Acreman *et al.*, 2003). Lane (2008) suggested that if the levées in the Ouse catchment reduce the effects of attenuation, the flood magnitudes at York could increase. This thesis suggests that by restricting the available attenuation of the floodplains, levées enhance the transmission of the flood wave more readily downstream, increasing the risk of flooding at York, albeit by a small amount.

In comparison, removing the levées with the scaled and shifted flow reduced the peak discharge by 4.2% (Table 6.1). The increased reduction of the peak indicates the effectiveness of blocking the grips in the Ouse catchment for reducing peak discharge. Solely removing the levées reduced peak discharge by 1.3%, but combined with the hypothetical blocked grip scenarios (scaled and shifted flows) this could be increased to 4.2%. The increased reduction of the peak by the scaled and shifted flows is a crucial finding illustrating the possible value of blocking grips in the Ouse catchment for reducing the magnitude of flooding at York. In addition, removing some or all of the flood levées along the Ouse could increase the effectiveness of any revised flood management strategy. The effect of blocked grips appears to be translated downstream, especially in a defended floodplain, but the degree of impact of the land management practice depends

on the magnitude of the grip effects, and hence the degree of scaling if blocked. As this study has shown that blocking grips could reduce peak discharges quite dramatically, the sustainability of removing flood levées is enhanced because the combined effect could be much more effective than removing flood levées alone. Peak timing delay is increased after using the scaled and shifted flow without the levées, but to a lesser extent than with the levées (Table 6.2). The smaller timing delay without the levées again shows a trend contrary to that of the literature (e.g. Whiting and Pomeranets, 1997; Morris *et al.*, 2004). A crucial link between grip blocking and levées is demonstrated here: by increasing the attenuation created by blocked grips and removing the levées in the Ouse catchment, peak discharge downstream is decreased by 4.2%, reducing the flood risk at York.

6.4.3 Varying channel Manning's *n*, flow and levée heights

With the levées included in the model, peak discharge reduces with the scaled and shifted flow and whilst Manning's *n* is increased. The reduction in peak discharge is increased further to 32.2% with the levées after increasing channel *n* to 0.1 and using the 150% scaled and shifted flow (Table 6.1). This demonstrates that combining each scenario (as shown in Figure 5.1) could greatly help to reduce peak discharge and therefore flood risk downstream. Subsequently removing the levées from the model (after using the scaled and shifted 150% flow and a channel *n* of 0.1) had the greatest impact on peak discharge throughout the modelling reducing it by 39.1% (Table 6.1). Individually all of these scenarios have a large influence on discharge. Flood risk for the floodplains upstream of York could decrease as the overall discharge in the system is reduced, as shown in Figure 5.1. Thus, when combined, they could make a real difference to reducing flood risk. However, the uncertainties surrounding this method must be considered. For example, increasing channel *n* to 0.1 may be not possible for the Ouse due to its large size. In addition, the scaled and shifted flows used in this study are end members of possible grip blocking responses. Thus, the results here are over-estimates and must be interpreted with caution. The influence of channel roughness is much greater than that of the scaled flows, as Manning's *n* plays a large role in controlling the friction exerted on the flow (Hunter *et al.*, 2006), thus increasing attenuation. For example, with the levées present, increasing channel Manning's *n* to 0.1 reduces peak discharge by 25.9% compared to the 150% scaled and shifted flow which reduces peak discharge by 2.3% (Table 6.1). The reduction in peak discharge after halving the levée height is very similar to that with the

levées at full height: 32.4% compared to 32.2% respectively (Table 6.1). This suggests that halving the height of the levées does not reduce peak discharge as much as might be expected. The results are similar to the 'with levées' scenario reduction rather than half way between the 'with' and 'without' levées scenarios. Therefore, adjusting the levées in this way is not as effective as removing the levées completely for reducing flood risk.

6.4.4 Varying floodplain Manning's *n*, flow and levée heights

Increasing floodplain roughness and introducing the scaled and shifted flows also decreased peak discharge (Table 6.1). The influence of floodplain roughness is smaller, however, as the flood wave is less sensitive to changes in floodplain roughness than channel roughness. With the levées included, floodplain *n* set to 0.3 and the flow scaled by 150%, the peak discharge can be reduced by 8.5% (Table 6.1). This reduction can be increased to 9.4% without the levées as the floodplains increase the attenuation in the system (Table 6.1). Unusually, the peak discharge was reduced the most by the 'added height levées' scenario, to 9.4% (Table 6.1). When the levée height is increased, storage dominates over attenuation. Thus, in this case the reduction of the peak created by storage (added height levées scenario) is greater than the reduction caused by attenuation (without levées scenario), explaining why the reduction in peak discharge was greater after increasing levée height. As with varying channel *n* and the scaled and shifted flows, when the levées were reduced to half height the peak discharge reduction was very similar to that produced with the original levée heights at 8.5% (Table 6.1).

For both levée scenarios (with and without levées) peak timing is delayed by increasing both channel and floodplain roughness and using the scaled and shifted flows (Figures 5.57 and 5.60). The peak timing is much later for increases in channel *n* as the model is most sensitive to channel roughness. Peak timing is later for the 150% scaled and shifted flow as would be expected, until channel *n* is increased to 0.1 where the 150% scaled flow produced the smallest lag time (Table 6.2). This may result from small instabilities created by the high Manning's *n* value. The influence of both Manning's *n* and the scaled and shifted flows is smaller without the levées, creating a smaller delay in peak timing as discovered in research question 1.

6.4.5 Reducing peak discharge below a threshold

Throughout this study the aim has been to investigate the extent to which the flood peak at York could be reduced by changing the flood management strategy for the Ouse catchment. It has shown that the levées lining the River Ouse do make the grip effect more noticeable, and thus by removing the levées and blocking grips in upland catchments the flood peak at York can be reduced. The reduction in the peak is fairly small, but if peak discharge is taken below a threshold, could reduce flood risk dramatically. If, for example, the peak flow could be reduced to bankfull discharge, the simulations used in this study could reduce flooding considerably for York. The bankfull discharge of a river is the discharge that fills the channel to the level of the floodplain (Chorley *et al.*, 1984). This varies between rivers but is generally considered to occur with an average return period of two years (Wolman and Leopold, 1957; Dury, 1961; Richards, 1982 ; Chorley *et al.*, 1984). Q_2 (2 year flood) was found to be 361.99 m^3/s for the Ouse using a magnitude-frequency plot. This is much lower than peak discharges simulated for the 2000 event. Thus, the peak discharge could not be taken below this threshold using the modifications explored here.

However, some simulations in the investigation reduced the peak discharge below peak flow associated with the 25 year return period (503.2 m^3/s). The peak flow return period for the 2000 event at Skelton was 25 to 50 years. Removing the levées from the model and running the scaled and shifted 150% flow reduced the peak discharge to 503.0 m^3/s, just below the flow for the 25 year return period. Furthermore, by also introducing the influence of floodplain roughness on the flow peak discharge could be reduced further. With a floodplain roughness of 0.1 (together with the scaled and shifted 150% flow) the peak is reduced to 494.0 m^3/s and to 483.3 m^3/s with a floodplain roughness of 0.3. This shows that by removing the levées and increasing the attenuation created by blocked grips, the peak flow of the Ouse can be reduced below the peak flow for the 25 year return period. Even though the reduction in discharge is small for the 2000 event, this could be considerable in terms of the number of people and properties that could potentially be protected from a flood event.

6.5 Conclusion

Levée height has an influence on flood peaks downstream as the levées channelise the flow, reducing attenuation available from the floodplains. By restoring the channel-floodplain connection, peak discharge is reduced in all scenarios tested. This is a valuable finding as it suggests that the levées enhance the transmission of the flood wave, transmitting the flood signal further downstream to York and increasing the volume of water travelling to York. Increasing and decreasing the height of the levées did not reduce peak discharges as much as completely removing them. Increasing Manning's *n* of the channel and floodplain reduced peak discharges downstream, as did scaling and shifting the flow to simulate the impact of blocking grips. The most dramatic reduction in peak discharge was found by modelling the effect of blocked grips on the flow *and* removing the levées *and* roughening the channel. This reduced local floodplain risk whilst also reducing downstream flood peaks at York. The findings suggest that, whilst blocking grips in the Ouse catchment may be effective for reducing peak flows, a large area would need to be blocked for an effect to be observed. It must be recognised that the effects of grip blocking appear to be translated downstream, especially in a defended floodplain, but the degree to which this is the case depends on the magnitude of the grip effects, and hence the degree of scaling if blocked. The simulations demonstrated that by removing the levées and using an extreme flow scaling of 150% (representing hypothetical attenuation from blocked grips), peak flow could be reduced below the threshold for peak flows associated with a 25 year return period. As separate approaches to floodplain management, both removing levées and blocking grips could aid the reduction of peak flows at York, but in combination they would create the most sustainable approach for future flood risk management in the Ouse catchment.

Chapter Seven

Conclusions

7.1 Introduction

This chapter will draw together the core findings of the investigation and place the findings in context. Section 7.2 draws out the key findings whilst Section 7.3 answers each of the research questions with reference to the key findings and to the literature. Section 7.4 sets out future avenues for developing the research presented in this thesis. Section 7.5 outlines the wider lessons learnt from the study. Section 7.6 assesses a number of issues arising during this investigation and Section 7.7 provides a summary of the chapter.

7.2 Impact of levées on propagation of the upland grip signal in the Ouse catchment

This thesis set out to assess whether or not the floodplains in the Ouse catchment upstream of York modify the propagation of upstream land management impacts on peak flows. The hydrological boundary conditions and geometry of the river system of interest were input into the hydrodynamic model HEC-RAS. In order to address the research questions the model was used to assess the impact of Manning's *n*, hypothetical flow scenarios and the levées on peak flow and peak timing. The findings specific to the Ouse catchment are summarised below:

- Levée removal restores the channel-floodplain connection, reducing discharge by 1.3%. In all scenarios, levée removal reduced peak discharge the most as flood water attenuates. This reduction is larger at upstream cross-sections thus suggesting dissipation of the attenuation effect in the system.

- Levée removal delays peak timing but the delay of the flood peak is larger at upstream cross-sections.

- Reducing levée height by half reduces peak discharge by only 0.2%. Raising levée height by 0.5 m reduces peak discharge by 0.7%. Both raising and reducing levée height decrease peak discharge due to the contrasting effects of storage and attenuation. Reducing levée height increases attenuation, reducing peak discharge, whilst raising levée height decreases attenuation but also storage is used later, countering the reduction in attenuation.

- Increasing Manning's *n* to 0.1 for the channel reduces peak discharge dramatically for all levée scenarios, but particularly without the levées at 32.4%. The magnitude

of the effect depends on the magnitude of change to Manning's *n*. Increasing Manning's *n* of the floodplain reduces peak discharge less than channel *n*. Manning's *n* might have a larger impact on the flood wave during smaller events.

- Peak timing delay is increased by both channel and floodplain roughness. The peak occurs later with the levées than without the levées in the model (Table 6.2).

- Blocking grips has the potential to increase attenuation and delay flood waves in the Ouse catchment with the current defences. Attenuation and translation both increase as the grip blocking effect is scaled by further degrees.

- Land use signals (the impact of blocked grips) are dissipated with distance as the flood wave travels downstream.

- Peak discharge is more sensitive to flow scaling and shifting (i.e. grip blocking) with the levées, demonstrating that the levées do make the grip effect more noticeable, but the influence of the levées is not large. Peak discharge is higher with the levées, suggesting that the levées do transmit the flood signal further. The degree to which grip effects are translated downstream depends on the magnitude of the grip effects and hence the degree of scaling if blocked.

- By scaling and shifting the flow (150%) in relation to the extreme hypothesised effect of blocked grips, and removing the levées in the Ouse catchment, peak discharge at York could be reduced by 4.2%. By combining increases to both channel and floodplain roughness, peak discharge could be reduced by as much as 39.1% (with a channel *n* of 0.1 and floodplain *n* set to original values).

- By removing the levées and using an extreme flow scaling (scaled by 150% and shifted by 1 hour) representing hypothetical attenuation from blocked grips, peak flow could be reduced below the threshold for peak flows associated with a 25 year return period.

7.3 Summary of Research Questions

The following section summaries the findings of this investigation relating to each research question posed in Chapter One.

7.3.1 Research Question 1 – In what way can the floodplain be used to reduce flood risk downstream?

The findings of this investigation agree with Nisbet (2004), Thomas and Nisbet (2007) and Helmio (2002): increasing Manning's *n* of the floodplain reduces peak discharge downstream. However, this reduction is not as great as that found by some previous studies, such as Woltenmade and Potter (1994), as the ease of reducing peak flows depends on floodplain characteristics. The smaller reduction in peak discharge created by floodplain *n* may also suggest that attenuation effects are diminished at high flow peaks and volumes during high magnitude events, as suggested by Archer (1989).

In accordance with literature concerning the temporary storage of water and flood risk (e.g. Whiting and Pomeranets, 1997; Morris *et al.*, 2003) the channel-floodplain connection has proved crucial for determining downstream discharges. As suggested by the studies conducted by Morris and Wheater (2007) and Acreman *et al.* (2003) it appears that the removal of levées does reduce peak discharges downstream, but only by a minimal amount (1.3%). An interesting result is that at upstream cross-sections the reduction in peak discharge caused by levée removal is higher, suggesting that the positive impact of removing the levées, in terms of decreasing the flood peak, is dissipated as the flood wave propagates downstream.

7.3.2 Research Question 2 – To what extent are land management signals impacted upon by flow attenuation?

Scaling and shifting the flow in accordance with the hypothesised influence of blocking grips from the literature (e.g. Environment Agency, 2000; Lane *et al.*, 2003b) has a large impact on peak discharge, particularly at high levels of scaling, attenuating and translating the flood peak. Further downstream the attenuation reduces, suggesting that land use signals are dissipated with distance downstream. This investigation has shown how scaling and shifting the flow in relation to land management change (blocked grips) can delay peak timing by as much as 2 hours (Table 6.2). This delay to the peak flow for the River Ouse is expected to desynchronise the peak flow from that of the River Swale and River Nidd, thus reducing downstream flood risk. The land management signals from blocked grips are noticeable downstream at York despite intervening attenuation. This investigation has shown that with a flow scaling of 150% and shift of 1 hour to represent

an extreme effect of blocking grips, peak discharge can be reduced by 3.2% with levées and 4.2% without levées.

7.3.3 Research Question 3 – Do flood levées aid the transmission of the upstream hydrograph?

This study has found that peak discharge is more sensitive to flow scaling with the levées, suggesting that levées do make the grip effect more noticeable, although the reduction in peak discharge is small. A valuable finding is that peak discharge is higher with the levées, suggesting that the levées do transmit the flood signal further downstream to York because they reduce (floodplain) attenuation, channelising the flood water (Acreman *et al.*, 2003).

Levée height has an influence on flood peaks downstream as the levées channelise the flow, reducing attenuation available from the floodplains as suggested by Buijse *et al.* (2002) and Acreman *et al.* (2003). Both raising and reducing levée height appear to reduce peak discharge in the system due to the countering effects of storage and attenuation. Although changing levée height only had a small influence on peak discharge, it illustrates how changing the geometry of the levées in the system can vary the propagation of the flood peak downstream. Removing the levées completely had the largest impact and it is suggested that using this method to reconnect the channel with its floodplain could reduce flood risk, if combined with increases to channel and floodplain roughness. The Ouse catchment has large areas of available floodplain storage which could greatly contribute to the reduction of flood flows.

As separate approaches to floodplain management, both removing levées and blocking grips could aid the reduction of peak flows at York. However, crucially, by combining the positive effects of levée removal and grip blocking (scaled 150%, shifted 1hr) downstream peak discharge for York could be reduced by 4.2%. This approach could also reduce the peak flow for the 2000 event below the threshold for peak flows associated with a 25 year return period. Therefore, this appears to be an effective and sustainable approach for future flood risk management in the Ouse catchment. As this study has shown that blocking grips could reduce peak discharges quite dramatically, the sustainability of removing flood banks is enhanced. The most dramatic reduction in peak discharge was found by roughening the channel whilst using the above method (removing levées and

scaling and shifting the flow). This reduced local floodplain risk whilst also reducing downstream flood peaks at York. However, increasing channel roughness to 0.1 is not readily achievable for large rivers so a combination of increasing channel and floodplain roughness may be the most beneficial approach.

7.4 Recommendations for future work

This thesis has provided a number of valuable conclusions regarding the future of flood management strategies, particularly for the Ouse catchment. The study demonstrated that there is a link between rural land management in the upper catchments and flood routing; the levées do make the grip blocking effect more noticeable with the effects still being detected at York despite intervening attenuation. This key finding suggests that a radical modification of the flood management strategy for York could reduce flood risk. Presented in the study is the attenuation provided by the available floodplains in the Ouse catchment. The understanding of the attenuation process in the Ouse system can be used to inform future flood risk policies for York. However, the extent to which this attenuation can aid flood reduction is expected to decrease for high magnitude events. By removing the embankments, allowing the floodplains to attenuate and translate the flood peak, peak discharge can be reduced. This approach to flood management would need the acceptance of relevant agricultural communities through the use of demonstration sites which have already been used within the Ouse catchment at Ripon. The implications of the project should be assessed holistically with consideration of the whole catchment. As this study suggests that the peak timing delay decreases following levée removal, the exact influence of the levées on the translation of the flood wave needs further investigation to gain a more conclusive result. Another avenue for future research is to assess how specific storage areas in the Ouse catchment, and other river systems, can be used to reduce peak flows downstream. Potential areas for further storage of floodwater have already been highlighted by the Environment Agency in the *River Ure and Tributaries Modelling Study.* Analysing the effectiveness of using specific storage areas for reducing flood risk downstream, once the levées are removed in critical reaches, could prove crucial for implementing the suggested modification to the flood management strategy for York.

7.5 Wider lessons learnt

A number of lessons can be taken from this study that could be relevant to other large river systems. The methodology can be applied to other catchments where similar routing problems are present and suitable data exist. The wider lessons that can be drawn from this study are:

1) Debates over upstream land management need to recognise that even if there is evidence of land management impacts on local flooding, those effects need to be propagated downstream and to take into account the network arrangement of downstream rivers. Land management practices will have the greatest impact in a river system where the peak flow of the tributaries are synchronised. By changing the land management practice in a catchment (such as blocking grips), it is possible to desynchronise the flood peaks, thus reducing the flood risk downstream.

2) The way that a river-floodplain is managed does impact upon its propagation. The removal of levées has the potential to reduce peak discharge downstream in a catchment. The reconnection of the river to the floodplain, through the removal of levées, allows the floodplains to attenuate and translate the flood peak. It is expected that the presence of levées in other river systems is propagating land management signals more strongly as found in the Ouse catchment.

3) There are complex and contradictory effects of levées on flood routing and downstream flows associated with the balancing of two effects – taking water off into storage, which is more likely at flood peaks, and so meaning higher levée heights are better at giving storage – and slowing water movement down by getting it onto the floodplain sooner – and the balance of these effects depends on location with respect to the downstream city where flooding occurs.

7.6 Assessment of the study

A number of issues must be highlighted before the results from this study can be used to inform future flood policies. First, many of the simulations involved varying Manning's *n* values for the channel and floodplain. Values for channel *n* ranged between 0.02 and 0.1 in order to capture any significant responses. However, it must be noted that an increase in channel roughness to 0.1 may not be deliverable in practice. Such a high value

describes a very weedy river channel with heavy stands of timber which is rarely found in large rivers. Large increases in Manning's *n* tend to be hard to achieve in very large rivers such as the Ouse, even through different restoration techniques, due to the large distances involved and conflicting interests of stakeholders (Chow, 1959). Second, the manipulations of the hydrograph (scaling and shifting) are end members of possible grip blocking responses, so the conclusions are likely to be over-estimates. The scaling of the hydrograph was used to hypothetically represent the influence of blocking grips on the system. The results serve a preliminary guide to the expected effect of grip blocking in the upland catchments on peak flows downstream. The degree to which grip blocking effects are translated downstream in a defended floodplain depends on the magnitude of grip effects (degree of scaling and shifting if blocked). Future enquiries will be necessary to understand how grip blocking affects the upstream flow. Moreover, recognising a relationship between flow attenuation and extent of grip blocking will be crucial for the Ouse catchment. Third, some issues with the HEC-RAS model need to be recognised. Some instabilities in water surface elevations remain along the Nidd reach of the model. Also, the correlation between the observed and modelled discharge following preliminary modelling was not very good. This is likely to have been due to the expected overestimation of flow at gauging stations on the River Swale and River Nidd (Environment Agency, 2010a). The issues relating to the reliability of the observed data may explain the variation between the simulated and observed flow data. If internal records could be provided, the results could be validated. The main error exists between the troughs of the observed and modelled hydrographs; however, as this investigation was primarily interested in the timing and magnitude of the flow peaks, this did not prove a problem. Although the discrepancy with the measured flow is an issue, the overall findings presented in this thesis do not change. Further enquiries will require a full calibration of the model, which was not possible here due to a lack of data.

7.7 Summary

Chapter Seven has highlighted the findings of this investigation and offered suggestions for the application of the research. It has shown that the levées do aid the propagation of the grip signal in the Ouse catchment as peak discharge is more sensitive to flow scaling with the levées in place. The reduction of peak discharge caused by levée removal is only small but if reduced below a critical threshold could prove vital for flood risk reduction.

For moderate sized floods (smaller than the 2000 event) the attenuation of the floodplains could reduce flood peaks considerably, reducing damage and losses to York. The 1-D model built in HEC-RAS could prove a useful tool for guiding future flood management policies for the City of York in order to mitigate the impact of land use changes and climate change.

References

Aber, J. D. (1997) Why don't we believe the models? *Bulletin of the Ecological Society of America* 78 (3): 232-233.

Acreman, M. C., Fisher, J., Stratford, C. J., Mould, D. J. and Mountford, J. O. (2007) Hydrological science and wetland restoration: some case studies from Europe *Hydrology and Earth System Sciences* 11 (1): 158-169.

Acreman, M. C., Riddington, R. and Booker, D. J. (2003) Hydrological impacts of floodplain restoration: a case study of the River Cherwell, UK *Hydrological and Earth System Sciences* 7 (1): 75-85.

Akanbi, A. A. and Singh, K. P. (1997) *Managed Flood Storage Option for Selected Levées along the Lower Illinois River for Enhancing Flood Protection, Agriculture, Wetlands, and Recreation* Illinois, Illinois State Water Survey.

Albertson, M. L., Barton, J. R. and Simons, D. B. (1966) *Fluid Mechanics for Engineers* USA: Prentice-Hall Inc.

Anderson, B. G., Rutherfurd, I. D. and Western, A. W. (2006) An analysis of the influence of riparian vegetation on the propagation of flood waves *Environmental Modelling and Software* 21: 1290-1296.

Anderson, M. G. and Burt, T. P. (1985) Modelling strategies *In*: Anderson, M. G. and Burt, T. P. (Eds.) *Hydrological Forecasting* Chichester: Wiley pp. 1-14.

Archer, D. R. (1989) Flood wave attenuation due to channel and flood storage and effects on flood frequency *In*: Beven, K. and Carling, P. (Eds.) *Floods - Hydological Sedimentological and Geomorphological Implications* Chichester: Wiley pp. 37-46.

Armstrong, A., Holden, J., Kay, P., Foulger, M., Gledhill, S., McDonald, A. T. and Walker, A. (2009) Drain-blocking techniques on blanket peat: a framework for best practice *Journal of Environmental Management* 90: 3512-2519.

Baker, R. D. (2001) A methodology for sensitivity analysis of models fitted to data using statistical methods *IMA Journal of Management Mathematics* 12 (1): 23-39.

Ball, T. (2008) Management approaches to floodplain restoration and stakeholder engagement in the UK: a survey *Ecohydrological Processes and Sustainable Floodplain Management* 8 (2-4): 273-280.

Bates, P. D. and De Roo, A. P. J. (2000) A simple raster-based model for flood inundation simulation *Journal of Hydrology* 236: 54-77.

Beven, K. (1989) Changing ideas in hydrology - the case of physically-based models *Journal of Hydrology* 105: 157-172.

Beven, K. J. (2004) *Rainfall-Runoff Modelling: The Primer* Chichester: Wiley.

Beven, K. J., O'Connell, P. E., Harris, G. and Clements, R. O. (2004) *Review of impacts of rural land use and management on flood generation: Impact study report Joint Defra/EA Flood and Coastal Erosion Risk Management R&D Programme*. London.

Blackwell, M. S. A. and Maltby, E. (2005) *Ecoflood guidelines: How to use floodplains for flood risk reduction* [online]. Available from: www.kennisonline.wur.nl/NR/rdonlyres/CDA379F4-BF44-4B01-8417-A5AFFF22A9F6/43433/Ecoflood_summary_report.pdf [Accessed 11 March 2010].

Buijse, A. D., Coops, H., Staras, M., Jans, L. H., Van Geest, G. J., Grifts, R. E., Ibelings, B. W., Oosterberg, W. and Roozen, F. C. J. M. (2002) Restoration strategies for river floodplains along large lowland rivers in Europe *Freshwater Biology* 47: 889-907.

Bullock, A. and Acreman, M. (2003) The role of wetlands in the hydrological cycle *Hydrology and Earth System Sciences* 7: 358-389.

Burke, W. (1975) Effect of drainage on hydrology of blanket bog *Irish Journal of Agricultural Research* 14: 145-162.

Burnham, M. W. and Davis, D. W. (1990) Effects of data errors on computed stead-flow profiles *Journal of Hydraulic Engineering* 116 (7): 914-929.

Burt, T. P., Bates, P. D., Stewart, M. D., Claxton, A. J., Anderson, M. G. and Price, D. A. (2002) Water table fluctuations within the floodplain of the river Severn, England *Journal of Hydrology* 262: 1-20.

Carson, E. C. (2006) Hydrologic modelling of flood conveyance and impacts of historic overbank sedimentation on West Fork Black's Fork, Uinta Mountains, northeastern Utah, USA *Geomorphology* 75: 368-383.

Chorley, R. J., Schumm, S. A. and Sugden, D. E. (1984) *Geomorphology* London: Routledge.

Chow, V. T. (1959) *Open-Channel Hydraulics* USA: McGraw-Hill.

Chuntian, C., Chau, K. W. and Chunping, O. (2001) *Flood control management system for reserviors as non-structural measures* Non-structural measures for water management problems, London, Ontario, Canada.

Conway, V. M. and Miller, A. (1960) The hydrology of some small peat-covered catchments in the northern Pennines *Journal of the Institute of Water Engineers* 14: 415-424.

Coultish, G. (2008) Farming and flood storage *Journal of Practical Ecology and Conservation* 7 (1): 40-41.

Crosetto, M. and Tarantola, S. (2001) Uncertainty and sensitivity analysis: Tools for GIS-based model implementation *International Journal of Geographical Information Science* 15 (5): 415-437.

Crosetto, M., Tarantola, S. and Saltelli, A. (2000) Sensitivity and uncertainty analysis in spatial modelling based on GIS *Agriculture, Ecosystems and Environment* 81 (1): 71-79.

Cuny, F. C. (1991) Living with floods: alternatives for riverine flood mitigation *Land Use Policy* 8 (4): 331-342.

Daniel, C. (1973) One-at-a-time-plans *Journal of American Statistical Association* 68: 353-360.

De Doncker, L., Troch, P., Verhoeven, R., Bal, K., Meire, P. and Quintelier, J. (2009) Determination of the Manning roughness coefficient influenced by vegetation in the river Aa and Biebrza river *Environmental Fluid Mechanics* 9: 549-567.

DEFRA (2002) *Working with the grain of nature: A biodiversity strategy for England*. London: DEFRA.

DEFRA (2005) *Making Space for Water: Taking forward a new Government Strategy for flood and coastal erosion risk management in England*. London: DEFRA.

DEFRA (2007) *Ripon Mulit-objective project lessons learned report* [online]. Available from: http://www.defra.gov.uk/defrasearch/search_results.jsp?template=&category=&doctype=&options=&date=&database=Internet_Files%2B&batchsize=20&query=ripon+multi+objective [Accessed 27 October 2009].

DeFries, R. and Eshleman, K. N. (2004) Land-use change and hydologic processes: a major focus for the future *Hydological Processes* 18: 2183-2186.

Diehl, T. H. (1990) *Hydrological and statistical characteristics of extreme floods*. Madison, University of Wisconsin Ph.D. dissertation.

Dooge, J. and Keane, R. (1975) Mathematical simulation of runoff from small plots of undrained and drained peat at Glenmoy, Ireland. In: *Hydrology Of March-Ridden Areas.* Studies and reports in Hydrology 19. IAHS.

Downs, P. W. and Thorne, C. R. (2000) Rehabilitation of a lowland river: Reconciling flood defence with habitat diversity and geomorphological sustainability *Journal of Environmental Management* 58: 249-268.

Dury, G. H. (1961) Bankfull discharge: an example of its statistical relationships *International Association of Scientific Hydrology.* Bulletin 6 (3): 48-55.

English Nature, Environment Agency, DEFRA and Forestry Commission (2002) *Wetlands, lane use change and flood management* [online]. Available from: www.defra.gov.uk/environment/flooding/documents/manage/jointstment.pdf [Accessed 26 March 2010].

Environment Agency (2000) *Upper Wharfedale Best Practice Project: Moorland Drainage - The Gripping Question*. Langstrothdale 3rd July 2000.

Environment Agency (2004) *The Ouse flood risk management strategy scoping report summary*. Leeds: Environment Agency.

Environment Agency (2010a) *Hiflows-UK* [online]. Available from: www.environment-agency.gov.uk/hiflows/ [Accessed 16 July 2010].

Environment Agency (2010b) *Managing Flood Risk: Draft Ouse Catchment Management Plan Summary Report January 2010* Leeds: Environment Agency.

Environment Agency/DEFRA (2004) *Flood and Coastal Defence R&D Programme. Review of current knowledge and practice. Annex 2: Hydraulic Model Implementation of Bridge and Culvert Afflux and Blockage*. Bristol.

Environment Agency/DEFRA (2009) *Desktop review of 2D hydraulic modelling packages*. Bristol: Environment Agency.

Ervine, D. A. and MacLeod, A. B. (1999) Modelling a river channel with distant floodbanks *Proceedings of the Institution of Civil Engineers - Water, Maritime and Energy* 136: 21-33.

Evans, E. P., Wicks, J. M., Whitlow, C. D. and Ramsbottom, D. M. (2007) The evolution of a river modelling system *Water Management* 160: 3-13.

Farahi, G., Khodashenas, S. R., Ghahraman, B. and Esmaeeli, K. (2009) Flood inundation extent in storage cell mode *Science in China Series E: Technological Sciences* 52 (11): 3376-3381.

Fathi-Maghadam, M. and Kouwen, B. (1997) Nonrigid, nonsubmerged, vegetative roughness on floodplains *Journal of Hydraulic Engineering* 123 (1): 51-57.

Fisher, R. A. (1935) *The Design of Experiments* Edinburgh: Oliver and Boyd.

Fread, D. L. (1991) Flood routing models and the Manning *n In*: Yen, B. C. (Ed.) *Channel Flow Resistance: Centennial of Manning's Formula* Littleton, Colorade: Water resources publications pp. 421-435.

Ghavasieh, A. R., Poulard, C. and Paquier, A. (2006) Effect of roughened strips on flood propagation: Assessment on representative virtual cases and validation *Journal of Hydrology* 318: 121-137.

Green, I. R. A. and Stephenson, D. (1986) Criteria for comparison of single event models *Hydrological Sciences* 31 (3): 395-411.

Hall, A. (2008) Policy and farming perspectives of flooding and flood risk *Journal of Practical Ecology and Conservation* 7 (1): 58-59.

Hall, J. W., Tarantola, S., Bates, P. D. and Horritt, M. S. (2005) Distributed sensitivity analysis of flood inundation model calibration *Journal of Hydraulic Engineering ASCE* 131 (2): 117-126.

Hamby, D. M. (1994) A review of techniques for parameter sensitivity analysis of environmental models *Environmental Monitoring and Assessment* 32: 135-154.

Hamer, B. A. and Mocke, R. (2002) Flood risk modelling: a crisis of confidence? *Civil Engineering* 150: 30-35.

Hamill, L. (1999) *Bridge Hydraulics* London: Routledge.

Helmio, T. (2002) Unsteady 1D flow model of compound channel with vegetated floodplains *Journal of Hydrology* 269: 89-99.

Helmio, T. (2005) Unsteady 1D flow model of a river with partly vegetated floodplains - application to the River Rhine *Environmental Modelling and Software* 20 (3): 361-375.

Hewlett, J. D. and Helvey, J. D. (1970) Effects of forest clear-felling on the storm hydrograph *Water Resources Research* 6 (3): 768-782.

Hillman, G. R. (1997) Flood wave attenuation by a wetland following a beaver dam failure on a second order boreal stream *Wetlands* 18 (1): 21-34.

Holden, J., Burt, T. P., Evans, M. G. and Horton, M. (2006) Impact of land drainage on peatland hydrology *Journal of Environmental Quality* 35: 1764-1778.

Holden, J., Chapman, P. J. and Labadz, J. C. (2004) Artificial drainage of peatlands: hydrological and hydrochemical process and wetland restoration *Progress in Physical Geography* 28 (1): 95-123.

Homma, T. and Saltelli, A. (1996) Importance measures in global sensitivity analysis of nonlinear models *Reliability Engineering and System Safety* 52: 1-17.

Hornberger, G. M., Raffensperger, J. P., Wiberg, P. L. and Eshleman, K. N. (1998) *Elements of Physical Hydrology* London: John Hopkins University Press.

Horritt, M. S. and Bates, P. D. (2001) Predicting floodplain inundation: raster-based modelling versus the finite-element approach *Hydrological Processes* 15: 825-842.

Horritt, M. S. and Bates, P. D. (2002) Evaluation of 1D and 2D numerical models for predicting river flood inundation *Journal of Hydrology* 268: 87-99.

Howes, S. I. and Anderson, M. G. (1988) Computer Simulation in Geomorphology *In*: Anderson, M. G. (Ed.) *Modelling Geomorphological Systems* New York: John Wiley and Sons pp. 421-440.

Hunter, N. M., Bates, P. D., Horritt, M. S. and Wilson, M. D. (2006) Improved simulation of flood flows using storage cell models *Proceedings of the Institution of Civil Engineers, Water Management* 159 (WM1): 9-18.

Fluent Inc. (1993) *FLUENT User's Guide.* New Hampshire: Fluent Europe.

Jackson, B. M., Wheater, H. S., Mcintyre, N. R., Chell, J., Francis, O. J., Frogbrook, Z., Marshall, M., Reynolds, B. and Solloway, I. (2008) The impact of upland management on flooding: insights from a mulitscale experimental and modelling programme *Journal of Flood Risk Management* 1: 71-80.

Janssen, P. H. M. and Heuberger, P. S. C. (1995) Calibration of process-orientated models *Ecological Modelling* 83: 55-66.

JBA (2009) *Strategic Flood Risk Assessment*, South Oxfordshire District Council and Vale of White Horse District Council.

Kalyanapu, J. A., Burian, S. J. and McPherson, T. M. (2009) Effect of land use based surface roughness on hydrologic model output *Journal of Spatial Hydrology* 9 (2): 51-71.

Kirkby, M. J. (1996) A role for theoretical models in geomorphology? *In*: Rhoads, B. L. and Thorn, C. E. (Eds.) *The Scientific Nature of Geomorphology* Chichester: Wiley pp. 257-272.

Kitson, R. L., Richards, K. S. and Carling, P. A. (2006) Hydraulic model calibration for extreme floods in bedrock-confined channels: case study from northern Thailand *Hydrological Processes* 20: 329-344.

Knight, D. W. (2005) River flood hydraulics: validation issues in one-dimensional flood routing models *In*: Knight, D. W. and Shamseldin, A. Y. (Eds.) *River Basin Modelling for Flood Risk Mitigation*: Taylor and Francis.

Kohane, R. and Westrich, B. (1994) Modelling of flood hydraulics in compound channels *In*: White, H. R. and Watts, J. (Eds.) *Second International Conference on River Flood Hyraulics* Chichester: Wiley**.**

Krishnappan, B. G. and Lau, Y. L. (1986) Turbulence modeling of flood plain flows *Journal of Hydraulic Engineering* 112 (4): 251-266.

Lane, S. N. (1998) Hydraulic modelling in hydrology and geomorphology: a review of high resolution approaches *In*: Bates, P. D. and Lane, S. N. (Eds.) *High Resolution Flow Modelling in Hydrology and Geomorphology* Chichester: Wiley pp. 15-34.

Lane, S. N. (2003a) More Floods Less Rain? Changing Hydrology in a Yorkshire Context *In*: Atherden, M. (Ed.) *Global Warming in a Yorkshire Context* York: York St. John Univeristy pp. 1-21.

Lane, S. N. (2003b) Numerical modelling in physical geography: understanding, explanation and prediction *In*: Clifford, N. J. and Valentine, G. (Eds.) *Key Methods in Geography*: Sage pp. 263-290.

Lane, S. N. (2006) *Key research questions - unresolved issues, climate change and the future* Yorkshire Dales Rivers Trust: Proceedings of a conference on moorland management and river catchments, Middleham, Yorkshire.

Lane, S. N. (2008) Slowing the floods in the U.K. Pennine uplands...A case of waiting for Godot? *In*: Rotherham, I. D. (Ed.) *Flooding, Water and the Landscape* Sheffield: Wildtrack Publishing pp. 75-91.

Lane, S. N. and Bates, P. D. (2000) Introduction *In*: Bates, P. D. and Lane, S. N. (Eds.) *High Resolution Flow Modelling in Hydrology and Geomorphology* Chichester: Wiley pp. 1-14.

Lane, S. N., Brookes, C., Holden, J. and Kirkby, M. (2003a) Assessment of the effects of land drainage upon upland flood generation using a quasi-distributed hydrological model *Geophysical Research Abstracts* 5 (08498) EGS - AGU - EUG Joint Assembly, Nice, France.

Lane, S. N., Brookes, C. J., Hardy, R. J., Holden, J., James, T. D., Kirkby, M. J., McDonald, A. T., Tayefi, V. and Yu, D. (2003b) *Land management, flooding and environmental risk: new approaches to a very old question*. CIWEM National Conference, Harrogate.

Lane, S. N. and Ferguson, R. I. (2005) Modelling reach-scale flows *In*: Bates, P. D., Lane, S. N. and Ferguson, R. I. (Eds.) *Computational Fluid Dynamics: Applications in Environmental Hydraulics* Chichetser: Wiley pp. 1-15.

Lane, S. N., Morris, J., O'Connell, P. E. and Quinn, P. F. (2007) Managing the rural landscape *In*: Thorne, C. R., Evans, E. P. and Penning-Rowsell, E. (Eds.) *Future Flooding and Coastal Erosion Risks* London: Thomas Telford pp. 297-319.

Lane, S. N., Richards, K. S. and Chandler, J. H. (1994) Application of distributed sensitivity analysis to a model of turbulent open channel flow inn a natural river channel *Proceedings: Mathematical and Physical Sciences* 447 (1929): 49-63.

Lane, S. N. and Thorne, C. R. (2007) River Processes *In*: Thorne, C. R., Evans, E. P. and Penning-Rowsell, E. (Eds.) *Future Flooding and Coastal Erosion Risks* London: Thomas Telford pp. 82-99.

Larson, L. and Plasencia, D. (2001) No adverse impact: a new direction in floodplain management policy *Natural Hazards Review* 2 (4): 167-181.

Leopold, L. B. (1994) Flood hydrology and the floodplain: Water Resources Update Issue *The Universities Council on Water Resources 94*: 11-15.

Lin, B., Wicks, J. M., Falconer, R. A. and Adams, K. (2006) Integrating 1D and 2D hydrodynamic models for flood simulation *Proceedings of the Institution of Civil Engineers* 159 (WM1): 19-25.

Longfield, S. A. and Macklin, M. G. (1999) The influence of recent environmental change on flooding and sediment fluxes in the Yorkshire Ouse Basin *Hydrological Processes* 13: 1051-1066.

Maidment, D. R. (Ed.) (2002) *Arc Hydro: GIS for Water Resources* Redlands, California: ESRI.

McCartney, M. P. and Naden, P. S. (1995) A semi-empirical investigation of the influence of flood-plain storage on flood flow *Journal of CIWEM* 9 (3): 236-246.

McGahey, C., Knight, D. W. and Samuels, P. G. (2009) Advice, methods and tools for estimating channel roughness *Water Management* 162 (WM6): 353-362.

McMillan, H. K. and Brasington, J. (2007) Reduced complexity strategies for modelling urban floodplain inundation *Geomorphology* 90 (3-4): 226-243.

Michaelides, K. and Wainwright, J. (2004) Modelling fluvial processes and interactions *In*: Wainwright, J. and Mulligan, M. (Eds.) *Environmental Modelling: Finding Simplicity in Complexity* Chichester: Wiley pp. 123-142.

Montaldo, N., Mancini, M. and Rosso, R. (2004) Flood hydrograph attenuation induced by a reservoir system: analysis with a distributed rainfall-runoff model *Hydrological Processes* 18: 545-563.

Morris, J. H., Bailey, A. P., Alsop, D., Vivash, R. M., Lawson, C. S. and Leeds-Harrison, P. B. (2003) Integrating Flood Management and Agri-environment through Washland Creation in the UK *Journal of Farm Management* 12 (1): 1-16.

Morris, J. H., Hess, T. M., G., G. D. J., Leeds-Harrison, P. B., Bannister, N., Vivash, R. and Wade, M. (2005) A framework for integrating flood defence and biodiversity in washlands in England *International Journal of River Basin Management* 3 (2): 1-11.

Morris, J. H., T. M., Gowing, D. J., Leeds-Harrison, P. B., Bannniester, N., Wade, M. and Vivash, R. M. (2004) *Integrated washland management for flood defence and biodiversity: Report to Department for Environment, Food and Rural Affairs & English Nature*. Bedfordshire,UK, Cranfield Univeristy.

Morris, J. H. and Wheater, H. S. (2007) Catchment land-use *In*: Thorne, C. R., Evans, E. p. and Penning-Rowsell, E. C. (Eds.) *Future Flooding and Coastal Erosion Risks* London: Thomas telford pp. 82-99.

Morris, M., Dyer, M. and Smith, P. (2007) *Management of flood embankments: A good practice review. R&D Technical Report FD2411/TR1*. London: DEFRA.

Mujumdar, P. P. (2001) Flood Wave Propagation: The Saint Venant Equations *Resonance* 6 (5): 66-73.

Mulligan, M. and Wainwright, J. (2004) Modelling and Model Building *In*: Wainwright, J. and Mulligan, M. (Eds.) *Environmental Modelling: Finding Simplicity in Complexity* Chichester: Wiley pp. 7-73.

Nash, J. E. and Sutcliffe, J. V. (1970) River flow forecasting through conceptual models. Part 1 - a discussion of principles *Journal of Hydrology* 10: 282-290.

Nisbet, T. (2004) *Interactions between floodplain woodland and the freshwater environment*, Forest Research annual report and accounts: 32-39.

Nisbet, T. R. and Broadmeadow, S. (2003) *Opportunity mapping for trees and floods: Final report to Parrett catchment project*. Surrey, Forest Research.

Nisbet, T. R. and Thomas, H. (2008) *Project SLD2316: Restoring Floodplain Woodland for Flood Alleviation*. London: Defra.

Nisbet, T. R., Thomas, H. and Broadmeadow, S. (2008) Trees and Water - A Forestry Perspective *Journal of Practical Ecology and Conservation* 7 (1): 100-102.

O'Connell, E., Ewen, J., O'Donnell, G. and Quinn, P. (2007) Is there a link between agricultural land-use management and flooding? *Hydology and Earth System Sciences* 11 (1): 96-107.

O'Donnell, G., Geris, J., Mayes, W., Ewen, J. and O'Connell, E. (2008) *Mulitscale experimentation, monitoring and anamysis of long-term land use changes and flood risk* BHS 10th national Hydrology Symposium, Exeter.

Olsen, J. R., Beling, P. A. and Lambert, J. H. (2000) Dynamic Models for Floodplain Management *Journal of Water Resource Planning and Management* 126 (3): 167-175.

Olsen, N. R. B. (2008) *Numerical modelling and hydraulics* [online]. Norway. Available from: http://folk.ntnu.no/nilsol/tvm4155/flures6.pdf [Accessed 29 October 2009].

Pappenberger, F., Beven, K., Frodsham, K., Romanowicz, R. and Matgen, P. (2007) Grasping the unavoidable subjectivity in calibration of flood inundation models: A vulnerability weighted approach *Journal of Hydrology* 333: 275-287.

Parrott, A., Brooks, W., Harmar, O. and Pygott, K. (2009) Role of rural land use management in flood and coastal risk management *Journal of Flood Risk Management* 2: 272-284.

Pasche, E. and Rouve, G. (1985) Overbank flow with vegetatively roughened flood plains *Journal of Hydraulic Engineering* 111 (9): 1262-1278.

Pattison, I., Lane, S. N., Hardy, R. J. and Reaney, S. (2008) *Sub-catchment peak flow magniyude and timing effects on downstream flood risk* BHS 10th National Hydrology Symposium, Exeter.

Pender, G. and Neelz, S. (2007) Use of computer models of flood inundation to facilitate communication in flood risk management *Environmental Hazards* 7: 106-114.

Pepper, A. T., Pettifer, D. and Fitzsimons, J. (1998) Challenges and opportunities for flood storage reservoirs *In*: Tedd, P. (Ed.) *The Prospect for Reservoirs in the 21st Century* London: Thomas Telford pp. 171-182.

Posthumus, H., Hewett, C. J. M., Morris, J. and Quinn, P. F. (2008) Agricultural land use and flood risk management: engaging with stakeholders in North Yorkshire *Agricultural Water Management* 95: 787-798.

Posthumus, H. and Morris, J. (2010) Implications of CAP-reform for land management and runoff control in England and Wales *Land Use Policy* 27: 42-50.

Ratto, M., Tarantola, S. and Saltelli, A. (2001) Sensitivity analysis in model calibration: GSA-GLUE approach *Computer Physics Communications* 136 (3): 212-224.

Richards, K. S. (1982) *Rivers, Form and Process in Alluvial Channels* London: Routledge.

Rickard, C., Day, R. and Purseglove, J. (2003) *River Weirs - Good Practice Guide R&D Publication W5B-023/HQP* Bristol: Environment Agency.

Robinson, M. (1986) Changes in catchment runoff following drainage and afforestation *Journal of Hydrology* 86: 71-84.

Robinson, M. (1989) *Impact of improved land drainage on river flows. Institute of Hydrology Report 113*. Wallingford.

Robinson, M. (2006) *Hydrological change in upland catchments* Yorkshire Dales Rivers Trust: Proceedings of a conference on moorland management and river catchments, Middleham, Yorkshire.

Saltelli, A. (2002) Sensitivity analysis for importance assessment *Risk Analysis* 22 (3): 579-590.

Saltelli, A., Chan, K. and Scott, E. M. (Eds.) (2000) *Sensitivity Analysis* Chichester: Wiley.

Samuels, P. G. (1990) *Cross-Section Location in 1-D models* International Conference on River Flood Hydraulics, Wiley.

Sholtes, J. (2009) *Hydraulic analysis of stream restoration on flood wave propagation*, North Carolina at Chapel Hill. MA.

Svensson, C., Hannaford, J., Kundzewicz, Z. W. and Marsh, T. J. (2006) Trends in river floods: why is there no clear signal in observations? *In*: Tchiguirinskaia, I., Thein, K.

N. N. and Hubert, P. (Eds.) *Frontiers in Flood Research* Oxford: IAHS Press pp. 1-18.

Swiatek, D. (2007) Unsteady 1D Flow Model of Natural Rivers with Vegetated Floodplain *Publications of the Institute of Geophysics Polish Academy of Sciences* E-7 (401): 237-244.

Tayefi, V., Lane, S. N., Hardy, R. J. and Yu, D. (2007) A comparison of one- and two-dimensional approaches to modelling flood inundation over complex upland floodplains *Hydrological Processes* 21: 3190-3202.

The Guardian Online (2000) *Floods leave York on edge of disaster* [online]. Available from: http://www.guardian.co.uk/environment/2000/nov/05/weather.climatechange [Accessed 18 June 2010].

Thomas, H. and Nisbet, T. R. (2007) An assessment of the impact of floodplain woodland on flood flows *Water and Environment Journal* 21: 114-126.

Turner-Gillespie, D. F., Smith, J. A. and Bates, P. D. (2003) Attenuating reaches and the regional flood response of an urbanizing drainage basin *Advances in Water Resources* 26: 673-684.

U. S. Army Corps of Engineers (1993) *River Hydraulics Engineer Manual Ep. No. EM 1110-2-1416* Washington, D. C.: Dept. of the Army.

U. S. Army Corps of Engineers (2008) *HEC-RAS River Analysis System: User's Manual* Davis: Dept. of the Army.

Wallingford, H. (2006) *Whitby Marina: Water Velocities* Wallingford: HR Wallingford Ltd.

Werner, M. G. F., Hunter, N. M. and Bates, P. D. (2005) Identifiability of distributed floodplain roughness values in flood extent estimation *Journal of Hydrology* 314: 139-157.

Whatmore, S. J. and Landstrom, C. (2009) Manning's *n* - putting roughness to work *In*: Morgan, M. and Howlett, P. (Eds.) *How Well Do We Know The Facts?* Cambridge: CUP pp. 1-27.

Whiting, P. J. and Pomeranets, M. (1997) A numerical study of bank storage and its contribution to streamflow *Journal of Hydrology* 202: 121-136.

Wise Use of Floodplains (2002) *EU Wise Use of Floodplains Project* [online]. Available from: http://www.floodplains.org.uk [Accessed 23 Feb 2010].

Wollf, C. G. and Burges, S. J. (1994) An analysis of the influence of river channel properties on flood frequency *Journal of Hydrology* 153: 317-337.

Wolman, M. G. and Leopold, L. B. (1957) River flood plains - Some observations on their formation *USGS Professional Paper* 282-C: 87-109.

Woltenmade, C. J. and Potter, K. W. (1994) A watershed modeling analysis of fluvial geomorphologic influences on flood peak attenuation *Water Resources Research* 30 (6): 1933-1942.

Wright, N. G. and Baker, C. (2004) Environmental Applications of Computational Fluid Dynamics *In*: Wainwright, J. and Mulligan, M. (Eds.) *Environmental Modelling: Finding Simplicity in Complexity* Chichester: Wiley pp. 335-348.

Yorkshire Post (2006) *Hi-tech flood defences to protect ancient city* [online]. Available from: http://www.yorkshirepost.co.uk/news/Hitech-flood-defences-to-protect.1537465.jp [Accessed 18 June 2010].

Yu, D. and Lane, S. N. (2006a) Urban fluvial flood modelling using a two-dimensional diffusion-wave treatment, part 1: mesh resolution effects *Hydrological Processes* 20: 1541-1565.

Yu, D. and Lane, S. N. (2006b) Urban fluvial flood modelling using a two-dimensional diffusion-wave treatment, part 2: development of a sub-grid-scale treatment *Hydrological Processes* 20: 1567-1583.

Yue, S., Ouarda, T. B. M. J., Bobee, B., Legendre, P. and Bruneau, P. (2002) Approach for describing statistical properties of flood hydrograph *Journal of Hydraulic Engineering* 7 (2): 147-153.

APPENDIX ONE – Number, grid reference, roughness and distance downstream for Left Over Bank (LOB), channel and Right Over Bank (ROB) for each cross-section in the HEC-RAS model.

				Roughness (Manning's *n*)			Distance to downstream cross-section (m)		
River	**No.**	**Grid Reference**		**LOB**	**Channel**	**ROB**	**LOB**	**Channel**	**ROB**
Ure-Ouse	1000	435043	467236	0.06	0.045	0.06	77.3	81.3	82.8
	999	435352	467248	0.06	0.045	0.06	68.5	54.0	52.5
	998	435484	467213	0.06	0.045	0.06	163.5	85.0	71.5
	996	435701	466986	0.06	0.045	0.06	47.5	78.5	53.0
	995	435686	466796	0.06	0.045	0.06	75.0	61.0	83.0
	994	435632	466656	0.06	0.045	0.06	78.8	83.6	97.6
	993	435753	466281	0.06	0.045	0.06	75.6	89.4	95.8
	992	436101	466428	0.06	0.045	0.06	94.3	83.8	83.8
	991	436416	466636	0.06	0.045	0.06	99.3	88.8	78.5
	990	436813	466647	0.06	0.045	0.06	90.8	88.2	90.4
	989	437248	466518	0.06	0.045	0.06	99.8	95.8	86.0
	988	437648	466220	0.06	0.045	0.06	82.6	87.2	99.6
	987	438011	466416	0.06	0.045	0.06	87.5	84.8	81.0
	986	438346	466313	0.06	0.045	0.06	97.5	97.5	97.5
	985	438346	466313	0.06	0.045	0.06	112.6	73.3	134.3
	984	438467	466629	0.06	0.045	0.06	95.0	90.3	88.0
	983	438536	467003	0.06	0.045	0.06	104.0	107.0	95.0
	982	438607	467080	0.06	0.045	0.06	165.0	53.0	43.5
	981	438653	467406	0.06	0.045	0.06	105.6	83.2	82.0
	980	439181	467429	0.06	0.045	0.06	50.0	54.0	52.5
	979	439281	467430	0.06	0.045	0.06	170.5	52.0	52.5
	978	439408	467114	0.06	0.045	0.06	98.0	53.5	109.5
	977	439408	467114	0.06	0.047	0.06	98.0	53.5	109.5
	976	439496	467124	0.06	0.05	0.06	45.0	40.0	27.0
	975	439538	467108	0.06	0.05	0.06	60.0	52.0	40.0
	974	439580	467065	0.06	0.05	0.06	36.0	33.0	30.0
	973	439616	467063	0.06	0.05	0.06	48.0	54.0	69.0
	972	439658	467039	0.06	0.05	0.06	136.0	134.0	190.0
	971	439691	467098	0.06	0.05	0.06	58.0	75.0	95.0
	970	439803	467129	0.06	0.05	0.06	68.0	77.5	79.0
	969	439913	467210	0.06	0.05	0.06	87.3	86.0	84.0
	968	440157	467305	0.06	0.05	0.06	54.5	56.0	63.5
	967	440233	467383	0.06	0.05	0.06	155.0	94.0	74.0
	966	440239	467538	0.06	0.05	0.06	545.0	393.0	353.0
	965	440687	467847	0.06	0.05	0.06	671.0	389.0	358.0
	964	441202	467417	0.06	0.05	0.06	81.0	90.5	120.3
	963	441387	467259	0.06	0.05	0.06	70.2	91.0	54.8
	962	441257	466933	0.06	0.05	0.06	119.0	97.5	237.0
	961	441328	466837	0.06	0.05	0.06	89.5	94.5	101.3
	960	441686	466838	0.06	0.05	0.06	303.0	100.0	240.0
	959	441941	466675	0.06	0.05	0.06	90.0	91.8	106.8
	958	442234	466334	0.06	0.05	0.06	92.0	96.8	124.8
	957	442565	466173	0.06	0.05	0.06	395.0	390.0	396.0
	956	442943	466060	0.06	0.05	0.06	86.7	79.0	69.3
	955	443161	465919	0.04	0.035	0.04	355.0	341.0	330.0

	954	443329	465606	0.04	0.035	0.04	84.8	93.5	105.3
	953	443477	465301	0.04	0.035	0.04	79.0	90.0	108.0
	952	443869	465253	0.04	0.035	0.04	95.3	95.3	102.8
	951	444208	465427	0.04	0.035	0.04	84.8	88.2	81.2
	950	444613	465301	0.04	0.035	0.04	95.3	93.3	90.8
	949	444992	465335	0.04	0.035	0.04	95.0	87.0	71.7
	948	445251	465217	0.04	0.035	0.04	88.6	88.0	84.2
	947	445362	464788	0.04	0.035	0.04	88.0	90.0	93.0
	946	445510	464469	0.04	0.035	0.04	94.3	93.0	90.8
	945	445755	464183	0.04	0.035	0.04	90.6	90.4	90.0
	944	445981	463790	0.04	0.035	0.04	85.2	92.8	94.6
	943	446250	463460	0.04	0.035	0.04	96.5	94.0	90.5
	942	446593	463284	0.04	0.035	0.04	83.4	81.6	75.8
	941	446811	462929	0.04	0.035	0.04	81.0	82.0	79.2
	940	446669	462550	0.04	0.035	0.04	86.0	95.5	83.5
	939	446749	462215	0.04	0.035	0.04	35.0	44.2	55.0
	938	446752	462181	0.06	0.035	0.06	263.0	76.4	296.0
	937	446916	461681	0.06	0.035	0.06	105.0	98.4	92.8
	936	447342	461218	0.06	0.035	0.06	571.0	278.7	548.0
	935	447301	460648	0.06	0.035	0.06	479.0	497.0	598.0
	934	447427	460186	0.06	0.035	0.06	113.2	89.5	139.0
	933	448106	460197	0.06	0.035	0.06	771.0	396.4	795.0
	932	448870	460297	0.06	0.035	0.06	412.0	414.5	409.0
	931	449255	460149	0.06	0.035	0.06	95.3	93.8	89.5
	930	449777	459913	0.06	0.035	0.06	209.0	100.0	234.0
	929	449951	460016	0.03	0.015	0.03	10.0	10.0	10.0
	928	449950	460023	0.04	0.04	0.06	340.0	20.0	249.0
	927	450195	460259	0.06	0.035	0.06	94.7	97.8	95.2
	926	450759	460194	0.06	0.035	0.06	99.3	97.8	76.0
	925	451197	459789	0.06	0.035	0.06	187.3	74.8	209.3
	924	451288	459235	0.06	0.035	0.06	361.0	98.5	337.0
	923	451333	458514	0.06	0.035	0.06	516.0	512.5	499.0
	922	451287	458001	0.06	0.035	0.06	418.0	180.0	490.0
	920	451702	458040	0.06	0.035	0.06	87.5	94.0	72.5
	919	452220	457949	0.06	0.035	0.06	82.1	90.4	81.4
	918	452676	457599	0.06	0.035	0.06	569.0	96.5	486.0
	917	453211	457406	0.06	0.035	0.06	138.0	99.0	181.3
	916	453595	457251	0.06	0.035	0.06	182.8	94.0	170.8
	915	453988	456634	0.06	0.035	0.06	175.3	84.3	158.7
	914	454456	456395	0.06	0.035	0.06	621.0	331.7	658.0
	913	454804	455881	0.06	0.035	0.06	155.5	77.7	146.5
	912	455304	455511	0.06	0.035	0.06	88.5	90.5	100.2
	911	455707	455165	0.06	0.035	0.06	659.0	89.2	826.0
	910	456361	455248	0.06	0.035	0.06	98.0	51.7	113.0
	909	456443	455302	0.06	0.035	0.06	103.0	117.0	110.0
	908	456527	455354	0.06	0.046	0.16	10.0	10.0	10.0
	907	456528	455350	0.16	0.046	0.07	75.0	69.5	58.0
	906	456601	455367	0.16	0.046	0.07	91.0	85.8	76.0
	905	456692	455381	0.07	0.046	0.06	98.0	97.1	95.0
	904	456790	455379	0.15	0.046	0.06	30.0	24.0	19.0
	903	456819	455389	0.05	0.046	0.06	29.0	27.0	25.0
	902	456808	455296	0.05	0.046	0.06	0.0	0.0	0.0
Swale	100	442709	473531	0.06	0.045	0.06	291.0	75.0	318.0
	99	442552	473329	0.06	0.045	0.06	10.0	10.0	10.0
	98	442518	473322	0.06	0.045	0.06	339.0	14.0	382.0
	97	442815	473159	0.06	0.045	0.06	124.0	86.0	108.8

	96	443435	473154	0.06	0.045	0.06	93.8	99.8	99.6
	95	443280	472711	0.06	0.045	0.06	80.0	97.2	88.4
	94	443640	472885	0.06	0.045	0.06	107.8	98.8	78.8
	93	443839	472503	0.06	0.045	0.06	110.0	90.3	89.8
	92	443916	472070	0.06	0.045	0.06	89.6	86.6	82.8
	91	443737	471659	0.06	0.045	0.06	92.4	86.2	70.8
	90	443447	471299	0.06	0.045	0.06	168.0	90.0	94.0
	89	443290	471360	0.06	0.045	0.06	84.4	99.0	93.4
	88	443238	470941	0.06	0.045	0.06	91.3	93.0	94.3
	87	443259	470577	0.06	0.045	0.06	107.0	91.3	106.7
	85	443395	470291	0.06	0.045	0.06	76.5	81.0	90.3
	84	443479	469997	0.06	0.045	0.06	87.0	87.5	66.5
	83	443641	469689	0.06	0.045	0.06	93.3	99.3	103.5
	82	443648	469316	0.06	0.045	0.06	93.3	92.3	88.0
	81	443493	468977	0.06	0.045	0.06	96.5	82.5	86.8
	80	443435	468595	0.06	0.045	0.06	86.0	97.4	104.4
	79	443270	468198	0.06	0.045	0.06	41.0	88.8	65.7
	78	443492	468091	0.06	0.045	0.06	65.0	93.0	37.5
	77	443739	468302	0.06	0.045	0.06	309.0	80.0	285.0
	76	443884	468029	0.06	0.045	0.06	86.3	76.7	80.7
	75	443864	467771	0.06	0.045	0.06	62.3	80.5	70.5
	74	444061	467618	0.06	0.045	0.06	72.7	89.2	70.7
	73	443866	467228	0.06	0.045	0.06	95.3	98.3	97.5
	72	443962	466859	0.06	0.045	0.06	66.6	96.0	56.0
	71	443659	466721	0.06	0.045	0.06	50.5	57.5	64.0
	70	443563	466691	0.06	0.045	0.06	81.2	98.8	78.6
	69	443221	466473	0.06	0.045	0.06	126.0	70.0	163.7
	68	443187	466551	0.06	0.045	0.06	0.0	0.0	0.0
Nidd	100	442827	453037	0.02	0.045	0.07	12.0	22.0	37.0
	99	442839	453036	0.07	0.045	0.07	36.0	25.0	125.0
	98	442868	453057	0.075	0.045	0.07	73.0	40.0	87.0
	97	442936	453084	0.07	0.045	0.045	336.0	20.0	279.0
	96	443272	453071	0.07	0.045	0.07	44.8	45.1	43.7
	95	443476	452725	0.07	0.045	0.07	38.6	45.4	47.5
	94	443857	452790	0.075	0.045	0.075	40.9	44.7	41.4
	93	444175	452865	0.105	0.045	0.105	39.5	47.6	40.2
	92	444036	453149	0.075	0.045	0.06	41.6	45.8	35.5
	91	444453	453151	0.045	0.045	0.06	45.8	45.8	45.1
	90	444811	453222	0.07	0.045	0.07	38.3	46.6	49.6
	89	444862	453602	0.075	0.045	0.105	38.3	49.1	45.5
	88	444650	453823	0.075	0.045	0.06	80.0	50.0	48.7
	87	444757	454038	0.075	0.045	0.075	343.0	20.0	301.0
	86	445097	454081	0.075	0.045	0.075	47.0	48.1	45.1
	85	445201	453720	0.075	0.045	0.075	68.8	40.9	77.6
	84	445541	453773	0.075	0.045	0.075	36.7	48.5	40.8
	83	445455	454053	0.075	0.045	0.075	50.1	49.3	44.1
	82	445616	454421	0.06	0.045	0.075	43.2	47.0	37.0
	81	445917	454175	0.075	0.045	0.075	121.0	43.3	131.7
	80	446247	454024	0.075	0.045	0.075	49.8	43.3	67.6
	79	446213	454271	0.075	0.045	0.075	43.8	44.6	43.0
	78	446002	454603	0.075	0.045	0.075	93.8	40.0	69.2
	77	446213	454913	0.05	0.045	0.09	122.5	49.5	91.3
	76	446627	455174	0.05	0.045	0.06	161.3	42.5	86.5
	75	446966	454626	0.105	0.045	0.105	32.0	27.9	31.0
	74	446951	454597	0.09	0.045	0.09	40.7	46.2	39.4
	73	446907	454274	0.045	0.045	0.075	44.0	48.0	55.8
	72	447100	454378	0.09	0.045	0.09	46.0	44.2	37.3

	71	447418	454430	0.105	0.045	0.075	71.3	42.2	60.3
	70	447656	454273	0.075	0.045	0.075	20.0	48.9	31.3
	69	447617	454159	0.075	0.045	0.075	31.9	45.1	41.6
	68	447755	454373	0.075	0.045	0.075	84.7	44.2	72.7
	67	447646	454603	0.075	0.045	0.075	49.4	48.0	53.6
	66	447959	454751	0.075	0.045	0.09	24.5	49.9	6.8
	65	447959	454751	0.075	0.045	0.09	76.3	50.0	103.0
	64	447748	454971	0.06	0.045	0.06	36.1	44.5	27.7
	63	447546	455177	0.06	0.045	0.06	48.4	48.4	42.0
	62	447658	455547	0.09	0.045	0.105	48.8	49.3	46.3
	61	447834	455782	0.075	0.045	0.06	54.3	49.5	44.5
	60	448151	455709	0.083	0.045	0.083	49.3	47.5	39.1
	59	448292	455394	0.075	0.045	0.075	13.6	48.1	25.1
	58	448342	455313	0.075	0.045	0.075	87.8	50.0	88.8
	57	448450	455647	0.075	0.045	0.075	236.0	20.0	339.0
	56	448686	455643	0.075	0.045	0.075	33.2	47.7	68.1
	55	448569	455918	0.06	0.045	0.06	46.3	47.5	36.9
	54	448206	455991	0.075	0.045	0.075	71.0	28.1	95.0
	53	448225	456059	0.06	0.045	0.06	182.0	20.0	142.0
	52	448046	456093	0.05	0.045	0.05	107.0	35.0	193.0
	51	448148	456124	0.09	0.045	0.075	122.8	46.6	68.8
	50	448439	456519	0.053	0.045	0.06	55.8	49.5	46.8
	49	448839	456718	0.05	0.045	0.075	58.2	47.2	49.8
	48	448956	456148	0.06	0.045	0.05	32.1	47.7	53.0
	47	449179	456181	0.06	0.045	0.06	39.8	48.6	36.8
	46	449256	456407	0.06	0.045	0.06	34.7	43.3	41.3
	45	449498	456379	0.06	0.045	0.075	42.4	47.2	35.6
	44	449305	456605	0.075	0.045	0.05	44.9	45.8	37.4
	43	449664	456613	0.09	0.045	0.05	55.8	48.0	64.0
	42	449758	456876	0.05	0.045	0.06	127.3	44.0	41.7
	40	449985	456702	0.075	0.045	0.06	19.3	49.4	15.0
	39	449958	456550	0.06	0.045	0.06	36.2	41.6	71.5
	38	449852	456452	0.068	0.045	0.06	40.0	48.0	53.6
	37	450156	456353	0.04	0.04	0.05	80.0	50.0	92.8
	36	450463	456608	0.06	0.04	0.06	63.6	44.2	86.0
	35	450514	456923	0.075	0.04	0.05	54.0	48.0	18.5
	34	450649	457333	0.05	0.09	0.05	27.4	41.7	18.2
	33	450643	457470	0.05	0.04	0.06	9.6	45.1	88.6
	32	450664	457514	0.06	0.04	0.06	12.7	42.5	40.8
	31	450736	457540	0.05	0.04	0.05	32.5	39.0	41.0
	30	450826	457633	0.06	0.04	0.06	81.4	40.7	50.0
	29	451134	457899	0.05	0.04	0.05	95.0	40.0	131.0
	28	451553	457673	0.075	0.045	0.075	0.0	0.0	0.0

APPENDIX TWO – Changes to the output hydrographs after varying Manning's *n* of the channel and floodplain (Chapter Five).

1) Whole model

WITH LEVÉES

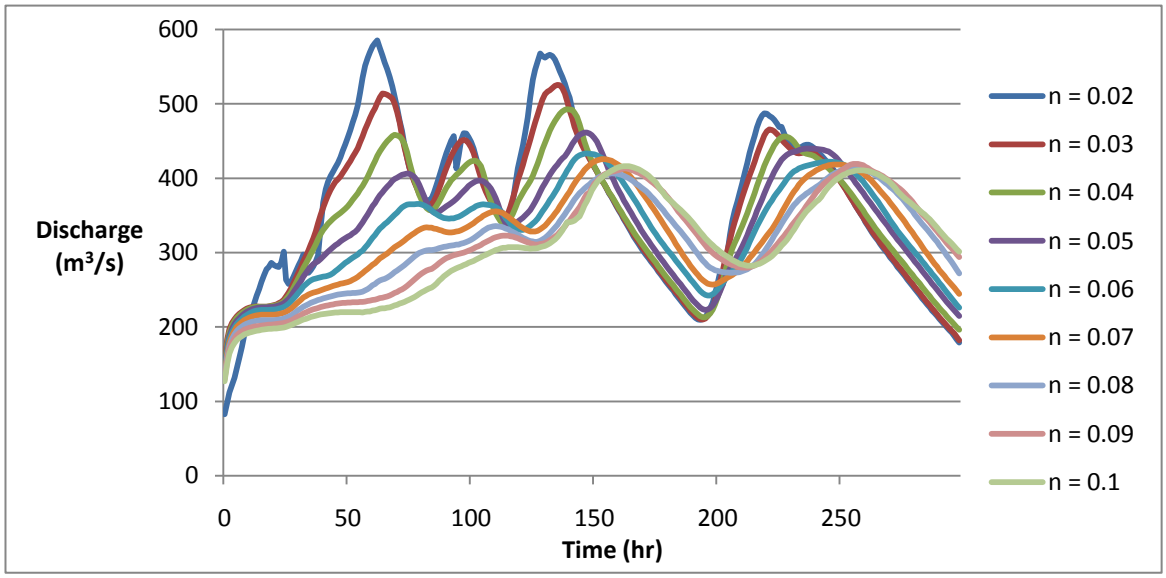

Manning's *n* for the channel varied.

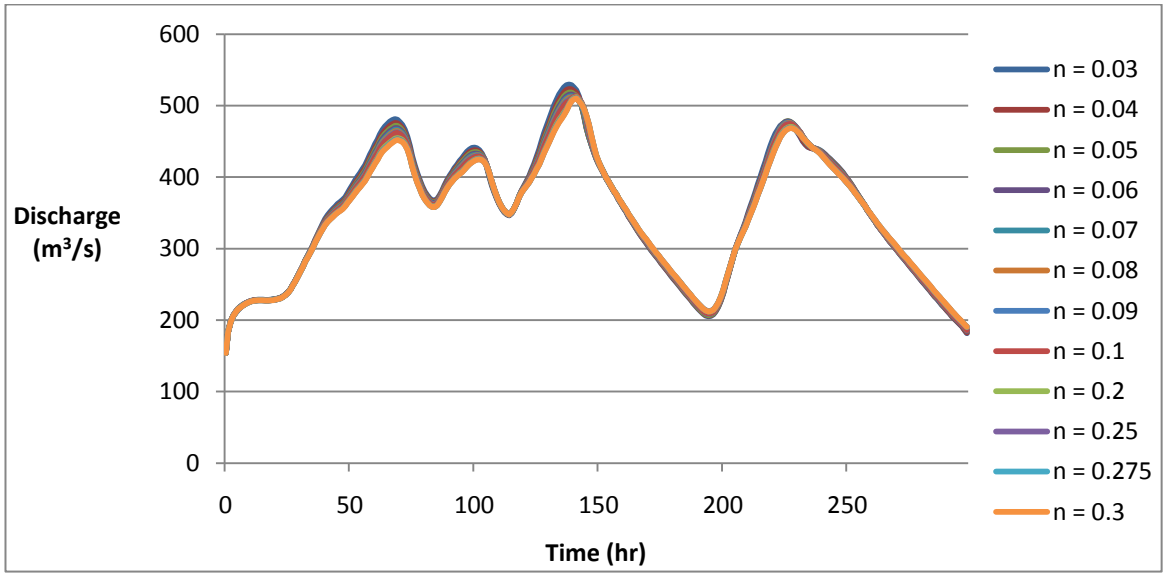

Manning's *n* for the floodplain varied.

WITHOUT LEVÉES

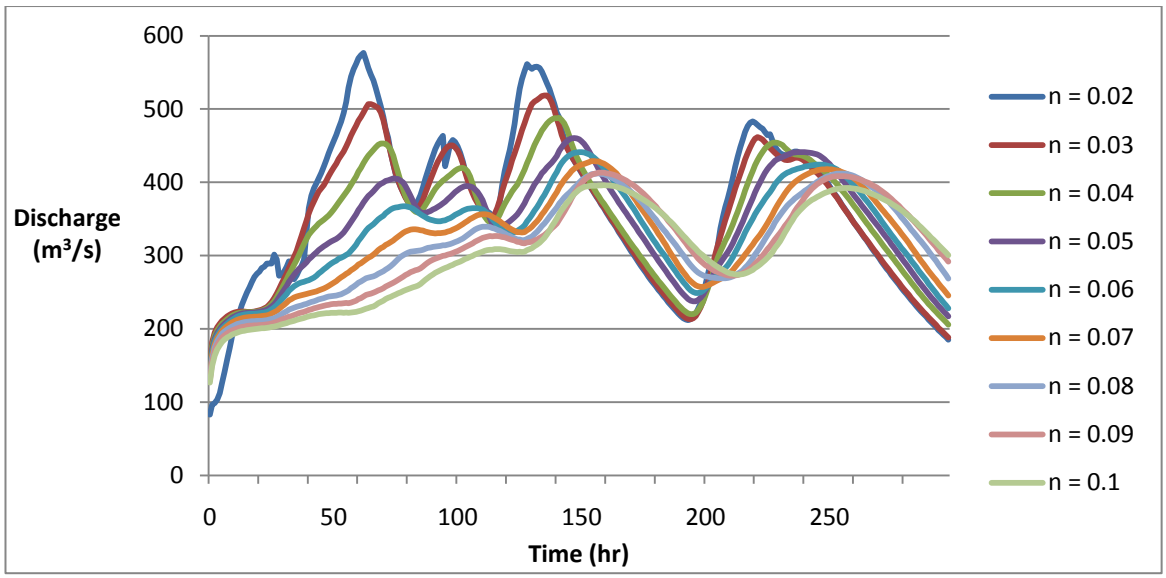

Manning's *n* for the channel varied.

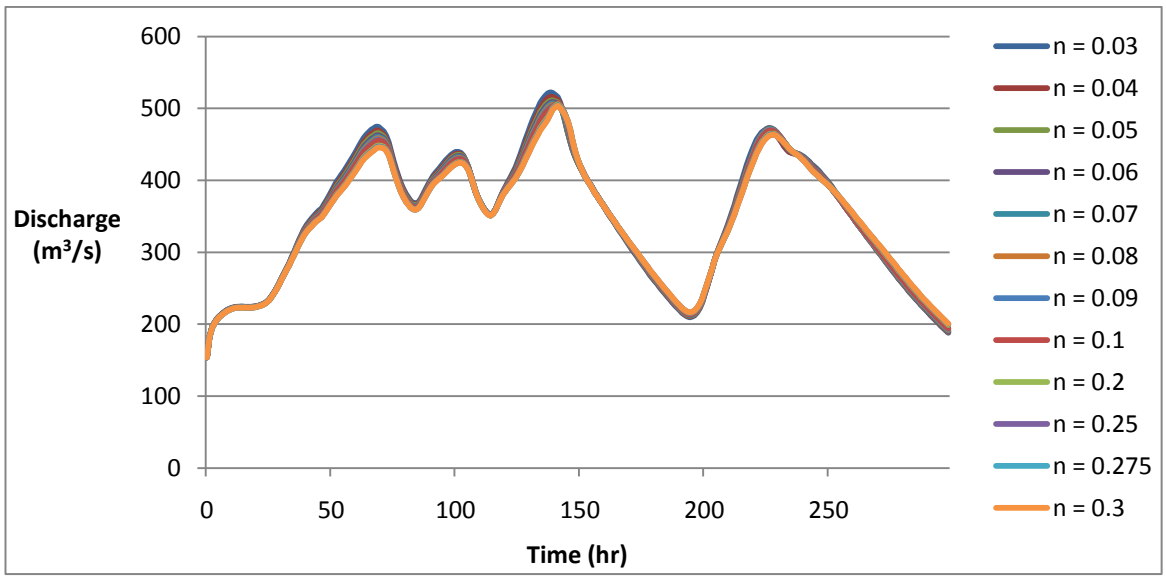

Manning's *n* for the floodplain varied.

2) River Ouse – WITH LEVÉES

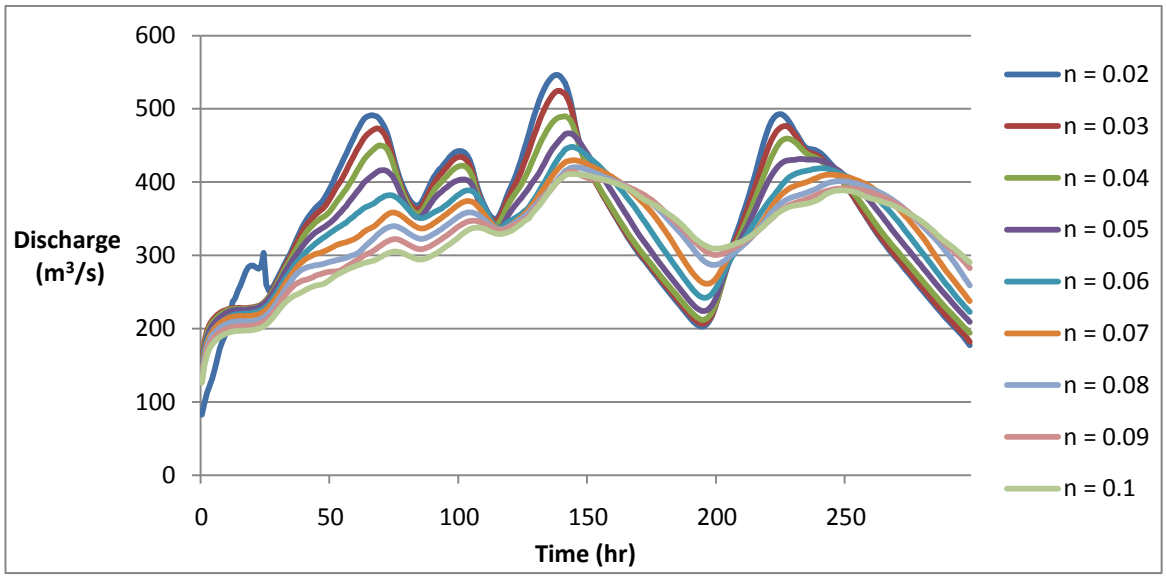

Manning's *n* for the channel varied.

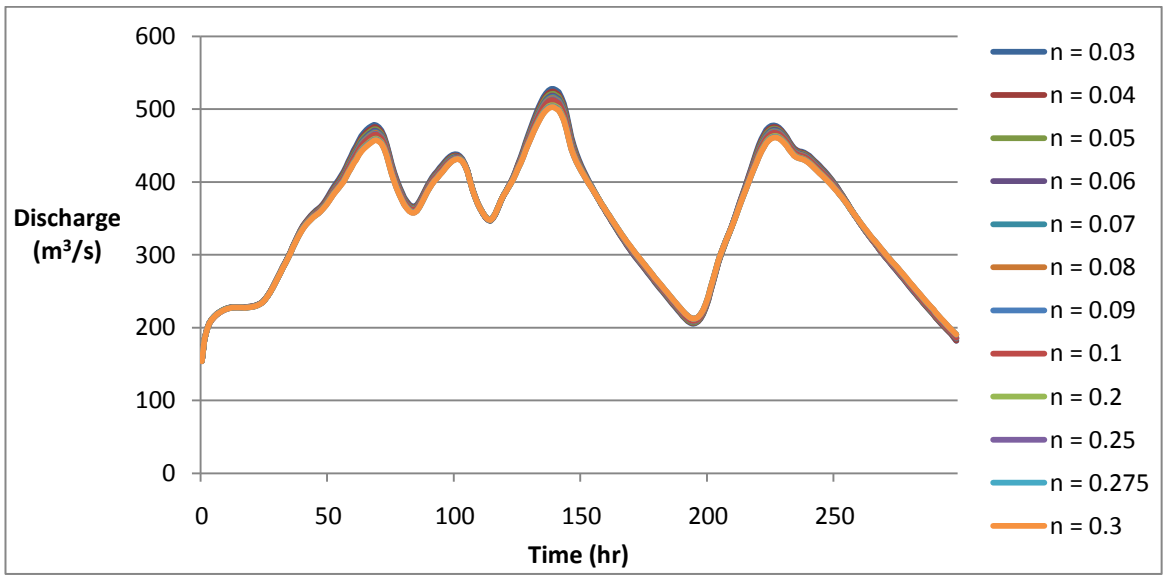

Manning's *n* for the floodplain varied.

WITHOUT LEVÉES

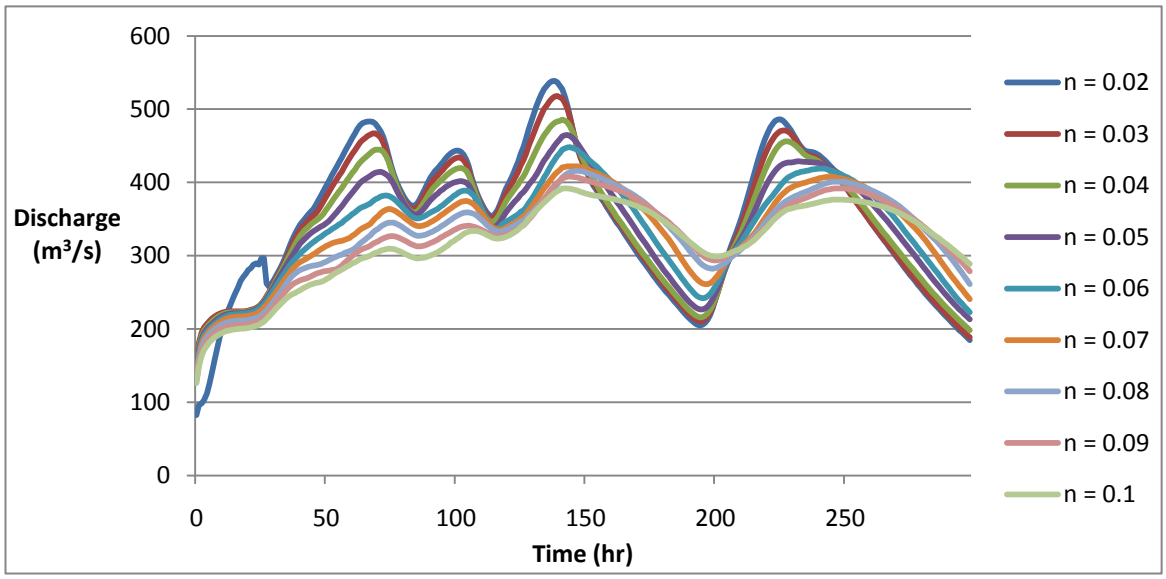

Manning's *n* for the channel varied.

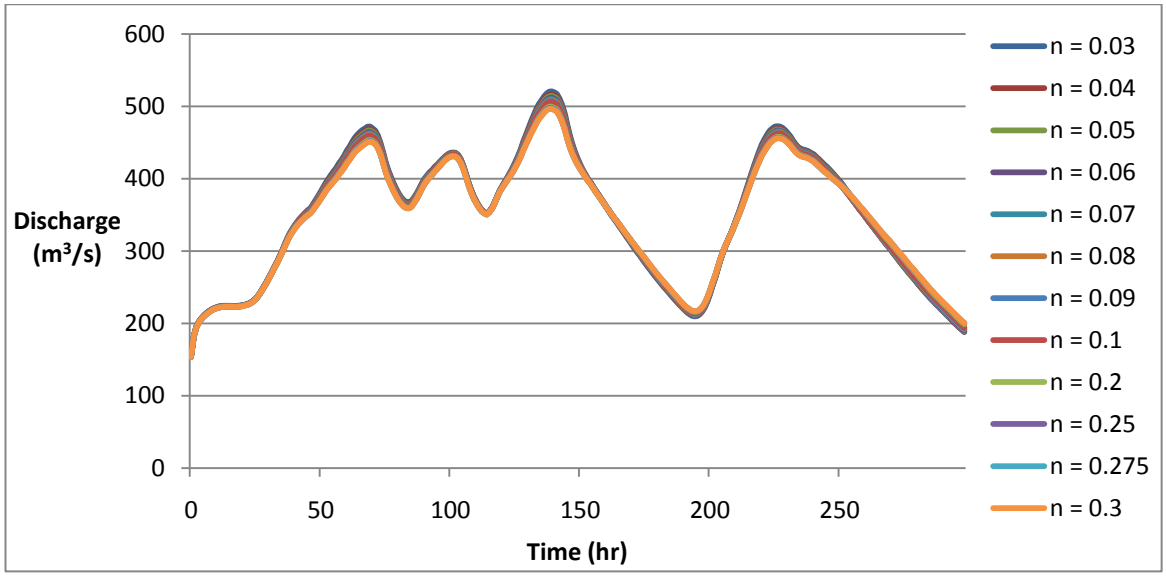

Manning's *n* for the floodplain varied.

3) River Swale – WITH LEVÉES

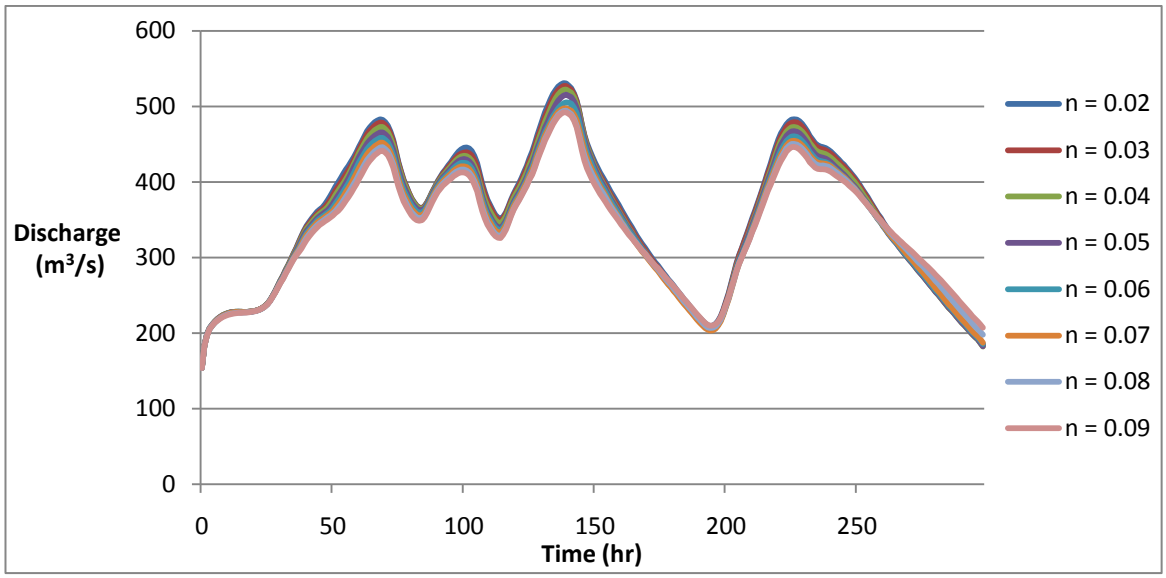

Manning's *n* for the channel varied.

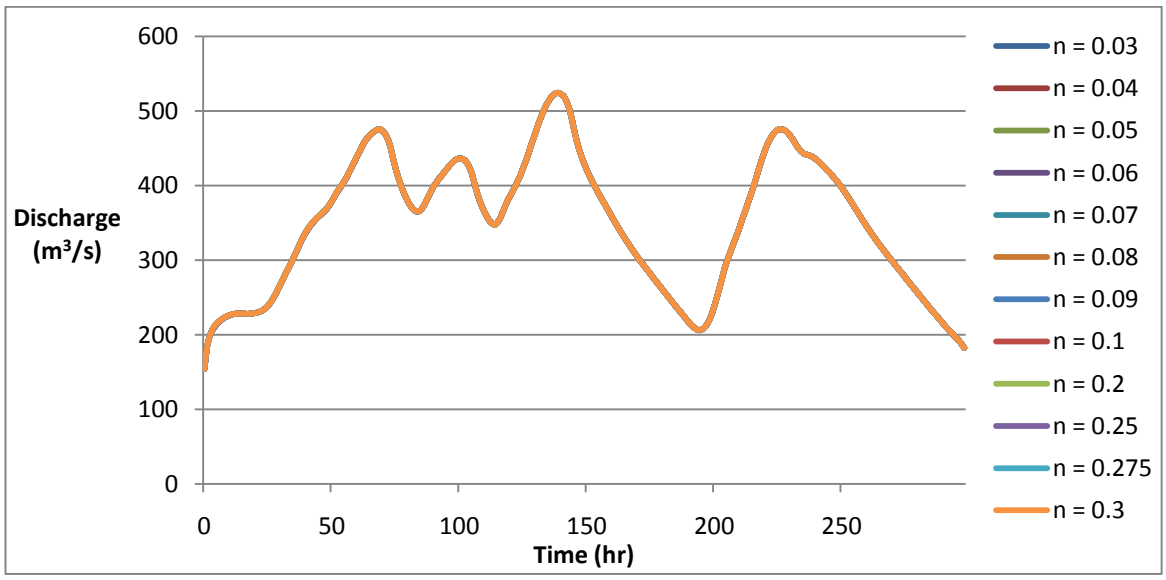

Manning's *n* for the floodplain varied. Variations to floodplain *n* did not change the hydrograph in these scenarios, thus all lines overlap on the graph.

WITHOUT LEVÉES

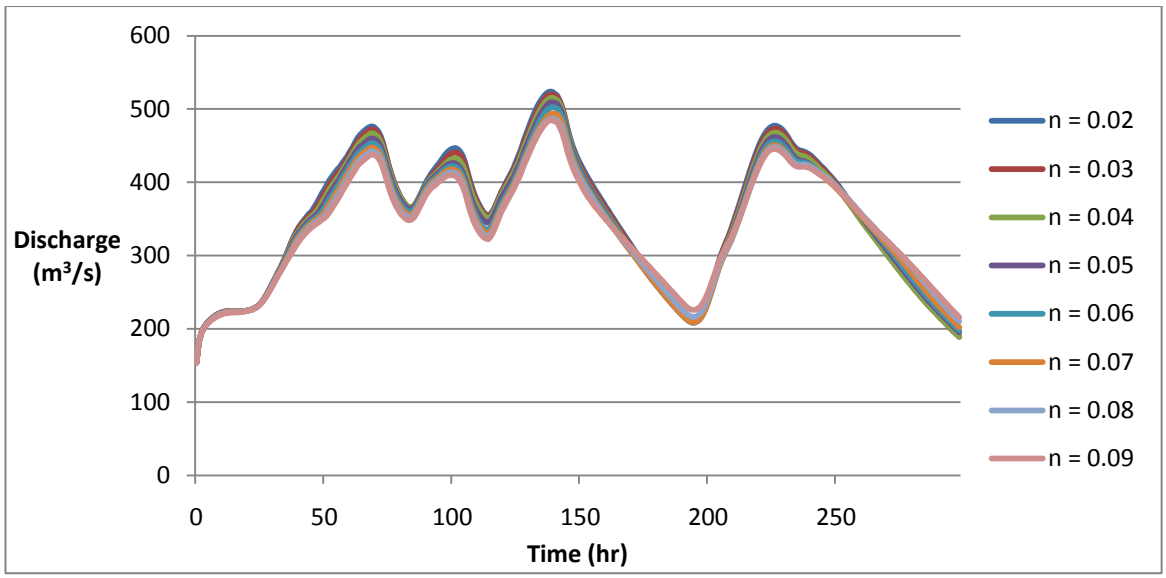

Manning's *n* for the channel varied.

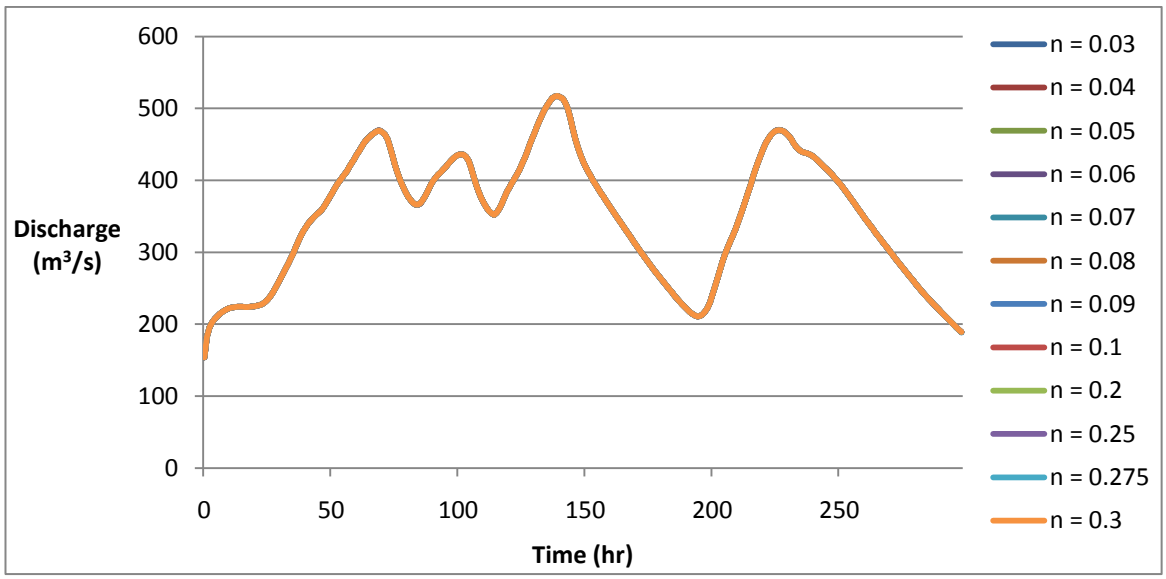

Manning's *n* for the floodplain varied. Variations to floodplain *n* did not change the hydrograph in these scenarios, thus all lines overlap on the graph.

4) River Nidd – WITH LEVÉES

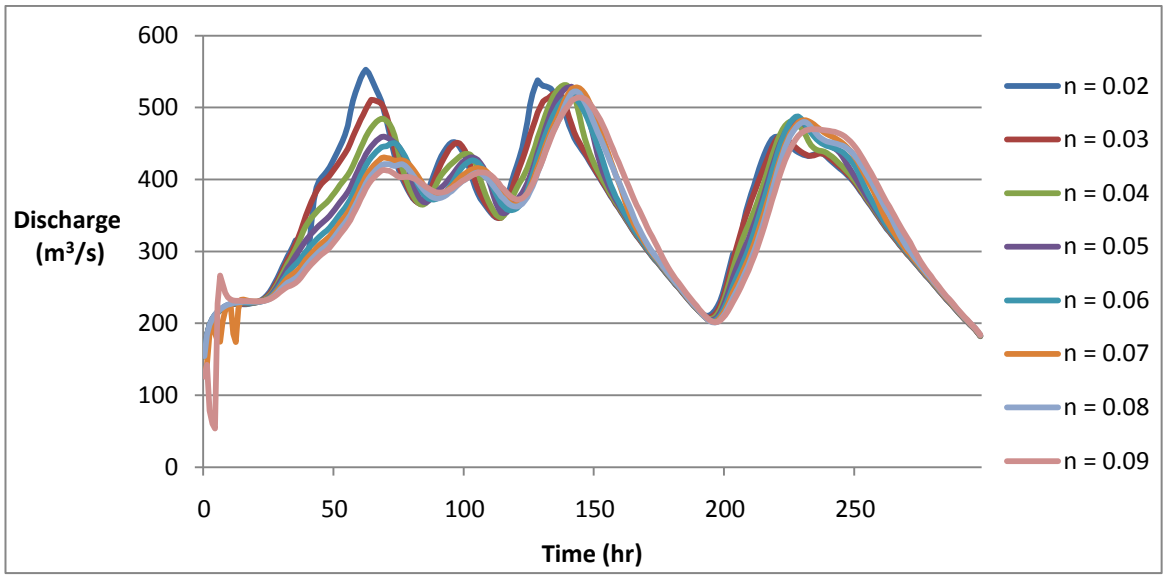

Manning's *n* for the channel varied.

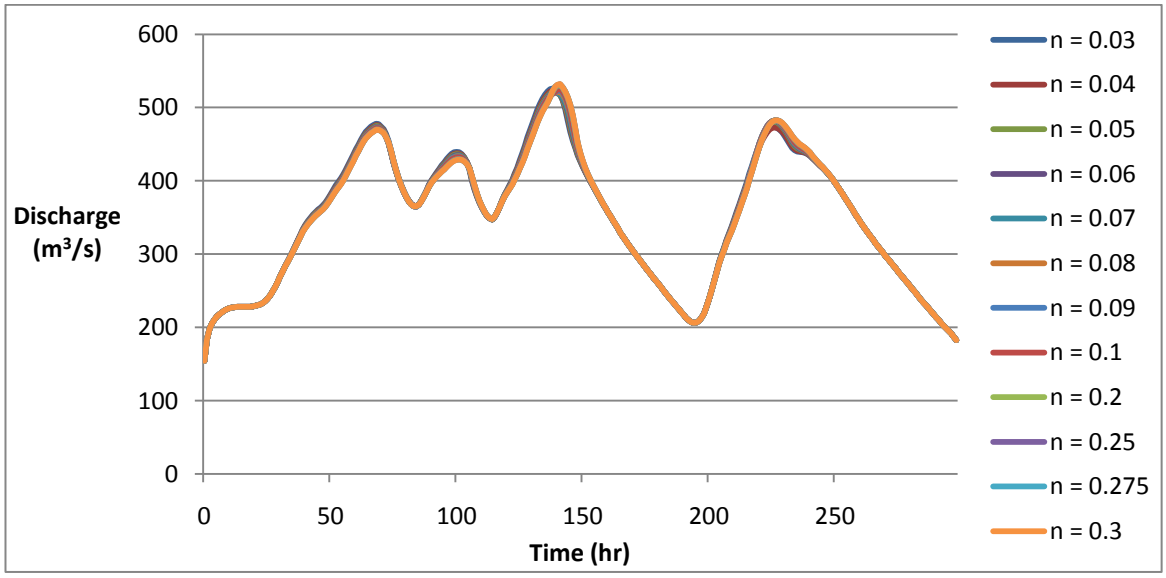

Manning's *n* for the floodplain varied.

WITHOUT LEVÉES

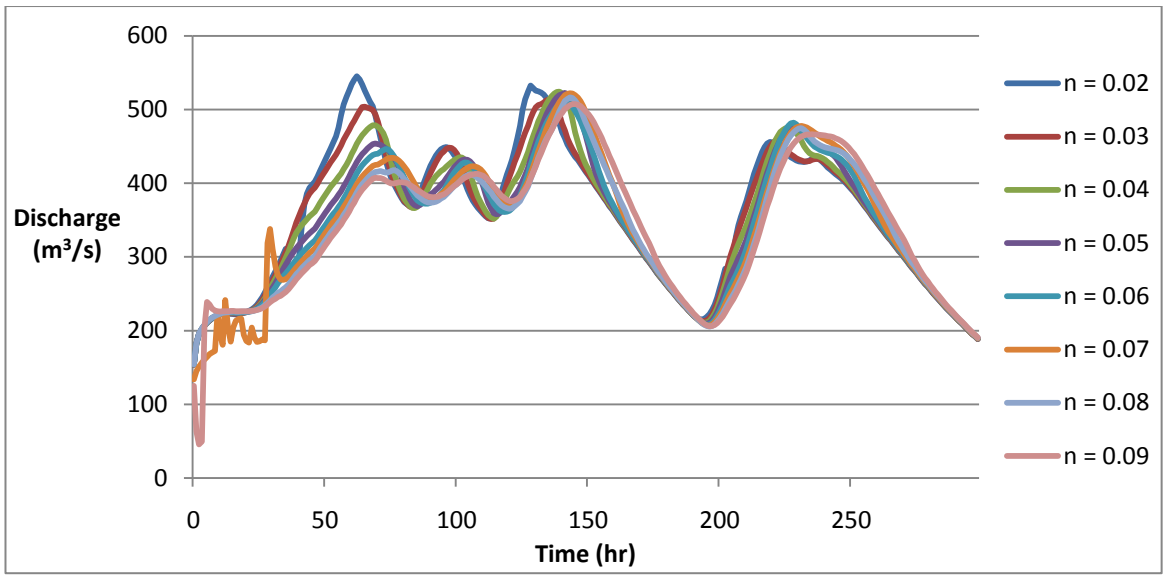

Manning's *n* for the channel varied.

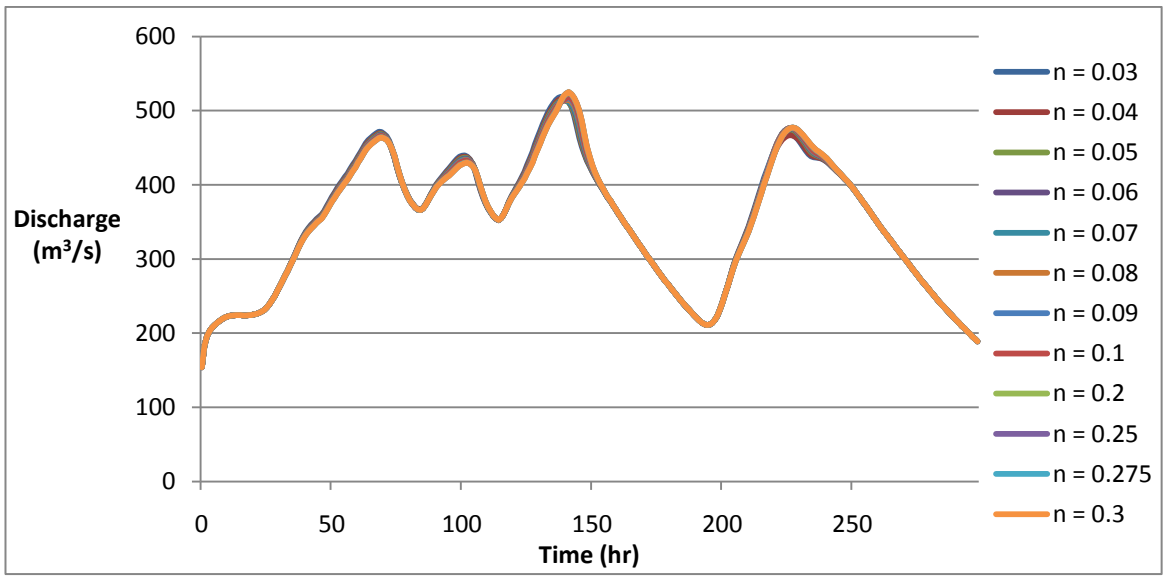

Manning's *n* for the channel varied.

5) Half height levées

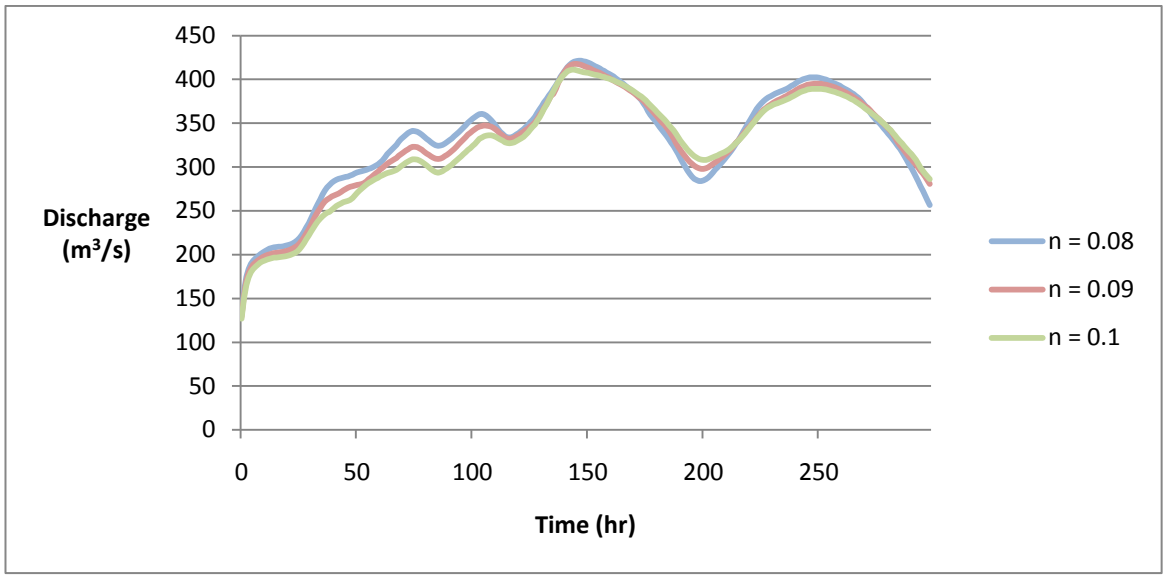

Manning's *n* for the channel varied.

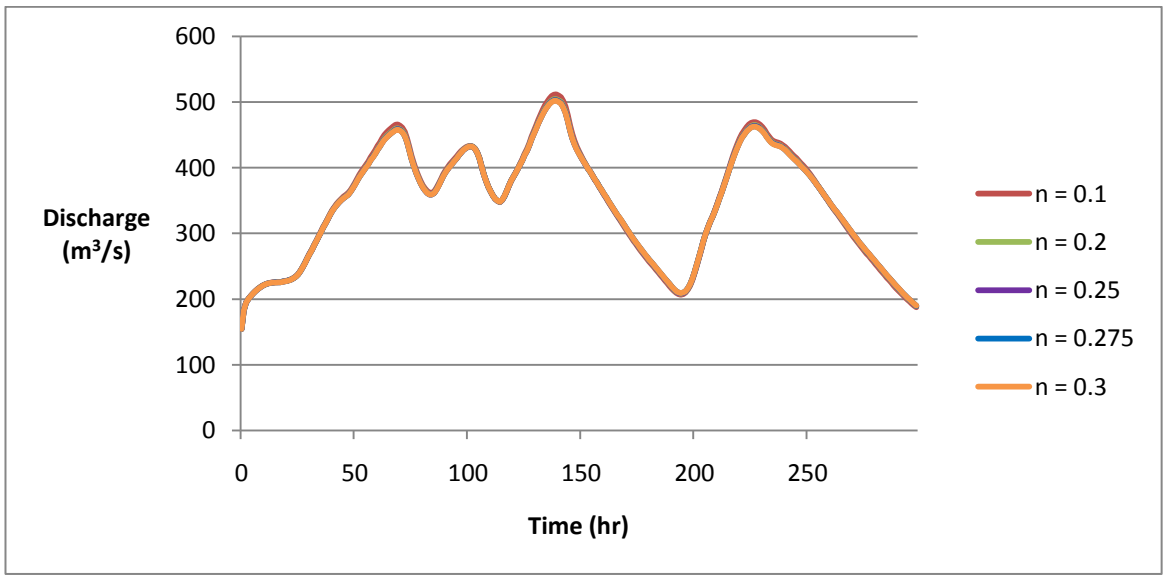

Manning's *n* for the floodplain varied.

6) Added height levées

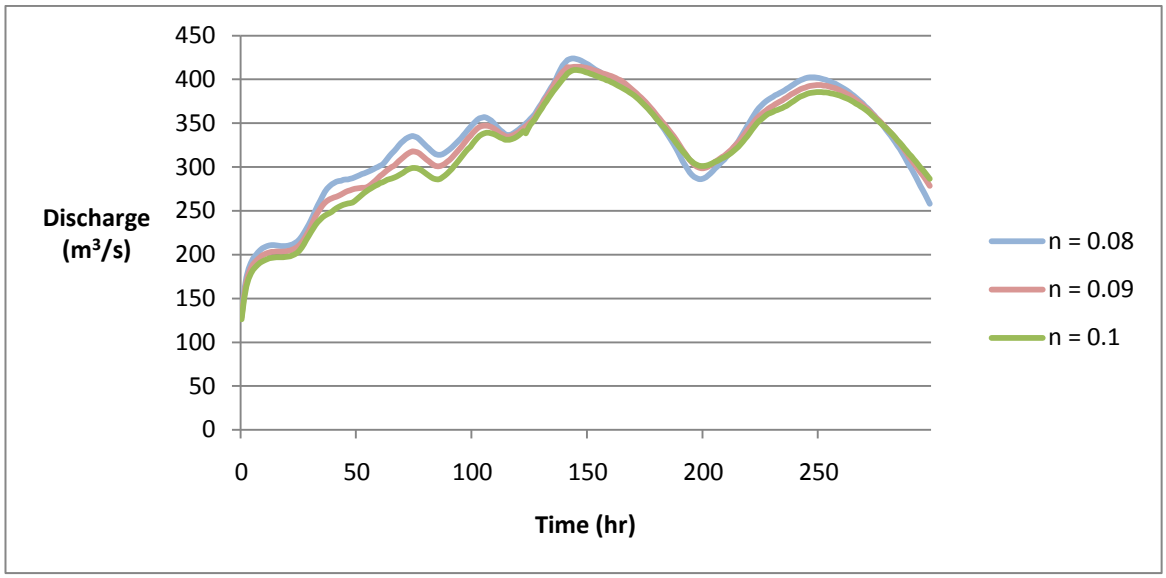

Manning's *n* for the channel varied.

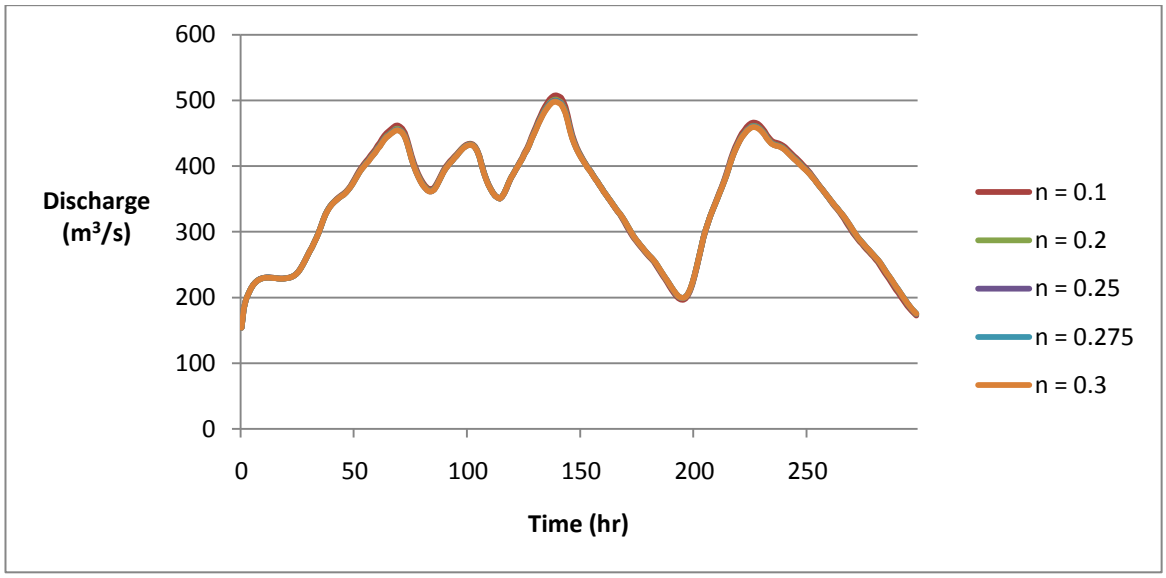

Manning's *n* for the floodplain varied.

APPENDIX THREE – Hydrographs produced after scaling and shifting the flow for each of the levée scenarios in Chapter Five.

1) Scaled flow

WITH LEVÉES

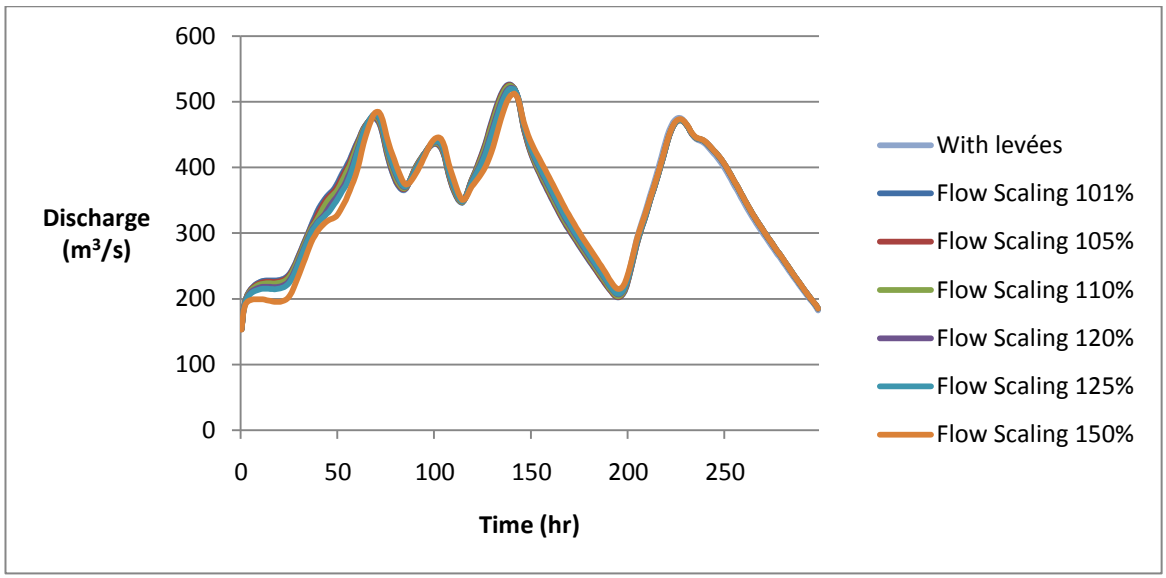

WITHOUT LEVÉES

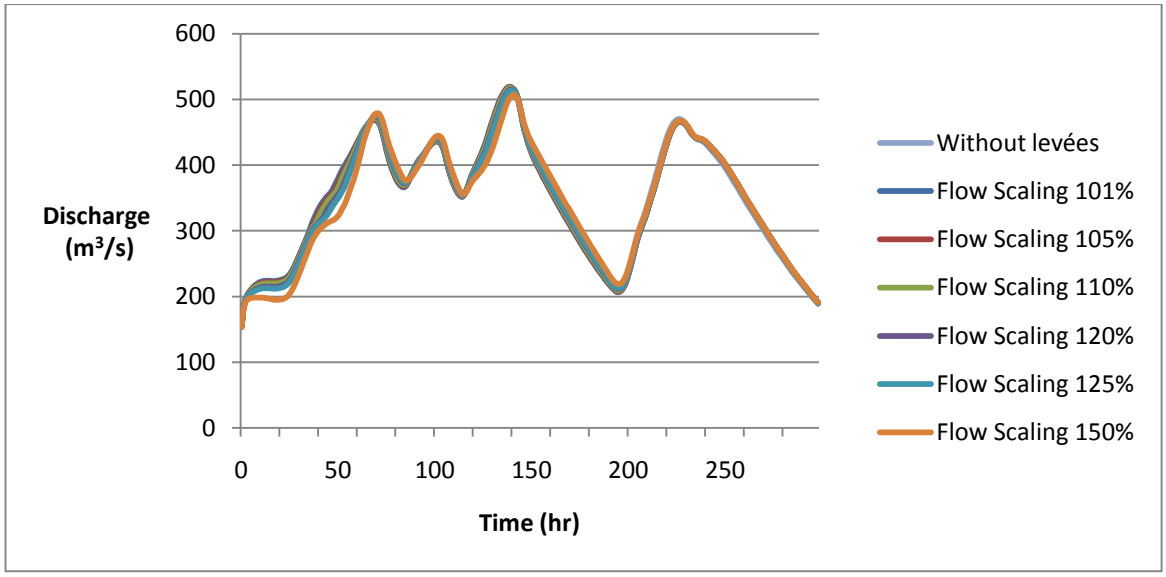

HALF LEVÉES

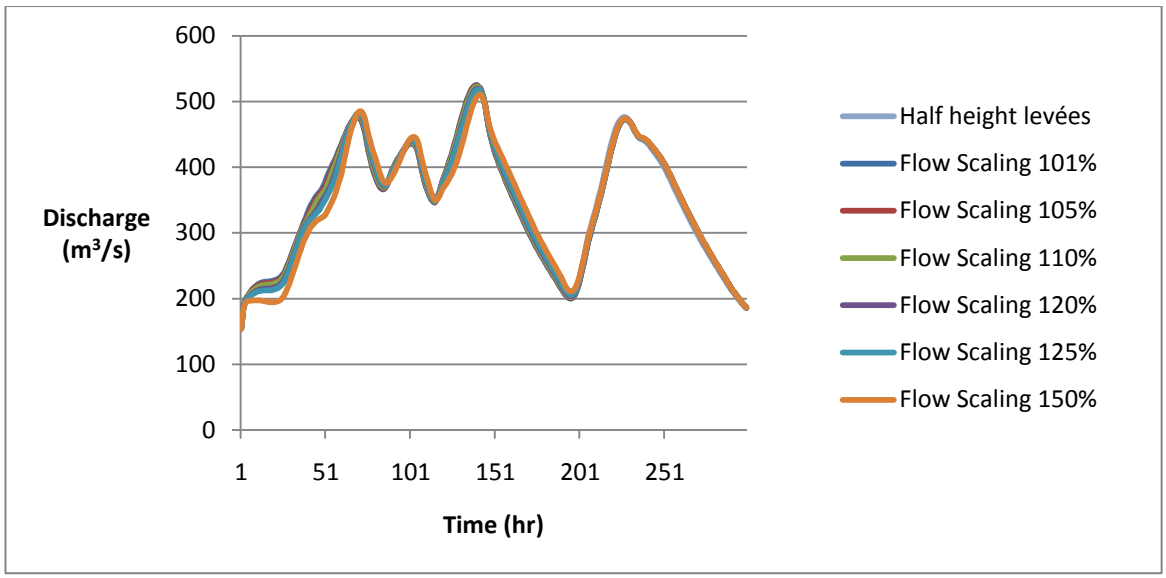

ADDED HEIGHT LEVÉES

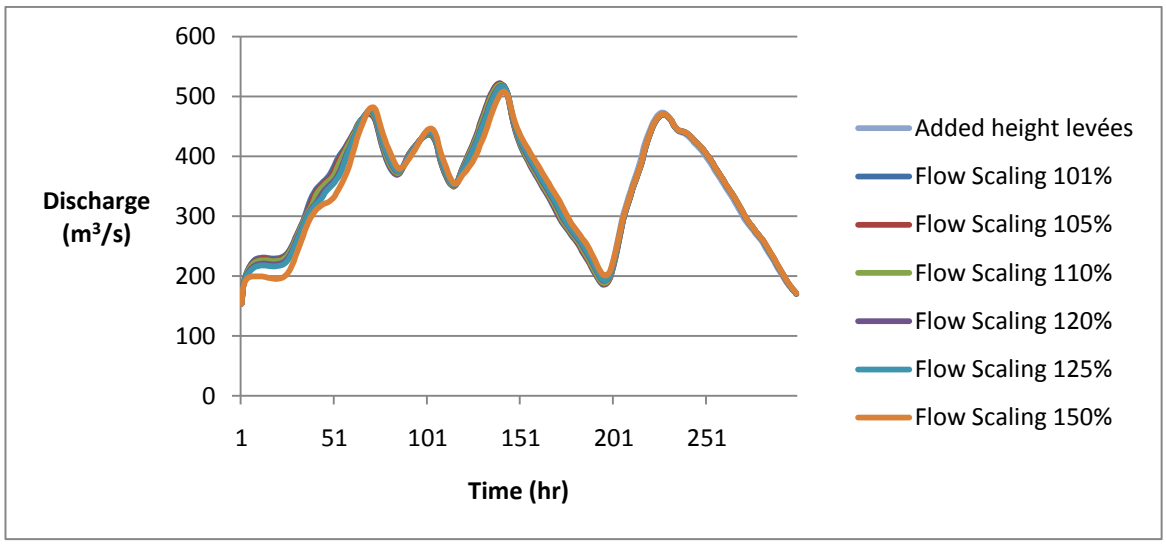

2) Scaled and shifted flow

WITH LEVÉES

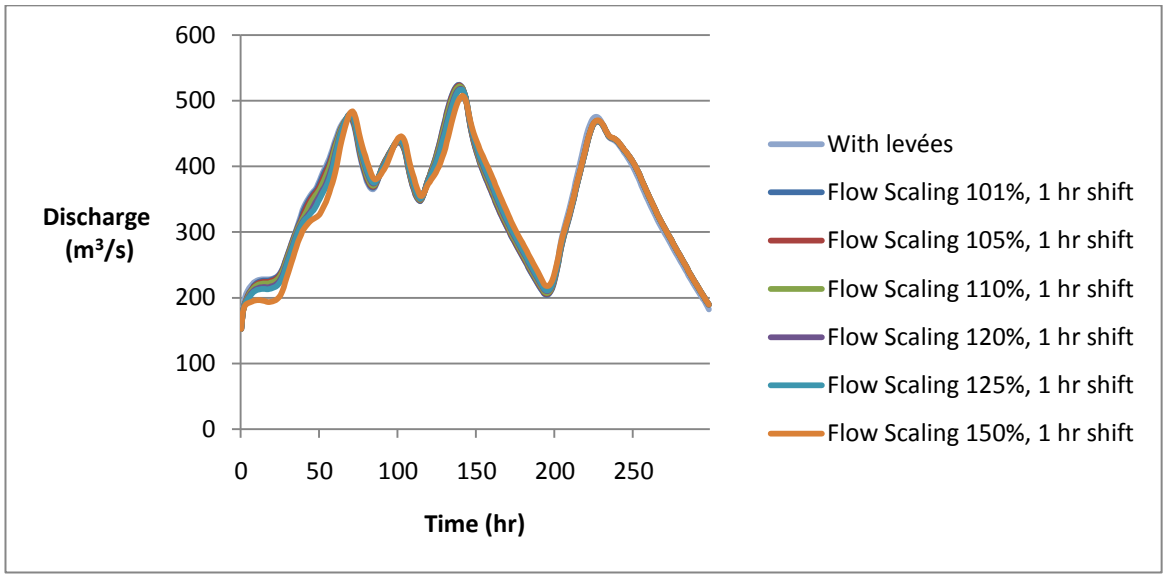

WITHOUT LEVÉES

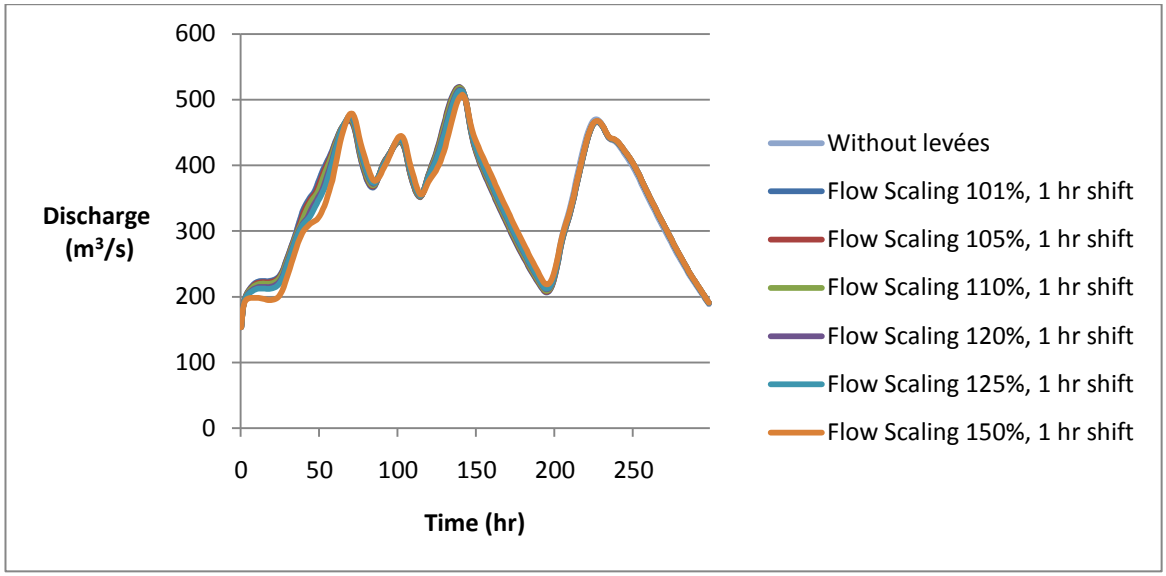

HALF HEIGHT LEVÉES

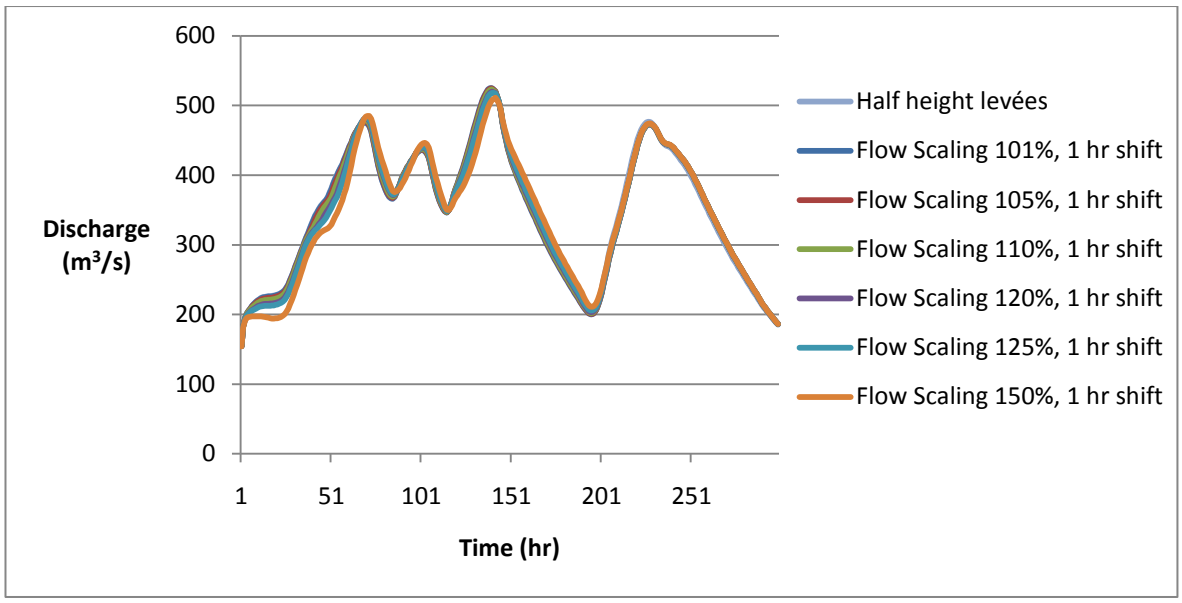

ADDED HEIGHT LEVÉES

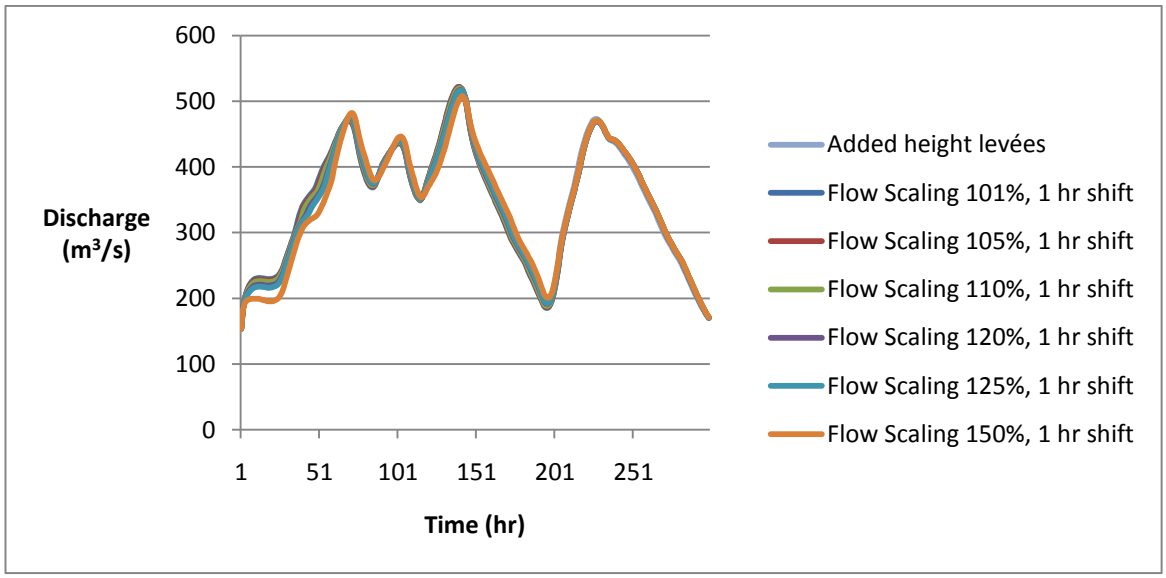

APPENDIX FOUR – Comparing the hydrographs for each variation presented in Chapter Five.

WITH LEVÉES

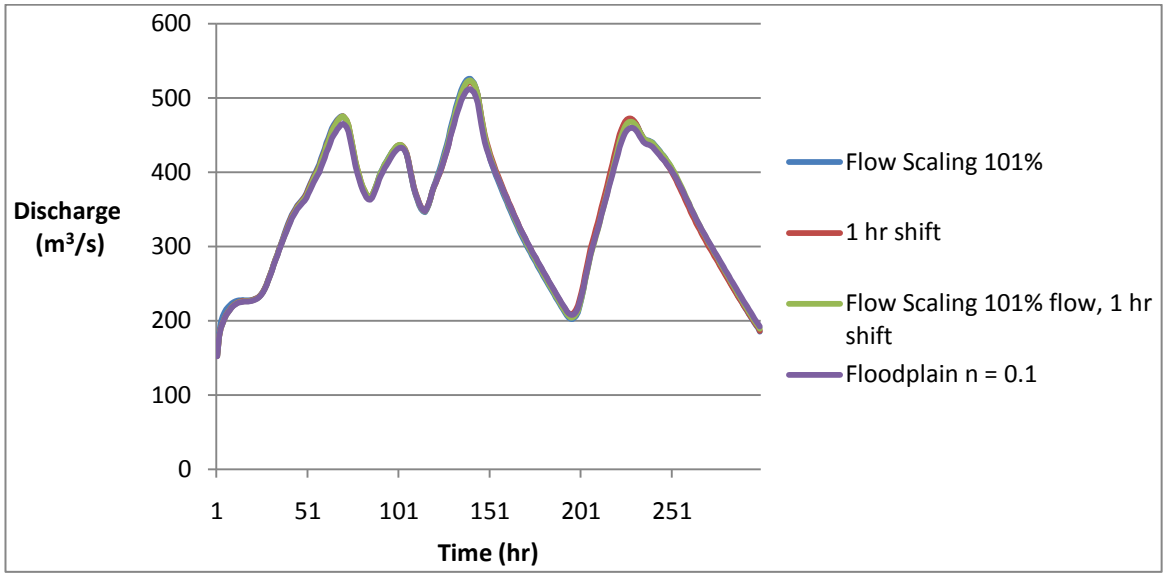

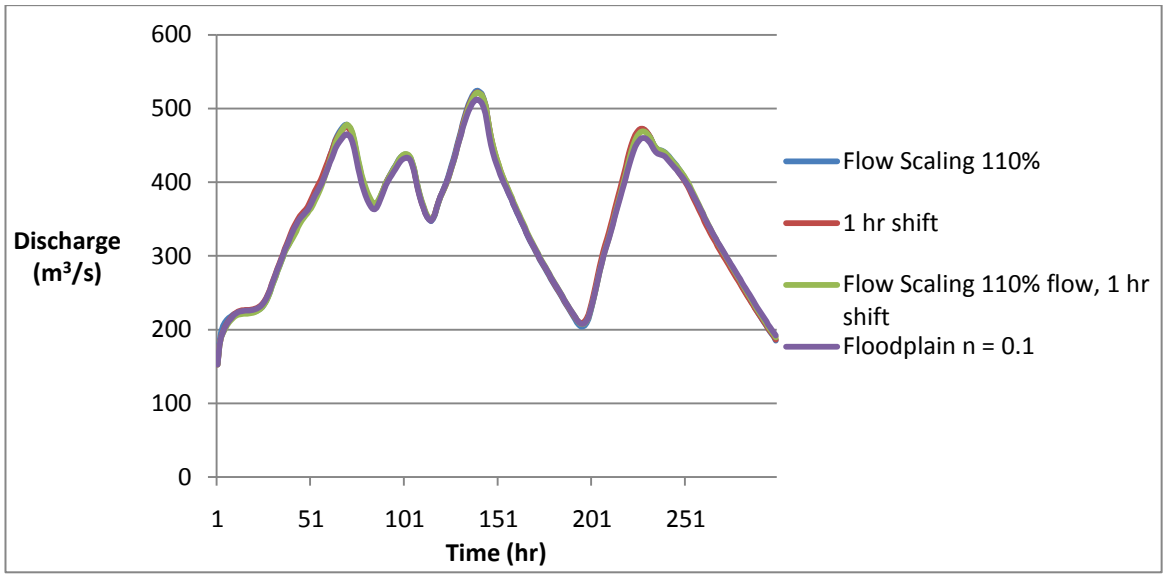

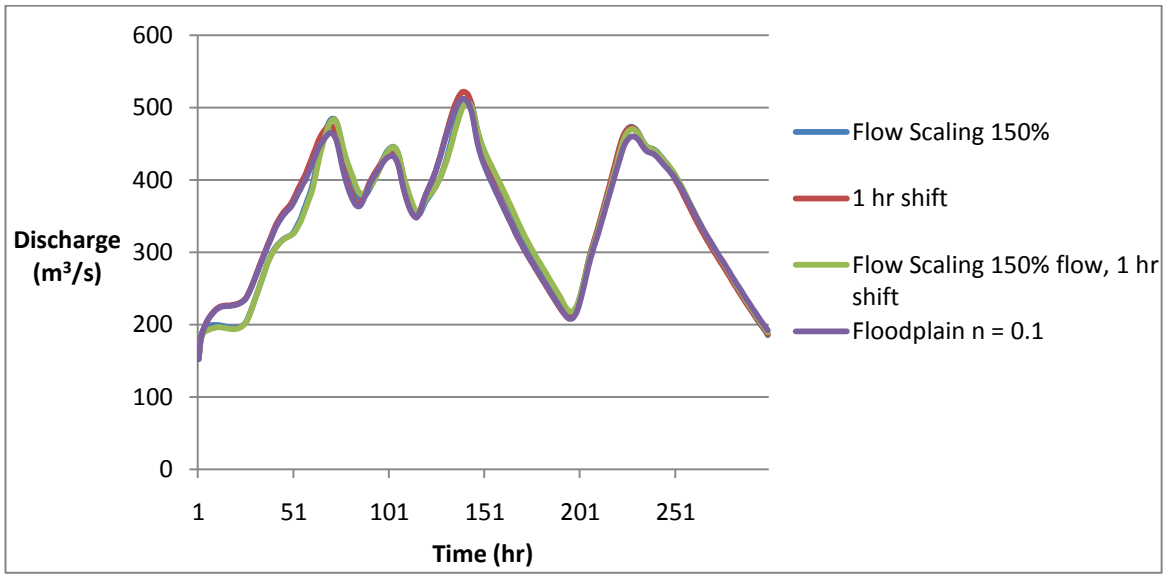
600
500
400
300
200
100
0
Discharge (m³/s)
1
51
101
151
201
251
Time (hr)
Flow Scaling 150%
1 hr shift
Flow Scaling 150% flow, 1 hr shift
Floodplain n = 0.1

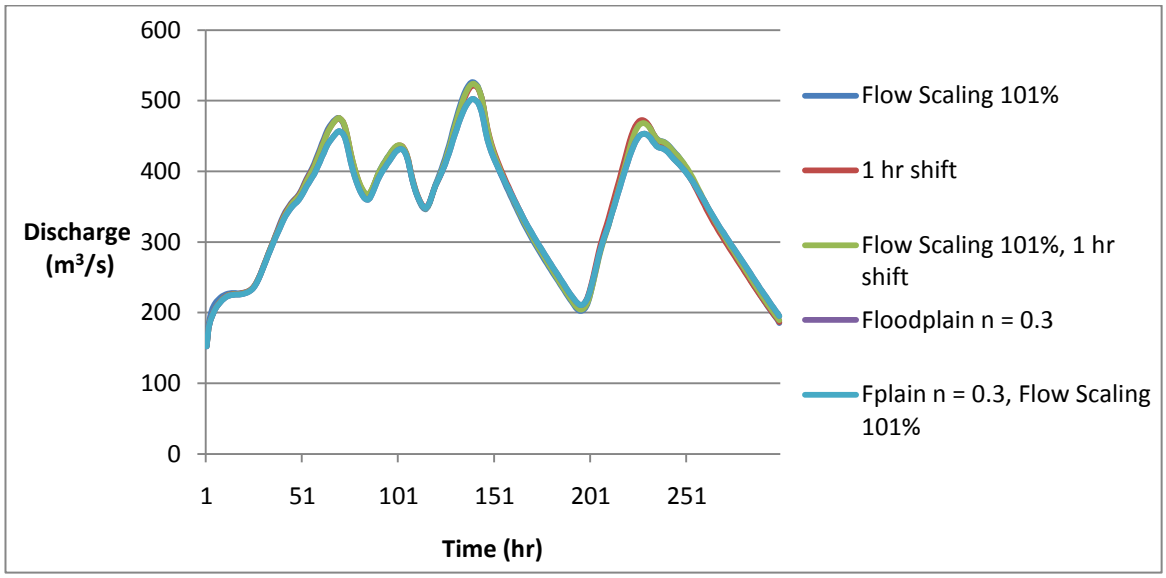
600
500
400
300
200
100
0
Discharge (m³/s)
1
51
101
151
201
251
Time (hr)
Flow Scaling 101%
1 hr shift
Flow Scaling 101%, 1 hr shift
Floodplain n = 0.3
Fplain n = 0.3, Flow Scaling 101%

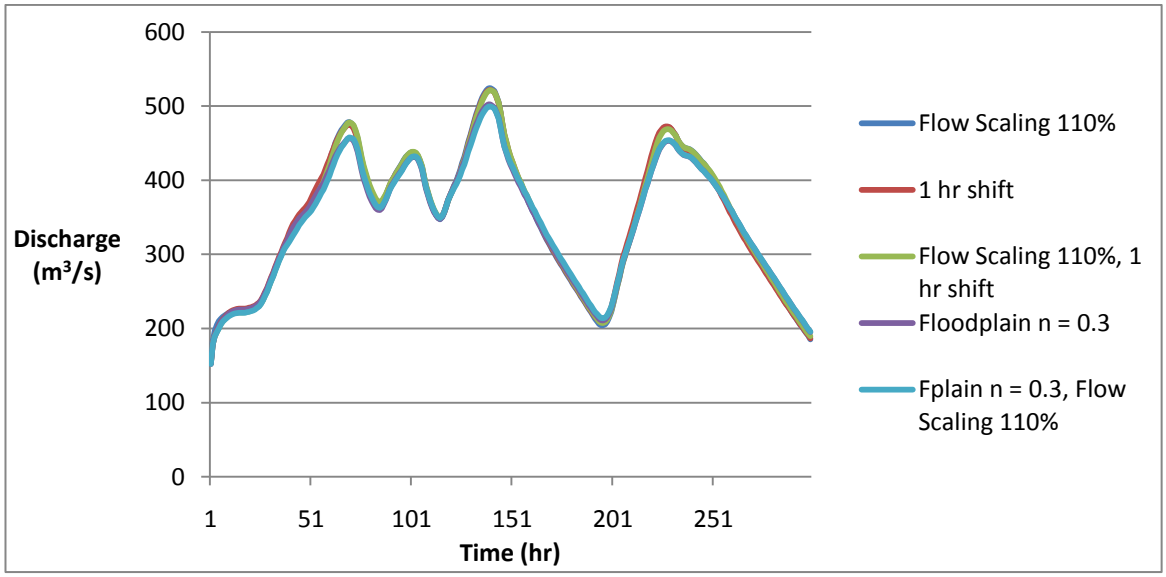
600
500
400
300
200
100
0
Discharge (m³/s)
1
51
101
151
201
251
Time (hr)
Flow Scaling 110%
1 hr shift
Flow Scaling 110%, 1 hr shift
Floodplain n = 0.3
Fplain n = 0.3, Flow Scaling 110%

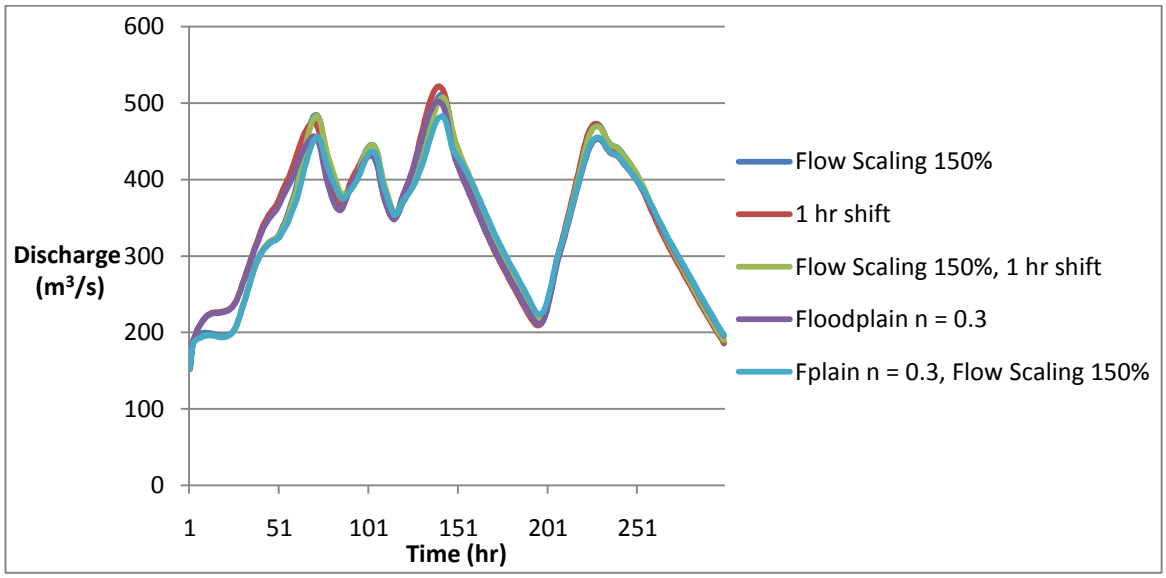
600
500
400
300
200
100
0
Discharge (m³/s)
1
51
101
151
201
251
Time (hr)
Flow Scaling 150%
1 hr shift
Flow Scaling 150%, 1 hr shift
Floodplain n = 0.3
Fplain n = 0.3, Flow Scaling 150%

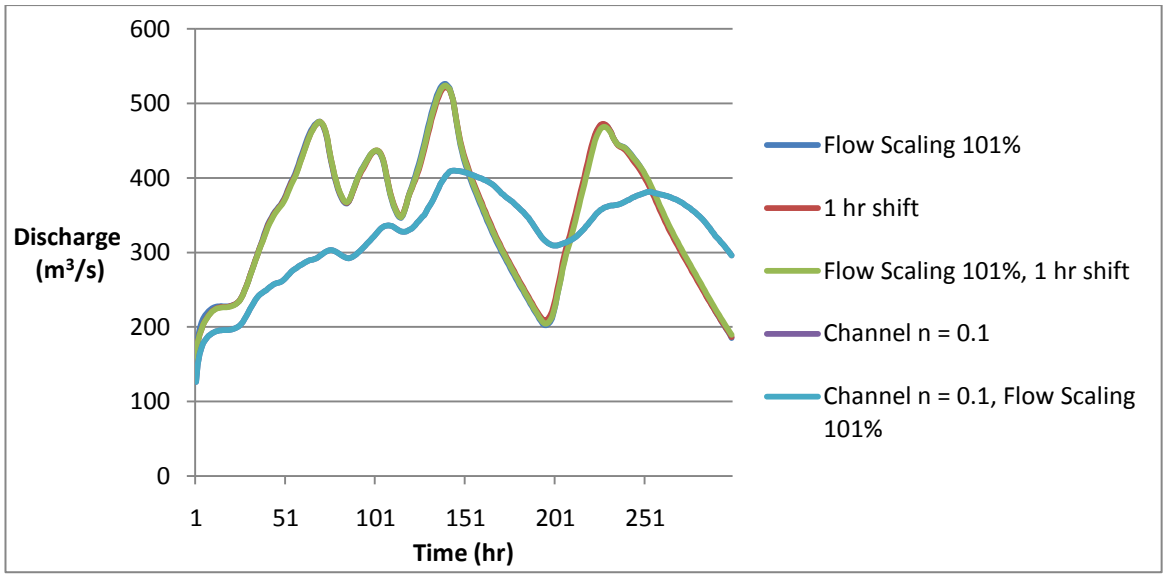
600
500
400
300
200
100
0
Discharge (m³/s)
1
51
101
151
201
251
Time (hr)
Flow Scaling 101%
1 hr shift
Flow Scaling 101%, 1 hr shift
Channel n = 0.1
Channel n = 0.1, Flow Scaling 101%

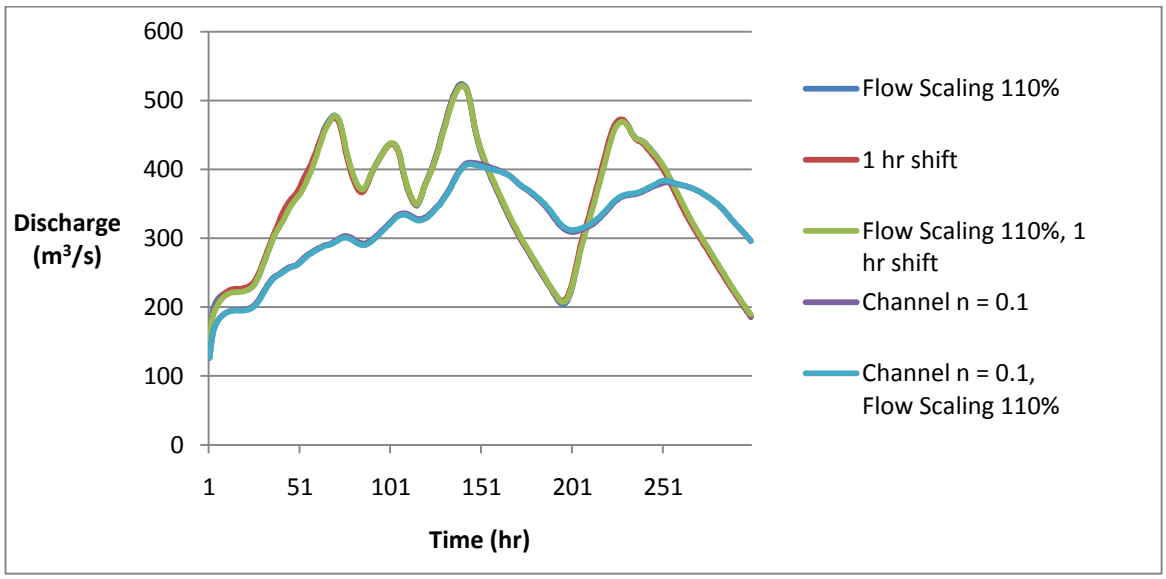
600
500
400
300
200
100
0
Discharge (m³/s)
1
51
101
151
201
251
Time (hr)
Flow Scaling 110%
1 hr shift
Flow Scaling 110%, 1 hr shift
Channel n = 0.1
Channel n = 0.1, Flow Scaling 110%

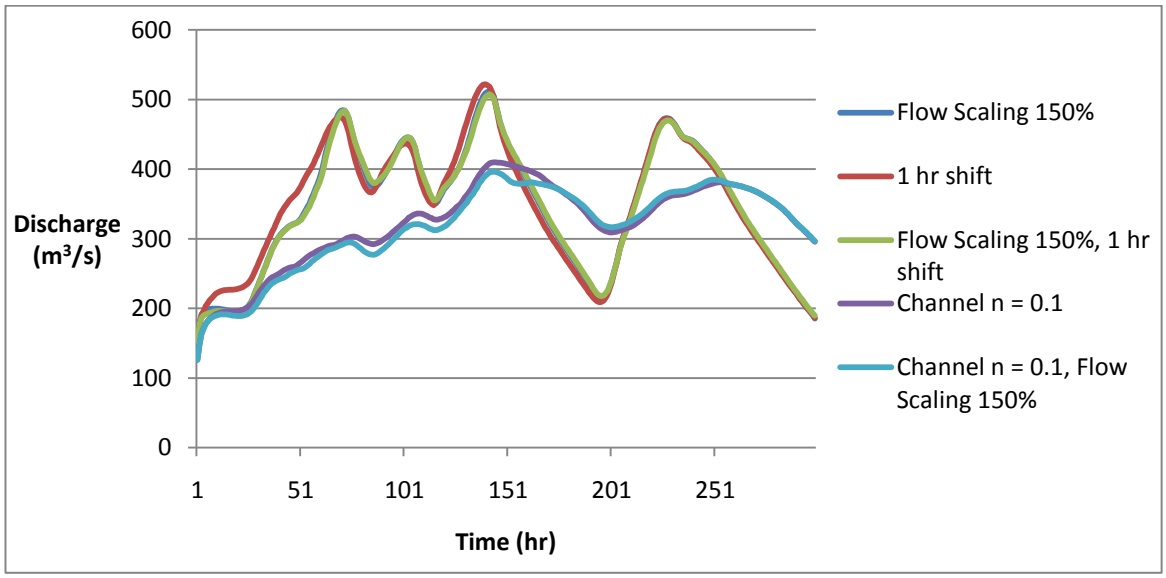
600
500
400
300
200
100
0
Discharge (m³/s)
1
51
101
151
201
251
Time (hr)
Flow Scaling 150%
1 hr shift
Flow Scaling 150%, 1 hr shift
Channel n = 0.1
Channel n = 0.1, Flow Scaling 150%

WITHOUT LEVÉES

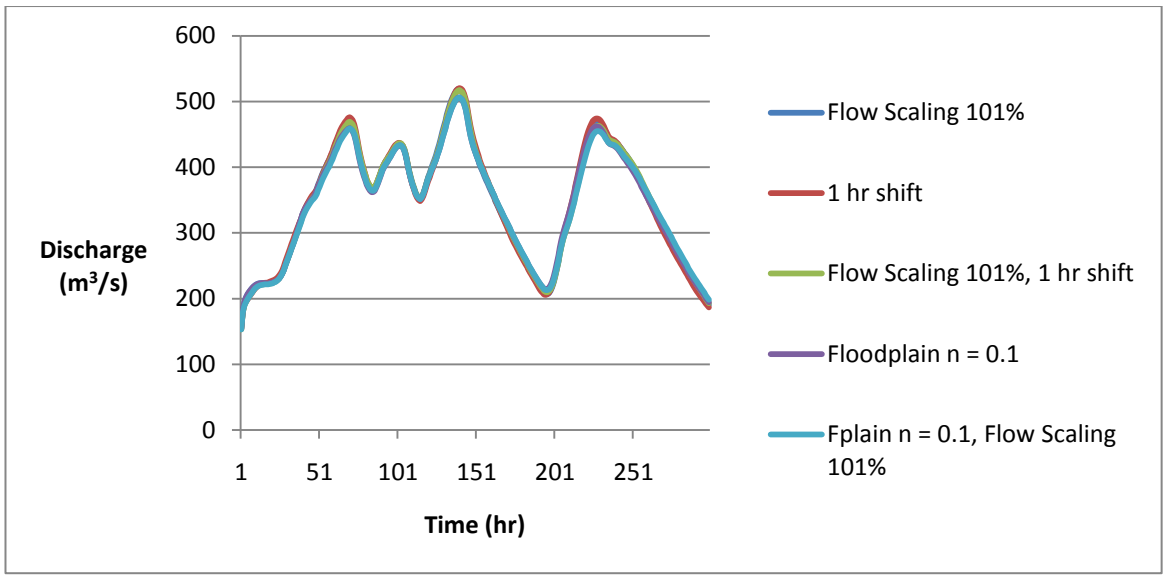

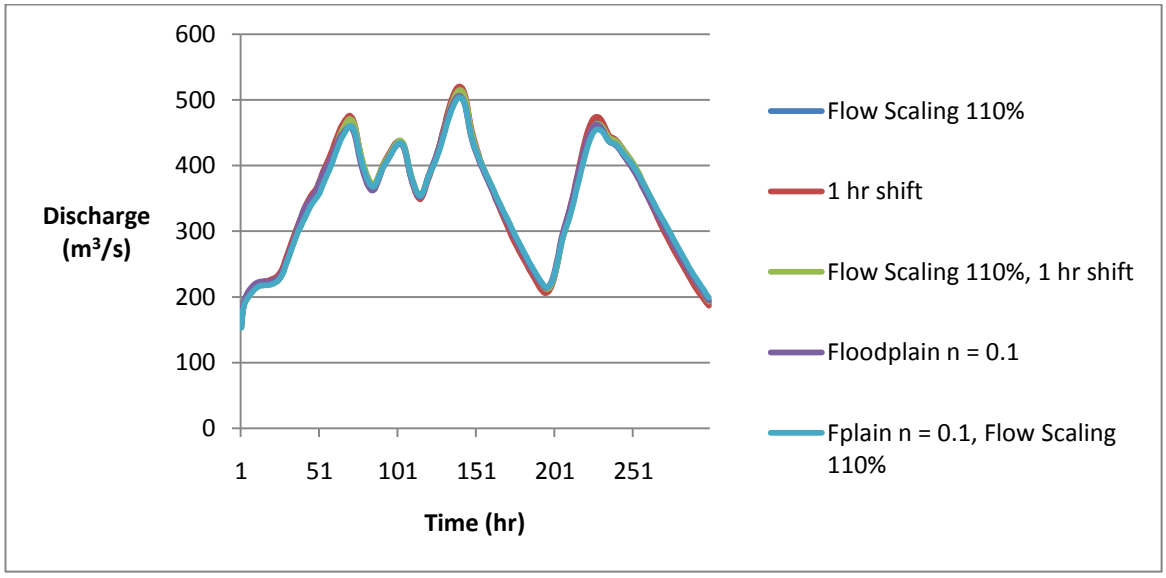

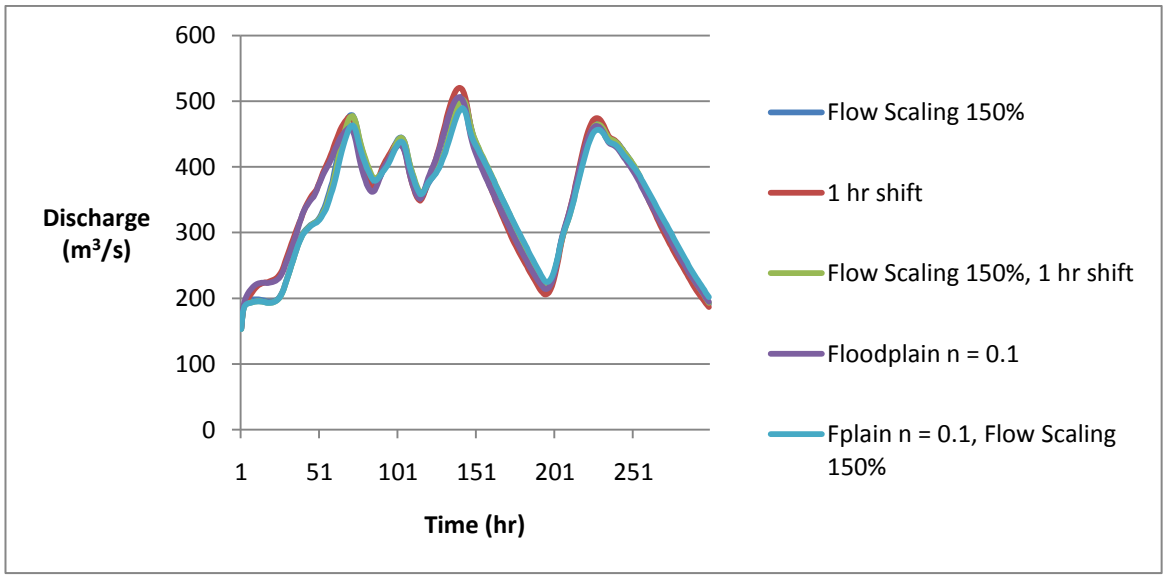

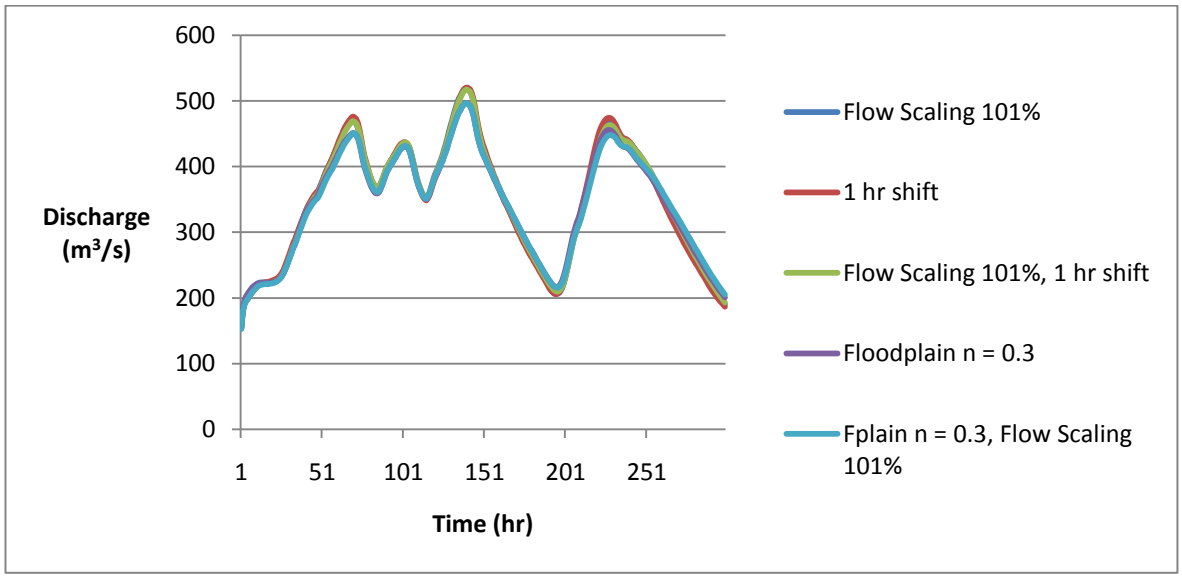
600
500
400
300
200
100
0
Discharge (m³/s)
1
51
101
151
201
251
Time (hr)
Flow Scaling 101%
1 hr shift
Flow Scaling 101%, 1 hr shift
Floodplain n = 0.3
Fplain n = 0.3, Flow Scaling 101%

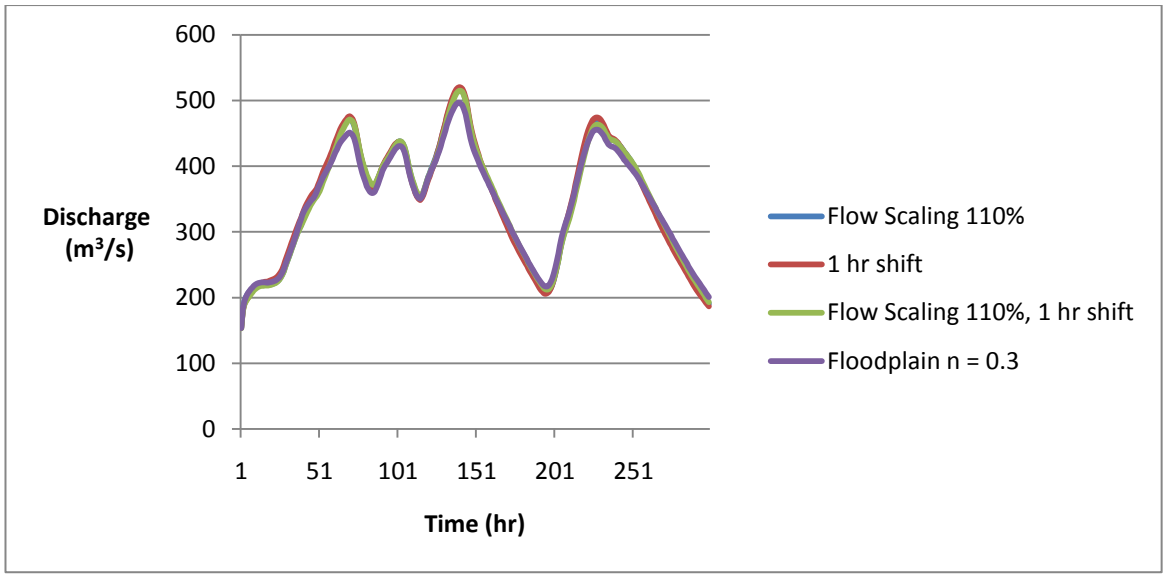
600
500
400
300
200
100
0
Discharge (m³/s)
1
51
101
151
201
251
Time (hr)
Flow Scaling 110%
1 hr shift
Flow Scaling 110%, 1 hr shift
Floodplain n = 0.3

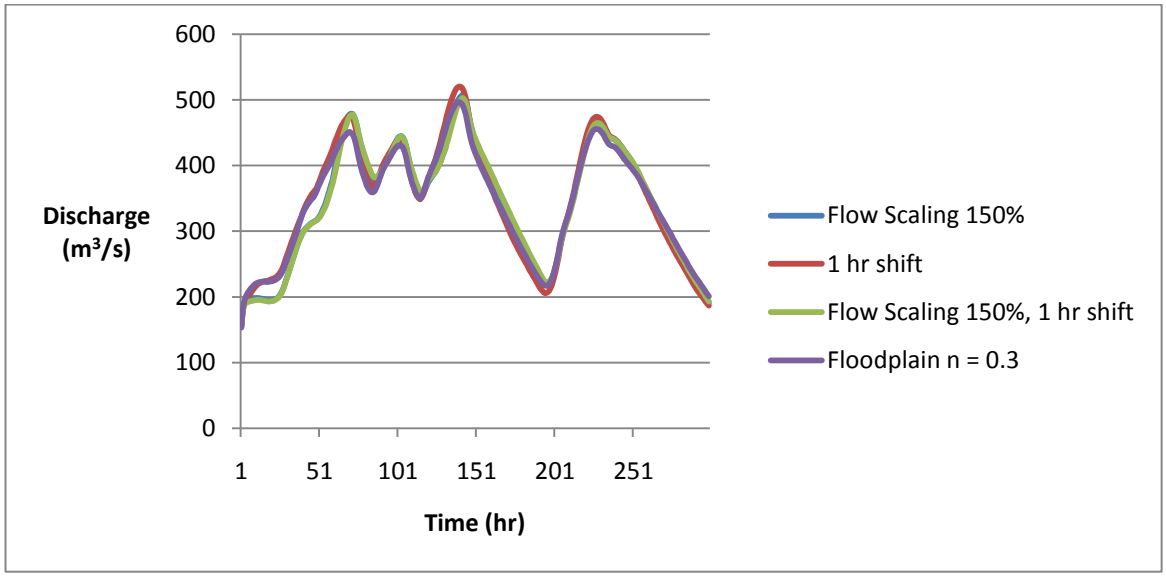
600
500
400
300
200
100
0
Discharge (m³/s)
1
51
101
151
201
251
Time (hr)
Flow Scaling 150%
1 hr shift
Flow Scaling 150%, 1 hr shift
Floodplain n = 0.3

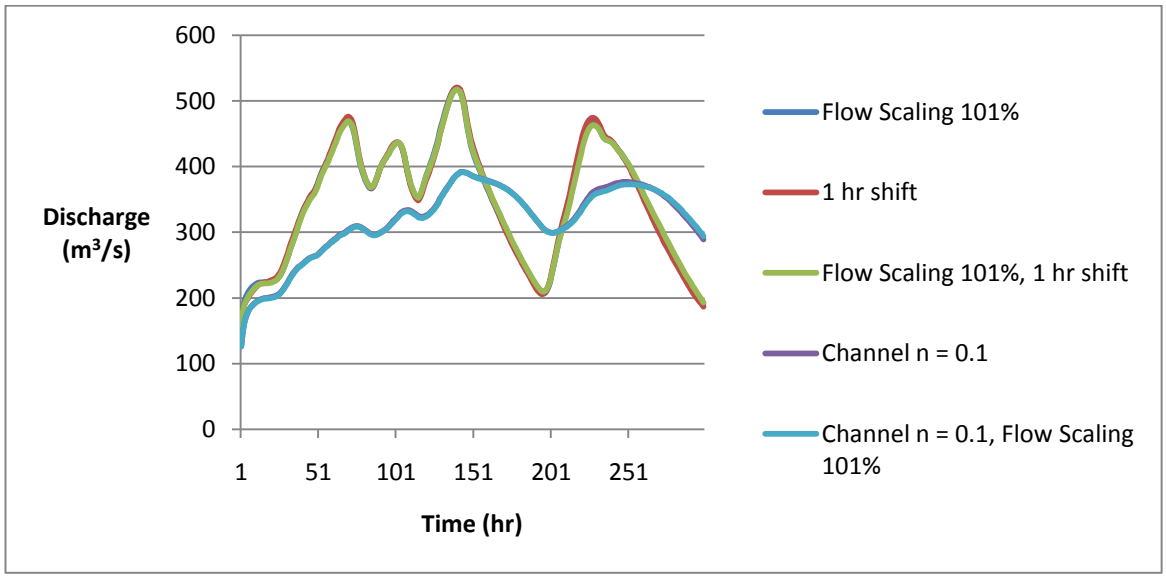
600
500
400
300
200
100
0
Discharge (m³/s)
1
51
101
151
201
251
Time (hr)
Flow Scaling 101%
1 hr shift
Flow Scaling 101%, 1 hr shift
Channel n = 0.1
Channel n = 0.1, Flow Scaling 101%

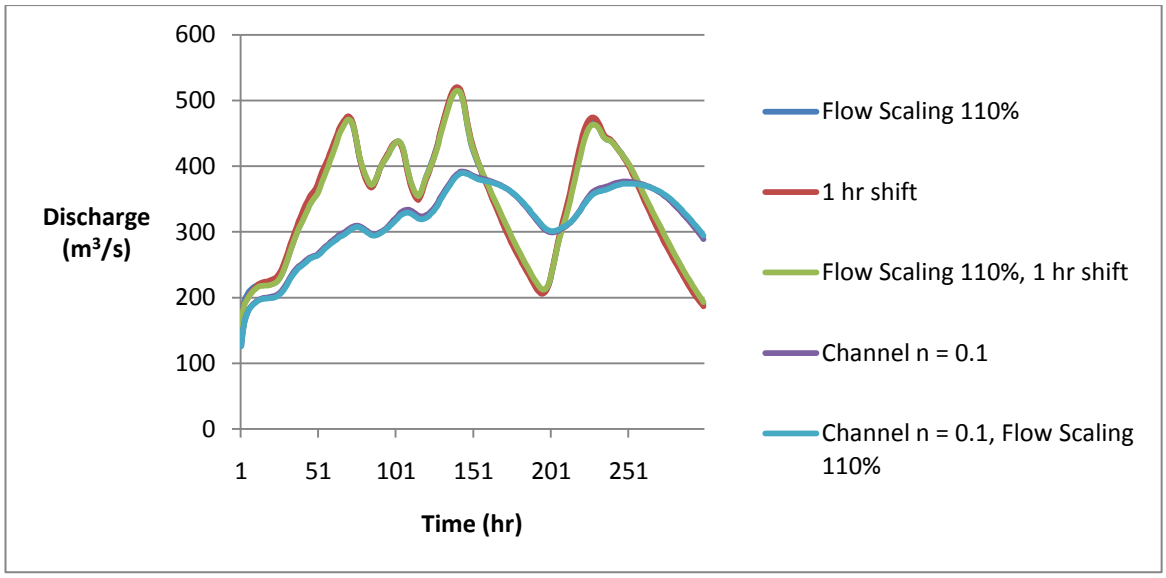
600
500
400
300
200
100
0
Discharge (m³/s)
1
51
101
151
201
251
Time (hr)
Flow Scaling 110%
1 hr shift
Flow Scaling 110%, 1 hr shift
Channel n = 0.1
Channel n = 0.1, Flow Scaling 110%

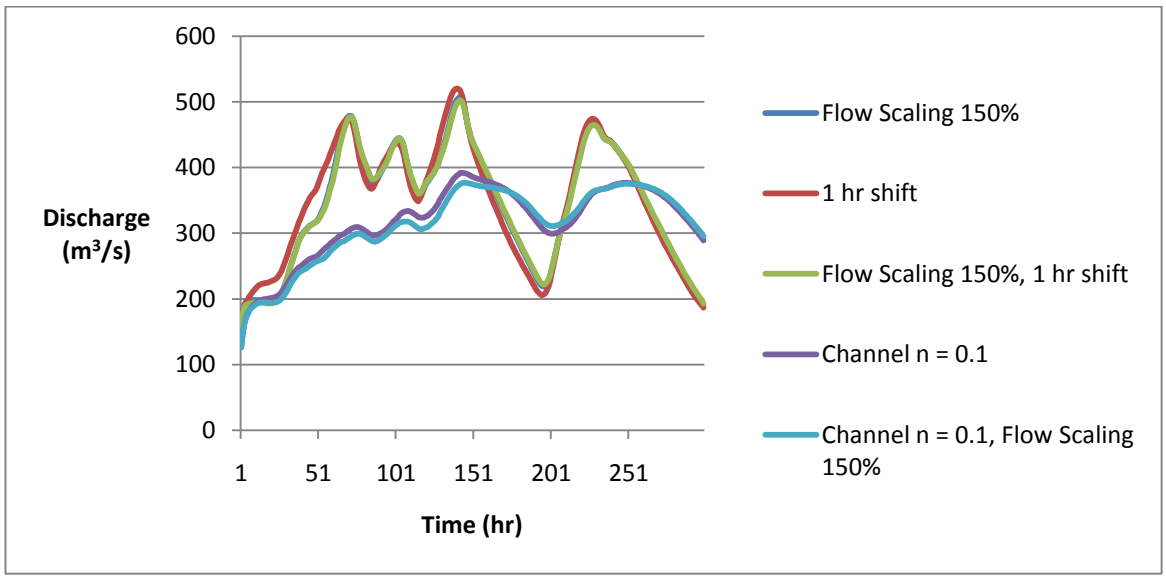
600
500
400
300
200
100
0
Discharge (m³/s)
1
51
101
151
201
251
Time (hr)
Flow Scaling 150%
1 hr shift
Flow Scaling 150%, 1 hr shift
Channel n = 0.1
Channel n = 0.1, Flow Scaling 150%